Calibration and application of foraminiferal based trace metal proxies in the Mediterranean Sea

Shauna Ní Fhlaithearta

Utrecht Studies in Earth Sciences

No. 169

MEMBERS OF THE DISSERTATION COMMITTEE

Prof. Dr. J. B. M. Middelburg
Prof. Dr. L. J. Lourens
Prof. Dr. A. Sluijs
Prof. Dr. D. Nürnberg
Dr. K. A. Koho

This research project was funded by the Darwin Center for Biogeosciences

ISBN: 978-90-6266-522-8
USES no. 169
Lay-out by Legatron Electronic Publishing, The Netherlands
Cover lay-out by Margot Stoete, UU Geo C&M
Printed by Ipskamp Printing, The Netherlands

Calibration and application of foraminiferal based trace metal proxies in the Mediterranean Sea

Kalibratie en applicatie van op foraminiferen gebaseerde spoormetalen proxies in de Middellandse Zee

(met een samenvatting in het Nederlands)

PROEFSCHRIFT

Ter verkrijging van de graad van doctor aan de Universiteit Utrecht
op gezag van de rector magnificus, prof. dr. H. R. B. M. Kummeling,
ingevolge het besluit van het college voor promoties in het openbaar te verdedigen
op vrijdag 25 januari 2019 des ochtends te 10.30 uur
door

Shauna Mairéad Ní Fhlaithearta
geboren op 14 maart 1980 te Galway, Ierland

PROMOTOREN

Prof. dr. G. J. Reichart
Prof. dr. G. J. de Lange

Na Blátha Craige

A dúirt mé leis na blátha:
"Nach suarach an áit a fuair sibh
le bheith ag déanamh aeir
Teannta suas anseo le bruach na haille,
Gan fúibh ach an chloch ghlas
Agus salachar na n-éan,
áit bhradach, lán le ceo
Agus farraige cháite,
Ní scairteann grian anseo
Ó Luan go Satharn
Le gliondar a chur oraibh"
A dúirt na blatha craige:
"Is cuma linn, a stór,
Táimid faoi dhraíocht
ag ceol na farraige."

– Liam Ó Flaithearta

Contents

1

Introduction and Outlook

1 | CLIMATE CHANGE

Studying the nature, causes and consequences of climate change allows a better understanding of the functioning of Earth's climate system, including forcing and feedbacks of the different components within the system. The impetus for present climate-change studies came from the observation of rapidly increasing carbon dioxide concentrations in the atmosphere (Keeling, 1960; Petit et al., 1999). Carbon dioxide, increasingly released since the industrial revolution, traps heat in the atmosphere, causing a rise in average global temperature (IPCC, 2013). Increasing temperature has a knock-on effect on the atmosphere, hydrosphere, cryosphere, lithosphere and biosphere, making the consequences of climate change far-reaching and complex. These consequences include changing precipitation pattern, drought, sea-level rise, ocean acidification and flooding, all leading to drastic socio-economic impacts. The complex nature of the interactions makes it very difficult, in both short and long time-scales, to predict the consequences for the different parameters involved.

Accurate predictions of climate change and the impact on the different components of the climate system are essential for informed policy making and for choosing the most suitable mitigation strategies. Numerical climate models are built specifically for this purpose and address either a specific aspect of on-going climate change, or try to assess the full complexity of the climate system. By capturing the complexity of the climate system in a numerical model, scientists are able to test the probability of different climate scenarios. However, interpretation of the results can be hindered due to the complexity of the system and the different responses, depending on the time scale considered. The complexity of the climate system and the multitude of feedback processes involved, make extensive testing and validation of climate models essential for their application.

Climate models are generally validated using cross correlations between models (inter-comparison) and different climate scenarios from the past, based on archives of past analogues. Instrumental records of temperature, precipitation and carbon dioxide concentrations are ideal for validating a climate model. However, they are relatively short term (~ 150 years), often limited in range, and lack true analogue conditions to the predicted climate scenarios. The latter largely exceed the more recent changes in temperature, precipitation and carbon dioxide concentration (IPCC, 2007). Conversely, the geological record provides a much longer archive with more extended extremes in temperature, precipitation and carbon dioxide concentration. Hence, to test the validity of climate model predictions for a high-CO_2 future, it is crucial to also delve into the high-CO_2 climates of the past. Additionally, because of the non-linear relationships between environmental variables, investigating non-analogue conditions adds substantial understanding of the processes involved. However, reconstructing past climates also requires adequate tools to read the geological record.

2 | PROXIES

Environmental recorders of past climate conditions have been developed to extend our knowledge of climate beyond instrumental records. Climate information is captured in tree rings, fossils, speleothems, ice cores and buried in sediments of lakes and oceans. An environmental recorder or a so-called 'proxy' for an environmental condition (for example, temperature) needs to have a quantifiable relationship with the environmental target condition. Ideally, the signal carrier needs to have a wide spatial distribution and should cover a significant period of the geological record. When these criteria are met, the proxy can be calibrated in the field, under controlled laboratory conditions, or by inter-comparison with other proxies and preferably is validated using sub-recent instrumental records. Most proxies are based on empirical calibrations, making it difficult to extend their calibrations to non-analogue settings. Hence the development of process-based proxies has become one of the major goals in paleoceanography and paleoclimate research. Especially the stable isotopic and trace metal composition of foraminiferal tests has been subject of much research in this respect.

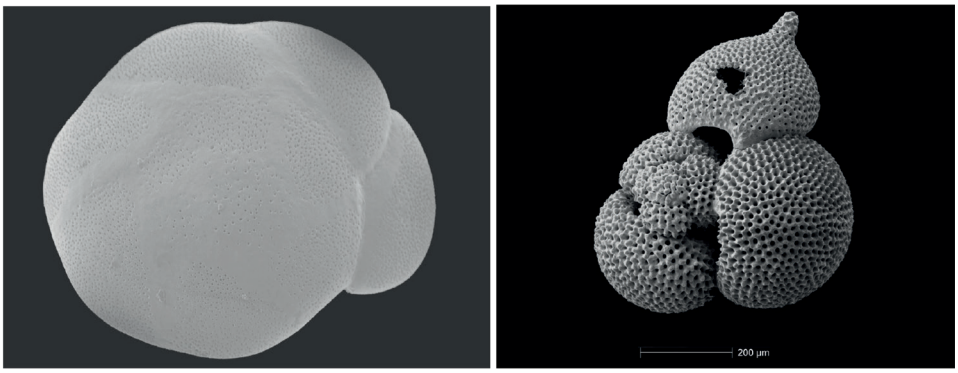

Figure 1 | Two species of foraminifera, on the left the benthic foraminifer *Ammonia tepida*. This species is often used for trace metal calibration studies in controlled growth experiments. On the right *Trilobatus sacculifer,* a shallow surface dwelling planktonic foraminiferal species. This species is often used in controlled growth experiments for proxy calibration purposes.

3 | FORAMINIFERA

Foraminifera (Figure 1) are unicellular marine organisms that are commonly used as proxy signal carriers. They are among the most widely occurring organisms on Earth, and are found in all marine environments. Fossil foraminifera are recovered from as far back as the Cambrian

(~ 520 Ma) (Pawlowski et al., 2003) at about the same time as the first skeletonized metazoans. There are approximately 900 genera and 10,000 species, with broad physiological divisions based on single- versus multi-chambered and calcareous- versus agglutinating-tests (Loeblich Jr. and Tappan, 1984). The majority of foraminiferal species, however, precipitate tests made of calcium carbonate. Both the relative distribution of foraminiferal species and the chemical and isotopic composition of their tests reflect the environment they were living in. By recovering and studying foraminiferal tests from marine sediments it is hence possible to reconstruct past environments. Test forming foraminifera are found in the water column (planktic foraminifera) and living on or within the seabed (benthic foraminifera).

Table 1 | Simplified overview of environment parameters and related foraminiferal proxies.

Environmental parameter	Foraminiferal based proxy	References
Temperature	Mg/Ca, $\delta^{18}O$	(McCrea, 1950; Nürnberg et al., 1996)
Nutrients	Ba/Ca, Cd/Ca, $\delta^{13}C$	(Boyle, 1981; Lea and Spero, 1994)
Bottom-water oxygenation	Assemblages, Mn/Ca	(Jorissen et al., 1995; Koho et al., 2017)
Salinity	Ba/Ca, Na/Ca, combi of Mg/Ca and $\delta^{18}O$	(Rohling and Bigg, 1998; Weldeab et al., 2007; Wit et al., 2013)
pH	$\delta^{11}B$	(Sanyal et al., 1995)
Carbonate ion	U/Ca, Sr/Ca, S/Ca	(Van Dijk et al., 2017; Keul et al., 2017; Russell et al., 2004)
Organic flux	Assemblages, $\delta^{13}C$	(Jorissen et al., 1995; Zahn et al., 1986)
Water mass	Assemblages, Ba/Ca, $\delta^{13}C$	(Lea and Boyle, 1989; Mackensen et al., 1993; Schmiedl et al., 1997)

The use of foraminifera as proxy carriers developed via two largely separate paths: an ecology based path and a test chemistry based path. Ecologically, changes through time in foraminiferal species diversity and relative abundance reflect environmental change, as foraminiferal communities react to primary variations in food- and oxygen- availability (Jorissen et al., 1995). Chemically, changes in oxygen- and carbon- isotope ratios in the test carbonate are correlated with changes in seawater temperature, water masses and food availability (Epstein et al., 1953; Shackleton, 1974; Bemis et al., 1995).

While constructing their tests, foraminifera also incorporate trace and minor elements into the carbonate in a way that reflects the environment of formation. The use of trace/minor elements to calcium ratios has gained considerable momentum in recent years due to advances in analytic techniques. The stable isotope ratio or trace and minor elements incorporated into foraminiferal tests often reflect more than one variable (Lea, 2013). These variables include influences from various components of the carbonate system ($[CO_3^{2-}]$, pH) and ecological preferences of the foraminifera (in-sediment habitat depth, metabolic rates) (Table 1). Robust interpretation of proxy information requires these different factors to be known. This can be

achieved through a multi-proxy approach. Some pertinent examples of such an approach are illustrated in the underlying dissertation, in particular using benthic foraminifera and their organic, elemental and isotopic composition.

Scope and framework of this thesis

This dissertation describes the development and application of proxies in benthic foraminifera. The aim is to better understand these proxies and thus expand our knowledge of climate change in the past. The different approaches followed have been ordered in Chapters 2 to 5, with the final Chapter 6 detailing an application of foraminiferal trace-metal proxies to the Mediterranean sedimentary record.

In Chapter 2 the organic geochemical composition of foraminiferal organic linings was investigated as a potential proxy signal carrier for the $\delta^{18}O$ and $\delta^{13}C$ of the seawater and $\delta^{13}C$ of the food source (i.e. trophic level). The macromolecular and stable isotopic composition of organic linings was characterized using Curie-point pyrolysis-GC-MS, showing that benthic foraminiferal linings consist of protein and polysaccharides, bound together in a complex macro-molecular structure. Both chitin derivatives and traces of guaiacols and syringols were found. Although for the five species investigated the linings all contain chitin derivatives and proteins, the relative contribution of the different compounds varied considerably between species. The stable oxygen isotopic composition of the organic linings was shown to be consistent with fractionation between seawater and organic matter. This makes the organic linings a potential independent source of information for the past stable oxygen isotopic composition of seawater. A deliberate tracer experiment showed that, in contrast, the $\delta^{13}C$ of the organic linings reflect the foraminiferal food source. These different pathways for carbon and oxygen have important implications for the potential use of organic linings as proxy signal carriers. However, their advanced application also relies on important analytical improvements to be made. Recent developments in the nano-scale analyses of stable carbon isotopes (Roij et al., 2017), in combination with the Chapter 2 approach now sets the stage for a whole new field of foraminiferal research.

In Chapter 3, the potential application of Mn/Ca ratios for the reconstruction of paleo-redox zonation was investigated in combination with foraminiferal microhabitat preferences. Manganese is ideally suited for such an approach as manganese geochemistry in deep-sea sediments is known to have a large systematic gradient, especially over the first few centimeters. This overlaps with the in-sediment depth habitats of several benthic foraminiferal species. Chapter 3 shows manganese incorporation in benthic foraminiferal test carbonate across a depth transect in the Gulf of Lions, NW Mediterranean. Manganese concentrations in the tests of living (Rose Bengal stained) benthic foraminiferal specimens of *Hoeglundina elegans*, *Melonis barleeanus, Uvigerina mediterranea*, *Uvigerina peregrina* were measured using laser ablation inductively coupled mass spectrometry (laser ablation ICP-MS). Porewater manganese concentrations decreased from shallow to deeper waters, which was consistent

with decreasing organic matter fluxes with water depth. Differences in organic matter loading at the sediment water interface affected oxygen penetration depth into the sediment and hence Mn porewater profiles. The foraminiferal Mn/Ca values of the different species link porewater geochemistry to species-specific depth habitat in the sediment. The observed variability within a single species is in-line with known ranges in depth habitat and measured dissolved Mn gradients under existing sedimentary redox conditions. Since Mn/Ca ratios and variability in foraminifera reflect past dynamics of foraminiferal depth habitats and Mn cycling, this limits the detailed application of such a proxy to settings with relatively stable environmental conditions.

Chapter 4 investigated other minor- and trace-metal incorporation into foraminiferal tests as a function of water and sediment depth across a 6-station depth transect of the Gulf of Lions, NW Mediterranean. The general aim was to investigate the link between trace metal incorporation in foraminiferal carbonate and ecological preference of foraminifera. Magnesium, strontium and barium concentrations in the tests of living (stained) specimens of the benthic foraminiferal species, *Hoeglundina elegans*, *Melonis barleeanus, Uvigerina mediterranea*, *Uvigerina peregrina* were measured using laser ablation inductively coupled mass spectrometry (laser ablation ICP-MS). Mg/Ca and Sr/Ca ratios remained relatively stable with increasing water depth, with Mg exhibiting much high inter-individual variability. Mg/Ca and Sr/Ca values were compared to existing temperature calibrations to validate applicability to the Mediterranean Sea. *Uvigerina peregrina* showed a distinctly different Mg/Ca signature compared to *U. mediterranea*, advising against grouping these species in the same empirical Mg/Ca-temperature relationships. Sr/Ca in *H. elegans* appears to follow temperature as expected based on existing calibrations. Although foraminiferal Mn has been shown to record pore water chemistry (Chapter 3), in-sediment changes in Ba^{2+} were not reflected by the Ba/Ca ratios in the test of living (i.e Rose-Bengal stained) foraminifera from the same cores. *Hoeglundina elegans* showed overall high Ba concentrations compared to the other species, which is in all likelihood mainly related to its aragonitic test (rather than a calcitic test like the other species). When comparing inter-specific differences in Ba/Ca, the calcitic foraminifera with the deepest living habitat in the sediment were characterized by the highest incorporation of Ba. Hence, although the Ba/Ca for individuals did not directly correspond to the in-situ Ba concentration, ecological preferences were clearly reflected by the Ba incorporation.

The fifth chapter deals with stable carbon and oxygen isotope fractionation of benthic foraminifera as a function of porewater carbonate chemistry. The stable oxygen and carbon isotope composition of the carbonate tests of benthic foraminifera is one of the most commonly used proxies in paleoceanography. Whereas the oxygen isotope signal is interpreted in terms of seawater temperature and global ice volume, the carbon isotope ratio is generally interpreted to reflect water mass and/or carbon flux to the seafloor. Most studies to date have, however, refrained from looking at both isotope systems in a coupled way. Here we show that the two isotopic systems are closely related when comparing benthic foraminiferal species

with contrasting microhabitats in the sediment. The good overall correlation of the carbon and oxygen isotopes suggests that these are primarily controlled by the same process. The near constant environmental conditions, irrespective of water depth in the setting studied here (the Gulf of Lions) permits the unravelling of this coupling between carbon and oxygen isotopes. The slope of the correlation supports a major impact of (seawater) carbonate ion concentration. Still, as these coupled oxygen and carbon isotopes cannot be interpreted purely in terms of depth habitat, it is likely that an additional impact of foraminiferal life processes, also known as vital effects, plays an important role.

In Chapter 6 the depositional environment of the Eastern Mediterranean was investigated using sediment geochemistry in combination with the trace elements incorporated in foraminiferal tests. Evolution of productivity, redox conditions, temperature, and ventilation during the deposition of Aegean sapropel S1 was investigated. The occurrence of benthic foraminifer, *Hoeglundina elegans* (*H. elegans*), throughout the sapropel, permitted for the first time a comparison between dissolved and particulate concentrations of Ba and Mn and the construction of a Mg/Ca-based temperature record through sapropel S1. A simultaneous increase in sedimentary Ba and Ba incorporated in foraminiferal test carbonate, points to a close coupling between Ba cycling and export productivity. During sapropel deposition, sedimentary Mn content ($(Mn/Al)_{sed}$) was reduced, corresponding to enhanced Mn^{2+} mobilization from sedimentary Mn oxides under suboxic conditions. The consequently elevated dissolved Mn^{2+} concentrations were reflected in enhanced ($Mn/Ca)_{H.\ elegans}$ levels, agreeing with observations today in the Gulf of Lions (Chapter 3). The magnitude and duration of the sapropel interruption and other short-term cooling events were constrained using Mg/Ca thermometry. Based on integrating productivity and ventilation records with the temperature record a two-mode hysteresis model was proposed for sapropel formation.

OUTLOOK

For advanced research and fundamental understanding of climate and ocean state, proxies will continue to be important. Whereas consensus exists on global warming, the sensitivity of the climate system with respect to atmospheric CO_2 is still under debate. More accurate and robust proxies are essential for our understanding of past climates. These provide essential boundary conditions for numerical climate reconstructions, hence are essential tools to improve forecasts of future climate change. However, for some components of the ocean-climate system proxies are not yet sufficiently constrained. For instance, many proxies exist for seawater temperature, such as Mg/Ca, Uk^{37} and clumped isotope thermometry, while other parameters, such as fluxes in organic matter and bottom-water oxygenation, are more difficult to capture in adequate proxies or be linked a single process. Also, the fact that multiple factors often affect a single proxy, such as Ba/Ca in foraminifera being affected by water mass,

diagenetic cycling close to the sediment water interface and salinity, requires more work to be done in constraining parameters using a multi-proxy approach. Ecological factors, defining which foraminifer calcifies where, both in the water column and in the sediment, require better constraints to make the foraminiferal trace and minor element proxies more robust and accurate. All these factors together urgently call for integration in a mechanistic approach. Modelling foraminiferal (micro) habitat preferences, life cycle and ontogenetic changes, impacts of live processes (Wolf-Gladrow et al., 1999), biomineralization (De Nooijer et al., 2014) in a common framework would give more insight into the potential inaccuracies in the proxies applied. In addition, it could also directly improve proxy-based reconstructions using a Bayesian approach in which the multi-elemental and multi-environmental impacts are actually improving the predictive power of proxies. The carbonate tests of foraminifera are in that sense ideal as the composition of these tests, both elemental and isotopic, is a carrier of a multitude of signals. This will require further controlled growth experiments, field calibrations, modelling studies and their application in relevant settings.

REFERENCES

Boyle, E. A.: Cadmium, zinc, copper, and barium in foraminifera tests, Earth Planet. Sci. Lett., 53(1), 11–35, 1981.

Van Dijk, I., Nooijer De, L. J. and Reichart, G. J.: Trends in element incorporation in hyaline and porcelaneous foraminifera as a function of pCO2, Biogeosciences, 14(3), 497–510, doi:10.5194/bg-14-497-2017, 2017.

IPCC: Working Group I Contribution to the IPCC Fifth Assessment Report, Climate Change 2013: The Physical Science Basis, IPCC, AR5 (March 2013), 2014, doi:10.1017/CBO9781107415324.Summary, 2013.

IPCC: IPCC Fourth Assessment Report (AR4), Ipcc, 1, 976, doi:ISSN: 02767783, 2007.

Jorissen, F. J., de Stigter, H. C. and Widmark, J. G. V: A conceptual model explaining benthic foraminiferal microhabitats, Mar. Micropaleontol., 26(1–4), 3–15, doi:10.1016/0377-8398(95)00047-X, 1995.

Keeling, C. D.: The Concentration and Isotopic Abundances of Carbon Dioxide in the Atmosphere, Tellus, 12(2), 200–203, doi:10.3402/tellusa.v12i2.9366, 1960.

Keul, N., Langer, G., Thoms, S., de Nooijer, L. J., Reichart, G.-J. and Bijma, J.: Exploring foraminiferal Sr/Ca as a new carbonate system proxy, Geochim. Cosmochim. Acta, 202, 374–386, 2017.

Koho, K. A., De Nooijer, L. J., Fontanier, C., Toyofuku, T., Oguri, K., Kitazato, H. and Reichart, G. J.: Benthic foraminiferal Mn/Ca ratios reflect microhabitat preferences, Biogeosciences, 14(12), 3067–3082, doi:10.5194/bg-14-3067-2017, 2017.

Lea, D. and Boyle, E.: Barium content of benthic foraminifera controlled by bottom-water composition, Nature, 338(6218), 751–753, doi:10.1038/338751a0, 1989.

Lea, D. W.: Elemental and Isotopic Proxies of Past Ocean Temperatures, in Treatise on Geochemistry: Second Edition, vol. 8, pp. 373–397., 2013.

Lea, D. W. and Spero, H. J.: Assessing the reliability of paleochemical tracers: Barium uptake in the shells of planktonic foraminifera, Paleoceanography, 9(3), 445–452, 1994.

Loeblich Jr., A. R. and Tappan, H.: Suprageneric Classification of the Foraminiferida (Protozoa), Micropaleon-tology, 30, 1–70, doi:10.2307/1485456, 1984.

Mackensen, A., Hubberten, H.-W., Bickert, T., Fischer, G. and Fütterer, D. K.: The $\delta^{13}C$ in benthic foraminiferal tests of Fontbotia wuellerstorfi (Schwager) relative to the $\delta^{13}C$ of dissolved inorganic carbon in southern ocean deep water: implications for glacial ocean circulation models, Paleoceanography, 8(5), 587–610, 1993.

McCrea, J. M.: On the isotopic chemistry of carbonates and a paleotemperature scale, J. Chem. Phys., 18(6), 849–857, 1950.

De Nooijer, L. J., Spero, H. J., Erez, J., Bijma, J. and Reichart, G. J.: Biomineralization in perforate foraminifera, Earth-Science Rev., 135, 48–58, doi:10.1016/j.earscirev.2014.03.013, 2014.

Nürnberg, D., Bijma, J. and Hemleben, C.: Assessing the reliability of magnesium in foraminiferal calcite as a proxy for water mass temperatures, Geochim. Cosmochim. Acta, 60(5), 803–814, doi:10.1016/0016-7037(95)00446-7, 1996.

Pawlowski, J., Holzmann, M., Berney, C., Fahrni, J., Gooday, A. J., Cedhagen, T., Habura, A. and Bowser, S. S.: The evolution of early Foraminifera., Proc. Natl. Acad. Sci. U. S. A., 100(20), 11494–8, doi:10.1073/pnas.2035132100, 2003.

Petit, J.-R., Jouzel, J., Raynaud, D., Barkov, N. I., Barnola, J.-M., Basile, I., Bender, M., Chappellaz, J., Davis, M., Delaygue, G. and others: Climate and atmospheric history of the past 420,000 years from the Vostok ice core, Antarctica, Nature, 399(6735), 429, 1999.

Rohling, E. J. and Bigg, G. R.: Paleosalinity and $\delta^{18}O$: a critical assessment, J. Geophys. Res. Ocean., 103(C1), 1307–1318, 1998.

Roij, L., Sluijs, A., Laks, J. J. and Reichart, G.-J.: Stable carbon isotope analyses of nanogram quantities of particulate organic carbon (pollen) with laser ablation nano combustion gas chromatography/ isotope ratio mass spectrometry, Rapid Commun. Mass Spectrom., 31(1), 47–58, 2017.

Russell, A. D., Hönisch, B., Spero, H. J. and Lea, D. W.: Effects of seawater carbonate ion concentration and temperature on shell U, Mg, and Sr in cultured planktonic foraminifera, Geochim. Cosmochim. Acta, 68(21), 4347–4361, 2004.

Sanyal, A., Hemming, N. G., Hanson, G. N. and Broecker, W. S.: Evidence for a higher pH in the glacial ocean from boron isotopes in foraminifera, Nature, 373(6511), 234, 1995.

Schmiedl, G., Mackensen, A. and Müller, P. J.: Recent benthic foraminifera from the eastern South Atlantic Ocean: dependence on food supply and water masses, Mar. Micropaleontol., 32(3), 249–287, 1997.

Wang, Y. and Van Cappellen, P.: A multicomponent reactive transport model of early diagenesis: Application to redox cycling in coastal marine sediments, Geochim. Cosmochim. Acta, 60(16), 2993–3014, doi:10.1016/0016-7037(96)00140-8, 1996.

Weldeab, S., Lea, D. W., Schneider, R. R. and Andersen, N.: 155,000 years of West African monsoon and ocean thermal evolution, Science (80-.)., 316(5829), 1303–1307, 2007.

Wit, J. C., De Nooijer, L. J., Wolthers, M. and Reichart, G. J.: A novel salinity proxy based on na incorporation into foraminiferal calcite, Biogeosciences, 10(10), 6375–6387, doi:10.5194/bg-10-6375-2013, 2013.

Wolf-Gladrow, D. A., Bijma, J. and Zeebe, R. E.: Model simulation of the carbonate chemistry in the microenvironment of symbiont bearing foraminifera, Mar. Chem., 64(3), 181–198, doi:10.1016/ S0304-4203(98)00074-7, 1999.

Zahn, R., Winn, K. and Sarnthein, M.: Benthic foraminiferal $\delta^{13}C$ and accumulation rates of organic carbon: Uvigerina peregrina group and Cibicidoides wuellerstorfi, Paleoceanography, 1(1), 27–42, 1986.

2

Molecular and isotopic composition of foraminiferal organic linings

Shauna Ní Fhlaithearta[a], Sander R. Ernst[a], Klaas G. J. Nierop[a], Gert J. de Lange[a], Gert-Jan Reichart[a,b]

[a] Department of Geosciences, Utrecht University, Utrecht, The Netherlands
[b] Alfred Wegener Institute for Polar and Marine Research, Biogeosciences, Bremerhaven, Germany

Marine Micropaleontology 102 (2013) 69-78
doi: 10.1016/j.marmicro.2013.06.004

ABSTRACT

Fossil remnants of benthic foraminifera consist of carbonate tests and their organic linings. The macromolecular and stable isotopic composition of these benthic foraminiferal organic linings was characterized to evaluate their potential use as paleoclimate proxies. Using Curie point pyrolysis–GC–MS (Py–GC–MS) we show that benthic foraminiferal organic linings consist of protein and polysaccharides, bound together in a complex macromolecular structure. Both chitin derivatives and traces of guaiacols and syringols, usually assigned to lignin, are found. Although the five species of benthic foraminifera all contain chitin derivatives and proteins, the relative contribution of these compounds tends to vary considerably. Oxygen stable isotopic analyses of the organic linings of the benthic foraminiferal species *Ammonia tepida* indicates that $\delta^{18}O_{OL}$ values are in line with fractionation between seawater and organic matter. In contrast a $\delta^{13}C$ deliberate tracer experiment showed that metabolic carbon is the main source for the carbon fixed in the organic lining. The different pathways of carbon and oxygen stable isotopes into the foraminiferal linings have important implications for future proxy development as they reflect different components of the environment compared to the carbonate bound stable isotopes. Still, the future application of benthic foraminiferal organic linings and their isotopic values critically relies on improvements in calibration and sample size required for isotopic analyses.

1 | INTRODUCTION

Since the 1970's foraminiferal tests have successfully been exploited in terms of their stable isotopic composition in order to reconstruct past climate conditions (Shackleton, 1974; Erez and Luz, 1983; Bemis et al., 1998). Oxygen isotopes measured on foraminiferal tests record changes in ice volume, seawater temperature and salinity, whereas the carbon isotopes provide information on carbon cycling. Over the last two decades the trace metal composition of foraminiferal tests has become an important extra indicator of past oceanic conditions (Lea, 1993; Rosenthal et al., 1997; Reichart et al., 2003; Elderfield et al., 2010). For example, the Mg–Ca ratio is used to reconstruct past temperatures and B–Ca ratios reveal past changes in seawater carbonate chemistry. Whereas the proxy potential of the inorganic part of foraminifer tests has thus been extensively explored (Lea, 1993; Rosenthal et al., 1997; Reichart et al., 2003; Elderfield et al., 2010), relatively few studies exist on the proxy potential of the organic component of foraminiferal tests.

The organic component of benthic foraminifera can be divided into two parts, the cytoplasm and the organic matrix of the test. The organic matrix can further be divided into two operationally defined components, (1) the soluble organic matrix and (2) the insoluble organic matrix (hereafter known as the organic lining (OL)) (Figure 1). While the cytoplasm degrades quickly upon death of the foraminifer, the soluble organic matrix and the OL remain intact (Stancliffe, 1989; Robbins and Brew, 1990). Studies of the soluble organic matrix show that it consists of proteins (Weiner and Erez, 1984; Robbins and Brew, 1990), while OLs are composed predominantly of polysaccharides with traces of proteins (Angell, 1967; Weiner and Erez, 1984), known collectively as 'glycosaminoglycans'. This compound is found in agglutinating, perforate and imperforate foraminifera (see Langer, 1992 and references therein). Most work on benthic foraminiferal OLs has focussed on the morphology of their remains in the fossil record (Stancliffe, 1989; Winchester-Seeto and Bell, 1999).

Benthic foraminiferal organic linings are often found preserved alongside pollen, spores and dinoflagellate cysts in palynological preparations, and at least partially maintain the internal test morphology of the original foraminifer (Figure 1). To date, the macromolecular composition of OLs has not been studied systematically. Knowing the composition of OLs yields insight into their function, structure and susceptibility to diagenesis. Furthermore, the macromolecular composition of OLs can be compared to other resistant-membrane bearing organisms (Van Bergen et al., 2004; De Leeuw et al., 2006; Versteegh et al., 2007; Verbruggen et al., 2010), as a tool to gain insight into any evolutionary linkages between their biochemical pathways. The susceptibility of OLs to diagenesis can be constrained by comparing the macromolecular composition of extant and fossil foraminiferal tests. Doing so sheds light on the molecular preservation potential of OLs and their applicability as a paleoceanographic proxy. Constraining the macromolecular composition is also a prerequisite for testing the application of OLs as carriers of oxygen and carbon stable isotopic signals and susceptibility to isotopic alteration.

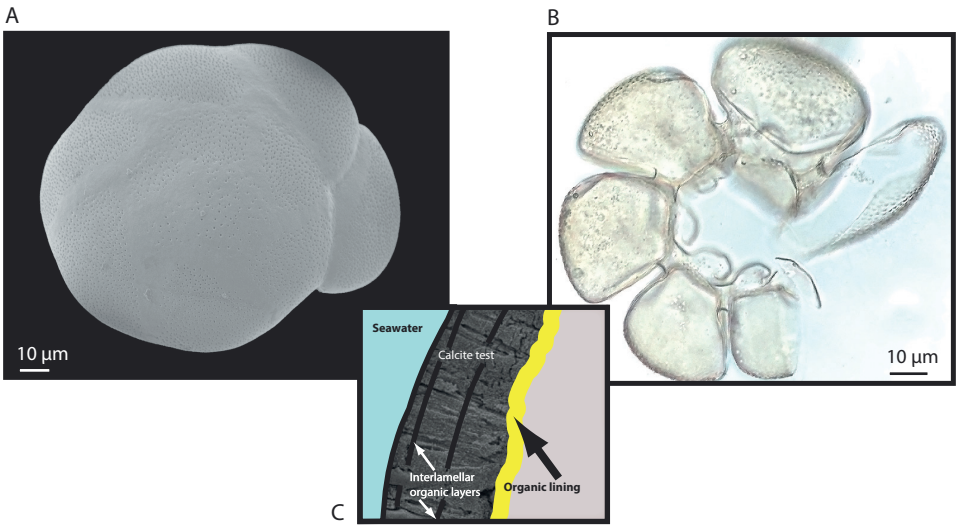

Figure 1 | Overview of organic lining structure in *Ammonia* sp. A. SEM image of *Ammonia* sp. B. Image of organic lining of *Ammonia* sp. C. Schematic cross section of *Ammonia* test (SEM courtesy of L. de Nooijer).

To date, carbon and oxygen isotope values of benthic foraminiferal OLs are unreported. Carbon and oxygen stable isotopes measured on decay-resistant organic matter are currently being developed for application in both marine (Sluijs et al., 2007) and lacustrine (Verbruggen et al., 2010) environments. In environments where carbonate is absent (due to calcite undersaturation), such information can provide insight into past environmental conditions. Whereas the oxygen stable isotopes of the organic matter can be related to the seawater the foraminifera grew in, carbon isotopes could reflect both food source and/or the isotopic values of seawater DIC. Additionally, by coupling oxygen isotope values from foraminiferal OLs and their carbonate tests, the first step could be taken towards the development of an independent proxy for past seawater $\delta^{18}O$ values.

In this study, the macromolecular and isotopic composition of foraminiferal OLs is constrained, giving insight into their potential as paleoceanographic proxies. The organic linings of four species of extant benthic foraminifer (*Ammonia* sp., *Sorites* sp., *Calcarina* sp., *Cycloclypeus* sp.) and one fossil foraminifer (*Amphistegina* sp.) are isolated and their macromolecular structure characterized using pyrolysis GC–MS. The organic test of *Gromia sphaerica*, a 'distant cousin' of foraminifera is also characterized, to investigate any biochemical evolutionary linkages and to cover the widest possible range in OL compositions. For the first time, carbon and oxygen isotopes are measured in isolated foraminiferal OLs and a carbon tracer study is carried out to unravel the influence of food source on the carbon isotopic composition of OLs.

2 | METHODS

2.1 | Qualitative survey of OL in benthic foraminifera

Cytoplasm-free individuals belonging to twenty-nine different benthic foraminiferal species (Table 1) were picked and placed in a solution of 0.1 M hydrochloric acid (HCl) to dissolve the calcitic test. The remaining organic lining was described based on completeness compared to the original test morphology. Although this approach is qualitative only, this comparison yields a first order overview of species that are potentially suited for an OL approach. Based on this first inventory species were selected for further investigation.

2.2 | Isolation of organic linings for pyrolysis GC–MS

Specimens of *Ammonia tepida* were picked from surface sediments collected at an intertidal flat of the Wadden Sea (near Den Oever, the Netherlands). Specimens of *Calcarina* sp. and *Cycloclypeus* sp. were recovered from a boxcore from a coastal shelf off East Kalimantan, Indonesia. Live *Sorites* sp. specimens were recovered by divers off the coast of Maratua, Indonesia.

Individuals of *G. sphaerica* were picked from the surface sediments of a multicore, recovered during the PASOM cruise (2009) in the Arabian Sea. Fossil *Amphistegina* specimens were Late Oligocene in age and recovered from the Aquitaine Basin in Bordeaux, France. Individuals of *Ammonia* sp., *Calcarina* sp., *Sorites* sp., *Cycloclypeus* sp. and *Amphistegina* sp. were picked after visually inspecting their test. All selected tests were clean and free of infill. The samples were subsequently rinsed in UHQ water and placed in a sonic bath for 20 s to remove small particles possibly still adhering to the test. This was repeated five times. Isolation of OLs was achieved by placing the foraminifera into dialysis tubing (CelluSEP T1 Dialysis Membrane, MW cutoff 3500), which was placed in a cylinder containing UHQ water and ion exchange resin (Dowex cation-exchange resin 50 × 8, mesh 50–100) (Gotliv et al., 2003). The cylinders containing both sample and resin were placed on a roller bench and regularly flushed with new UHQ water until the carbonate test was fully removed. The remaining OL was extracted with an ultrasonic needle using organic solvents, methanol (MeOH) and dichloromethane (DCM), following a sonification/centrifugation scheme of 1 × 1:1 MeOH:DCM and 4 × 1:9 MeOH:DCM, after which the sample was dried under a stream of N_2. For *G. sphaerica*, the cell was pierced and the contents removed under a stream of UHQ water. After visual inspection, the remaining membrane was extracted following the same scheme as described above for the foraminifera.

2.3 | Pyrolysis GC–MS

The isolated and extracted OL was pressed onto a flattened ferromagnetic wire with a Curie point temperature of 610 °C. The wire was subsequently inserted into a glass liner, which was placed into a RF coil in a He flow and heated for 10 s at its Curie point. The Curie point pyrolyzer (FOM-5XL) was coupled to a gas chromatograph (Thermo Finnigan Trace GC Ultra),

which was interfaced to a mass spectrometer (Thermo Finnigan Trace DSQ). Separation of the compounds released during pyrolysis was achieved in a silica capillary column (inner diameter 0.32 mm) coated with a 0.40 µm film (Varian, CP-Sil-5CB). The GC was programmed to change temperature from 40 °C to 230 °C at a rate of 3 °C/min and to 300 °C at a rate of 20 °C/min, followed by a 15 min isothermal stage. The MS was in full scan mode (*m/z* 50–800,2.5 scans/s, 70 eV electron energy, 250 °C source temperature). Blanks and standard (PE) were run prior to each sample series. Identification of the macromolecular structure was based on mass spectra and retention times from literature (Pouwels et al., 1987; Pouwels and Boon, 1990; Stankiewicz et al., 1996; Van Heemst et al., 1996; Nierop et al., 2001; NIST Library).

For the *Gromia* sample pyrolysis was carried out on a Horizon Instruments Curie-Point pyrolyser. Samples were heated for 5 s at 590 °C. The pyrolysis unit was connected to a Carlo Erba gas chromatograph GC8000 and the products were separated by a fused silica column (Varian Factor Four, 25 m, 0.32 mm i.d.) coated with VF-1 ms (film thickness 0.40 µm). Helium was used as carrier gas. The oven was initially kept at 40 °C for 1 min, next it was heated at a rate of 7 °C/min to 320 °C and maintained at that temperature for 15 min. The column was coupled to a Fisons MD800 mass spectrometer (mass range *m/z* 45–600, ionization energy 70 eV, cycle time 1 s).

2.4 | $\delta^{13}C$ labeling experiment

A culture of the micro-algae *Dunaliella salina* ('Label') was grown in filtered (0.2 µm) seawater amended with 99% ^{13}C labeled sodium bicarbonate (Cambridge Isotope Laboratories) (see Moodley et al., 2000). A further culture of *D. salina* ('Control') was grown in unaltered and filtered seawater. After two weeks both *D. salina* cultures were harvested by filtration, rinsed and centrifuged in UHQ water multiple times and dried in an oven. Subsequently, four bottles containing living stocks of *A. tepida* were spiked with the fluorescent dye calcein (Bis [N,N bis(carboxymethyl)aminomethyl]-fluorescein)).

Calcein is incorporated into carbonate during biomineralization, allowing the recognition of chambers grown when viewing under epifluorescence (470 nm excitation, 509 nm emission). The 'labeled' algae, were added to two bottles, 'Label A' and 'Label B', respectively, while unlabeled algae were added to the remaining two bottles, 'Control A' and 'Control B'.

After 6 weeks, the foraminifera in all bottles were harvested, thoroughly rinsed in filtered (0.2 µm) seawater and brushed clean of any adhering particles. All foraminiferal stocks were systematically inspected under an epifluorescent microscope, allowing the selection of tests that had grown during the experiment. Organic linings were isolated by dissolving the carbonate test in 0.1 M hydrochloric acid, extracting the soluble organic compounds using organic solvents (based on the same sonification/centrifugation scheme used prior to pyrolysis), and drying them under a stream of N_2.

Table 1 | Survey of various benthic foraminifera species with a description of their organic lining remains after decalcification.

	Visible organic lining[1]	Physical description of organic lining[2]
Rotaliida		
Ammonia tepida	Yes	Complete
Amphicoryna scalaris	No/?	–
Bolivina lata	Yes	Thin, only single fragment of lining
Bolivina striatula/ seminuda	Yes	Thin, only single fragment of lining
Bulimida marginata	Yes	Thin, only single fragment of lining
Bulimina striata	Yes	Thin, only single fragment of lining
Calcarina sp.	Yes	Thick, fairly complete series of chamber linings
Cassidulina laevigata	No	–
Chilostomella sp.	No/?	–
Cibicides kullenbergi/ pachyderma?	Yes	Thick to thin, single and series of chamber linings
Cibicides lobatulus	Yes	Thick, fairly complete series of chamber linings
Cibicides ungerianus?	Yes	Thick, only single chamber linings
Cycloclypeus sp.	Yes	Thick, fairly complete series of chamber linings
Elphidium crispum	No	–
Globobulimina ssp.	No/?	–
Gyroidina altiformis	Yes	Thick, fairly complete series of chamber linings
Gyroidina orbicularis	Yes	Thick, fairly complete series of chamber linings
Hoeglundina elegans	Yes	Thin, only single fragment linings
Melonis barleenum	Yes	Thin, single fragments/chamber and series of chamber linings
Planulina ariminensi	Yes	Thick, fairly complete series of chamber linings
Sphaeroidina bulloides	Yes	Thin, single fragments/chamber and series of chamber linings
Trifarina sp.	No/?	–
Uvigerina mediterranea	Yes	Thin, single fragments/chamber and series of chamber linings
Uvigerina peregrina	Yes	–
Miliolida		
Pyrgo	Yes	Thick, fairly complete series of chamber linings
Sorites sp.	Yes	Thick, fairly complete series of chamber linings
Spiroloculina	Yes	Thick, fairly complete series of chamber linings
Triloculina	Yes	Thin, fairly complete series of chamber linings

[1] Based on viewing under a stereo microscope.

[2] The description 'Thin' or 'Thick' is a relative term based on visual inspection only.

2.5 | Stable isotopes

Stable oxygen isotopes of the organic linings ($\delta^{18}O_{OL}$) were measured on an elemental analyzer (TC-EA; Thermo Finnigan) coupled to an isotope ratio mass spectrometer (IRMS; Thermo Finnigan Delta^{plus}).

Each sample consisted of multiple individuals; for *Ammonia* sp., a minimum of 50 individuals was required to reach the minimum required sample weight. Approximately > 50 µg are required for reliable $\delta^{18}O$ measurements. This conforms to Verbruggen et al. (2010) who found similar values using chironomid head capsules. Cellulose standard (IAEA-C3), benzoic acid standard (HEKAtech, batch number 33822501) and two potassium nitrate standards (IAEA-NO-3 and USGS-32) were used for standardization. The $\delta^{18}O$ data for organic linings are reported in per mille (‰) relative to V-SMOW (Vienna Standard Mean Ocean Water). The standard deviation for $\delta^{18}O_{OL}$ was 0.3 ‰. The $\delta^{13}C$ of the organic linings ($\delta^{13}C_{OL}$) was measured on a CNS analyser (Carbo Erba NA1500) coupled online to an IRMS (Thermo Finigan Delta^{plus}) and are reported relative to V-PDB (Vienna Pee Dee Belemnite). Approximately > 20 µg were required for reliable $\delta^{13}C$ measurements. Standard deviation of $\delta^{13}C_{OL}$ was better than 0.1 ‰. The $\delta^{13}C$ and $\delta^{18}O$ of the carbonate was measured using a Kiel-type (III) automated carbonate preparation device coupled online to an isotope ratio mass spectrometer (Thermo Finnigan 253). Ratios are reported relative to the V-PDB scale and calibration was achieved using an international (NBS-19) and in-house standard (Naxos). The standard deviations are 0.03 ‰ for $\delta^{13}C$ and 0.08 ‰ for $\delta^{18}O$. For the $\delta^{13}C$ labeling experiment, the carbon isotopic composition of the organic linings ($\delta^{13}C_{OL}$) was determined using a Fisons CN analyzer coupled on line, via a Finnigan conflo 2 interface, with a Finnigan Delta S mass-spectrometer. Carbon isotope ratios are expressed in ‰ relative to V-PDB. Reproducibility of $\delta^{13}C_{OL}$ was better than 0.1 ‰. The carbon isotopic composition of the carbonate ($\delta^{13}C_{carb}$) from the labeling experiments was determined with a Finnigan MAT252 equipped with a Kiel (II) automated carbonate preparation device at the Free University Amsterdam. The long-term external reproducibility of the $\delta^{13}C_{carb}$ measurements, based on repeated analyses of an in-house standard, is ± 0.05 ‰.

3 | RESULTS

3.1 | Qualitative survey of OL in benthic foraminifera

The survey shows that after dissolving the carbonate test of various benthic foraminiferal species, organic lining remained in almost all cases (Table 1). The notable exceptions were the *Amphicoryna scalaris*, *Chilostomella* sp., *Cassidulina laevigata*, *Globobulumina* spp., *Elphidium crispum* and *Trifarina* sp. Inspecting the isolated linings with a binocular showed differences in both completeness relative to the original morphology and robustness of the general appearance. This is qualitatively indicated in Table 1. The organic lining of *Ammonia* sp. looked

especially robust (Figure 1B) and this species was selected as the target species for the $\delta^{13}C$ labeling experiment.

3.2 | Pyrolysis products

The pyrolysis products of extant benthic foraminifera comprise a variety of compounds classes, including aromatics, non-aromatics and aromatic hetero-compounds (Figure 2A–D). The pyrolysis products can be divided into two major groups: proteins and polysaccharides, along with several minor compound groups (Table 2).

Common to all four benthic foraminiferal species are protein derivatives associated with pyrroles, indoles and benzenes. Pyrolysates of all species comprise phenol, methylpyrroles, pyridine, pyrrole, methylbenzene, ethylbenzene and styrene. Present in *Calcarina* sp., *Sorites* sp. and *Cycloclypeus* sp. pyrolysates are methylpyridine, C3-benzenes, 1-methyl-4-ethenylbenzene, indene, 2-methylphenol, 3- and 4-methylphenol, 2-methylindene, 3-methylindole, diketodipyrrole, while benzyl cyanide and acetamide were present in *Ammonia* sp., *Calcarina* sp., and *Sorites* sp.

Polysaccharide derived pyrolysis products comprised cyclic monosaccharides and furaldehydes. Pyrolysates of all species comprised (5H)-furan-2-one, 3-furaldehyde and 5-methyl-2-furaldehyde.

Polysaccharides present in *Ammonia* sp., *Calcarina* sp., and *Sorites* sp. were reflected by pyrolysis products (2H)-furan-3-one; 4-hydroxy-5, 6-dihydro-(2H)-pyran-2-one, levoglucosenone, while benzofuran was present in *Calcarina* sp., *Sorites* sp. and *Cycloclypeus* sp. The dominant peaks in the pyrolysate of *Ammonia* sp. contained a trio of polysaccharide isomers (levogalactosan, levomannosan and levoglucosan) of which levogalactosan was also found in *Cycloclypeus* sp. and levoglucosan also found in *Sorites* sp. pyrolysates. The pyrolysate of *Ammonia* sp. further contained dianhydrorhamnose isomer and the three isomers 1,4:3,6-anhydro-a-D-galactopyranose, 1,4:3,6-anhydro-a-D-mannopyranose and 1,4:3,6-anhydro-a-D-glucopyranose, which were absent from all other species' pyrolysates (Figure 2A inset). The identification of 1,4:3,6-anhydro-a-D-glucopyranose was based on mass spectral comparison published in Pouwels et al., (1989), the other two compounds had very similar mass spectra and we tentatively assigned them to the galactose and mannose based isomers similar to the three anhydrosugars levogalactosan, levomannosan and levoglucosan.

Minor compound groups consisted of polycyclic aromatic hydrocarbons n-alkanes/enes, and several methoxyphenols in trace amounts. *Calcarin* sp. *a*, *Sorites* sp. and *Cycloclypeus* sp. contain naphthalene, 1-methylnaphthalene, 2-(1-methylethyl)-naphthalene, fluorene and anthracene. Traces of pyrolysis products associated with lignin were recognized in the OLs isolated from three benthic foraminiferal species. Isomers eugenol, *cis*-isoeugenol and *trans*-isoeugenol were identified in *Ammonia* sp., *Sorites* sp. and *Cycloclypeus* sp., while 4-ethylsyringol was identified in *Calcarina* sp. and *Cycloclypeus* sp. and 4-methylguaiacol in *Sorites* sp.

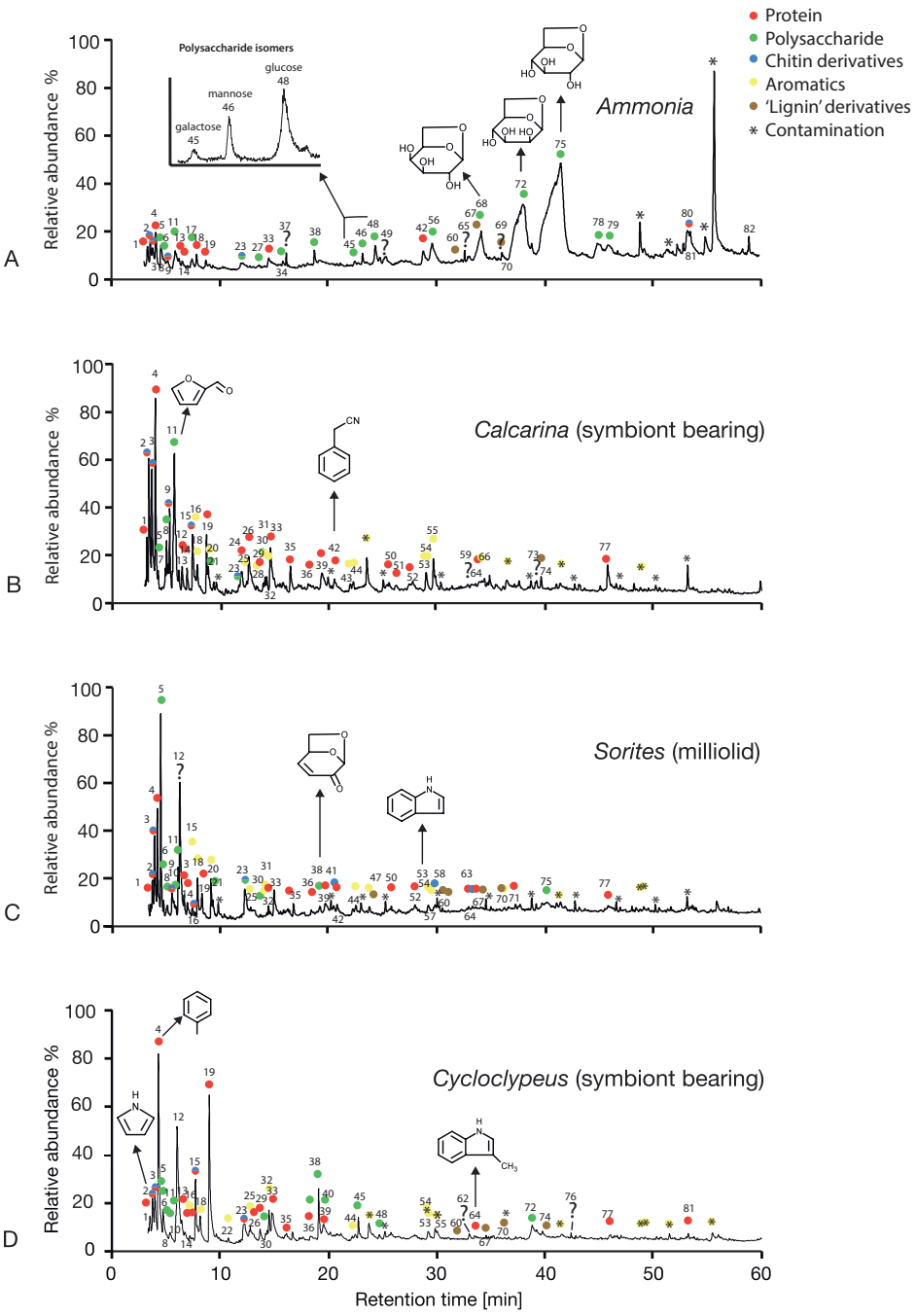

Figure 2 | Total ion current traces obtained by Curie-point pyrolysis-gas chromatography mass spectrometric analysis of foraminiferal organic linings. A. *Ammonia* sp. Inset: Total ion current traces for polysaccharide isomers galactose, mannose, glucose. B. *Calcarina* sp., C. *Sorites* sp., D. *Cycloclypeus* sp. Numbers indicate components as listed in Table 2.

Table 2 | List of pyrolysis products derived from benthic foraminifera *Ammonia* sp., *Calcarina* sp., *Sorites* sp. and *Cycloclypeus* sp.

Peak	MS characteristics[1]	Name	Origin[2]	*Ammonia* sp.	*Calcarina* sp.	*Sorites* sp.	*Cycloclypeus* sp.
1	**81**, 80	N-methylpyrrole	Pr	x	x	x	x
2	**79**, 52	Pyridine	Pr	x	x	x	x
3	**67**	Pyrrole	Pr	x	x	x	x
4	92, **91**	Toluene (methylbenzene)	Pr	x	x	x	x
5	84, 55	(5H)-furan-2-one	Ps	x	x	x	x
6	**84**, 54, 55	(2H)-furan-3-one	Ps	x		x	x
7	**70**, 55	?			x		
8	96, **95**	3-Furaldehyde	Ps	x	x	x	x
9	**59**	Acetamide	Ch, Pr	x	x	x	
10	**82**	3-Methylfuran				x	x
11	**96**, 95	2-Furaldehyde	Ps	x	x	x	x
12	**108**, 107	Methylphenol			x	x	x
13	81, **80**	2-Methylpyrrole	Pr	x	x	x	x
14	81,**80**	3-Methylpyrrole	Pr	x	x	x	x
15	**93**, 66	Methylpyridine	Pr		x	x	x
16	106, **91**	Ethylbenzene	Pr		x	x	x
17	**98**, 97, 81	2-(Hydroxymethyl)furan	Ps	x			
18	106, **91**	Ethylbenzene	Pr	x	x	x	x
19	**104**, 103, 78, 51	Styrene	Pr	x	x	x	x
20	106, **91**, 77, 60	1, 2-Dimethylbenzene			x	x	
21	**96**, 67, 53	2-Methyl-2-cyclopenten-1-one	Ps		x	x	
22	120, **105**	Ethylmethylbenzene					x
23	**110**, 109, 81, 53	5-Methyl-2-furaldehyde	Ps, Ch	x	x	x	x

Table 2 | *Continued*

Peak	MS characteristics[1]	Name	Origin[2]	*Ammonia* sp.	*Calcarina* sp.	*Sorites* sp.	*Cycloclypeus* sp.
24	120, **91**, 65	C3 benzene	Pr		x		
25	120, **105**, 77	C3 benzene (1-methyl-3-ethylbenzene)	Pr		x	x	x
26	**103**, 76	Benzonitrile			x		x
27	**114**, 58	4-Hydroxy-5,6-dihydro-(2H)-pyran-2-one	Ps	x		x	x
28	120, **105**	Ethylmethylbenzene	Pr		x		
29	118, 117, **103**	a-Methylstyrene	Pr		x		x
30	**118**, 89	Benzofuran			x	x	x
31	120, **105**, 91, 77	C3 benzene	Pr		x	x	
32	**118**, 117, 115, 91	1-Methyl-4-ethenylbenzene			x	x	x
33	**94**, 66	Phenol	Pr	x	x	x	x
34	**128**, 113	Dianhydrorhamnose isomer	Ps	x			
35	**116**, 115, 57	Indene			x	x	x
36	**108**, 107, 79	2-Methylphenol			x	x	x
37	136, 121, 107, 94, 93, **68**, 67	?		x			
38	**98**, 97, 96, 68, 53	Levoglucosenone	Ps	x		x	x
39	**108**, 107, 77	3- and 4-Methylphenol			x	x	x
40	132, **131**	?					x
41	137, **95**	3-Acetoxypyridine	Ch			x	
42	**117**, 116, 90, 89	Ethylcyanobenzene	Pr	x	x	x	
43	**130**, 129, 115	Methylindene	Pr		x		
44	**130**, 129, 115	Methylindene	Pr		x	x	x
45	**69**, 57	1,4:3,6-Anhydro-a-D-galactopyranose?	Ps	x			x
46	**69**, 57	1,4:3,6-Anhydro-a-D-mannopyranose ?	Ps	x			

Table 2 | *Continued*

Peak	MS characteristics[1]	Name	Origin[2]	*Ammonia* sp.	*Calcarina* sp.	*Sorites* sp.	*Cycloclypeus* sp.
◆	**128**	Naphthalene	PAH		x	x	x
47	**138**, 123	4-Methylguaiacol (?)	Lg			x	
48	**69**, 57	1,4:3,6-Anhydro-a-D-glucopyranose	Ps	x			x
49	**135**, 56	Benzothiozole ??		x			
50	131, **91**, 65	Propylcyanobenzene	Pr		x	x	
51	129	Quinoline ?	Pr		x		
52	**129**	Iso-quinoline ?	Pr		x	x	
53	**117**, 90, 89	Indole	Pr		x	x	x
54	**142**, 141	1-Methylnaphthalene	Pr		x	x	x
55	**142**, 141	1-Methylnaphthalene	Pr		x		x
56	144, **97**, 87, 69	1,4-Dideoxy-$_D$-glycero-hex-1-enpyranos-3-ulose ?	Ps	x			
57	139, **97**, 69	3-Acetamido-5-methylfuran	Ch			x	
58	**150**, 135	4-Vinylguaiacol	Lg			x	
59	**154**, 105	?			x		
60	**164**	Eugenol? (trace)	Lg	x		x	x
61	**92**, 91	C7 alkylbenzene	Pr				
62	**154**	?					x
63	151, **109**, 80	N-hydroxyphenylacetamide ?	Ch, Pr			x	
64	131, **130**	3-Methylindole	Pr		x	x	x
65	216, 125, 117, **116**, 86, 70	?		x			
66	**91**	Alkylbenzene	Pr			x	
67	**164**	Cis-Isoeugenol (trace)	Lg	x			x
68	73, **60**, 57	Levogalactosan	Ps	x			

Table 2 | *Continued*

Peak	MS characteristics[1]	Name	Origin[2]	*Ammonia* sp.	*Calcarina* sp.	*Sorites* sp.	*Cycloclypeus* sp.
69	176, **161**	C3-benzothiophene ??		x			
70	**164**	Trans-isoeugenol?	Lg	x		x	x
◆	**155**, 154	2-(1-Methylethyl)-naphthalene (?)	Pr		x	x	x
71	**92**, 91	Alkylbenzene	Pr			x	
72	73, **60**, 57	Levomannosan	Ps	x			x
73	182, **167**, 152, 144, 104,115, 116, 69, 55, 83				x		
74	182, **167**	4-Ethylsyringol ? (trace)	Lg		x		x
75	73, **60**, 57	Levoglucosan	Ps	x		x	
◆	**166**, 165	Fluorene	PAH		x	x	x
76	**71**	?					x
77	**186**, 93	Diketodipyrrole ?	Pr		x	x	x
78	**73**, 69	Ps ?	Ps?	x			
79	73, 70, **69**	Ps ?	Ps?	x			
◆	**178**	Anthracene	PAH		x	x	x
◆	**178**	Phenanthrene	PAH			x	x
◆	**204**, 203, 202, 101	Aromatic ?					x
80	194, 154, **70**	2,5-Diketopiperazine der.	Pr	x			x
◆	**204**, 203, 202, 101	Aromatic ?	PAH				x
81	204, 114, 101, **59**, 57	1,6-Anhydro-2-acetamido-2-deoxyglucose	Ch	x			
82	113, **100**, 57	?		x			

◆ Contamination.

[1] Fragment ions in bold indicate the base peak. M/z values after base peak are in descending order of relative abundance.

[2] Origin of macromolecules — Pr —protein, Ps — polysaccharide, Ch — chitin, PAH — polycyclic aromatic hydrocarbon, Lg — lignin.

Gromia lining pyrolysis products consisted exclusively of protein-derived compounds, of which 20 were previously described as pyrolysis products of foraminiferal linings (see numbering in Figure 3), although the trace of acetamide could also be related to chitin (Table 2). The protein-derived compounds are dominated by pyrroles and diketopiperazines (Table 2).

3.3 | Stable carbon and oxygen isotopes

The stable isotopic (^{13}C and ^{18}O) composition of the organic lining and carbonate test were determined for specimens of *Ammonia* sp. Additional measurements were carried out for *Heterostegina* sp. for $\delta^{18}O_{OL}$. For *Ammonia* sp. the $\delta^{13}C_{OL}$ was -17.4 ‰ (with a C content of 42.9%) and the $\delta^{18}O_{OL}$ was 20.2 ‰ while test carbonate had a $\delta^{13}C_{CARB}$ of -4.89 ‰ and a $\delta^{18}O_{CARB}$ of 28.7 ‰ (V-SMOW, -2.1 V-PDB) (Figures 4 and 6). Additional measurements on the $\delta^{18}O$ of *Heterostegina* sp. linings yielded a $\delta^{18}O_{OL}$ value of 19.7 ‰ (V-SMOW).

3.4 | Labeling experiment

Using 99 % labeled DIC, algae were grown with an enrichment of $\delta^{13}C$ 9677 ‰. In experiment 'Label A' this enrichment was measured, in decreasing order, into the lining (4787 ‰), seawater (2427 ‰) and carbonate (1098 ‰). In experiment 'Label B', using the same labeled biomass, the lining (1981 ‰) and seawater (1980 ‰) were both enriched to the same degree and the carbonate less so (1002 ‰).

In the two control experiments 'Control A' and 'Control B' seawater $\delta^{13}C$ values were -1.99 and -1.53, respectively. Control organic lining values were $\delta^{13}C_{OL}$ -37.64 (V-PDB), based on a single measurement. Due to limited sample size it was not possible to measure carbonate produced during the control experiment.

4 | DISCUSSION

4.1 | Differences in organic linings between benthic foraminiferal species

It is likely that all benthic and planktonic foraminifera produce organic linings to some degree (Hemleben et al., 1977, 1986). Still, not all species, upon dissolution of their carbonate test, left a visible lining. Either the lining was not robust enough to survive this isolation and disintegrated, or it dissolved as a result of the acid leach used. Although agglutinated foraminifera most likely contain very robust OLs, we omitted them from this study due to methodological difficulties associated with their isolation. Most of the species studied here left visible organic linings upon dissolving their test. Of the species with no visible organic lining, several were deep infaunal species with comparatively thin tests. This would suggest some sort of mechanistic link between test wall thickness and organic lining robustness. Such a mechanism may suggest a link with the Mg binding capacity of some foraminiferal organics (Erez, 2003). Studies show that removal of dissolved Mg from the foraminiferal cytoplasm increased carbonate saturation state, which

Table 3 | List of pyrolysis products derived from *Gromia*.

Peak*	MS characteristics[1]	Name	Origin[2]
1	**81**, 80	N-methylpyrrole	Pr
2	**79**, 52	Pyridine	Pr
3	67	Pyrrole	Pr
4	92, **91**	Toluene (methylbenzene)	Pr
15	**93**, 66	Methylpyridine	Pr
9	**59**	Acetamide	Ch, Pr
13	81, **80**	2-Methylpyrrole	Pr
14	81, **80**	3-Methylpyrrole	Pr
20	106, **91**, 77, 60	1, 2-Dimethylbenzene	
19	**104**, 103, 78, 51	Styrene	Pr
A	95, 94, **80**	Ethylpyrrole + dimethylpyrrole	Pr
B	106, 105, **77**, 51	Benzaldehyde	?
26	**103**, 76	Benzonitrile	
33	**94**, 66	Phenol	Pr
C	109, **94**, 67	C3-pyrrole	Pr
36	**108**, 107, 79	2-Methylphenol	Pr
39	**108**, 107, 77	3- and 4-Methylphenol	Pr
42	**117**, 116, 90, 89	Ethylcyanobenzene	Pr
D	**99**, 56	2,5-Pyrrolidinedione (?)	Pr
?	125, 97, **59**	same as no. 21 Stankiewicz et al. (1996)	
50	131, **91**, 65	Propylcyanobenzene	Pr
E	**129**, 128, 103, 102, 76	Propenecyanobenzene	Pr
53	117, 90, 89	Indole?	Pr
F	138, 110, **56**	Trimethylpyrimidone (?)	Pr?
64	131, **130**	1H-indole, 3-methyl-	Pr
G	147, 104, 76	Isoindole-1,3(2H)-dione	Pr
H	187, 159, **117**, 90, 89	C6-cyanobenzene ?Pr	
77	186, 93	Diketodipyrrole ?	Pr
I	113	Pyrrolidindione-derivative?	Pr?
J	154, 125, 72, 70	2,5-Diketopiperazine der.	Pr
K	154, 125, 70	2,5-Diketopiperazine der.	Pr
L	154, **84**, 70	2,5-Diketopiperazine der.	Pr
80	194, 154, **70**	2,5-Diketopiperazine der.	Pr
M	244, 153, **125**, 91, 70	3-Benzylhexahydropyrrolo[1,2-a] pyrazine-1,4-dione	Pr
N	244, 153, **125**, 91, 70	3-Benzylhexahydropyrrolo[1,2-a] pyrazine-1,4-dione (isomer)	Pr

* Numbers refer to components also found in Foraminifera and letters to components found only in the *Gromia* sample.

[1] Fragment ions in bold indicate the base peak. *M/z* values after base peak are in descending order of relative abundance.

[2] Origin of macromolecules — Pr —protein, Ps — polysaccharide, Ch — chitin, PAH — polycyclic aromatic hydrocarbon, Lg — lignin.

is a key requirement to build test carbonate (Bentov and Erez, 2005). Thicker tests would thus require more Mg binding capacity, resulting in more robust organic linings. At the same time the Mg binding capacity of these linings would reduce the amount of Mg incorporated into the carbonate, explaining the low D_{Mg} values in foraminifera. *Ammonia* sp., characterized by very robust linings, indeed has very low values of D_{Mg} (Raitzsch et al., 2009; Dissard et al., 2010; Toyofuku et al., 2011). Milliolids also have robust linings but a rather high D_{Mg} (Toyofuku et al., 2000). By implication, the binding of Mg to organic matter alone cannot explain the removal of Mg from protoplasm, as suggested by Erez (2003).

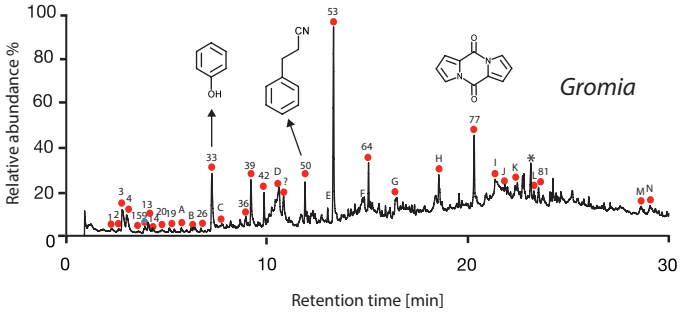

Figure 3 | Total ion current traces obtained by Curie-point pyrolysis–gas chromatography mass spectrometric analysis of a *Gromia sphaerica* test. Numbers indicate components as listed in Tables 2 & 3 and letters indicate components exclusive to *G. sphaerica* and listed in Table 3.

4.2 | Pyrolysis products

Two features dominate the pyrolysis results from foraminiferal organic linings: first, foraminiferal linings are composed predominantly of a mix of polysaccharides and proteins, and second, there is a distinct difference in compound composition and abundance between *Ammonia* sp. and *Calcarina* sp., *Cycloclypeus* sp. and *Sorites* sp. Based on the markers of a variety of different sugars, i.e. markers of galactose, mannose, glucose, rhamnose and the pentose related 4-hydroxy-5,6-dihydro-(2H)- pyran-2-one, the polysaccharide fraction of the various foraminiferal organic linings comprises a complex mixture which cannot be attributed to a well-defined carbohydrates such as cellulose or chitin.

Early studies repeatedly refer to the organic linings of foraminifera and the test structure of agglutinating foraminifera as chitinous or pseudochitin (Loeblich and Tappan, 1964; Banner and Williams, 1973). Although the organic remains of protists are sometimes also referred to as tectin, this merely implies a non-specific mixture of sugars and proteins and not a structural or compositional definition (Hedley, 1963). Our results show that foraminiferal organic linings, while certainly sharing some pyrolysis products considered chitin markers (Stankiewicz et al., 1996), are not made of chitin, or to a minor extent at best. This rather agrees with an earlier

assertion for agglutinating foraminifera using histochemical staining methods (Hedley, 1963; Angell, 1967; Schwab and Plapp, 1983).

The foraminiferal species looked at in this study use two different biomineralization pathways to produce their carbonate test. *Ammonia* sp., *Calcarina* sp. and *Cycloclypeus* sp. belong to the order of Rotaliida and produce hyaline tests, while *Sorites* sp. belongs to the order of Miliolida and produces a porcelaneous test (Hottinger, 2000; Pawlowski et al., 2003). While molecular and fossil data support an earlier divergence for multilocular milliolids compared to rotaliids (Pawlowski et al., 2003), no major differences were observed in macromolecular composition between the organic linings of the two types. This may suggest that the biosynthesis of these linings evolved prior to the separation of the two lineages. The earliest foraminiferal assemblages comprise agglutinating benthic taxa, thought to originate from an organic-walled ancestor (Pawlowski et al., 2003). Unfortunately, it was not possible to characterize the macromolecular composition of agglutinating foraminifera in this study, due to technical issues associated with the isolation of their organic envelope.

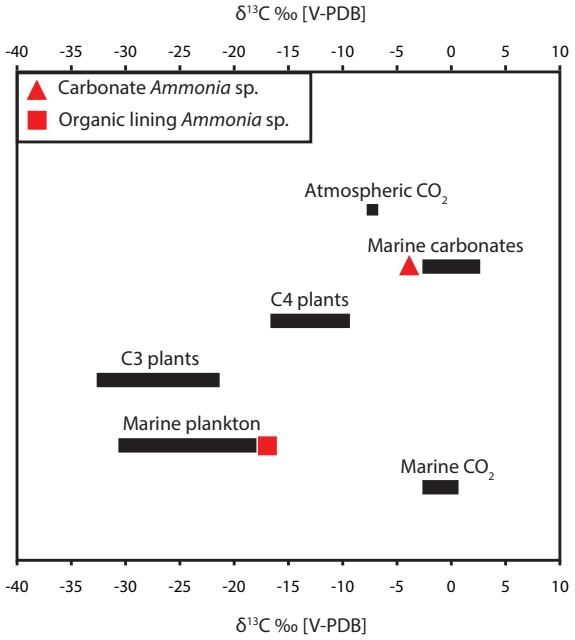

Figure 4 | Natural variation in $\delta^{13}C$ (black bars) including data from isolated *Ammonia tepida* organic linings (red square) and *A. tepida* carbonate test (red triangle), (amended from Zeebe and Wolf-Gladrow, 2005).

Gromia (organic walled rhizarian protists) are considered living relatives of Foraminifera. In fact, RNA phylogenies show them to be related to predecessors of thecate and unilocular

foraminifera, which evolved earlier than the fossil biomineralizing forms (Berney and Pawlowski, 2003; Longet et al., 2003). As such, they present a glimpse into the relatively poorly constrained evolution of non-fossilizing foraminifera and more specifically, the evolution of decay resistant macromolecules. The *G. sphaerica* theca studied here have a distinctly different macromolecular composition than the organic lining of the calcareous foraminifera. Their organic envelope is almost exclusively dominated by protein compounds (Figure 3), in agreement with a previous histochemical study by Hedley (1962). While other biological traits, such as the ability to denitrify, may be shared (Piña-Ochoa et al., 2010) between foraminifera and *gromia*, they clearly use a distinct biochemical pathway for the synthesis of their organic envelope. This does not necessarily undermine the evolutionary links between foraminifera and *gromia*, as it is not uncommon for foraminifera to display 'evolutionary plasticity' (Pawlowski et al., 2003) in morphotypes and trophic strategies, which may be true as well for the biochemical pathways required for organic lining synthesis.

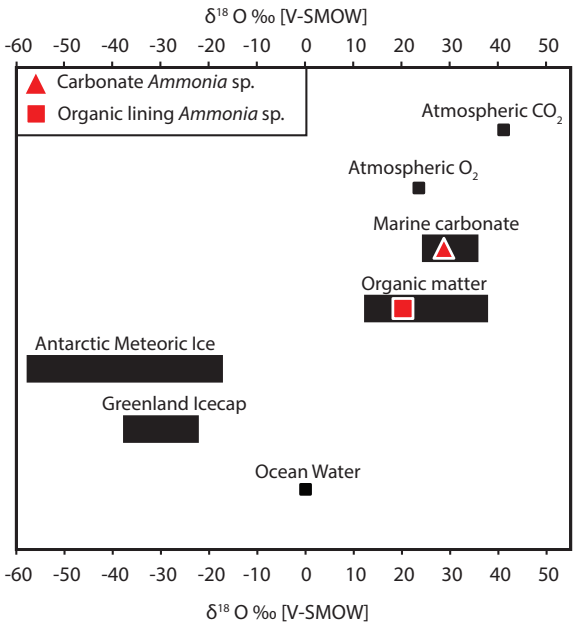

Figure 5 | Natural variation in $\delta^{18}O$ (black bars) including data from isolated *Ammonia tepida* organic linings (red square) and *A. tepida* carbonate test (red triangle), (amended from Zeebe and Wolf-Gladrow, 2005).

Since foraminiferal organic linings play a major role in foraminiferal biomineralization (Langer, 1992; Erez, 2003), their composition must have evolved in parallel with foraminiferal calcification. Indeed, a link between organic linings and foraminiferal biomineralization is suggested by Toler and Hallock (1997), who show that stressed *Amphistegina* populations with

a damaged cytoplasm have less organic matrix and linings, leading to reduced tensile strength and increased test breakages.

Somewhat surprisingly, guaiacol and syringol based pyrolysis products commonly assigned to lignin were identified for some of the linings. Generally, lignin is associated with higher terrestrial plants, however, Martone et al., (2009) found red algae to contain lignin. This led Popper and Tuohy (2010) to suggest several evolutionary scenarios explaining how this may have occurred. Given the small traces of guaiacols and syringols and the small number of these pyrolysis products identified in each pyrolysate, they represent both quantitatively and compositionally a kind of 'immature' or pseudolignin.

Measurements on fossil *Amphistegina* sp. (Late Oligocene, Aquitaine Basin, France) show that the levoglucosanone peak is still by far the largest pyrolysis product (data not shown). In addition 2-furaldehyde, 2-acetylfuran, 5-methyl-2-furaldehyde and pyridine were observed. This suggests that at least some of the sugar components from the macromolecular structure are well preserved. This high preservation potential offers the opportunity to use analyses of the stable isotopic composition of the fossil OL for environmental reconstructions over geological time scales.

4.3 | Stable isotopes

Marine plankton has a natural variability in ^{13}C of -18 to -30 ‰ (Zeebe and Wolf-Gladrow, 2005) (Figure 4). The stable isotopic composition of *Ammonia* sp. organic lining ($\delta^{13}C_{OL}$) was at the edge of this range (-17.4 ‰), being slightly more enriched in ^{13}C (Figure 4). This is the first time ^{13}C has been measured in isolated benthic foraminiferal organic linings. For comparison, a $\delta^{13}C$ range of -19.5 to -25.3 ‰ has been measured in benthic foraminiferal cytoplasm (Moodley et al., 2002; Panieri, 2006; Enge et al., 2011) and -26.5 to -27.0 ‰ in core top samples of planktonic foraminifera (Maslin et al., 1996). In the studies of benthic foraminifera, the measured 'cytoplasm' was in fact a mixture of cytoplasm, organic linings and matrix material. In general, carbon isotopes in organic matter reflect the food source of the organism (Moodley et al., 2000). However, the relative ^{13}C enrichment in the isolated organic linings measured in this study, may reflect the relatively high contribution of sugar components to its macromolecular structure (see Section 3.2), as the isotopic value of sugars is relatively heavy compared to proteins (Teece and Fogel, 2007). The $\delta^{13}C_{CARB}$ from the same sample of foraminifera, was slightly more depleted than the standard marine carbonates range (Figure 4). This may be explained by the so-called 'Mackensen effect', whereby at sites of intense organic matter degradation seawater ^{13}C becomes depleted (Mackensen et al., 1993). This is likely considering that the *Ammonia* sp. samples were recovered from an organic-rich mudflat. Alternatively, a so-called carbonate ion effect due to release of metabolic CO_2 could also have resulted in depleted $\delta^{13}C$ values (McCrea, 1950; Spero et al., 1997).

The carbon labeling experiment shows that *Ammonia* sp. assimilated ^{13}C from their food source (labeled algae) into their organic lining. Previous studies show that *Ammonia* sp. readily

ingests algal carbon (Moodley et al., 2000) and that benthic foraminifera can assimilate carbon within a matter of hours (Rivkin and DeLaca, 1990). The exact fractionation between OL and food source could not be constrained in this study, as the labeled OL sample also partially contained linings from chambers that had grown prior to the experiment. This could not be avoided since a considerable amount of lining was needed for isotopic analysis. However, the OL sample from Label Experiment A contained almost exclusively individuals grown in the experiment, while the OL sample from Label Experiment B contained more individuals partially grown in the experiment. This is reflected in the substantial difference in their $\delta^{13}C_{OL}$ values (Figure 6). That OL $\delta^{13}C$ changes as a function of food source suggests that these linings could be used to reconstruct these food sources and relative changes therein. For example, OL ^{13}C could be used to trace methane seep dynamics, provided that the used foraminiferal species primarily feed on the available isotropically depleted bacteria (Panieri, 2006).

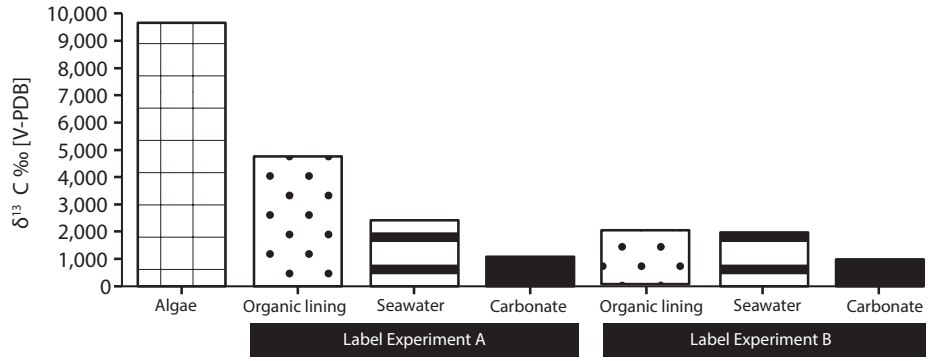

Figure 6 | The $\delta^{13}C$ enrichment values for *Ammonia tepida* carbonate, culture seawater and *A. tepida* organic linings. Conditions in Experiment A and B were identical.

The $\delta^{18}O_{OL}$ value fell within the standard range of values for organic matter (Figure 5). The offset from seawater $\delta^{18}O$ is in line with other aquatic organisms, caused by biosynthetic fractionation (Epstein et al., 1977; DeNiro and Epstein, 1981; Schimmelmann and DeNiro, 1986). A constant offset from seawater would potentially allow OL oxygen isotopes to be used as an independent tool for reconstructing the seawater oxygen isotopic composition. When subsequently combined with the oxygen isotopic ratios from the carbonate, preferably from the same specimen this sets the stage for determining absolute paleo-temperatures. The $\delta^{18}O_{OL}$ of *Heterostegina* sp., a foraminifer species found in shallow warm water has a similar $\delta^{18}O_{OL}$ to *Ammonia* sp. (19.7 ‰ versus 20.2 ‰) suggesting that foraminiferal $\delta^{18}O_{OL}$ might indeed be temperature independent. Due to the limited coverage of the data, it is currently not possible to test this hypothesis. However, by comparing the $\delta^{18}O_{OL}$ of the foraminifera with

that of the seawater from the site of recovery, it is possible to approximate the variance in the $\delta^{18}O_{OL}$–$\delta^{18}O_{SW}$ offset. Using average $\delta^{18}O_{SW}$ for the North Sea (0.5 ‰) and Adriatic (1.2 ‰) (Schmidt et al., 1999) the $\delta^{18}O_{OL}$–$\delta^{18}O_{SW}$ offset is calculated as 19.7 ‰ for *Ammonia* sp. and 18.5 ‰ for *Heterostegina* sp. A variable small contribution of isotopically depleted metabolic water might explain the observed offset. Clearly, further development of this proxy hinges on overcoming sample size constraints. The species analyzed above were either available in abundance (*Ammonia* sp.) or large in size (*Heterostegina* sp.). For paleo-oceanographic applications, species of interest are often deep sea taxa, which are inherently smaller and less abundant than shallow water taxa. A sample size calibration study is recommended to further develop this research direction.

5 | CONCLUSIONS

This study provides an in-depth analysis of the macromolecular structure of benthic foraminiferal organic linings. The OLs consist of complex mixture of polysaccharide and protein based macromolecules, with some chitin markers and traces of lignin or 'lignin-like' derivatives. This is, to our knowledge, the first report of carbon and oxygen stable isotope values for benthic foraminiferal OLs. The stable carbon isotopic composition of these linings reflects the relative contribution of sugar moieties in the lining and the foraminiferal food source. The oxygen isotopic composition of the linings falls within the standard range for organic matter and potentially allows reconstructing seawater oxygen isotopes, albeit with a possible metabolic offset. Together with the carbonate stable oxygen isotopes, this might facilitate reconstructing absolute seawater temperatures, although the amount of lining needed for a reliable analysis currently inhibits the routine application of this novel proxy. A sample size calibration would be the next logical step towards further development of this new research direction.

ACKNOWLEDGMENTS

We would like to thank and acknowledge the assistance of A. E. van Dijk (Utrecht University), P. van Rijswijk (Netherlands Institute of Ecology) and G. Ganssen (Free University, Amsterdam) with the stable isotope measurements. Thanks also to the two anonymous reviewers for their comments and suggestions, which greatly improved this manuscript. This is publication number DW-2013-1002 of the Darwin Center for Biogeosciences, which partially funded this project.

REFERENCES

Angell, R. W., 1967. The test structure and composition of the Foraminifer *Rosalina floridana*. Journal of Protozoology 14 (2), 299–307.

Banner, F. T., Williams, E., 1973. Test structure, organic skeleton and extrathalamous cytoplasm of *Ammonia bruennich*. Journal of Foraminiferal Research 3 (2), 49–69. doi:10.2113/gsjfr.3.2.49.

Bemis, B., Bijma, J., Spero, H., Lea, D. W., 1998. Reevaluation of the oxygen isotopic composition of planktonic foraminifera: experimental results and revised paleotemperature equations. Paleoceanography 13, 150–160.

Bentov, S., Erez, J., 2005. Novel observations on biomineralization processes in foraminifera and implications for Mg/Ca ratio in the shells. Geology 33, 841–844.

Berney, C., Pawlowski, J., 2003. Revised small subunit rRNA analysis provides further evidence that foraminifera are related to Cercozoa. Journal of Molecular Evolution 57, 1–8. doi:10.1007/s00239-003-0015-2.

De Leeuw, J. W., Versteegh, G. J. M., Van Bergen, P. F., 2006. Biomacromolecules of algae and plants and their fossil analogues. Plant Ecology 209–233.

De Niro, M. J., Epstein, S., 1981. Isotopic composition of cellulose from aquatic organisms. Geochimica et Cosmochimica Acta 45 (10), 1885–1894.

Dissard, D., Nehrke, G., Reichart, G. J., Bijma, J., 2010. The impact of salinity on the Mg/Ca and Sr/Ca ratio in the benthic foraminifera *Ammonia tepida*: results from culture experiments. Geochimica et Cosmochimica Acta 74 (3), 928–940.

Elderfield, H., Greaves, M., Barker, S., Hall, I. R., Tripati, A., Ferretti, P., Crowhurst, S., Booth, L., Daunt, C., 2010. A record of bottom water temperature and seawater $\delta^{18}O$ for the Southern Ocean over the past 440 kyr based on Mg/Ca of benthic foraminiferal Uvigerina spp. Quaternary Science Reviews 29 (1–2), 160–169. doi:10.1016/j.quascirev.2009.07.013.

Enge, A. J., Nomaki, H., Ogawa, N. O., Witte, U., Moeseneder, M. M., Lavik, G., Ohkouchi, N., Kitazato, H., Kucera, M., Heinz, P., 2011. Response of the benthic foraminiferal community to a simulated short-term phytodetritus pulse in the abyssal North Pacific. Marine Ecology Progress Series 438, 129–142. doi:10.3354/meps09298.

Epstein, S., Thompson, P., Yaap, C. J., 1977. Oxygen and hydrogen isotopic ratios in plant cellulose. Science 198 (4323), 1209–1215.

Erez, J., 2003. The source ions for biomineralization in Foraminifera and their implications for paleoceanographic proxies. Reviews in Mineralogy and Geochemistry 54, 115–149.

Erez, J., Luz, B., 1983. Experimental paleotemperature equation for planktonic foraminifera. Geochimica et Cosmochimica Acta 47, 1025–1031. doi:10.2113/0540115.

Gotliv, B., Addadi, L., Weiner, S., 2003. Mollusk shell acidic proteins: in search of individual functions. Chembiochem 4 (6), 522–529. doi:10.1002/cbic.200200548.

Hedley, R. H., 1962. *Gromia oviformis* (Rhizopodea) from New Zealand, with comments on the fossil chitinozoa. New Zealand Journal of Science 5, 121–136.

Hedley, R. H., 1963. Cement and iron in the arenaceous foraminifera. Micropaleontology 9 (4), 433–441.

Hemleben, C., Be, A. W. H., Anderson, O. R., Tuntivate, S., 1977. Test morphology, organic layers and chamber formation of the planktonic foraminifer *Globorotalia menardii* (d'Orbigny). Journal of Foraminiferal Research 7 (1), 1–25.

Hemleben, C., Anderson, O. R., Berthold, W., Spindler, M., 1986. Calcification and chamber formation in Foraminifera – A brief overview. In: Leadbeater, B.S.C., Riding, R. (Eds.), Biomineralization in Lower Plants and Animals. Oxford University Press, New York, pp. 237–249. doi: 10.2113/gsjfr.7.1.1.

Hottinger, L., 2000. Functional morphology of benthic foraminiferal shells, envelopes of cells beyond measure. micropaleontology 46, 57–86 (suppl. 1).

Langer, M. R., 1992. Biosynthesis of glycosaminoglycans in foraminifera: a review. Marine Micropaleontology 19, 245–255.

Lea, D. W., 1993. Constraints on the alkalinity and circulation of glacial circumpolar deep water from benthic foraminiferal barium. Global Biogeochemical Cycles 7 (3), 695–710.

Loeblich Jr., A. R., Tappan, H., 1964. Foraminiferal classification and evolution. Journal of the Geological Society of India 5, 5–39.

Longet, D., Archibald, J. M., Keeling, P. J., Pawlowski, J., 2003. Foraminifera and Cercozoa share a common origin according to RNA polymerase II phylogenies. International Journal of Systematic and Evolutionary Microbiology 53, 1735–1739. doi:10.1099/ijs.0.02597-0.

Mackensen, A., Hubberten, H., Bickert, T., Fischer, G., Fütterer, D. K., 1993. The $\delta^{13}C$ in benthic foraminiferal tests of *Fontbotia Wuellerstorf*i (Schwager) relative to the $\delta^{13}C$ of dissolved inorganic carbon in Southern Ocean deep water: implications for glacial ocean circulation models. Paleoceanography 8 (5), 587–610. doi:10.1029/93PA01291.

Martone, P. T., Estevez, J. M., Lu, F., Ruel, K., Denny, M. W., Somerville, C., Ralph, J., 2009. Discovery of lignin in seaweed reveals convergent evolution of cell wall architecture. Current Biology 19, 169–175.

Maslin, M. A., Hall, M. A., Shackleton, N. J., Thomas, E., 1996. Calculating surface water pCO_2 from foraminiferal organic $\delta^{13}C$. Geochimica et Cosmochimica Acta 60 (24), 5089–5100.

McCrea, J. M., 1950. On the isotopic chemistry of carbonates and a paleotemperature scale. Journal of Chemical Physics 18, 849–857.

Moodley, L., Boschker, H. T. S., Middelburg, J. J., Pel, R., De Herman, P. M. J., Deckere, E., Heip, C. H. R., 2000. Ecological significance of benthic foraminifera: ^{13}C labelling experiments. Marine Ecology Progress Series 202, 289–295.

Moodley, L., Middelburg, J. J., Boschker, H. T. S., Duineveld, G. C. A., Pel, R., Herman, P. M. J., Heip, C. H. R., 2002. Bacteria and Foraminifera: key players in a short-term deep-sea benthic response to phytodetritus. Marine Ecology Progress Series 236, 23–29.

Nierop, K. G. J., Pulleman, M. M., Marinissen, J. C. Y., 2001. Management induced organic matter differentiation in grassland and arable soil: a study using pyrolysis techniques. Soil Biology and Biochemistry 33 (6), 755–764. doi:10.1016/S0038-0717(00)00223-6.

Panieri, G., 2006. Foraminiferal response to an active methane seep environment: a case study from the Adriatic Sea. Marine Micropaleontology 61, 116–130.

Pawlowski, J., Holzmann, M., Berney, C., Fahrni, J., Gooday, A. J., Cedhagen, T., Habura, A., Bowser, S. S., 2003. The evolution of early Foraminifera. Proceedings of the National Academy of Sciences of the United States of America 100 (20), 11494–11498. doi:10.1073/pnas.2035132100.

Piña-Ochoa, E., Høgslund, S., Geslin, E., Cedhagen, T., Revsbech, N. P., Nielsen, L. P., Schweizer, M., Jorissen, F., Rysgaard, S., Risgaard-Petersen, N., 2010. Widespread occurrence of nitrate storage and denitrification among Foraminifera and Gromiida. Proceedings of the National Academy of Sciences of the United States of America 107, 1148–1153. doi:10.1073/pnas.0908440107.

Popper, Z. A., Tuohy, M. G., 2010. Beyond the green: understanding the evolutionary puzzle of plant and algal cell walls. Plant Physiology 153, 373–383.

Pouwels, A. D., Boon, J. J., 1990. Analysis of beech wood samples, its milled wood lignin and polysaccharide fractions by curie-point and platinum filament pyrolysis-mass spectrometry. Journal of Analytical and Applied Pyrolysis 17 (2), 97–126. doi:10.1016/0165-2370(90)85026-J.

Pouwels, A. D., Tom, A., Eijkel, G. B., Boon, J. J., 1987. Characterisation of beech wood and its holocellulose and xylan fractions by pyrolysis-gas chromatography–mass spectrometry. Journal of Analytical and Applied Pyrolysis 11, 417–436. doi:10.1016/0165-2370(87)85045-3.

Pouwels, A. D., Eijkel, G. B., Boon, J. J., 1989. Curie point pyrolysis-capillary gas chromatography-high-resolution mass spectrometry of microcrystalline cellulose. Journal of Analytical and Applied Pyrolysis 14, 237–280.

Raitzsch, M., Dueñas-Bohórquez, A., Reichart, G.-J., de Nooijer, L. J., Bickert, T., 2009. The impact of seawater calcite saturation state by modifying Ca ion concentrations on Mg and Sr incorporation in cultured benthic foraminifera. Biogeosciences Discussions 6 (6), 11347–11375.

Reichart, G.-J., Jorissen, F., Mason, P. R. D., Anschutz, P., 2003. Single foraminiferal test chemistry records the marine environment. Geology 31, 355–358.

Rivkin, R. B., DeLaca, T. E., 1990. Trophic dynamics in Antarctic benthic communities. I. In situ ingestion of microalgae by foraminifera and metazoan meiofauna. Marine Ecology Progress Series 64, 129–136.

Robbins, L. L., Brew, K., 1990. Proteins from the organic matrix of core-top and fossil planktonic foraminifera. Geochimica et Cosmochimica Acta 54 (8), 2285–2292.

Rosenthal, Y., Boyle, E. A., Slowey, N., 1997. Temperature control on the incorporation of magnesium, strontium, fluorine, and cadmium into benthic foraminiferal shells from Little Bahama Bank: prospects for thermocline paleoceanography. Geochimica et Cosmochimica Acta 61 (17), 3633–3643. doi:10.1016/S0016-7037(97)00181-6.

Schimmelmann, A., DeNiro, M. J., 1986. Stable isotope studies of chitin. III. The D/H 18O/ 16O ratios in arthropod chitin. Geochimica et Cosmochimica Acta 50 (7), 1485–1496.

Schmidt, G. A., Bigg, G. R., Rohling, E. J., 1999. Global Seawater Oxygen-18 Database -v1.20.

Schwab, D., Plapp, R., 1983. Quantitative chemical analysis of the shell or the monthalamous foraminifer *Allogromia laticollaris* Arnold. Journal of Foraminiferal Research 13 (1), 69–71.

Shackleton, N. J., 1974. Attainment of isotopic equilibrium between ocean water and the benthonic foraminifera genus *Uvigerina*: isotopic changes in the ocean during the last glacial. Cent. Nat. Rech Science Colloquium International 219, 203–209.

Sluijs, A., Brinkhuis, H., Schouten, S., Bohaty, S. M., John, C., Zachos, J. C., Reichart, G. J., Sinninghe Damsté, J. S., Crouch, E. M., Dickens, G. R., 2007. Environmental precursors to rapid light carbon injection at the Palaeocene/Eocene boundary. Nature 450 (7173), 1218–1221. doi:10.1038/nature06400.

Spero, H., Bijma, J., Lea, D. W., Bemis, B. E., 1997. Effect of seawater carbonate concentration on foraminiferal carbon and oxygen isotopes. Nature 390, 497–500. doi:10.1038/37333.

Stancliffe, R. P. W., 1989. Microforaminiferal linings: their classification, biostratigraphy and paleoecology, with special reference to specimens from British Oxfordian sediments. Micropaleontology 35, 337–352.

Stankiewicz, A. B., Van Bergen, P. F., Duncan, I. J., Carter, J. F., Briggs, D. E. G., Evershed, R. P., 1996. Recognition of chitin and proteins in invertebrate cuticles using analytical pyrolysis/gas chromatography and pyrolysis/gas chromatography/mass spectrometry. Rapid Communications in Mass Spectrometry 10 (14), 1747–1757. doi: 10.1002/(SICI)1097-0231(199611)10:14b1747: AID-RCM713>3.0.CO;2-H.

Teece, M. A., Fogel, M. L., 2007. Stable carbon isotope biogeochemistry of monosaccha-rides in aquatic organisms and terrestrial plants. Organic Geochemistry 38 (3), 458–473. doi:10.1016/j.orggeochem.2006.06.008.

Toler, S. K., Hallock, P., 1997. Shell malformation in stressed *Amphistegina* populations: relation to biomineralization and paleoenvironmental potential. Marine Micropaleontology 34, 107–115.

Toyofuku, T., Kitazato, H., Kawahata, H., Tsuchiya, M., Nohara, N., 2000. Evaluation of Mg/Ca thermometry in foraminifera: comparison of experimental results and measurements in nature. Paleoceanography 15, 456–464.

Toyofuku, T., Suzuki, M., Suga, H., Sakai, S., Suzuki, A., Ishikawa, T., de Nooijer, L. J., Schiebel, R., Kawahata, H., Kitazat, H., 2011. Mg/Ca and [delta]^{18}O in the brackish shallow-water benthic foraminifer *Ammonia* '*beccarii*'. Marine Micropaleontology 78, 13–120. doi:10.1016/j.marmicro.2010.11.003.

Van Bergen, P. F., Blokker, P. M., Collinson, E., Sinninghe Damsté, J. S., De Leeuw, J. W., 2004. Structural biomacromolecules in plants: what can be learnt from the fossil record? In: Hemsley, A. R., Poole, I. (Eds.), The Evolution of Plant Physiology. Academic Press, Oxford, pp. 133–154.

Van Heemst, J. D. H., Peulve, S., De Leeuw, J. W., 1996. Novel algal polyphenolic biomacromolecules as significant contributors to resistant fractions of marine dissolved and particulate organic matter. Organic Geochemistry 24 (6–7), 629–640. doi:10.1016/0146-6380(96)00054-X.

Verbruggen, F., Heiri, O., Reichart, G.-J., de Leeuw, J. W., Nierop, K. G. J., Lotter, A., 2010. Effects of chemical pretreatments on δ^{18}O measurements, chemical composition, and morphology of chironomid head capsules. Journal of Paleolimnology 43 (4), 857–872. doi:10.1007/s10933-009-9374-z.

Versteegh, G. J. M., Blokker, P., Marshall, C., Pross, J., 2007. Macromolecular composition of the dinoflagellate cyst *Thalassiphora pelagica* (Oligocene, SW Germany). Organic Geochemistry 38 (10), 1643–1656.

Weiner, S., Erez, J., 1984. Organic matrix of the shell of the foraminifer, *Heterostegina depressa*. Journal of Foraminiferal Research 14 (3), 206–212.

Winchester-Seeto, T. M., Bell, K. N., 1999. Foraminiferal linings and other organic walled microfossils from the Devonian of the Tamworth Belt, northern New South Wales, Australia. Alcheringa 31 (08), 155–175.

Zeebe, R. E., Wolf-Gladrow, D., 2005. CO_2 in seawater: equilibrium, kinetics, isotopes. In: Halpern, D. (Ed.), Elsevier Oceanography Series 65. Elsevier, Amsterdam.

3

Manganese incorporation in living (stained) benthic foraminiferal shells: A bathymetric and in-sediment study in the Gulf of Lions (NW Mediterranean)

Shauna Ní Fhlaithearta[1], Christophe Fontanier[2,3,4], Frans Jorissen[4], Aurélia Mouret[4], Adriana Dueñas-Bohórquez[1], Pierre Anschutz[2], Mattias B. Fricker[5], Detlef Günther[5], Gert J. de Lange[1], Gert-Jan Reichart[1,7]

[1]Faculty of Geosciences, Utrecht University, Utrecht, the Netherlands
[2]EPOC, UMR CNRS 5805, University of Bordeaux, Pessac, France
[3]FORAM, Foraminiferal Study Group, 29200, Brest, France
[4]Faculty of Sciences, Université d'Angers, Angers, France
[5]Université d'Angers, LPG-BIAF, UMR CNRS 6112, 49045 Angers Cedex, France
[6]Laboratory of Inorganic Chemistry, ETH Zurich, 8093 Zurich, Switzerland
[7]Royal Netherlands Institute of Sea Research, Landsdiep 4, 1797 SZ 't Horntje, the Netherland

Biogeosciences, 15, 6315–6328, 2018
doi.org/10.5194/bg-15-6315-2018

ABSTRACT

Manganese geochemistry in deep-sea sediments is known to vary greatly over the first few centimeters, which overlaps with the in-sediment depth habitats of several benthic foraminiferal species. Here we investigated manganese incorporation in benthic foraminiferal shell carbonate across a 6-station depth transect in the Gulf of Lions, NW Mediterranean to unravel the impacts of foraminiferal ecology and Mn pore water geochemistry. Over this transect water depth increases from 350 to 1987 m, while temperature (~ 13 °C) and salinity (~ 38.5) remained relatively constant. Manganese concentrations in the tests of living (Rose Bengal stained) benthic foraminiferal specimens of *Hoeglundina elegans*, *Melonis barleeanus, Uvigerina mediterranea*, *Uvigerina peregrina* were measured using laser ablation inductively coupled mass spectrometry (laser ablation ICP-MS). Pore water manganese concentrations show a decrease from shallow to deeper waters, which corresponds to a generally decreasing organic matter flux with water depth. Differences in organic matter loading at the sediment water interface affects oxygen penetration depth into the sediment and hence Mn pore water profiles. Mn/Ca values for the investigated foraminiferal species reflect pore water geochemistry and species-specific microhabitat in the sediment. The observed degree of variability within a single species is in–line with know ranges in depth habitat and gradients in redox conditions. Both Mn/Ca ratio and inter-specific variability hence reflect past Mn cycling and related early diagenetic processes within the sediment, making this a potential tool for bottom-water oxygenation and organic-matter fluxes. Dynamics of both in-sediment foraminiferal depth habitats and Mn cycling, however, limit the application of such a proxy to settings with relatively stable environmental conditions.

1 | INTRODUCTION

Reconstructing past climate and environmental change largely depends on so-called proxies. These proxies relate measurable variables in the geological record to target parameters, such as e.g. temperature, biological productivity and bottom water oxygenation. The carbonate shells of unicellular protists, foraminifera, are one of the most utilized signal carriers for reconstructing past environments. Both the census data of foraminifera and the geochemical composition of the shells are used in this context. The geochemical composition of the shells is investigated for their stable isotopic composition as well as for their trace and minor element incorporation. Both pelagic and bottom water conditions are reconstructed this way, using planktonic and benthic foraminiferal species respectively.

Most existing calibrations of trace element uptake in foraminiferal test carbonate are based on comparing their composition with bottom water conditions (Elderfield et al., 2006; Nürnberg et al., 1996; Yu and Elderfield, 2007). Many benthic foraminiferal species live, however, within the sediment and precipitate their calcium carbonate test in contact with pore water. As a result, the trace metal composition of pore water exerts a control on the uptake of trace metals in their test. This effectively links benthic foraminiferal microhabitat preference and pore water chemistry. On the one hand, this creates complications when using foraminiferal trace metal ratios for reconstructing bottom water conditions, whereas on the other hand, it offers the possibility to develop proxies of pore water chemistry in the past.

Linking foraminiferal test chemistry with pore water chemistry requires in-depth knowledge of, (1) how early diagenesis in sediments affects pore water chemistry, (2) the habitat preference of the foraminiferal species, (3) foraminiferal migration (and the depth at which they calcify) within the uppermost sediment layer. In principle, the chemical composition of living (stained) benthic foraminifera will reflect all these processes.

For many elements an important inter-specific difference in uptake of trace metals has been observed (Hintz et al., 2006; Wit et al., 2012; Barras et al., 2018), a so-called vital effect. This implies that in addition to ecology and pore water geochemistry, trace metal partitioning also needs to be taken into consideration. This requires a comparative study between locations where all three of these aspects have been quantified.

Reconstructing past pore water trace metal profiles is important since it provides valuable information on organic carbon degradation and recycling of nutrients at the seafloor (Van Cappellen and Wang, 1996; De Lange, 1986). Knowledge of such profiles in the past could thus help to reconstruct past carbon cycles.

Benthic foraminiferal species have a specific preference for their depth-habitat (Jorissen et al., 1995). Some benthic foraminiferal species are limited to a very narrow environmental in-sediment range, for example, along redox fronts, whereas others have a wider distribution, thriving under variable conditions and consequently occupy a broader niche. These differences in depth-habitat preferences could be related to the presence of different types of metabolism (Koho et al., 2011; Risgaard-Petersen et al., 2006). As such, trace metal profiles and foraminiferal in-sediment depth habitat can be related, such as recently proposed in a conceptual (TROXCHEM^3) model for the redox sensitive element, manganese, by Koho et al., (2015). Studying the interplay between benthic foraminiferal habitat preference and incorporation of redox-sensitive trace elements is key to verifying such models.

Studying manganese bound in foraminiferal shell carbonate lies at the intersection of foraminiferal ecology and early diagenesis in sediments. Manganese is a redox sensitive element and exists as Mn-(hydr)oxides in the presence of oxygen. As oxygen concentrations in the sediment decreases due to ongoing organic matter remineralization, Mn-(hydr)oxides are reduced to aqueous Mn^{2+}, (Froelich et al., 1979). Manganese in sediments cycles continuously between solid and aqueous state as a result of upward diffusion of Mn^{2+} and consequent remineralization to Mn-(hydr)oxides. Hence proxy studies must account for both ecological controls, like foraminiferal habitat preference, as well as geochemical controls like oxygen concentrations and organic matter loading (Glock et al., 2012; Groeneveld and Filipsson, 2013; Koho et al., 2015, 2017; McKay et al., 2015; Reichart et al., 2003). Notably, both benthic foraminifera and trace metal geochemistry react to organic matter recycling and bottom water oxygenation (Jorissen et al., 1995). This implies that locations with contrasting conditions, both low and high bottom-water oxygenation as well as low and high productivity, are required for testing. Whereas most of these studies focused on the role of bottom water oxygenation in relatively oxygen poor settings, here we focus on the well-oxygenated western Mediterranean.

In this study we combine pore water geochemistry, foraminiferal habitat preference and test geochemistry in an area characterized by well-oxygenated bottom water conditions and average productivity. Results are compared with earlier studies from high productivity regimes and low-oxygen conditions at the sediment-water interface (e.g. Arabian Sea, Koho et al., 2015 and Mediterranean sapropel deposition, Ní Fhlaithearta et al., 2010). Specifically, we investigate the link between manganese incorporation and benthic foraminiferal ecology and compare this to the recently proposed TROXCHEM^3 model (Koho et al., 2015). Four species of living (stained) foraminifera were sampled along a 6-station bathymetric transect in the Gulf of Lions, NW Mediterranean. Individuals were picked from a series of in-sediment depths and analyzed by laser ablation ICP-MS, enabling multiple analyses of single specimens.

2 | MATERIAL AND METHODS

2.1 | Study area and sediment sampling

Cores were collected with a classical Barnett multicorer (Barnett et al., 1984) at 6 stations in the Gulf of Lions (NW Mediterranean) during the August-September 2006 BEHEMOTH cruise (Figure 1, Table 1). The 6 stations describe a bathymetric transect from 350 m to 1987 m depth. The shallowest site, station F, is bathed in Mediterranean Intermediate Water (MIW). Stations E (552 m) and D (745 m) are positioned at the transition of MIW and Western Mediterranean Deep Water (WMDW). Stations C (980 m), B (1488 m) and A (1987 m) are bathed by the WMDW. Bottom water temperature is stable through the part of the water column studied here (~ 13.1 °C) (Xavier Durrieu de Madron, personal communication, 2006). Salinity ranges between 38.4 and 38.5. The multicorer allowed sampling of the first decimeters of the sediment, the overlying bottom waters, and an undisturbed sediment-water interface. Cores were sliced for foraminiferal studies with a 0.5 cm resolution down to 4 cm, followed by 1 cm slices down to 10 cm depth. Sediments were put in an ethanol-Rose Bengal mixture (95% ethanol with 1 g/l Rose Bengal), in order to identify living (stained) specimens. For more detailed information about methods, please consult Fontanier et al., (2008).

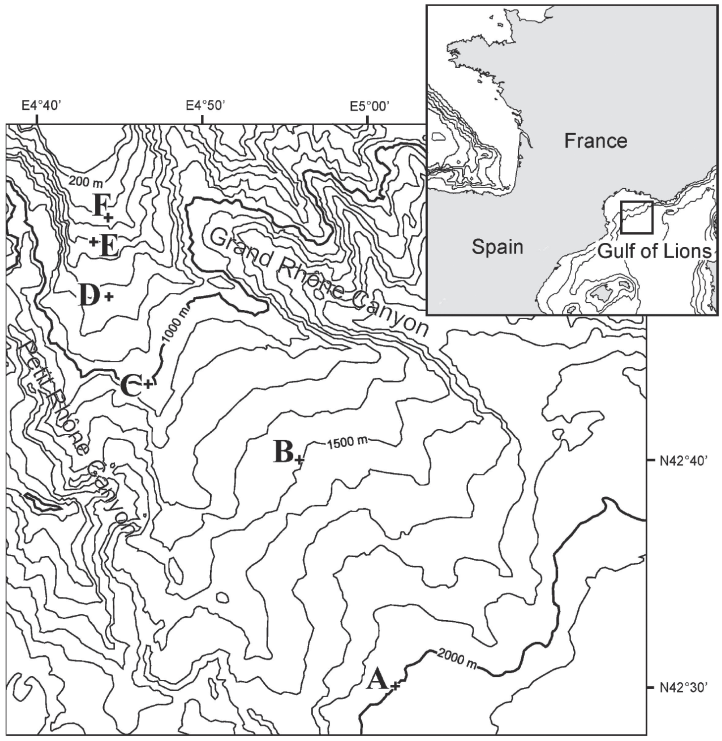

Figure 1 | Location map showing sampling stations and bathymetry.

Table 1 | Water depth, coordinates and bottom water physio-chemical parameters: Temperature (°C), salinity, and oxygen penetration depth mm) for six stations F-A.

Station	Depth (m)	Latitude (N)	Longitude (E)	Bottom water temperature* (°C)	Bottom water salinity *	Oxygen penetration depth (mm)
F	350	42°52'32	4°42'43	13.2	~ 38.5	20.5 ± 3.3
E	552	42°48'78	4°43'21	13.2	~ 38.5	57.2 ± 4.5
D	745	42°46'66	4°43'91	13.1	~ 38.5	36.5 ± 1.6
C	980	42°43'18	4°46'58	13.1	~ 38.48	50.7 ± 6.3
B	1488	42°38'83	4°56'03	13.1	~ 38.46	141.5 ±0.0
A	1987	42°28'25	5°00'61	13.1	~ 38.46	197.0 ± 11.0

(* Xavier Durrieu de Madron, personal communication, 2006)

2.2 | Pore water geochemistry

Sediment sampling for pore water extraction was carried out under an inert atmosphere (N_2). Hereafter, samples were centrifuged at 3500 rpm for 20 min. The supernatant was filtered and acidified (HNO_3 *suprapure*) for analyzing dissolved metals. Dissolved Mn concentrations were determined with flame atomic absorption spectrometry (Perkin Elmer AA 300). Precision for this method is ± 5%. A pore water subsample was also analyzed for Mn using ICP-MS (Agilent 7500 Series). Relative precision for this method is 3%. Total alkalinity of pore water was measured at Utrecht University using an automated titrator (702 SM Titrino, Metrohm) making Gran plots. Dissolved Inorganic Carbon (DIC) was measured using a Dissolved Carbon Analyser (Shimadzu, Model TOC-5050A). Carbonate ion concentrations were calculated using the CO2SYS software (version 01.05; Lewis and Wallace, 1998). Analytical uncertainty for the alkalinity is about 10 µeq, relative standard deviation for the DIC analyses is 0.8%.

Oxygen concentration profiles were determined using Clark-type microelectrodes (Unisense©, Denmark). Labile organic matter was derived from the sum of lipids, amino acids and sugars measured in the top cm of sediment; for details, see Fontanier et al., 2008.

2.3 | Foraminiferal trace metal geochemistry

Foraminiferal trace element concentrations were determined using two laser ablation ICP-MS systems. Prior to laser ablation, all samples were gently cleaned in methanol (× 1) and UHQ water (× 4). Between each rinse, the samples were placed in a sonic bath for several seconds to thoroughly clean the tests. Benthic foraminifera from 745 m (station D), 980 m (station C), 1488 m (station B) and 1987 m (station A) were measured at Utrecht University using a deep UV (193 nm) ArF excimer laser (Lambda Physik) with GeoLas 200Q optics. Ablation was performed at a pulse repetition rate of 10 Hz, and energy density of 1.4 J/cm^2, with a crater size of 80 µm. Ablated particles were measured by a quadrupole ICP-MS (Micromass Platform) equipped with a collision and reaction cell. Such a collision and reaction cell improves carbonate analyses by

eliminating interferences on mass 44. Scanned masses included ^{24}Mg, ^{26}Mg, ^{27}Al, ^{42}Ca, ^{43}Ca, ^{55}Mn, ^{88}Sr, ^{137}Ba, ^{138}Ba, ^{208}Pb. Benthic foraminifera from stations F (350 m) and E (552 m) were analyzed at ETH-Zurich (due to laboratory renovations at Utrecht University). The laser type and ablation parameters were identical to those detailed above. The ablated particles were measured using a quadrupole ICP-MS (ELAN 6100 DRC, Perkin-Elmer). In both cases, calibration was performed using an international standard (NIST610) with Ca as an internal standard (Jochum et al., 2011). The same masses as measured in Utrecht were monitored, in addition to ^{7}Li, ^{23}Na, ^{47}Ti, ^{60}Ni, ^{61}Ni and ^{89}Y. Inter-laboratory compatibility was monitored using a matrix-matched calcite standard. For Mn this standard showed a precision better than 3% over all analyses, at ETH and UU, and with an offset of less than 5% from an off line determined (solution ICP-AES) concentration analyzing discrete sub-samples. The matrix matched standard is routinely included in the analyses and has been monitored since 2010 (Duenas Bohorquez et al., 2011).

Analytical error (equivalent to 1 sigma), based on repeated measurement of an external standard, was < 5% for reported elements. Each laser ablation measurement was screened for contamination by monitoring Al and Pb. On encountering surface contamination, the data integration interval was adjusted to exclude any Al or Pb enrichment. Cross-plots between Al and Pb versus Mn showed that they are unrelated, confirming accuracy of the integrations.

During the laser ablation analyses the different trace elements were monitored with respect to time, thus representing a cross section of the test wall. This allows not only quantification of the different trace metals of interest, but also to observe variability within individual tests. Each species has a distinct test-wall thickness, permitting the study of intra-test variability. A typical ablation profile for *H. elegans* is shown in Figure 2.

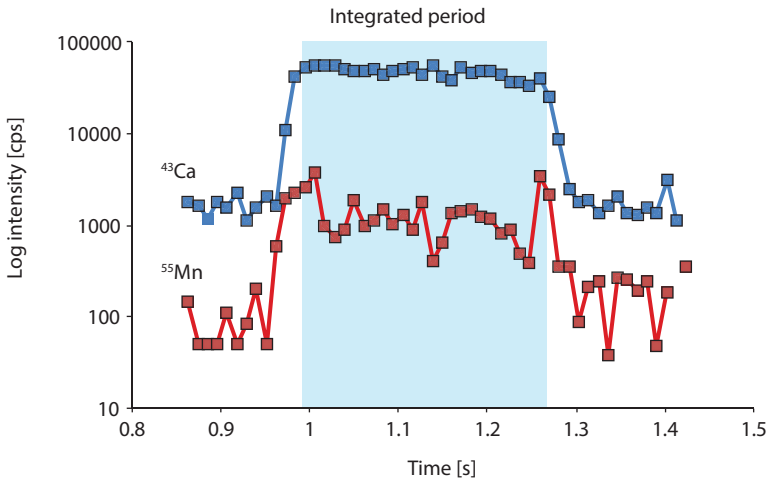

Figure 2 | Example of a laser ablation profile with signal log intensity counts per second (cps) through time. The integrated signal is shaded.

2.4 | Analyses of manganese in foraminiferal tests

Contamination and presence of secondary Mn-rich coatings on benthic foraminiferal tests has been a longstanding challenge in trace metal analyses of benthic foraminifera (Boyle 1983, Lea and Boyle 1989). In this study the trace metal data are based exclusively on living (Rose Bengal stained) foraminifera, which effectively rules out the impact of Mn-rich coatings on trace metal concentrations. At the time of sampling, the collected tests were still enveloped by foraminiferal cytoplasm, preventing the formation of extraneous inorganic precipitates. Although benthic foraminifera live within the sediment, their test is physically separated from the environment as they are enveloped in an organic sheath (Ní Fhlaithearta et al., 2013). In case a recently deceased foraminifer was mistakenly analyzed (still with sufficient protoplasm to stain with Rose Bengal) the Mn oxide would not only have had limited time to develop, but it would also show up as a Mn spike at the start of a laser ablation profile. The ablation profiles confirm that no Mn-rich phases are present at the test surfaces (Figure 2).

Comparing LA-ICP-MS data with traditional solution analyses for foraminiferal Mg/Ca values showed that data are directly comparable (Rosenthal et al., 2011). Also for trace metals such as Ni^{2+}, Cu^{2+} and Mn^{2+}, cross-calibration of LA-ICP-MS and micro-XRF shows those analytical results are robust (Munsel et al., 2010).

2.5 | Benthic foraminiferal Mn/Ca

Manganese incorporation in benthic foraminiferal test carbonate was analyzed from 4 different species (*Hoeglundina elegans, Melonis barleeanus, Uvigerina mediterranea, Uvigerina peregrina*), from 6 coring sites, for up to 9 depths in the sediment. Sample coverage for all stations is described in Table 2. Descriptive statistics are presented in Table 3.

From the largest taxon, *Uvigerina mediterranea*, 3–4 analyses were routinely carried out per test, and no trend in Mn/Ca values was seen in consecutive growth stages. From the other species two analyses were performed per test. The resolution of the ablation profiles themselves does not allow quantifying changes in trace metals within the test wall. Still, comparing the data within individual ablation profiles shows that the intratest variability is generally limited for Mn (Table 4). As the ablation profiles typically target only one chamber, this does not include the full potential range. Comparing different ablation profiles between chambers in a single test would circumvent this, but this data is somewhat limited.

Boxplots are used to describe the range of Mn/Ca values and how the distribution, median, average and skewness compares between species. All ICP-MS measurements are included, and as such represent both intra- and inter-individual variation.

Table 2 | Number of LA-ICP-MS analyses per benthic foraminifera species per sample per station.

Station	Depth (m)	Sample intervals (cm)	*Hoeglundina elegans* no. analyses	*Uvigerina mediterranea* no. analyses	*Uvigerina peregrina* no. analyses	*Melonis barleeanus* no. analyses
F	350	0–0.5	2	18	5	1
		0.5–1	4	13		2
		1–1.5		3		
		1.5–2				10
		2–2.5	1			2
		3–3.5				3
		5–6				3
E	552	0–0.5		5	26	
		0.5–1			9	4
		1–1.5			14	3
		1.5–2			5	3
		2–2.5			7	3
		2.5–3			6	2
		3–3.5			6	
		3.5–4			8	1
		4–5		3		
		7–8				1
D	745	0–0.5		20	13	
		0.5–1		6		5
		1–1.5		3	6	
		1.5–2		7	8	6
		2–2.5			4	
		3.5–4			2	
		4–5			2	4
		8–9			2	
C	980	0–0.5		20		2
		0.5–1		20		2
		1–1.5		4		
B	1488	0–0.5	3	4	10	4
		0.5–1	9	5	3	5
A	1987	0–0.5	15		10	
		1–1.5				3

Table 3 | Descriptive statistics (minimum, maximum, mean, median, standard deviation and interval of maximum frequency of total analyses for *H. elegans*, *U. mediterranea*, *U. peregrina* and *M. barleeanus* for Mn/Ca µmol/mol.

Mn/Ca µmol/mol	*H. elegans*	*U. mediterranea*	*U. peregrina*	*M. barleeanus*
Min	DL*	DL*	DL*	3.91
Max	0.69	22.71	35.38	149.50
Mean	0.04	4.03	8.28	37.22
Median	DL*	1.04	7.45	24.76
Std. deviation	0.16	5.03	7.17	35.17
Max. frequency interval	DL-7.50 (100% < 1)	DL-7.50 (80%)	DL-7.50 (53%)	7.5–15 (23%)

DL: detection limit

Table 4 | Relative standard deviation (% RSD) of intra-individual values in Mn/Ca within four species of benthic foraminifera (*H. elegans*, *U. mediterranea*, *U. peregrina* and *M. barleeanus*).

Element	*H. elegans* % RSD	*U. mediterranea* % RSD	*U. peregrina* % RSD	*M. barleeanus* % RSD
Mn	21	23	20	51

3 | RESULTS

3.1 | Pore water data

Pore water dissolved manganese (Mn^{2+}) concentrations were measured at all six stations. Manganese concentrations increase below the oxygen penetration depth at stations C and D (Figure 3), with the highest in-sediment Mn^{2+} concentrations reached at station D. At stations E and F manganese concentrations remain low after crossing the oxygen penetration depth. At stations A and B the oxygen penetration depth and MnO_2/Mn^{2+} redox boundary are deeper than 10 cm's. Dissolved inorganic carbon (DIC) and total alkalinity (TA), were measured at stations E, C and B (Figure 4). At stations D, C and E, DIC concentrations in the top 10 cm have a similar range (2350–2700 µmol/kg). The DIC profile at station B has a narrower range, ranging from 2400-2550 µmol/kg. Total alkalinity values range from 3242 µmol/kg at station E to a minimum of 2774 at station B. Carbonate ion concentrations [CO_3^{2-}] were derived based on TA and DIC values. The [CO_3^{2-}] profiles were relatively similar (Figure 4) for stations E and C and B. Values for all three stations ranged from a maximum of 419 µmol/kg at station E to a minimum of 192 µmol/kg at station C (Figure 4).

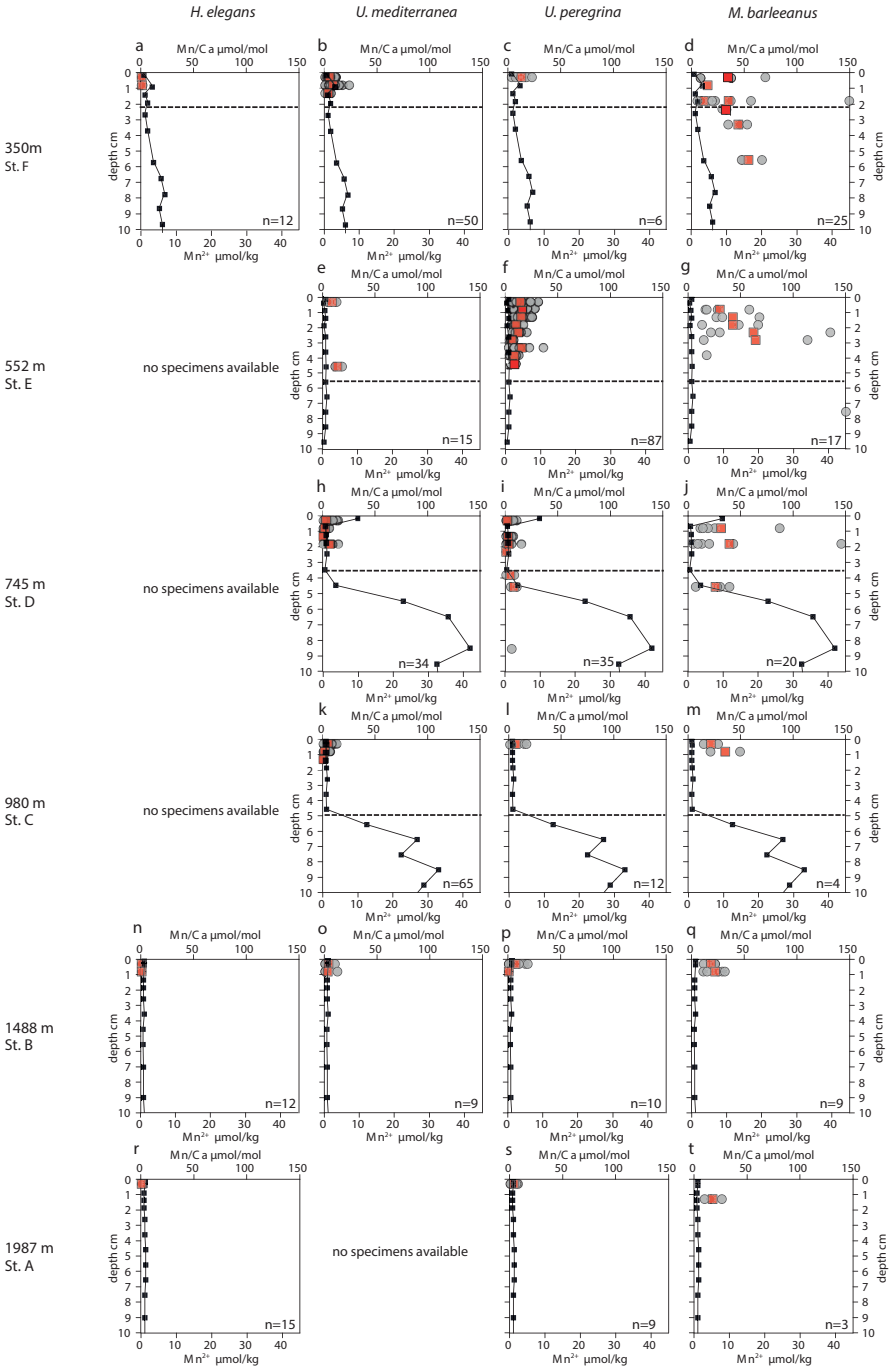

Figure 3 | Plots of Mn/Ca (µmol mol^{-1}) (a-t) measured in living (stained) *Hoeglundina elegans*, *Uvigerina mediterranea*, *Uvigerina peregrina*, and *Melonis barleeanus*. Individual analyses are plotted (grey circles) alongside average values for a given depth in the sediment (red squares). Pore water Mn^{2+} (µmol kg^{-1}) profiles (black line) are plotted for all stations. The dashed grey line indicates the oxygen penetration depth (OPD).

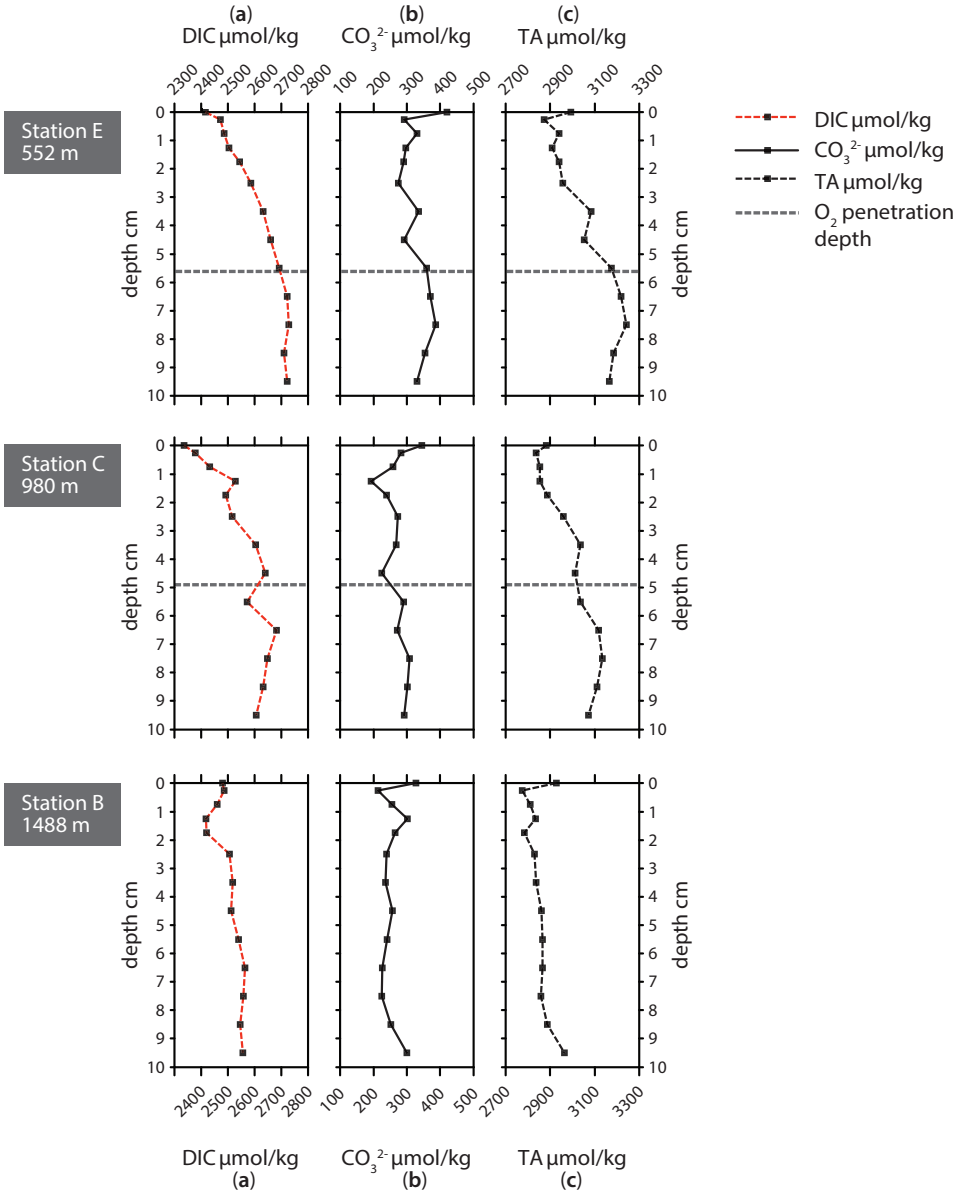

Figure 4 | Carbonate chemistry parameters for stations E, C, and B. (**a**) Dissolved inorganic carbon (DIC), (**b**) [CO_3^{2-}] in µmol kg^{-1}, and (**c**) total alkalinity (TA) in µmol kg^{-1}.

3.2 | Mn/Ca data

3.2.1 | *Intra-individual variability*

For most species some Mn/Ca analyses were below detection limit, except for *M. barleeanus,* which contained measurable quantities of Mn in all tests analyzed. This was most evident for *H. elegans*, where all but three Mn/Ca measurements were below detection limit (dl). *Uvigerina peregrina* had a wider range of Mn/Ca values than *U. mediterranea*. *Melonis barleeanus* exhibited the largest range of Mn/Ca values of the four studied species (Figure 5 and Table 5). For all species, except *H. elegans,* values are somewhat skewed towards higher values.

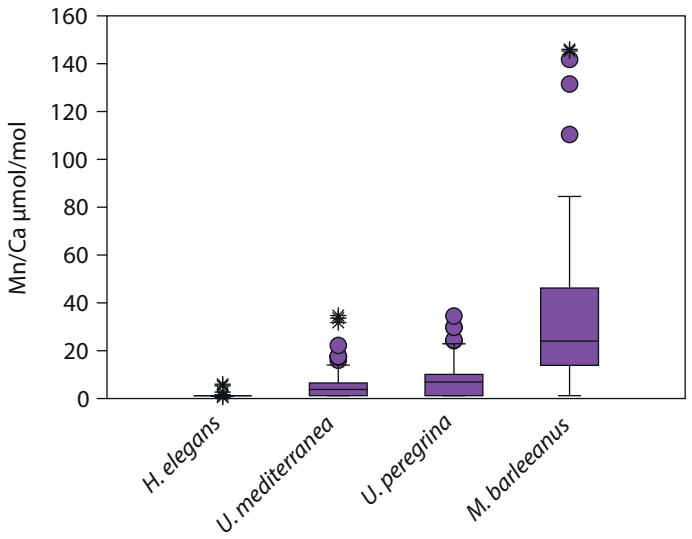

Figure 5 | Box plots describing the distribution of Mn/Ca values measured in living (stained) individuals of *Hoeglundina elegans*, *Uvigerina mediterranea*, *Uvigerina peregrina*, and *Melonis barleeanus*. The box represents all values between the 25th and 75th percentile. The dissection line through the box denotes the median. The whiskers are drawn from the top of the box up to the largest data point less than 1.5 times the box height from the box and similarly below the box. Values outside the whiskers are shown as circles, and values further than 3 times the box height are denoted as stars.

3.2.3 | *Foraminiferal Mn/Ca variation across a depth transect*

A trend of decreasing manganese incorporation with increasing water depth (350–1987 m) is most clearly visible in *M. barleeanus* (Figure 6), except that the maximum values are observed at station E at 552 m. *Melonis barleeanus* shows the highest Mn/Ca values and the largest Mn/Ca variability. Station E registers the broadest Mn/Ca variability, which decreases with increasing water depth. *U. peregrina* also exhibits the largest variability in Mn/Ca values at

station E. For *U. peregrina*, Mn^{2+} incorporation decreases from 350 m to 1987 m, except for station D (745 m), where Mn/Ca values (between the 10–90th percentile) are approximately equivalent to those at station A (350 m; Figure 6). For *U. mediterranea* a trend of decreasing Mn incorporation with increasing depth is found in specimens of *U. mediterranea* from the sediments at 552, 745 and 980 m. The highest values are reached at the shallowest station (350 m). Station E is also marked by the highest minimum Mn/Ca values for *U. mediterranea*. At station A only two *U. mediterranea* measurements are above the detection limit. *Hoeglundina elegans* tests from three stations (350 m, 1488 m and 1987 m) were analyzed, however, all but three measurements were below detection limit (Figure 6). These slightly elevated values were recorded at the shallowest station (station F). These Mn/Ca values are still very low compared to ranges in Mn/Ca values observed for the other species (Figure 6).

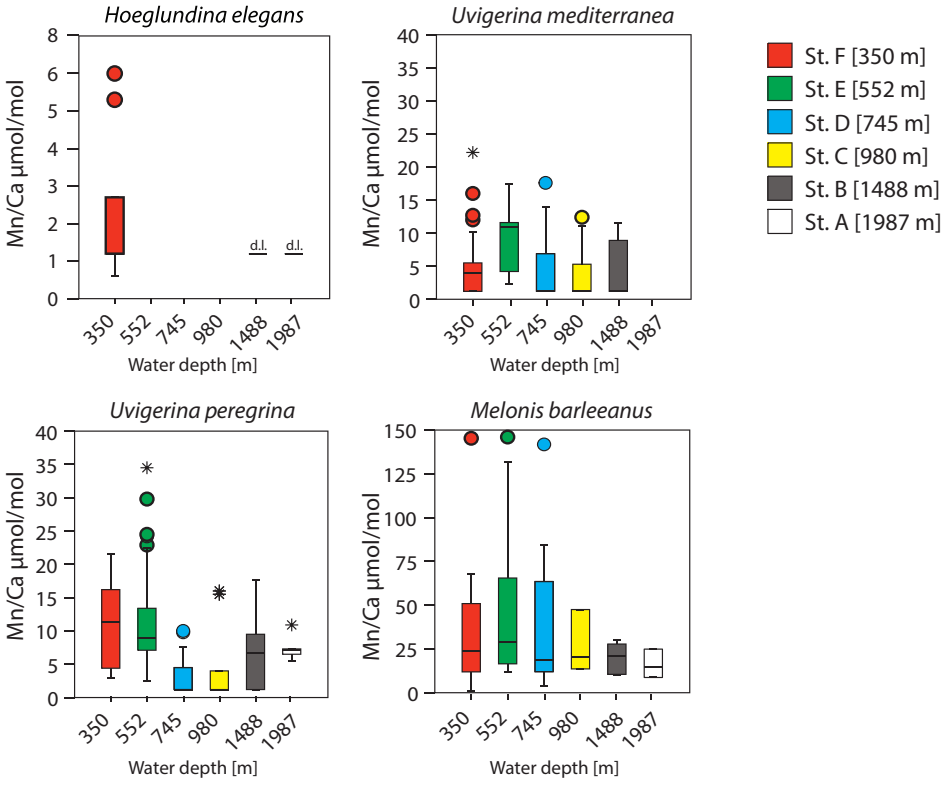

Figure 6 | Box plots describing the distribution of Mn/Ca values across a depth transect (350–1987 m) measured in living (stained) individuals of *Hoeglundina elegans*, *Uvigerina mediterranea*, *Uvigerina peregrina*, and *Melonis barleeanus*. Note that the scale of the y axis varies. The box represents all values between the 25th and 75th percentile with the whiskers extending less than 1.5 times the box height. The dissection line through the box denotes the median. Values outside the whiskers are shown as circles, and values further than 3 times the box height are denoted as stars. Detection limit (DL) for *H. elegans* is indicated when specimens have been measured but the signal was too low.

Variability in Mn/Ca increases together with the overall Mn/Ca concentration within benthic foraminiferal species (Table 4). This suggests that even at those stations and depth levels where the highest Mn concentrations are recorded, individuals with relatively low amounts of Mn in their calcitic test were found. Comparing relative standard deviations, as a measure for the inter-specimen variability, for the different stations and species suggests that with increasing Mn concentration for *M. barleeanus* and *U. mediterranea* variability increases, whereas for *U. peregrina* it decreases.

3.2.4 | *In-sediment variation*

For most species Mn/Ca values are more or less constant with in-sediment depth (Figure 3). However, *M. barleeanus* shows increasing Mn/Ca values with in-sediment depth. This is most apparent at the shallowest station (station F – 350 m) (Figure 3d).

4 | DISCUSSION

Incorporation of Mn in benthic foraminiferal carbonate depends both on foraminiferal ecology and early diagenesis in sediments. Although other factors such as temperature, seawater carbonate chemistry, growth rate etc., might also affect the uptake of Mn in the test carbonate (Koho et al., 2017), these effects are most likely several orders of magnitude smaller compared to the large range in dissolved Mn in pore water. Since pore water Mn is the dominant factor controlling Mn incorporation, studies must account for ecological controls, like foraminiferal depth habitat preference, as well as for geochemical controls like oxygen concentrations and organic matter fluxes (Koho et al., 2015; De Lange, 1986; Reichart et al., 2003). The fact that this study was based on living foraminifera circumvents potential complications due to Mn-rich coatings. Such coatings would likely not affect the aragonitic test of *H. elegans* (Ní Fhlaithearta et al., 2010), but might interfere when analyzing fossil calcite tests. Still, a spatially resolved analytical technique like LA-ICP-MS allows the detection of such coatings in fossil specimens.

4.1 | Impact of redox conditions and foraminiferal habitat preference on Mn incorporation

In general, flux of organic matter arriving at the seafloor decreases with increasing water depth, due to ongoing degradation during settling (Arndt et al., 2013 and references theirein). Consequently, redox boundaries within the sediment generally also deepen as a function of water depth, as oxygen consumption in the sediment decreases. Such a fundamental organic matter-depth relation is in line with the much deeper oxygen penetration depths at stations A and B compared to the more shallow stations. At station F the relative shallow oxygen penetration depth observed is consistent with it's relatively shallow water depth, although the organic matter which arrives here at the seafloor apparently undergoes winnowing (Fontanier

et al., 2008). The organic matter along the transect studied is concentrated at a so-called depocenter, which largely coincides with the depths of stations C and D (Fontanier et al., 2008). As bottom waters at all stations are well oxygenated, organic matter concentration can be considered the main control for redox conditions at stations F-A, with the amount of organic matter arriving at the seabed being regulated by water depth and sedimentary processes, such as focusing versus winnowing.

At stations C, D and F, the oxygen penetration depth and the Mn^{2+} redox boundaries are at the same depth, as expected. Station F shows the shallowest OPD of all stations, although the organic matter concentration is relatively low. One explanation for this observation is that a lower porosity at F (56% versus 76% and 79% at stations D and E, respectively) impedes oxygen diffusion through the sediment. Alternatively, the pore water profile reflects an earlier organic matter deposition event, with this organic matter being largely consumed at the time of sampling. The pore water profiles require more time to re-equilibrate to the new conditions (Burdige and Gieskes, 1983). At station E there is a mismatch between oxygen penetration depth and the Mn^{2+} redox boundary as the Mn^{2+} redox boundary is considerably deeper than the OPD. Although this is in line with the observed higher bioirrigation at this station (Fontanier et al., 2008), this might reflect non-equilibrium conditions as well.

The vertical distribution of benthic foraminiferal species varies between stations, in accordance with organic matter concentrations and redox zonation, which is consistent with the TROX model (Jorissen et al., 1995; Fontanier et al., 2008). In case of a shallower redox zone, infaunal benthic foraminifera biomineralize in contact with Mn-enriched pore water, with highest dissolved manganese concentrations occurring just below the oxygen penetration depth at all stations, except for station E (552 m). This is in contrast to low bottom-water oxygen environments often studied in the context of proxy development studies, where pore water Mn^{2+} is released from the pore water (Koho et al., 2015, 2017; Mangini et al., 2001).

The species studied here cover the range of shallow-infauna to intermediate-infauna niches. Both *U. mediterranea* and *M. barleeanus* were in the Gulf of Lions found to occupy shallow to intermediate infaunal habitat, with *U. peregrina* having a somewhat shallower infaunal habitat (Fontanier et al., 2008). *Hoeglundina elegans*, a typically shallow infaunal species, is often found close to the sediment-water interface (Jorissen et al., 1998; Schönfeld 2001; Fontanier et al., 2002; Fontanier et al., 2008) and contains the lowest concentration of Mn in its test. Only at the shallowest station (350 m) do three specimens of *H. elegans* show concentrations above the detection level, with values still low compared to the values observed for the other species (Figure 6). In the Bay of Biscay Reichart et al., (2003) also suggested that elevated Mn concentrations in *H. elegans* were confined to stations with oxygen depleted bottom waters and/or with a shallow oxygen penetration depth. *Uvigerina mediterranea* and *Uvigerina peregrina* are also classed as shallow-infaunal species; they are typically found within the top few centimeters of the sediment column (Fontanier et al., 2002, Fontanier et al., 2008). The calculated average living depth (ALD_{10}) as calculated in Fontanier et al., (2008) is consistently

shallower than the ALD_{10} for *U. mediterranea*. This is at odds with previous reports suggesting *U. peregrina* has a slightly deeper microhabitat than *U. mediterranea* (Fontanier et al., 2002; 2006). That *U. peregrina* has a deeper microhabitat is further supported by the distinct $\delta^{13}C$ offset in *U. peregrina,* which is more depleted compared to *U. mediterranea* (Schmiedl et al., 2004; Fontanier et al., 2002, 2006). The higher Mn/Ca values observed here for *U. peregrina* (Figure 6) supports the idea that it calcifies somewhat deeper in the sediment compared to *U. mediterranea*. Alternatively, *U. peregrina* may migrate downwards within burrows to track food resources, recording redox steepness (Loubere et al., 1995). This could highlight a disparity between the assumed living depth (the depth interval of recovery) and biomineralization depth of foraminifera. Still, this would also result in a higher variability of Mn/Ca values at higher Mn/Ca levels, which is not observed. Hence, more likely the observed disparity between the geochemical signals incorporated into foraminiferal calcite and depth of recovery in *U. peregrina* reflects opportunistic behaviour, with calcification at a shallower in-sediment depth in response to more favourable conditions after e.g. seasonal peaks in organic matter fluxes (Accornero et al., 2003), when the OPD is close to the sediment water interface.

Melonis barleeanus, generally considered an intermediate-infaunal species (Fontanier et al., 2002, 2008), contains the highest concentrations of Mn in its test, which is in line with the deepest habitat of the species studied here. Manganese incorporation in this species increases with increasing labile organic matter (Figure 7a).

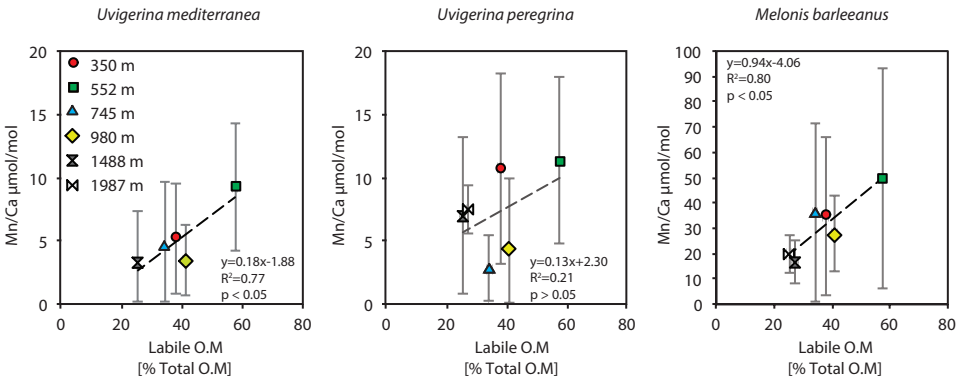

Figure 7 | Plots of average Mn/Ca µmol mol^{-1} versus labile organic matter (% total organic matter).

In summary, the habitat preference of the benthic foraminiferal species studied here is reflected in the Mn/Ca values recorded in their tests. This is in contrast with other results showing lower Mn/Ca values in foraminiferal tests with shallower redox fronts (Koho et al., 2015). This, however, critically depends on the Mn being released to the water column, which only occurs when the bottom waters are disoxic. In case of a seasonal organic matter deposition event,

an increase of Mn concentration in foraminiferal test carbonate would initially occur in the deeper and ultimately also in the more shallow calcifying foraminifera. This is in line with the conceptual TROXCHEM[3] model, with the conditions studied here falling within the first stage of the temporal succession considered in the model. Bottom water remains well oxygenated (O_2 concentrations at the study area: 199–219 µmol/l (Fontanier et al., 2008)) and organic matter loading is controlling Mn^{2+} concentrations in the sediment. To what extent species are high in Mn/Ca depends on living depth and opportunistic behavior.

At a given location, a benthic foraminiferal species' depth preference or biomineralization depth, is reflected in its average Mn/Ca value (Figure 5). The trend across a depth transect shows a strong correlation to labile organic matter concentrations in the surface sediments (Figure 7). The strong correlation between labile organic matter (i.e. sedimentary lipid content) and Mn incorporation in shallow and intermediate infaunal species *U. mediterranea* ($R^2 = 0.80$ ($p < 0.05$) suggests that test Mn has potential as a proxy for detecting past labile organic matter fluxes. Noteably, *M. barleeanus* has a very strong correlation (0.81), though this correlation lacks statistical significance ($p > 0.05$). In contrast, *U. peregrina* shows a correlation coefficient of only 0.45 (R^2) between test Mn and labile organic matter. *Uvigerina peregrina* is reported to respond opportunistically to the concentration and quality of organic matter produced during bloom events (Fontanier et al., 2003; Koho et al., 2008; Barras et al., 2010). This response is in the form of increased reproduction and growth. Perhaps *U. peregrina* calcifies preferentially at shallower depths and therefore does not capture the full Mn^{2+} gradient.

At low oxygen concentrations Mn is released through the reduction of manganese (oxy) hydroxides. Here we show an increase in Mn/Ca incorporation in several species, from shallow to intermediate-depth infaunal habitats, as a function of oxygen penetration depth. Such a correlation agrees with studies by Ní Fhlaithearta et al., (2010) and McKay et al., (2015) from a down core record of $Mn/Ca_{H.\ elegans}$ during the formation of sapropel (S1) in the Eastern Mediterranean and a paleoproductivity study of an upwelling system in the NE Atlantic, respectively. Here, a comparison of Mn (oxy)hydroxides in the sediment and foraminiferal Mn^{2+} showed that Mn^{2+} incorporation in an epifaunal to shallow infaunal species was higher during times of enhanced Mn^{2+} remobilization and hence higher pore water Mn^{2+}. Such a correlation, however, requires that the bottom waters remain somewhat oxygenated to retain the dissolved Mn^{2+} in the pore water. With disoxic bottom waters Mn^{2+} escapes the pore water and foraminiferal Mn/Ca values decrease (Koho et al., 2015). However, with high organic matter deposition, which might be concentrated in events, also foraminiferal species living at or close to the sediment water interface may show elevated Mn concentrations.

In addition to the here observed changes, biomineralization could affect Mn^{2+} incorporation. In a controlled laboratory study by Munsel et al., (2010) Mn incorporation in *Ammonia tepida* increased with increasing Mn^{2+} concentrations in the culture water and the partition coefficient was well above 1. The lack of an appreciable discrimination argues against a major biomineralization impact on Mn^{2+} partitioning. Recently Barras et al., (2018), also

using controlled growth experiments, showed, however, that Mn partitioning in *B. marginata* differs from that in *A. tepida*, with that in *B. marginat* being close to one and that of *A. tepida* being 4 times lower. Inter-specific differences are considerable and hence an impact of biomineralization on Mn incorporation cannot be disregarded.

In summary, Mn incorporation seems primarily controlled by pore water conditions in close proximity to the test, biomineralization and with a secondary control determined by the ability of a foraminifer to seasonally calcify and migrate within the sediment.

4.2 | Pore water Mn dynamics and foraminiferal migration within the sediment

Manganese is incorporated in foraminiferal carbonate with a partition coefficient (D) close to 1 or somewhat lower (Munsel et al., 2010; Barras et al., 2018). We calculated Mn partition coefficients for *U. mediterranea*, *U. peregrina* and *M. barleeanus* at stations E, C and B (Table 6) based on average Mn/Ca_{foram} and average $Mn/Ca_{pore\ water}$ values found above the Mn^{2+}–MnO(H) redox boundary. Calculated D_{Mn} agrees with the previously reported D_{Mn} by Munsel et al., (2010), with values varying between ~ 1–2 for *U. mediterranea* and *U. peregrina*. The Mn partition coefficient for *Melonis barleeanus* ranges from ~ 4–7. The partition coefficient for this species most likely reflects its capacity to calcify under dysoxic conditions, close to or even below the oxygen penetration depth. Still, this calculation is based on two assumptions: (1) the depth foraminifera are recovered from during sampling corresponds with the average depth of calcification and, (2) variation in pore water is limited. Establishing species specific Mn partitioning coefficients using culture experiments might, however, be needed for unlocking the full potential of this proxy (Barras et al., 2018).

Table 5 | Relative standard deviation (% RSD) of inter-individual values in Mn/Ca within four species of benthic foraminifera (*H. elegans*, *U. mediterranea*, *U. peregrina* and *M. barleeanus*).

Element	*H. elegans* % RSD	*U. mediterranea* % RSD	*U. peregrina* % RSD	*M. barleeanus* % RSD
Mn	400	125	87	97

Table 6 | Manganese pore water – carbonate partition coefficient for foraminiferal species *U. mediterranea*, *U. peregrina* and *M. barleeanus*.

	Partition coefficient (D)[1]		
Station	*U. mediterranea*	*U. peregrina*	*M. barleeanus*
E (552 m)	1.7	1.8	7.0
C (980 m)	1.2	–	5.1
B (1488 m)	2.2	2.3	4.1

[1] Pore water-carbonate partition coefficients were calculated using the average pore water Mn/Ca [µmol/mol^{-1}] measured above the oxygen penetration depth and the average carbonate Mn/Ca [umol/mol^{-1}] measured in *U. mediterranea*, *U. peregrina* and *M. barleenanus*, for all specimens recovered above the reported oxygen penetration depth (Fontanier et al., 2008).

A foraminifer calcifying within a steep Mn^{2+} gradient is exposed to a higher range of Mn^{2+} concentrations (over a fixed depth interval) compared to specimens living along a more gradual Mn^{2+} concentration gradient. Since foraminifera can migrate through the sediment as a response to food availability and oxygen concentrations (Alve and Bernhard 1995; Gross, 2000), not only the slope of the Mn gradient, but also the in-sediment depth range (microhabitat) of the foraminifer in relation to the Mn redox boundary, should be considered (Figure 8). Although the analyses of foraminiferal test Mn/Ca is challenging, which adds to the inter-specimen variability, we observe systematic differences between species in Mn/Ca variability. A shallow-infaunal species, with a limited in-sediment range, would be expected to exhibit lower variability than an intermediate- infauna species, which possibly migrates considerably in depth. This is exemplified at station F (350 m) where we note an increase in foraminiferal test Mn/Ca variability at 2 cm depth, consistent with the oxygen penetration depth at that station (Figure 3). Moreover, the variability in Mn/Ca values increases towards higher Mn/Ca values. This is in line with the depth habitat of *M. barleeanus* being consistently deeper and this species traveling more actively through the redox zones than *U. mediterranea* or *U. peregrina*. Nitrate respiration could be a mechanism allowing this dynamic behaviour by *M. barleeanus* in the intermediate depth habitat. However, Pina-Ochao et al., (2010), studying denitrification in foraminifera, reports nitrate storage in all three species mentioned here. Notably, nitrate storage in *M. barleeanus* is lower than *U. mediterranea* and *U. peregrina*. Alternatively *M. barleeanus* thrives in habitats with varying oxygenation and hence also varying Mn levels, whereas the stable but high Mn/Ca values in the Uvigerinids are related to their opportunistic behaviour.

With a redox-sensitive element such as Mn, in a dynamic geochemical environment, it is not surprising that foraminifera exhibit high inter-individual variability in their Mn/Ca incorporation. Benthic foraminifera reside in a 3D geochemical mosaic, as reflected by a large spread of Mn values, in addition to undergoing substantial temporal variability. Still, using Mn/Ca as a potential proxy for redox conditions or primary productivity seems promising, as established ecological characteristics of species are reflected by differences in Mn incorporation. Apparently the large variability on both spatial and temporal scales averages out, making Mn into a promising proxy for paleo-redox and organic matter flux.

5 | CONCLUSION

This study investigates the link between benthic foraminiferal habitat preferences and manganese incorporation in their tests. Manganese incorporation increases with bottom-arriving labile organic matter content, driven by enhanced oxygen demand. This results in a more shallow oxygen penetration depth with immediately below it enhanced dissolved Mn levels. Shallow infaunal species calcify under lower concentrations of Mn compared to

intermediate infauna, agreement with their depth preference. Their depth habitat is related to in-sediment changes in redox conditions. However, their distribution does not necessarily vary synchronously with changes in redox zonation, as illustrated by the Mn/Ca variability in their tests (Figure 8). The latter reflects the Mn/Ca pore water composition, which itself is directly related to reactive organic matter concentration and redox conditions. The foraminiferal Mn/Ca ratio and inter-specimen variability, therefore, provides information on past Mn cycling within the sediment. Consequently, foraminiferal Mn/Ca ratio is a potential proxy for bottom-water oxygenation and organic matter fluxes.

ACKNOWLEDGEMENTS

We thank captain and crew of the N/O Téthys 2 (CNRS-INSU) for their assistance during the *BEHEMOTH* campaign. We acknowledge the technical assistance given by Christine Barras, Mélissa Gaultier, Sophie Terrien and Gérard Chabaud from Angers and Bordeaux University. We thank Serge Berné and Laetitia Maltese (Ifremer), for providing us with maps of the study area and Xavier Durrieu de Madron (Perpignan University) for discussions about water column structure. Helen de Waard (LA-ICP-MS) and Karoliina Koho (SEM) (Utrecht University) are acknowledged for their laboratory assistance. The associate editor and two anonymous reviewers are acknowledged for their helpful comments. The Darwin Center for Biogeosciences provided partial funding for this project. This paper contributes to the Netherlands Earth Systems Science Center (NESSC -www.nessc.nl)

REFERENCES

Accornero, A., Picon, P., De Bovée, F., Charrière, B., & Buscail, R.: Organic carbon budget at the sediment-water interface on the Gulf of Lions continental margin. Continental Shelf Research, 23(1), 79–92, 2003.

Alve, E., & Bernhard, J. M.: Vertical migratory response of benthic foraminifera to controlled oxygen concentrations in an experimental mesocosm. Oceanographic Literature Review, 9(42), 771, 137–151, 1995.

Arndt, S., Jørgensen, B. B., LaRowe, D. E., Middelburg, J. J., Pancost, R. D. and Regnier, P.: Quantifying the degradation of organic matter in marine sediments: A review and synthesis, Earth-Science Rev., 123, 53–86, doi:10.1016/j.earscirev.2013.02.008, 2013.

Barnett, P. R. O., Watson, J. and Connely, D.: A multiple corer for taking virtually undisturbed sample from shelf, bathyal and abyssal sediments, Oceanologica Acta, 7, 399–408, 1984.

Barras, C., Fontanier, C., Jorissen, F. and Hohenegger, J.: A comparison of spatial and temporal variability of living benthic foraminiferal faunas at 550 m depth in the Bay of Biscay, Micropaleontology, 56, 275–295, 2010.

Barras, C., Mouret, A., Nardelli, M. P., Metzger, E., Petersen, J., La, C., Filipsson, H. L., Jorissen, F.: Experimental calibration of manganese incorporation in foraminiferal calcite, Geochim. Cosmochim. Acta, 237, 49–64, 2018.

Boyle, E. A.: Manganese carbonate overgrowths on foraminifera tests, Geochim. Cosmochim. Acta, 47, 1815–1819, doi:10.1016/0016-7037(83)90029-7, 1983.

Burdige, D. J. and Gieskes, J. M.: A pore water/solid phase diagenetic model for manganese in marine sediments. American Journal of Science, 283(1), 29–47, 1983.

De Lange, G. J.: Early diagenetic reactions in interbedded pelagic and turbiditic sediments in the Nares Abyssal Plain (western North Atlantic): Consequences for the composition of sediment and interstitial water, Geochim. Cosmochim. Acta, 50(12), 2543–2561, doi:10.1016/0016-7037(86)90209-7, 1986.

Dueñas-Bohórquez, A., Rocha, R., Kuroyanagi, A., de Nooijer, L., Bijma, J., Reichart, G. J.: Interindividual variability and ontogenetic effects on Mg and Sr incorporation in the planktonic foraminifer *Globigerinoides sacculifer.* Geochim. Cosmochim. Acta, 75 (2), 520–532, 2011.

Elderfield, H., Yu, J., Anand, P., Kiefer, T. and Nyland, B.: Calibrations for benthic foraminiferal Mg/Ca paleothermometry and the carbonate ion hypothesis, Earth Planet. Sci. Lett., 250(3–4), 633–649, doi:10.1016/j.epsl.2006.07.041, 2006.

Fontanier, C., Jorissen, F. J., Licari, L., Alexandre, A., Anschutz, P. and Carbonel, P.: Live benthic foraminiferal faunas from the Bay of Biscay: faunal density, composition, and microhabitats, Deep Sea Research Part I: Oceanographic Research Papers, 49, 751–785, doi:10.1016/S0967-0637(01)00078-4, 2002.

Fontanier, C., Jorissen, F. J., David, C., Anschutz, P., Chaillou, G. and Lafon, V.: Seasonal and interannual variability of benthic foraminiferal faunas at 550m depth in the Bay of Biscay. Deep-Sea Research I, 50, 457–494, 2003.

Fontanier, C., Mackensen, A., Jorissen, F. J., Anschutz, P., Licari, L., & Griveaud, C.: Stable oxygen and carbon isotopes of live benthic foraminifera from the Bay of Biscay: Microhabitat impact and seasonal variability. Marine Micropaleontology, 58(3), 159–183, 2006.

Fontanier, C., Jorissen, F. J., Lansard, B., Mouret, A., Buscail, R., Schmidt, S., Kerhervé, P., Buron, F., Zaragosi, S., Hunault, G., Ernoult, E., Artero, C., Anschutz, P. and Rabouille, C.: Live foraminifera from the open slope between Grand Rhône and Petit Rhône Canyons (Gulf of Lions, NW Mediterranean), Deep. Res. Part I Oceanogr. Res. Pap., 55(11), 1532–1553, doi:10.1016/j.dsr.2008.07.003, 2008.

Froelich P. N., Klinkhammer G. P., Bender M. L., Luedtke N. A., Heath G. R., Cullen D., Dauphin P., Hammond D., Hartman B. and Maynard V.: Early oxidation of organic matter in pelagic sediments of the eastern equatorial Atlantic: suboxic diagenesis. Geochim. Cosmochim. Acta 43(1075), 1075–1090, 1979.

Glock, N., Eisenhauer, A., Liebetrau, V., Wiedenbeck, M., Hensen, C. and Nehrke, G.: EMP and SIMS studies on Mn/Ca and Fe/Ca systematics in benthic foraminifera from the Peruvian OMZ: A contribution to the identification of potential redox proxies and the impact of cleaning protocols, Biogeosciences, 9(1), 341–359, doi:10.5194/bg-9-341-2012, 2012.

Groeneveld, J. and Filipsson, H. L.: Mg/Ca and Mn/Ca ratios in benthic foraminifera: the potential to reconstruct past variations in temperature and hypoxia in shelf regions, Biogeosciences, 10(7), 5125–5138, doi:10.5194/bg-10-5125-2013, 2013.

Gross, O.: Influence of temperature, oxygen and food availability on the migrational activity of bathyal benthic foraminifera: evidence by microcosm experiments. In Life at Interfaces and Under Extreme Conditions (pp. 123–137). Springer Netherlands, 2000.

Hintz, C. J., Shaw, T. J., Chandler, G. T., Bernhard, J. M., McCorkle, D. C. and Blanks, J. K.: Trace/minor element : calcium ratios in cultured benthic foraminifera. Part I: Inter-species and inter-individual variability, Geochim. Cosmochim. Acta, 70(8), 1952–1963, doi:10.1016/j.gca.2005.12.018, 2006a.

Jochum, K. P., Weis, U., Stoll, B., Kuzmin, D., Yang, Q., Raczek, I., Jacob, D. E., Stracke, A., Birbaum, K., Frick, D. A., Gunther, D., Enzweiler, J.: Determination of Reference Values for NIST SRM 610–617 Glasses Following ISO Guidelines, Geostandards and Geoanalytical Research, 35, 4, 397–421, 2011.

Jorissen, F. J., de Stigter, H. C. and Widmark, J. G. V: A conceptual model explaining benthic foraminiferal microhabitats, Mar. Micropaleontol., 26(1–4), 3–15, doi:10.1016/0377-8398(95)00047-X, 1995.

Jorissen, F. J., Wittling, I., Peypouquet, J. P., Rabouille, C. and Relexans, J. C.: Live benthic foraminiferal faunas off Cape Blanc, NW-Africa: Community structure and microhabitats, Deep Sea Research Part I: Oceanographic Research Papers, 45, 2157–2188, doi:10.1016/S0967-0637(98)00056-9, 1998.

Koho, K. A., Langezaal, A. M., van Lith, Y. A., Duijnstee, I. A. P. and van der Zwaan, G. J.: The influence of a simulated diatom bloom on deep-sea benthic foraminifera and the activity of bacteria: A mesocosm study, Deep. Res. Part I Oceanogr. Res. Pap., 55(5), 696–719, doi:10.1016/j.dsr.2008.02.003, 2008.

Koho, K. A., Piña-Ochoa, E., Geslin, E. and Risgaard-Petersen, N.: Vertical migration, nitrate uptake and denitrification: Survival mechanisms of foraminifers (Globobulimina turgida) under low oxygen conditions, FEMS Microbiol. Ecol., 75(2), 273–283, doi:10.1111/j.1574-6941.2010.01010.x, 2011.

Koho, K. A., de Nooijer, L. J. and Reichart, G. J.: Combining benthic foraminiferal ecology and shell Mn/Ca to deconvolve past bottom water oxygenation and paleoproductivity, Geochim. Cosmochim. Acta, 165, 294–306, doi:10.1016/j.gca.2015.06.003, 2015.

Koho, K. A., De Nooijer, L. J., Fontanier, C., Toyofuku, T., Oguri, K., Kitazato, H. and Reichart, G. J.: Benthic foraminiferal Mn/Ca ratios reflect microhabitat preferences, Biogeosciences, 14(12), 3067–3082, doi:10.5194/bg-14-3067-2017, 2017

Lea, D. and Boyle, E.: Barium content of benthic foraminifera controlled by bottom-water composition, Nature, 338, 751–753, 1989.

Lewis, E., and Wallace, D. W. R.: Program Developed for CO2 Systems Calculations. ORNL/CDIAC-105, Carbon Dioxide Information Analysis Centre, Oak Ridge National Laboratory U.S. Department of Energy, Oak Ridge, Tennessee, 1998.

Loubere, P., Meyers, P., and Gary, A.: Benthic foraminiferal microhabitat selection, carbon isotope values, and association with larger animals: A test with uvigerina peregrina, Journal of Foraminiferal Research, 25, 83–95. doi:10.2113/gsjfr.25.1.83, 1995.

Mangini, A., Jung, M. and Laukenmann, S.: What do we learn from peaks of uranium and of manganese in deep sea sediments?, Mar. Geol., 177(1–2), 63–78, doi:10.1016/S0025-3227(01)00124-4, 2001.

McKay, C. L., Groeneveld, J., Filipsson, H. L., Gallego-Torres, D., Whitehouse, M. J., Toyofuku, T. and Romero, O. E.: A comparison of benthic foraminiferal Mn/Ca and sedimentary Mn / Al as proxies of relative bottom-water oxygenation in the low-latitude NE Atlantic upwelling system, Biogeosciences, 12(18), 5415–5428, doi:10.5194/bg-12-5415-2015, 2015.

Munsel, D., Kramar, U., Dissard, D., Nehrke, G., Berner, Z., Bijma, J., Reichart, G. J. and Neumann, T.: Heavy metal incorporation in foraminiferal calcite: Results from multi-element enrichment culture experiments with Ammonia tepida, Biogeosciences, 7(8), 2339–2350, doi:10.5194/bg-7-2339-2010, 2010.

Ní Fhlaithearta, S., Reichart, G.-J., Jorissen, F. J., Fontanier, C., Rohling, E. J., Thomson, J. & de Lange, G. J.: Reconstructing the seafloor environment during sapropel formation using benthic foraminiferal trace metals, stable isotopes, and sediment composition. Paleoceanography, 25(4), PA4225, 2010. doi:10.1029/2009PA001869

Ní Fhlaithearta, S., Ernst, S. R., Nierop, K. G. J., de Lange, G. J. and Reichart, G.-J.: Molecular and isotopic composition of foraminiferal organic linings, Mar. Micropaleontol., 102, 69–78, doi:10.1016/j.marmicro.2013.06.004, 2013.

Nürnberg, D., Bijma, J. and Hemleben, C.: Assessing the reliability of magnesium in foraminiferal calcite as a proxy for water mass temperatures, Geochim. Cosmochim. Acta, 60(5), 803–814, doi:10.1016/0016-7037(95)00446-7, 1996.

Pina-Ochoa, E., Hogslund, S., Geslin, E., Cedhagen, T., Revsbech, N. P., Nielsen, L. P., Schweizer, M., Jorissen, F., Rysgaard, S. and Risgaard-Petersen, N.: Widespread occurrence of nitrate storage and denitrification among Foraminifera and Gromiida, Proc. Natl. Acad. Sci., 107(3), 1148–1153, doi:10.1073/pnas.0908440107, 2010.

Reichart, G. J., Jorissen, F., Anschutz, P. and Mason, P. R. D.: Single foraminiferal test chemistry records the marine environment, Geology, 31(4), 355–358, doi:10.1130/0091-7613(2003)031<0355:SFTCRT>2.0.CO;2, 2003.

Risgaard-Petersen, N., Langezaal, A. M., Ingvardsen, S., Schmid, M. C., Jetten, M. S. M., Op Den Camp, H. J. M., Derksen, J. W. M., Piña-Ochoa, E., Eriksson, S. P., Nielsen, L. P., Revsbech, N. P., Cedhagen, T. and Van Der Zwaan, G. J.: Evidence for complete denitrification in a benthic foraminifer, Nature, 443(7107), 93–96, doi:10.1038/nature05070, 2006.

Rosenthal, Y., Morley, A., Barras, C., Katz, M. E., Jorissen, F., Reichart, G.-J., Oppo, D. W. and Linsley, Braddock. K.: Temperature calibration of Mg/Ca ratios in the intermediate water benthic foraminifera Hyalinea Balthica, Geochem. Geophys. Geosyst., 12(4), 2011. doi:10.1029/2010GC003333

Schönfeld, J.: Benthic foraminifera and pore water oxygen profiles: A reassessment of species boundary conditions at the Western Iberian margin, Journal of Foraminiferal Research, 31, 86–107, doi:10.2113/0310086, 2001.

Schmiedl, G., Pfeilsticker, M., Hemleben, C., Mackensen, A.: Environmental and biological effects on the stable isotope composition of recent deep-sea benthic foraminifera from the western Mediterranean Sea Mar. Micropaleontol., 51, 129–152, doi:10.1016/j.marmicro.2003.10.001, 2004.

Van Cappellen, P. and Wang, Y.: Cycling of iron and manganese in surface sediments: A general theory for the coupled transport and reaction of carbon, oxygen, nitrogen, sulfur, iron, and manganese, Am. J. Sci., 296(3), 197–243, doi:10.2475/ajs.296.3.197, 1996.

Wang, Y. and Van Cappellen, P.: A multicomponent reactive transport model of early diagenesis: Application to redox cycling in coastal marine sediments, Geochim. Cosmochim. Acta, 60(16), 2993–3014, doi:10.1016/0016-7037(96)00140-8, 1996.

Wit, J. C., De Nooijer, L. J., Barras, C., Jorissen, F. J. and Reichart, G. J.: A reappraisal of the vital effect in cultured benthic foraminifer Bulimina marginata on Mg/Ca values: Assessing temperature uncertainty relationships, Biogeosciences, 9(9), 3693–3704, doi:10.5194/bg-9-3693-2012, 2012.

Yu, J. and Elderfield, H.: Benthic foraminiferal B/Ca ratios reflect deep water carbonate saturation state, Earth Planet. Sci. Lett., 258(1–2), 73–86, doi:10.1016/j.epsl.2007.03.025, 2007.

4

Mg/Ca, Sr/Ca and Ba/Ca incorporation in living (stained) benthic foraminifera: A bathymetric and microhabitat study in the Gulf of Lions (NW Mediterranean)

Shauna Ní Fhlaithearta[1], Christophe Fontanier[2,3,4], Frans Jorissen[4], Aurélia Mouret[5], Adriana Dueñas-Bohórquez[1], Pierre Anschutz[6], Mattias B. Fricker[7], Detlef Günther[7], Gert J. de Lange[1], Gert-Jan Reichart[1,8]

[1]Faculty of Geosciences, Utrecht University, Utrecht, The Netherlands.
[2]Université de Bordeaux, CNRS, Environnements et Paléo-environnements Océaniques et Continentaux, UMR 61125805, F-33600 Pessac, France
[3]FORAM, Foraminiferal Study Group, F-29200, Brest, France
[4]University of Angers, France
[5]CNRS UMR 6112 LPG-BIAF, Angers University, 49045 Angers Cedex, France
[6]UMR 5805 Environnements et Paléoenvironnements Océaniques et Continentaux (EPOC-OASU), University of Bordeaux, Avenue des Facultés, 33405 Talence Cedex, France.
[7]Laboratory of Inorganic Chemistry, ETH Zurich, 8093 Zurich, Switzerland.
[8]Royal NIOZ, Netherlands Institute for Sea Research, department of Ocean Systems.

ABSTRACT

Minor and trace element incorporation in benthic foraminiferal carbonate was investigated across a depth transect in the Gulf of Lions, NW Mediterranean, to investigate the link between trace-metal incorporation in foraminiferal carbonate and foraminiferal ecology. Water depth increases from 350 to 1987 m, while temperature (~ 13 °C) and salinity (~ 38.5) remain relatively constant. Magnesium, strontium and barium concentrations in the tests of living (stained) specimens of the benthic foraminiferal species, *Hoeglundina elegans*, *Melonis barleeanus, Uvigerina mediterranea*, *Uvigerina peregrina* were measured using laser ablation inductively coupled mass spectrometry (laser ablation ICP-MS). Mg/Ca and Sr/Ca ratios remain relatively stable with increasing water depth, with Mg exhibiting much high inter-individual variability. Mg/Ca and Sr/Ca values are compared to existing temperature calibrations to validate applicability to the Mediterranean. *Uvigerina peregrina* has a distinctly different Mg/Ca signature compared to *U. mediterranea*, advising against grouping these species in the same empirical Mg/Ca-temperature relationships. Sr/Ca in *H. elegans* appears to reflect temperature as expected on the basis of existing calibrations. Although foraminiferal Mn/Ca has been shown to record pore water chemistry (Chapter 4), in-sediment changes in Ba^{2+} are not reflected by the Ba/Ca ratios in the test of living (i.e stained) foraminifera from the same cores. *Hoeglundina elegans* shows overall high Ba concentrations compared to the other species, which seems mainly associated with its aragonitic test. *Melonis barleeanus* exhibits high variability, which may reflect its migration through the sediment.

1 | INTRODUCTION

Many benthic foraminiferal species live within the sediment and precipitate their calcium carbonate tests in contact with pore water. As such, the trace-metal composition of pore water affects the chemistry of their carbonate test and hence the incorporation of trace metals. This effectively links benthic foraminiferal microhabitat preference and pore water chemistry. This was shown for stable carbon isotopes (Fontanier et al., 2006; Chapter 5) and more recently also for Mn incorporation (Koho et al., 2015; 2017; Chapter 3). However, whether this also is applicable to other minor and trace elements and to what extent pore water profiles are reflected in foraminiferal carbonate test chemistry remains to be investigated.

Since the early 1990's the trace element composition of benthic foraminiferal tests has become a frequently used tool for the reconstruction of past ocean conditions (Boyle 1981, Elderfield and Ganssen, 2000, Lea et al., 2002, Nürnberg et al., 1996). For instance, Mg incorporated in test carbonate is used to reconstruct past temperatures, foraminiferal Ba and Cd records are used as a proxy for seawater nutrient conditions, and B has been related to the carbonate chemistry of seawater (Boyle et al., 1995, Lea and Boyle 1989, Lear et al., 2000, Yu and Elderfield 2007). Core top calibrations and controlled growth experiments both contributed to our knowledge of the incorporation of these elements into test carbonate and how this correlates to the environment. At the same time these studies also revealed the role of biomineralization on trace-metal incorporation (de Nooijer et al., 2014, and references therein), as well as an impact from metabolic growth rates. Biology in general probably also plays a role in affecting foraminiferal trace-metal proxies via species-specific ecology as foraminiferal microhabitats within the sediment exposes them to different pore water chemistries. Since this clearly impacts the correlation between bottom water composition and proxies, interestingly, with known depth habitat and ecological preferences of benthic foraminiferal species (and established partitioning coefficients) it might be possible to reconstruct past pore water trace-metal profiles. Such paleo pore water profiles ultimately would allow us to unravel past changes in bottom water oxygenation and organic matter fluxes arriving at the seafloor (Koho et al., 2015).

Here we investigate the link between trace-metal incorporation and benthic foraminiferal microhabitat preferences. Along a 6-station bathymetric transect in the Gulf of Lions, NW Mediterranean, four species with contrasting depth-habitat preferences were selected for investigating their minor and trace-metal incorporation. Living (i.e. Bengal Rose stained) individuals were picked from a series of sediment depths and analyzed by laser ablation ICP-MS, enabling multiple analyses of individual specimens. The Mn incorporation of these species was discussed recently in a separate paper (Chapter 3, Ní Fhlaithearta et al., 2018), specifically targeting the potential application of foraminiferal Mn incorporation as redox proxy. The study presented here is a first step towards a multi-species, multi-element, calibration ultimately needed to better constrain past pore water profiles.

2 | MATERIAL AND METHODS

Cores were collected with a classical Barnett multicorer (Barnett et al. 1984) at 6 stations from the Gulf of Lions (NW Mediterranean) during the 2006 BEHEMOTH cruise (Figure 1, Table 1). The 6 stations describe a bathymetric transect from 350 to 1987m depth. The shallowest site at 350 m (station F) is bathed by Mediterranean Intermediate Water (MIW). The stations at 552 m (station E) and 745 m (station D) water depth are positioned in the diffusive boundary layer separating MIW and Western Mediterranean Deep Water (WMDW). The stations at 980 m (Station C), 1488 m (station B) and 1987 m (station A) are bathed by the WMDW. Bottom water temperature is stable through the water column (~ 13.1°C) (Xavier Durrieu de Madron, personal communication, 2006). Salinity ranges between 38.4 and 38.5. The multicorer allowed sampling of the first decimeters of the sediment, the overlying bottom waters, and an undisturbed sediment-water interface. Cores were sliced for foraminiferal studies with a 0.5–cm resolution down to 4 cm, followed by 1 cm slices down to 10 cm depth. Sediments were put in an ethanol-Rose Bengal mixture (95% ethanol with 1g/l Rose Bengal), in order to identify living (stained) specimens.

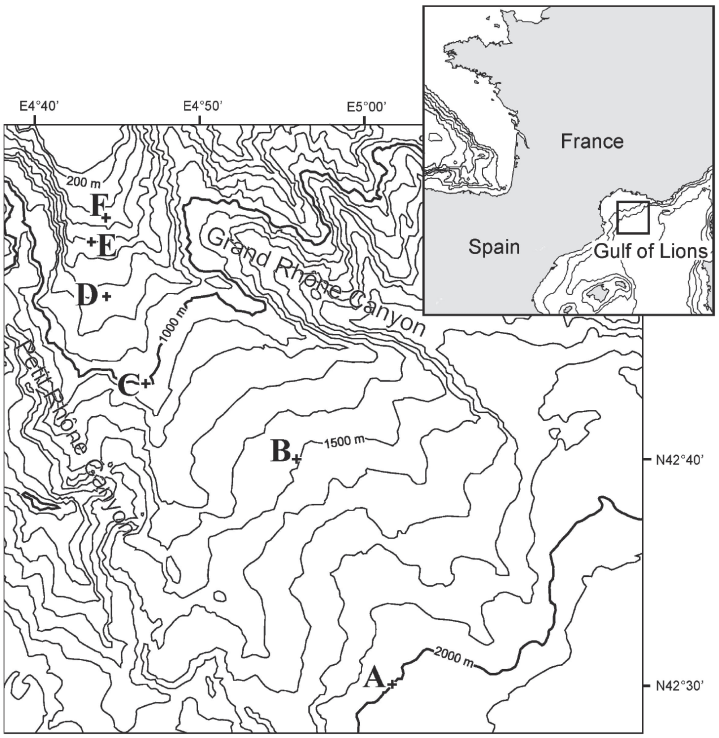

Figure 1 | Location map showing stations and bathymetry.

Table 1 | Water depth, coordinates and bottom water physio-chemical parameters: Temperature (°C), salinity, and oxygen penetration depth mm) for six stations F–A.

Station	Depth (m)	Latitude (N)	Longitude (E)	Bottom water temperature* (°C)	Bottom water salinity *	Oxygen penetration depth (mm)
F	350	42°52'32	4°42'43	13.2	~ 38.5	20.5 ± 3.3
E	552	42°48'78	4°43'21	13.2	~ 38.5	57.2 ± 4.5
D	745	42°46'66	4°43'91	13.1	~ 38.5	36.5 ± 1.6
C	980	42°43'18	4°46'58	13.1	~ 38.48	50.7 ± 6.3
B	1488	42°38'83	4°56'03	13.1	~ 38.46	141.5 ± 0.0
A	1987	42°28'25	5°00'61	13.1	~ 38.46	197.0 ± 11.0

(* Xavier Durrieu de Madron, personal communication, 2006)

Sediment sampling for pore water extraction was carried out under an inert atmosphere (N_2). Hereafter, samples were centrifuged at 5000 rpm for 20 min. The supernatant was filtered and acidified (HNO_3 s.p.) for dissolved metals analyses (Fontanier et al., 2008). A pore water subsample was analyzed for Ba from each depth, using an ICP-MS (Agilent 7500 Series). Relative precision for this method is better than 3%, based on analyses of duplicates and standards. Total alkalinity of pore water was measured at Utrecht University using an automated titrator (702 SM Titrino, Metrohm). Dissolved Inorganic Carbon (DIC) was measured using a Total Organic Carbon Analyser (Shimadzu, Model TOC-5050A). Carbonate ion concentrations were calculated using the CO2SYS software (version 01.05; Lewis and Wallace, 1998).

Pore water oxygen concentration profiles were determined using polarographic oxygen microelectrodes (Unisense); for details, see Fontanier et al., (2008). Labile organic matter was derived from sum of the lipids, amino acids and sugars measured in the top cm of sediment; for details, see Fontanier et al., (2008).

Foraminiferal trace element concentrations were determined using laser ablation ICP-MS at two different laboratories. Prior to laser ablation, all samples were gently cleaned in methanol (x 1) and UHQ water (x 4). Between each rinse, the samples were placed in a sonic bath for several seconds to thoroughly clean the tests. Benthic foraminifera from 745 m (station D), 980 m (station C), 1488 m (station B) and 1987 m (station A) were measured at Utrecht University using a deep UV (193 nm) ArF excimer laser (Lambda Physik) with GeoLas 200Q optics. Ablation was performed at a pulse repetition rate of 10 Hz, and energy density of 1.4 J/cm^2, with a crater size of 80 µm. Ablated particles were measured by a quadrupole ICP-MS (Micromass Platform) equipped with a collision and reaction cell. Such a collision and reaction cell improves carbonate analyses by eliminating interferences on mass 44. Benthic foraminifera from 350 m (station F) and 552 m (station E) were analyzed at ETH-Zurich. The laser type and ablation parameters were identical to those detailed above. The ablated particles were measured using a quadrupole ICP-MS (ELAN 6100 DRC, Perkin-Elmer). In both cases, calibration was performed using an international standard (NIST612) with Ca as an internal standard and

relative concentrations based on Jochum et al., (2011). Inter-laboratory compatibility was monitored using an in-house calcite standard (GJR). Isotopes used for element quantification were ^{27}Al, ^{24}Mg, ^{88}Sr, ^{138}Ba and ^{208}Pb. To rule out potential interference on ^{24}Mg by $^{12}C^{12}C^{+}$, ^{26}Mg was also measured to confirm the correct isotopic ratio between the Mg isotopes.

Analytical uncertainty (equivalent to 1 σ), based on repeated measurement of an external standard, was < 5% for reported elements. Each laser ablation measurement was screened for contamination by monitoring Al and Pb. On encountering surface contamination, the data integration interval was adjusted to exclude any Al or Pb enrichment. Cross-plots between Al and Pb versus Ba, Mg and Sr showed that they are unrelated.

During the laser ablation analyses the different trace elements were monitored with respect to time, thus representing a cross section of the test wall. This allows not only quantification of the different trace metals of interest, but also to observe variability within individual tests. A typical ablation profile for *Hoeglundina elegans* is shown in Figure 2.

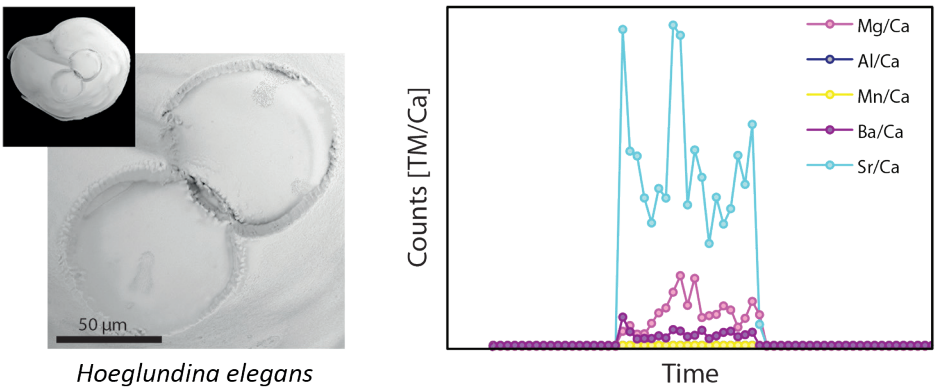

Figure 2 | (**a**) Detail of SEM laser ablation craters on *Hoeglundina elegans*. The inset is an overview SEM of a sampled test. (**b**) Example of laser ablation profiles, signal trace metal/Ca count ratios through time.

3 | RESULTS

3.1 | Pore water data

Pore-water dissolved barium (Ba^{2+}) was measured at 552 m, 980 m and 1488 m water depth (station E, C and B, respectively). Barium (Ba^{2+}) concentrations increased with sediment depth (Figure 3). Dissolved inorganic carbon (DIC) and total alkalinity (TA), were measured at 552 m (station E), 980 m (station C) and 1488 m (station B) (Figure 4). At 745 m and 552 m (stations D and E), dissolved inorganic carbon concentrations in the top 10 cm have a similar range

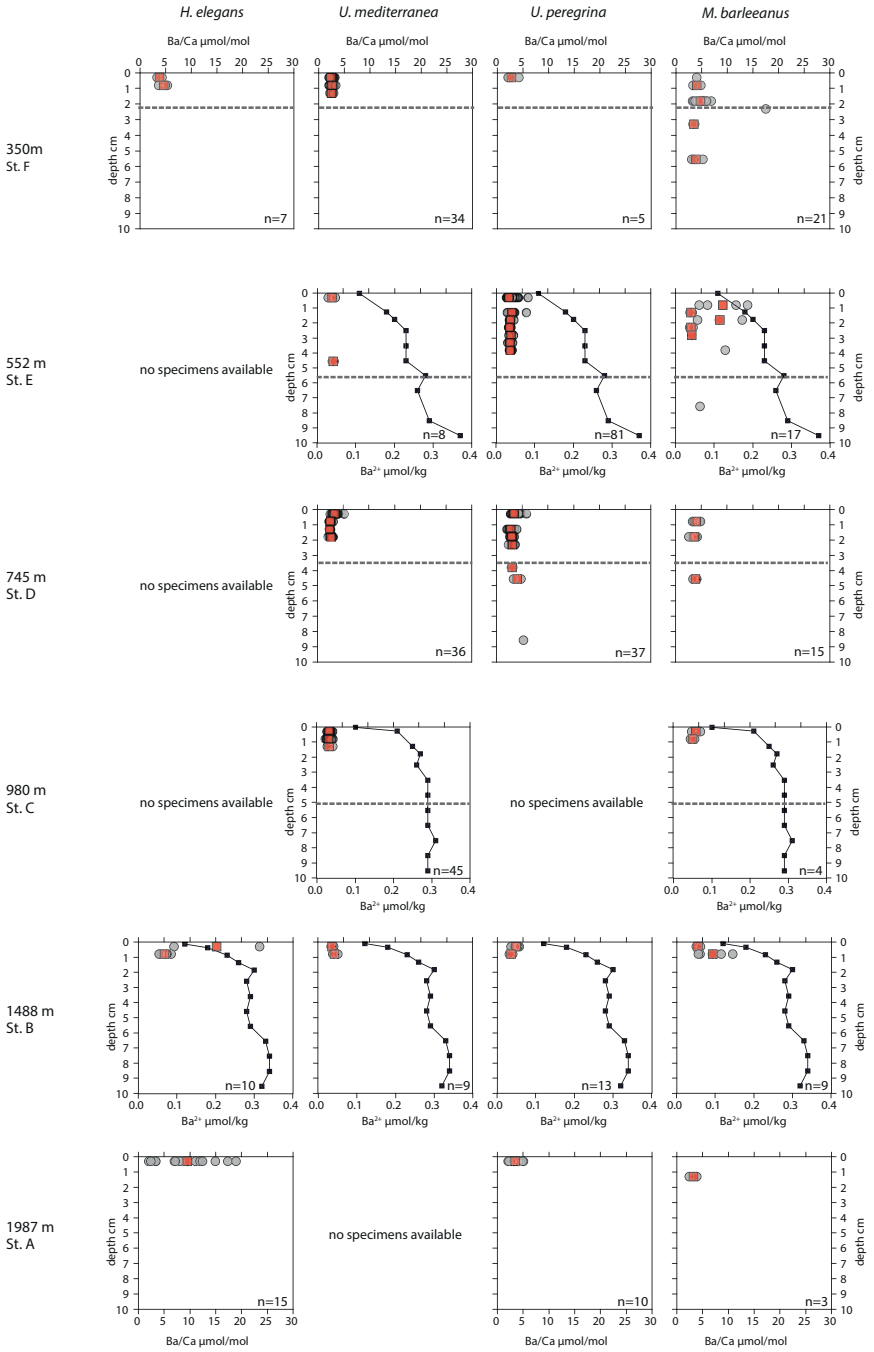

Figure 3 | Plots of Ba/Ca µmol/mol measured in *Hoeglundina elegans*, *Uvigerina mediterranea*, *Uvigerina peregrina* and *Melonis barleeanus*. Individual analyses are plotted (black circles) alongside average values for a given depth in the sediment (red squares). Pore water Ba^{2+} (µmol/kg) profiles (black line) are plotted for stations C and B. The dashed grey line indicates the oxygen penetration depth (OPD).

(2350–2700 µmol/kg). The DIC profile at 1488 m has a narrower range, and steeper slope, ranging from 2400–2550 µmol/kg. Total alkalinity values ranged from 3242 µmol/kg at 552 m to a minimum of 2774 at 1488 m. Carbonate ion concentrations [CO_3^{2-}] were derived based on the TA and DIC values. The [CO_3^{2-}] profiles were relatively similar (Figure 4) at 552 m and 980 m water depth, with measurements at 1488 m exhibiting the lowest overall values. Values for all three stations ranged from a maximum of 419 µmol/kg at 552 m to a minimum of 192 µmol/kg at 980 m (Figure 4).

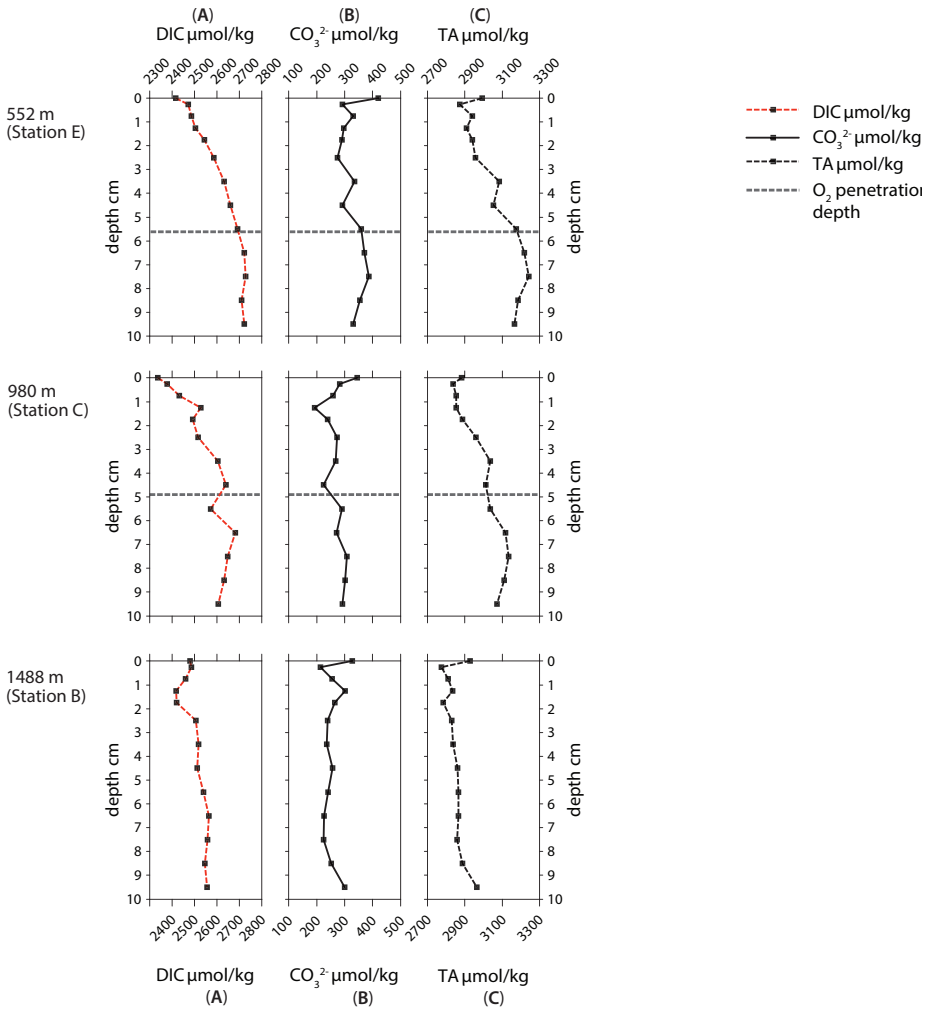

Figure 4 | Carbonate chemistry parameters for stations E, C and B. (**A**) Dissolved inorganic carbon (DIC), (**B**) [CO_3^{2-}] in µmol/kg, (**C**) Total alkalinity (TA) in µmol/kg.

Table 2 | Number of LA-ICP-MS analyses per benthic foraminifera species per sample per station.

Station	Depth (m)	Sample intervals (cm)	*Hoeglundina elegans* no. analyses	*Uvigerina mediterranea* no. analyses	*Uvigerina peregrina* no. analyses	*Melonis barleeanus* no. analyses
F	350	0–0.5	2	18	5	1
		0.5–1	4	13		2
		1–1.5		3		
		1.5–2				10
		2–2.5	1			2
		3–3.5				3
		5–6				3
E	552	0–0.5		5	26	
		0.5–1			9	4
		1–1.5			14	3
		1.5–2			5	3
		2–2.5			7	3
		2.5–3			6	2
		3–3.5			6	
		3.5–4			8	1
		4–5		3		
		7–8				1
D	745	0–0.5		20	13	
		0.5–1		6		5
		1–1.5		3	6	
		1.5–2		7	8	6
		2–2.5			4	
		3.5–4			2	
		4–5			2	4
		8–9			2	
C	980	0–0.5		20		2
		0.5–1		20		2
		1–1.5		4		
B	1488	0–0.5	3	4	10	4
		0.5–1	9	5	3	5
A	1987	0–0.5	15		10	
		1–1.5				3

3.2 | Benthic foraminiferal trace and minor element data

Trace-metal incorporation in benthic foraminiferal test carbonate was analyzed for 4 different species (*Hoeglundina elegans, Melonis barleeanus, Uvigerina mediterranea, Uvigerina peregrina*), from 6 sites. Sample coverage for all stations is described in Table 2.

3.2.1 | *Intra-individual variability*

The taxon with the largest individuals, *Uvigerina mediterranea*, allowed multiple analyses on a single test and routinely 3–4 analyses were carried out per test. No trend was observed for Mg/Ca or Sr/Ca values between the consecutive growth stages. Among the studied benthic foraminiferal species, no noteworthy difference in signal stability (i.e. elemental homogeneity) was observed within the test wall profiles. In general, concentrations of Sr were relatively stable, whereas Mg and Ba were more variable (Table 3).

Table 3 | Descriptive statistics (minimum, maximum, mean, median, standard deviation and interval of maximum frequency of total analyses for *H. elegans*, *U. mediterranea*, *U. peregrina* and *M. barleeanus* for Mg/Ca mmol/mol, Sr/Ca mmol/mol, Ba/Ca µmol/mol and Mn/Ca µmol/mol.

Mg/Ca mmol/mol	***H. elegans***	***U. mediterranea***	***U. peregrina***	***M. barleeanus***
Min	0.38	0.85	1.31	1.12
Max	1.99	6.07	5.99	4.20
Mean	0.98	2.23	3.01	1.98
Median	0.96	1.96	2.90	1.79
Std. deviation	0.40	0.89	0.91	0.67
Max. frequency interval	1.00–1.50 (42%)	1.50–2.00 (36%)	3.00–3.50 (34%)	1.50–2.00 (41%)
Sr/Ca mmol/mol	***H. elegans***	***U. mediterranea***	***U. peregrina***	***M. barleeanus***
Min	1.55	1.05	0.98	1.12
Max	3.38	1.57	1.53	1.75
Mean	2.55	1.27	1.27	1.39
Median	2.59	1.27	1.27	1.40
Std. deviation	0.39	0.10	0.11	0.12
Max. frequency interval	2.40–2.55 (23%), 2.55–2.70 (23%)	1.20–1.35 (48%)	1.20–1.35 (41%)	1.35–1.50 (44%)
Ba/Ca µmol/mol	***H. elegans***	***U. mediterranea***	***U. peregrina***	***M. barleeanus***
Min	1.85	1.54	1.80	2.24
Max	23.30	5.02	5.93	17.36
Mean	7.65	2.53	2.88	4.82
Median	5.40	2.47	2.71	3.86
Std. deviation	5.17	0.51	0.77	2.96
Max. frequency interval	3.00–4.00 (23%)	2.00–3.00 (67%)	2.00–3.00 (64%)	3.00–4.00 (39%)

3.2.2 | *Mg/Ca, Sr/Ca and Ba/Ca in benthic foraminiferal calcite*

Boxplots are used to describe the range of Mg/Ca, Sr/Ca and Ba/Ca values and how the distribution, median, average and skewness compares between the different species studied here (Figure 5). All ICP-MS measurements are included, and as such represent both intra- and inter-individual variability.

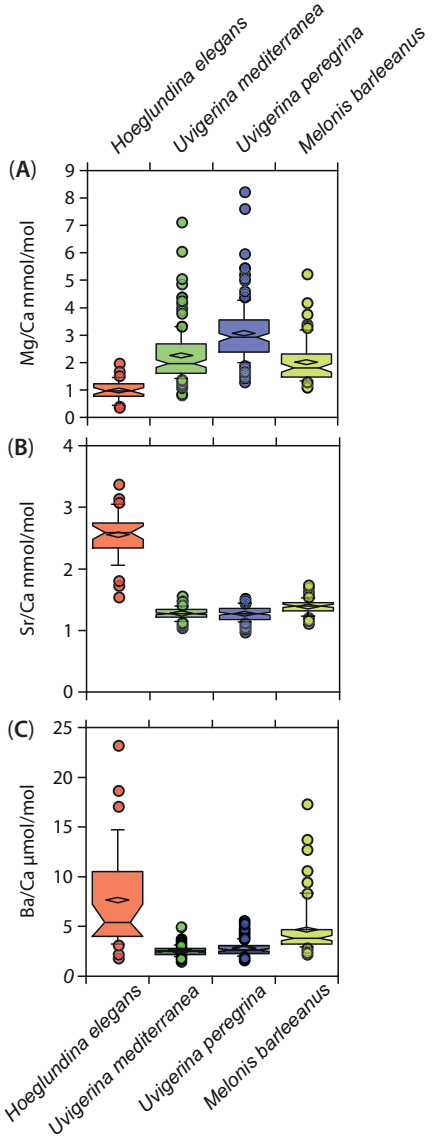

Figure 5 | Box plots describing the distribution in: (**A**) Mg/Ca, (**B**) Sr/Ca, and (**C**) Ba/Ca values measured in living (stained) individuals *of Hoeglundina elegans, Uvigerina mediterranea, Uvigerina peregrina* and *Melonis barleeanus*. The box represents all values between the 25th and 75th percentile with the line bars extending between the 10th to 90th percentiles. The dissection line through the box denotes the median. The half width (HW) of the notch is calculated using HW = 75th percentile – 25th percentile *1.57/(√N). The empty diamond shape denotes the average value of the distribution. Outliers are denoted by coloured circles.

The range observed in Mg/Ca values (between the 10th and 90th percentile) is widest for *Uvigerina peregrina*, and decreases in the order *Uvigerina mediterranea*, *Melonis barleeanus* and *Hoeglundina elegans* (Figure 5). All species display a positive skew in values, which most likely reflects a methodological bias. Noteworthy are the significantly higher (median) Mg/Ca ratios in *U. peregrina* compared to *U. mediterranea*. The range and distribution of Sr/Ca values for *U. mediterranea*, *U. peregrina* and *M. barleeanus* are similar, while *H. elegans* clearly differs in both its Sr range and distribution. The ranges in Ba/Ca values for *U. mediterranea* and *U. peregrina* are similar, while that of *M. barleeanus* and *H. elegans* are larger and exhibit more skewing.

3.2.3 | Trace-metal variation across a depth transect

In the case of Mg/Ca, no appreciable differences were observed across the depth transect for the benthic foraminiferal species analyzed (Figure 6). Strontium to calcium ratios are also similar for the different stations (Figure 7). Barium incorporation in *Hoeglundina elegans* had a larger spread at 1987 m compared to the 350 m station (Figure 3). However, this has to be regarded with some caution as the station at 350 m also has the lowest amount of analyses (n = 5). In *Melonis barleeanus*, a markedly large spread of values is observed only at 552 m, whereas values remain relatively stable at the other stations.

3.2.4 | Trace-metal varation with sediment depth

Magnesium to calcium ratios in living (stained) foraminifera remain similar with sediment depth (Figure 6). The spread in Mg/Ca values varies in most species, however, no depth-related trend is observed. Also Sr/Ca ratios for all species remain quite stable with sediment depth (Figure 7). *Hoeglundina elegans* show somewhat more variation compared to the other taxa. Barium to calcium ratios exhibit some variability with sediment depth (particularly in *Melonis barleeanus* and *H. elegans*), but with no clear depth related trend for any of the species studied here (Figure 3).

4 | DISCUSSION

4.1 | Trace element analyses

Contamination with detritus and presence of secondary trace-metal coatings on benthic foraminiferal tests has been a longstanding challenge in trace-metal analyses of benthic foraminifera (Boyle 1983, Lea and Boyle, 1989). In this study, however, the trace-metal data are based exclusively on living (Rose Bengal stained) foraminifera and thus the impact of trace-metal coatings on built-in elemental concentrations can be ruled out: at the time of sampling, the collected tests were still enveloped by foraminiferal cytoplasm, thus preventing the formation of extraneous inorganic precipitates. This is confirmed by the ablation profiles, which show that no Mg, Sr or Ba -rich phases are present at the test surfaces (Figure 2). This

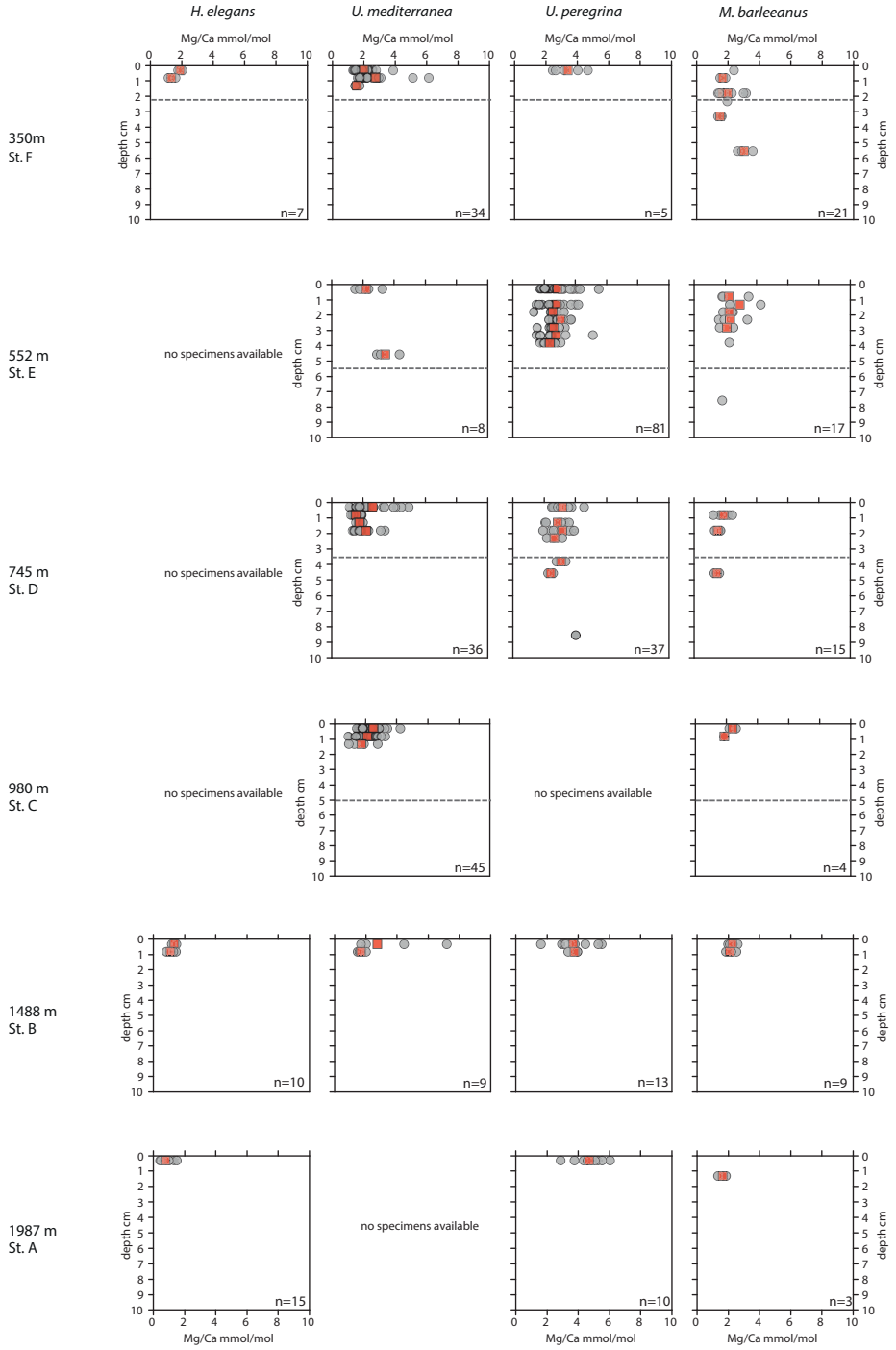

Figure 6 | Plots of Mg/Ca mmol/mol measured in living (stained) *Hoeglundina elegans*, *Uvigerina mediterranea*, *Uvigerina peregrina* and *Melonis barleeanus*. Individual analyses are plotted (black circles) alongside average values for a given depth in the sediment (red squares).

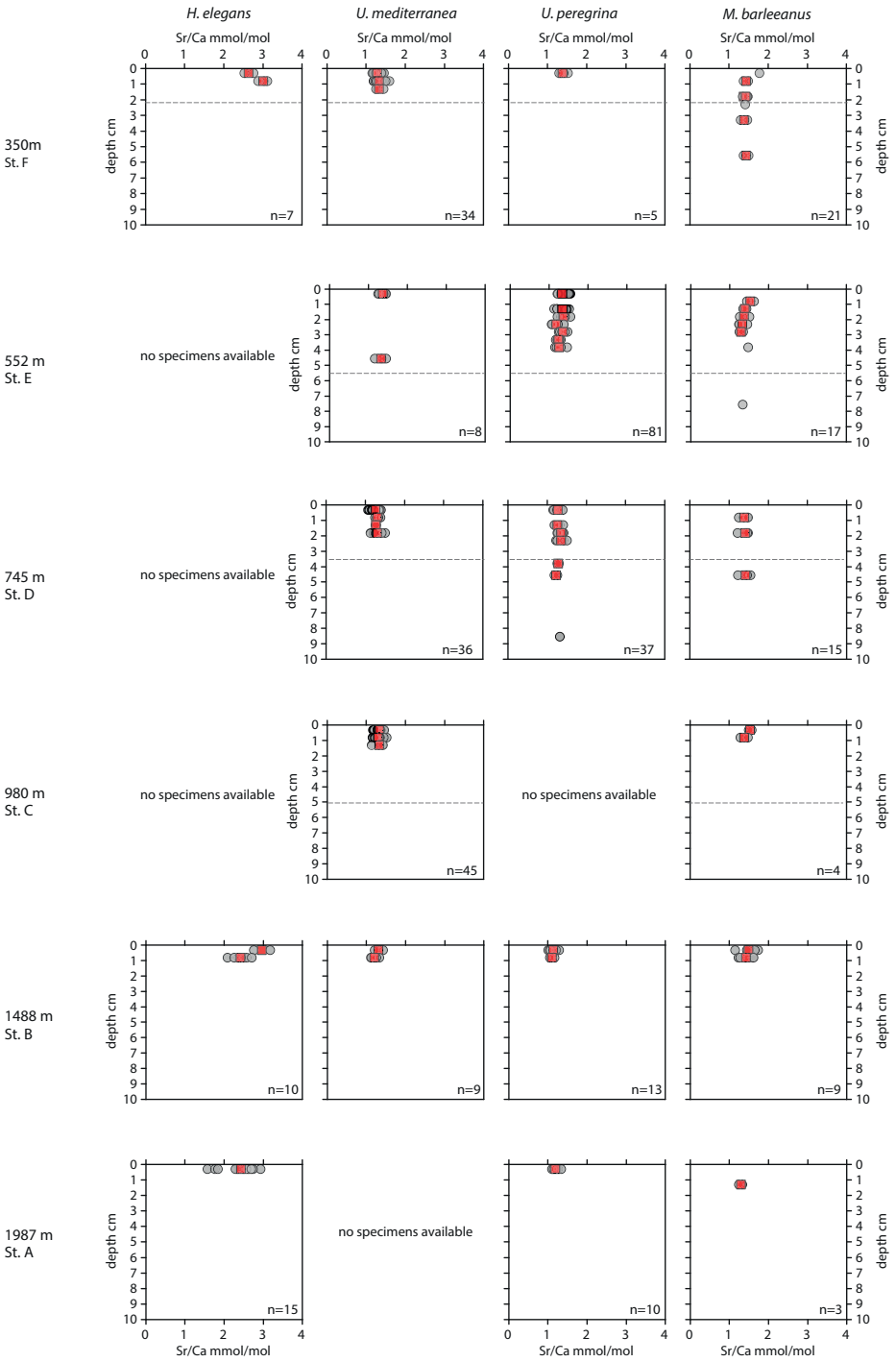

Figure 7 | Plots of Sr/Ca mmol/mol measured in living (stained) *Hoeglundina elegans*, *Uvigerina mediterranea*, *Uvigerina peregrina* and *Melonis barleeanus*. Individual analyses are plotted (black circles) alongside average values for a given depth in the sediment (red squares).

implies that the measured Mg, Sr and Ba concentrations are primary, test carbonate related signals. Results obtained by LA-ICP-MS can be directly compared with traditional solution based analyses as independent cross calibration of LA-ICP-MS, traditional solution analyses and micro- XRF showed no analytical offsets (Munsel et al., 2010, Rosenthal et al., 2011).

4.2 | Aragonite versus calcite

The observed difference in Mg and Sr incorporation between *Hoeglundina elegans* and the other benthic foraminiferal species is most likely due to *H. elegans* having an aragonitic test. (Figures 6 and 7). The orthorhombic crystal lattice of aragonite permits higher Sr incorporation and at the same time limits Mg incorporation, relative to calcite (Lorens 1981). Strontium incorporation in *H. elegans* is about two times higher than in the calcitic species used in this study, which is slightly higher than previous observations for this species (Reichart et al., 2003, Rosenthal et al., 2006, Rosenthal et al., 1997). Conversely, Mg/Ca values in *H. elegans* are somewhat less than half of those observed for *Uvigerina mediterranea*, *Uvigerina peregrina* and *Melonis barleeanus*, in line with earlier observations (Reichart et al., 2003, Rosenthal et al., 2006, Rosenthal et al., 1997).

4.3 | Temperature effects

Temperature at all stations is similar to within half a degree (Durrieu de Madron, Pers. Com.) and is therefore not expected to cause appreciable differences in trace-metal uptake. The similarity in Mg and Sr values across the transect (Figures 6 & 7) confirms that Mg and Sr incorporation is largely determined by ambient temperature (Lear et al., 2002, Rosenthal et al., 1997). To test the fidelity with which Mg/Ca- and Sr/Ca-temperature calibrations reproduce the in-situ temperature in the western Mediterranean, the measured Mg/Ca or Sr/Ca ratios for *Hoeglundina elegans* have been used to calculate the average apparent temperature (Figure 8). This has been done for *H. elegans* as it is the only species studied here that has previously reported temperature calibrations at the species level. For *H. elegans*, the three derived Sr/Ca temperatures correspond well to the in-situ temperatures, suggesting a particularly robust Sr/Ca – temperature relationship for *H. elegans*. Conversely, two of the three derived Mg/Ca temperatures are appreciably offset to lower temperatures (Figure 8). The Mg/Ca values of *H. elegans* are lower than previously reported for this species in the Bay of Biscay (Reichart et al., 2003). In both this study and that of Reichart et al., (2003), individual living (stained) specimens were analyzed using LA-ICP-MS. Even so, the temperature derived from Rosenthal's Atlantic (A) dataset (10.5 °C, Figure 8) corresponds best to the in-situ temperature (Rosenthal et al., 1997). The final Reichart et al., (2003) temperature relationship was based on a non-linear regression of Mg/Ca and Sr/Ca with temperature and here is offset by approximately 4 °C.

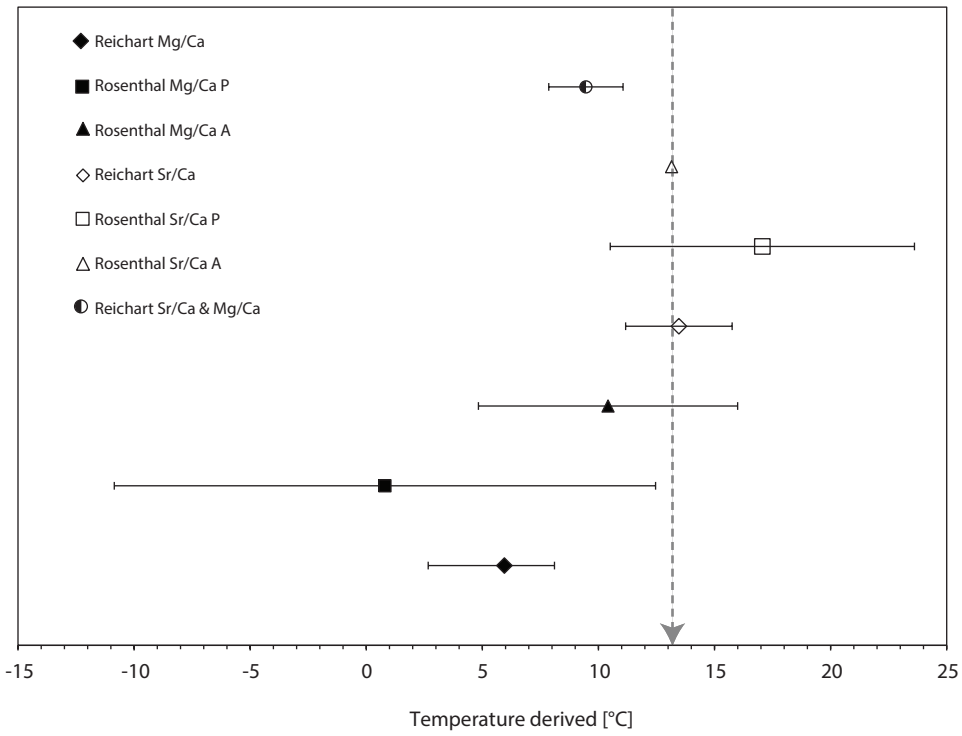

Figure 8 | Derived temperature from empirical Mg/Ca and Sr/Ca relationships for *Hoeglundina elegans*. Dashed grey line indicates in-situ temperature (P – Pacific, A – Atlantic) (Rosenthal et al., 1997; Reichart at al., 2003).

For the Uvigerinids, the Lear et al., (2002) calibration relationship gives a derived temperature with an offset of 6.3 °C for *U. mediterranea* and 0.3 °C for *U. peregrina* from the actual in-situ temperature (Figure 9). It is, however, difficult to evaluate how well this fits as the existing temperature calibration groups several Uvigerinid species. The distinctly different Mg/Ca signatures for *U. mediterranea* and *U. peregrina* observed here at identical temperatures suggest that species-specific Mg/Ca–temperature calibrations are required. The cause for this offset may reflect species' different responses to carbonate chemistry (Dissard et al., 2010; Duenas Bohorquez et al., 2009) or different species-specific vital effects resulting in differences in biomineralization (Wit et al., 2012). *Uvigerina peregrina* has a distinctly lower carbon isotope signature than *U. mediterranea* (Fontanier et al., 2006, 2002; Schmiedl et al., 2004; Chapter 5). Such a lower $\partial^{13}C$ signature suggests calcification in a (micro) environment characterized by lower carbonate ion [CO_3^{2-}] concentrations (Spero et al., 1997). As [CO_3^{2-}] covaries with Mg in the same direction, this does not explain the observed higher Mg/Ca values in *U. peregrina*. Alternatively, molecular and fossil phylogeny shows *U. peregrina* to have evolved during the Early Oligocene, while *U. mediterranea* evolved during the Pliocene (Schweizer, 2006). Seawater

Mg concentrations were lower during the Early Oligocene (Tyrrell and Zeebe, 2004; Coggon et al., 2010) and hence *U. peregrina* may have developed less efficient Mg pumping mechanisms compared to *U. mediterranea*, which evolved during the Pliocene. A recent comparison of carbonate test types and ocean chemistry suggests the two to be linked (Van Dijk et al., 2016). The differences in ocean chemistry at the time these species evolved might also have affected efficiency and hence selectiveness of their biomineralization pathway (Nehrke et al., 2013; De Nooijer et al., 2017). An offset of 6.6 °C is also calculated between the Mg/Ca signature for *M. barleeanus* in this study and the empirically related Mg/Ca signature for the genus derived by Lear et al., (2002). Also here, two *Melonis* species were grouped by Lear et al (2002), preventing a direct comparison between Mg/Ca temperature relationships, but emphasizing the need for species-specific calibrations.

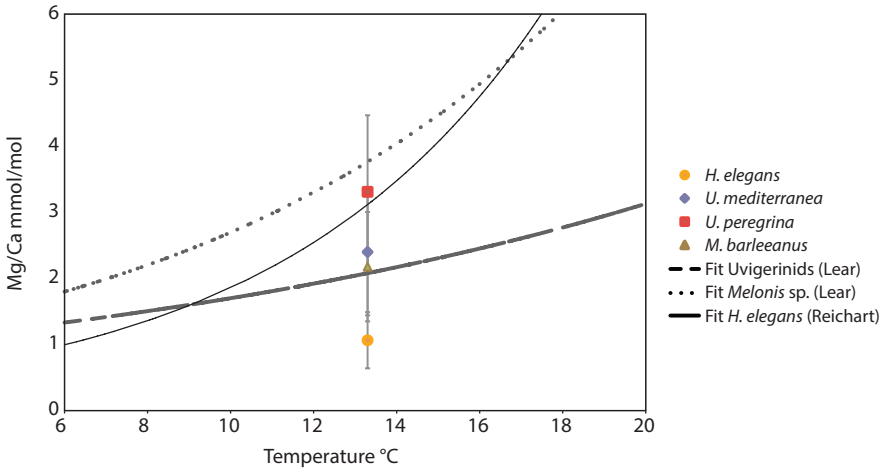

Figure 9 | Plots of average Mg/Ca mmol/mol versus temperature based on different calibrations. Dots indicate average values measured here for *Hoeglundina elegans, Uvigerina Mediterranea, Uvigerina peregrina* and *Melonis barleeanus*.

4.3.1 | *Variability in Mg/Ca and Sr/Ca*

A clear observation for the Mg/Ca records for all species is the high degree of variability between individual test values. Across all species, the range of relative standard deviation in Mg/Ca and Sr/Ca within a test (intra-individual variation) is 12–24% and 5–8% respectively (Table 4) and 30–41% and 8–15% between tests (inter-individual variation) (Table 5). For *Hoeglundina elegans*, the observed range of inter-individual variability corresponds to a temperature range (derived from the Rosenthal et al., (1997) Atlantic Mg/Ca-temperature relationship) of 3.6–15.5 °C. As the in-situ temperature is 13.1 °C and the annual range in temperature at the studied sites is very limited, temperature variability is not responsible for the observed spread of values. Hence other physico-chemical and biological parameters must be considered.

Table 4 | Relative standard deviation (% RSD) of intra-individual values in Mg/Ca, Sr/Ca, and Ba/Ca within four species of benthic foraminifera (*H. elegans*, *U. mediterranea*, *U. peregrina* and *M. barleeanus*).

Element	*H. elegans* % RSD	*U. mediterranea* % RSD	*U. peregrina* % RSD	*M. barleeanus* % RSD
Mg	24	15	16	12
Sr	8	5	5	6
Ba	30	16	11	18

Table 5 | Relative standard deviation (% RSD) of inter-individual values in Mg/Ca, Sr/Ca, and Ba/Ca within four species of benthic foraminifera (*H. elegans*, *U. mediterranea*, *U. peregrina* and *M. barleeanus*).

Element	*H. elegans* % RSD	*U. mediterranea* % RSD	*U. peregrina* % RSD	*M. barleeanus* % RSD
Mg	41	40	30	34
Sr	15	8	9	9
Ba	68	20	27	61

Since Mg and Sr are conservative elements in seawater, and salinity does not vary across the depth transect, salinity variations cannot explain the observed variation. The same obviously also holds within shallow sediment depths (< 10 cm). Magnesium and strontium are also known to vary with carbonate chemistry (Dissard et al., 2010; Russell et al., 2004; Keul et al., 2017). The uptake of Mg and Sr by foraminifera can be influenced by carbonate chemistry at two spatial scales: (1) along the pore water depth gradient; (2) within the foraminiferal respiratory sphere. A foraminifer migrating or undergoing vertical migration is exposed to changing carbonate chemistry with depth. If individual foraminifera are harvested from different depths from where they actual calcified, Mg and Sr incorporation can be offset from empirically derived Mg/Ca_{test}-$Mg/Ca_{pore\ water}$ relationships. In this study, no changes in inter-individual variability were observed as a function of sediment depth. In addition, changes in carbonate chemistry within the sediment are smaller than the variation seen in Mg/Ca values that could be explained with carbonate chemistry, using any of the known calibrations (Figure 9). On a smaller scale, differences in the carbonate chemistry within the respiratory sphere surrounding individual benthic foraminifera might be much larger and could hence explain the spread of values observed here. Previous studies show that ontogenetic control play a role in intra-test trace-metal variations (Anand and Elderfield 2005, Toyofuku and Kitazato 2005). In fact, different metabolic rates during various growth phases (juveniles, pre-adults and adults) result in different trace element incorporation signatures (Hintz et al., 2006b). Individuals with higher metabolic rates potentially alter the pH and hence carbonate chemistry in their respiratory sphere to a larger extent than others. Diz et al., (2012) showed that difference in size and hence

differences in respiratory activity are reflected in the stable oxygen and carbon isotopes, but do not alter either Sr/Ca or Mg/Ca. Unfortunately, the relative contribution of ontogeny cannot be quantified in this study, but the variability observed is very much comparable to Diz et al., (2012). A positive relationship between carbonate ion effect and Sr/Ca has been reported for *H. elegans*, when conditions are undersaturated with respect to aragonite (Rosenthal et al., 2006). The latter is, however, excluded here as the western Mediterranean is saturated with respect to aragonite at all depths (Millero et al., 1979). Indeed, intact pteropods (aragonitic gastropods) were reported even in surface sediments from the deepest station (1987 m) (Fontanier et al., 2008). Accordingly, Sr/Ca in *H. elegans* is here unrelated to carbonate ion concentration.

All evidence presented here supports an inherent biological control on the inter- and intra-individual variation of Mg in foraminifera, which is in line with the strong fractionation exerted against Mg by most foraminiferal species (Hintz et al., 2006a, b; Lear et al., 2002; De Nooijer et al., 2009; De Nooijer et al., 2014). This fractionation, as evidenced by low Mg-partition coefficients between pore water and calcium carbonate, has previously been invoked as an explanation for strong intra-individual variability. This is caused by differences in the efficiency whereby Mg is pumped out of the protoplasm (De Nooijer et al., 2009). Using a clone group of *Ammonia tepida* De Nooijer et al., (2014) showed similar ranges in inter and intra-test variability in specimens cultured under identical conditions, which suggests that the observed inherent variability is similar between species and somehow related to the biological functioning of the organism. Apparently, the differences underlying this natural variability are similar under natural and controlled growth conditions.

4.4 | Barium incorporation in response to organic fluxes

Solid phase barium concentrations in (oxic) sediments are predominantly controlled by organic matter fluxes (McManus et al., 1998) and are mostly present as barite. Dissolved barium is also easily incorporated in foraminiferal test carbonate (Boyle, 1981; Lea and Boyle, 1991; Lea and Spero, 1992; 1994; Hönisch et al., 2011; De Nooijer et al., 2017) making Ba/Ca potentially suited for tracking pore water chemistry in relation to foraminiferal ecology. This is potentially important for paleoceanographic applications as incorporation of pore water Ba in test carbonate would offset calibrations based on bottom water Ba concentrations (Lea and Boyle, 1991).

Pore water Ba is known to rapidly increase within the first few centimetres of the sediment, as a consequence of ongoing release of Ba from barite (Dehairs et al., 1992; Dymond et al., 1992; Schenau et al., 2001). Indeed, an upward flux of Ba^{2+} is seen at 980 m (station C), 1488 m (station B) and 552 m (station E) (Figure 3). The higher Ba^{2+} concentrations in the pore waters of the upper 2 cm at 980 m compared to those at 1488 m, are consistent with the generally higher total organic carbon contents reported at 980 m (Fontanier et al., 2008). Still, the benthic foraminifera studied here do not appear to record increasing Ba incorporation with increasing sediment depth habitat. In fact, foraminiferal Ba/Ca remains relatively stable with

depth in the sediment. Exceptions to this are *Hoeglundina elegans* and *M. barleeanus*, the two species with the most disparate microhabitat preferences. Variability in Ba/Ca_{foram} values can reflect two processes: (1) migration of the foraminifer along the Ba pore water gradient or (2) a disparity between the Ba concentrations sampled during pore water sampling and the Ba conditions the foraminifera were exposed to during the time they added new chambers: i.e. a 'snapshot' effect. *Melonis barleeanus* displays a large spread in Ba/Ca values at 552 m and *H. elegans* at 1987 m and 1488 m. Barium is more easily incorporated into an aragonitic crystal lattice because of the generally more open structure of aragonite (Lorens, 1981), explaining the slightly higher Ba/Ca values in *H. elegans*. The spread of Ba/Ca values in *M. barleeanus* is similar to that seen in Mn/Ca values for the same specimens (Chapter 3, Ni Fhlaithearta et al., 2018)) and may reflect its migration through the sediment column. The variability and high Ba/Ca values in *H. elegans* within the surface sediments at 1987 m is unexpected due to the relatively low total organic carbon content and labile organic matter measured at this station (Chapter 5, Figure 2). Upon degradation, organic matter releases Ba^{2+} into undersaturated bottom waters (Schenau et al., 2001). As such, variable Ba/Ca in *H. elegans* could indicate temporally variable organic matter fluxes (Ní Fhlaithearta et al., 2010; Chapter 6) at that station, which are not recorded in measured organic matter concentrations as this organic matter becomes remineralized. The incorporation of Ba in specific benthic foraminifera might thus provide an additional tool to investigate past variability in fluxes of organic matter (and thus barite) to the seafloor, even when the organic matter has been (almost) fully remineralized.

5 | CONCLUSION

The observed variability of Mg and Sr in the different foraminiferal species corresponds with that in foraminifera grown under relatively constant conditions and hence reflects the variability inherent in species-specific biomineralization. The differences observed between specimens is similar for the different species studied here. Differences in Mg incorporation between species calcifying at the same temperature observed here and in existing calibrations suggest that for accurate temperature calibrations species-specific calibrations are needed. The deepest living species, *Melonis barleeanus*, records high variability in Ba concentrations. The elevated Ba/Ca values in *Hoeglundina elegans* are observed at the depth with the lowest recorded organic matter content at the seafloor. This suggests Ba incorporation in these species to be a potential proxy for past organic matter fluxes at the seafloor.

ACKNOWLEDGEMENTS

We thank captain and crew of the N/O Téthys 2 (CNRS-INSU) for their assistance during the *BEHEMOTH* campaign. We acknowledge the technical assistance given by Christine Barras, Mélissa Gaultier, Sophie Terrien and Gérard Chabaud from Angers and Bordeaux University. We thank Serge Berné and Laetitia Maltese (IFREMER), for providing us with maps of the study area and Xavier Durrieu de Madron (Perpignan University) for discussions about water column structure. Helen de Waard (LA-ICP-MS) and Karoliina Koho (SEM) (Utrecht University) are acknowledged for their laboratory assistance. This is a publication from the Darwin Center for Biogeosciences, which provided partial funding for this project. The authors acknowledge NESSC for funding part of this research.

REFERENCES

Anand, P. and Elderfield, H.: Variability of Mg/Ca and Sr/Ca between and within the planktonic foraminifers Globigerina bulloides and Globorotalia truncatulinoides, Geochem. Geophys. Geosyst., 6, Q11D15, 2005.

Barnett, P. R. O., Watson, J. and Connely, D.: A multiple corer for taking virtually undisturbed sample from shelf, bathyal and abyssal sediments, Oceanologica Acta, 7, 399-408, 1984.

Boyle, E. A., Labeyrie, L. and Duplessly, J. -.: Calcitic Foraminiferal Data Confirmed by Cadmium in Aragonitic *Hoeglundina*: Application to the Last Glacial Maximum in the Northern Indian Ocean, Paleoceanography, 10, 881-900, 1995.

Boyle, E. A.: Manganese carbonate overgrowths on foraminifera tests, Geochim. Cosmochim. Acta, 47, 1815-1819, doi:10.1016/0016-7037(83)90029-7, 1983.

Boyle, E. A.: Cadmium, zinc, copper, and barium in foraminifera tests, Earth Planet. Sci. Lett., 53, 11-35, doi:10.1016/0012-821X(81)90022-4, 1981.

Coggon, R, M., Teagle, D. A. H., Smith-Duque, C. E., Alt, J. C. and Cooper, M. J.: Reconstructing Past Seawater Mg/Ca and Sr/Ca from Mid-Ocean Ridge Flank Calcium Carbonate Veins, Science, 327, 1114, doi:10.1126/science.1182252, 2010.

Dehairs, F., Baevens, W. and Goeyens, L.: Accumulation of Suspended Barite at Mesopelagic Depths and Export Production in the Southern Ocean Science, 258, 5086, http://www.jstor.org/stable/2880421, 1992.

De Nooijer, L. J., van Dijk, I., Toyofuku, T., & Reichart, G. J.: The Impacts of Seawater Mg/Ca and Temperature on Element Incorporation in Benthic Foraminiferal Calcite. Geochemistry, Geophysics, Geosystems, 18(10), 3617-3630, doi:10.1002/2017GC007183, 2017.

De Nooijer, L. J., Spero, H. J., Erez, J., Bijma, J., and Reichart, G.J.: Biomineralization in perforate foraminifera, Earth-Sci. Rev., 135, 48–58, 2014.

De Nooijer, L. J., Toyofuku, T. and Kitazato, H.: Foraminifera promote calcification by elevating their intracellular pH, Proceedings of the National Academy of Sciences, 106, 15374-15378, doi:10.1073/pnas.0904306106, 2009.

Dissard, D., Nehrke, G., Reichart, G. J. and Bijma, J.: Impact of seawater pco2 on calcification and Mg/Ca and Sr/Ca ratios in benthic foraminifera calcite: Results from culturing experiments with Ammonia tepida, Biogeosciences, 7, 81-93, 2010.

Diz, P., Barras, C., Geslin, E., Reichart, G. J., Metzger, E., Jorissen, F., & Bijma, J.: Incorporation of Mg and Sr and oxygen and carbon stable isotope fractionation in cultured Ammonia tepida. Marine Micropaleontology, 92, 16-28. 10.1016/j.marmicro.2012.04.006, 2012.

Duenas-Bohorquez, A., da Rocha, R. E., Kuroyanagi, A., Bijma, J., & Reichart, G.-J.: Effect of salinity and seawater calcite saturation state on Mg and Sr incorporation in cultured planktonic foraminifera, Mar. Micropaleontol., 73, 178–189, 2009.

Dymond, J., Suess, E., & Lyle, M.: Barium in deep-sea sediment: A geochemical proxy for paleoproductivity. Paleoceanography, 7(2), 163-181, doi:10.1029/92PA00181, 1992.

Elderfield, H., Ganssen, G.: Past temperature and $\delta^{18}O$ of surface ocean waters inferred from foraminiferal Mg/Ca ratios, Nature, 405, 442-445, 2000.

Fontanier C., Mackensen A., Jorissen F. J., Anschutz P., Licari L., Griveaud C.: Stable oxygen and carbon isotopes of live benthic foraminifera from the Bay of Biscay: microhabitats impact and seasonal variability. Marine Micropaleontology, 58, 159-183, 2006.

Fontanier, C., Jorissen, F. J., Lansard, B., Mouret, A., Buscail, R., Schmidt, S., Kerhervé, P., Buron, F., Zaragosi, S., Hunault, G., Ernoult, E., Artero, C., Anschutz, P. and Rabouille, C.: Live foraminifera from the open slope between Grand Rhône and Petit Rhône Canyons (Gulf of Lions, NW Mediterranean), Deep Sea Research Part I: Oceanographic Research Papers, 55, 1532-1553, doi:10.1016/j.dsr.2008.07.003, 2008.

Fontanier, C., Jorissen, F. J., Licari, L., Alexandre, A., Anschutz, P. and Carbonel, P.: Live benthic foraminiferal faunas from the Bay of Biscay: faunal density, composition, and microhabitats, Deep Sea Research Part I: Oceanographic Research Papers, 49, 751-785, doi:10.1016/S0967-0637(01)00078-4, 2002.

Hönisch, B., Allen, K. A., Russell, A. D., Eggins, S. M., Bijma, J., Spero, H. J., Lea, D. W., and Yu, J.: Planktic foraminifers as recorders of seawater Ba/Ca, Mar. Micropaleontol., 79, 52–57, 2011.

Hintz, C. J., Shaw, J. M., Chandler, T. J., Bernhard, G. T., McCorkle, D. C. and Blanks, J. K.: Trace/minor element:calcium ratios in cultured benthic foraminifera. Part I: Inter-species and Inter-individual variability, Geochim. Cosmochim. Acta, 70, 1952-1963, 2006a.

Hintz, C. J., Shaw, T. J., Bernhard, J. M., Chandler, G. T., McCorkle, D. C. and Blanks, J. K.: Trace/minor element:calcium ratios in cultured benthic foraminifera. Part II: Ontogenetic variation, Geochim. Cosmochim. Acta, 70, 1964-1976, 2006b.

Jochum, K. P., Weis, U., Stoll, B., Kuzmin, D., Yang, Q., Raczek, I., Jacob, D. E., Stracke, A., Birbaum, K., Frick, D. A., Gunther, D., Enzweiler, J.: Determination of Reference Values for NIST SRM 610-617 Glasses Following ISO Guidelines, Geostandards and Geoanalytical Research, 35, 4, 397-421, 2011.

Keul, N., Langer, G., Thoms, S., de Nooijer, L. J., Reichart, G. J., & Bijma, J.: Exploring foraminiferal Sr/Ca as a new carbonate system proxy. Geochimica et Cosmochimica Acta, 202, 374-386, 2017.

Koho, K. A., de Nooijer, L. J. and Reichart, G. J.: Combining benthic foraminiferal ecology and shell Mn/Ca to deconvolve past bottom water oxygenation and paleoproductivity, Geochim. Cosmochim. Acta, 165, 294–306, doi:10.1016/j.gca.2015.06.003, 2015.

Koho, K. A., De Nooijer, L. J., Fontanier, C., Toyofuku, T., Oguri, K., Kitazato, H. and Reichart, G. J.: Benthic foraminiferal Mn/Ca ratios reflect microhabitat preferences, Biogeosciences, 14(12), 3067–3082, doi:10.5194/bg-14-3067-2017, 2017

Lea, D. and Boyle, E.: Barium content of benthic foraminifera controlled by bottom-water composition, Nature, 338, 751-753, 1989.

Lea, D. W. and Boyle, E. A.: Barium in planktonic foraminifera, Geochim. Cosmochim. Ac., 55, 3321–3331, 1991.

Lea, D. W. and Spero, H. J.: Experimental determination of barium uptake in shells of the planktonic foraminifera Orbulina universa at 22°C, Geochim. Cosmochim. Ac., 56, 2673–2680, 1992.

Lea, D. W. and Spero, H. J.: Assessing the reliability of paleochemical tracers: Barium uptake in the shells of planktonic foraminifera, Paleoceanography, 9, 445–452, 1994.

Lea, D., Martin, P., Pak, D. and Spero, H.: Reconstructing a 350 ky history of sea level using planktonic Mg/Ca and oxygen isotope records from a Cocos Ridge core, Quaternary Science Reviews, 21, 283-293, 2002.

Lear, C. H., Elderfield, H. and Wilson, P. A.: Cenozoic Deep-Sea Temperatures and Global Ice Volumes from Mg/Ca in Benthic Foraminiferal Calcite, Science, 287, 269-272, 10.1126/science.287.5451.269, 2000.

Lear, C. H., Rosenthal, Y. and Slowey, N.: Benthic foraminiferal Mg/Ca-paleothermometry: a revised core-top calibration, Geochim. Cosmochim. Acta, 66, 3375-3387, doi:10.1016/S0016-7037(02)00941-9, 2002.

Lewis, E., and Wallace, D. W. R. (1998) Program Developed for CO_2 Systems Calculations. ORNL/CDIAC-105, Carbon Dioxide Information Analysis Centre, Oak Ridge National Laboratory U.S. Department of Energy, Oak Ridge, Tennessee.

McManus, J., Berelson, W. M., Klinkhammer, G. P., Johnson, K. S., Coale, K. H., Anderson, R. F., Kumar, N., Burdige, D. J., Hammond, D. E., Brumsack, H. J., McCorkle, D. C. and Rushdi, A.: Geochemistry of barium in marine sediments: implications for its use as a paleoproxy, Geochim. Cosmochim. Acta, 62, 3453-3473, doi:10.1016/S0016-7037(98)00248-8, 1998.

Millero, F. J., Morse, J. and Chen-Tung, C.: The carbonate system in the western Mediterranean Sea, Deep-Sea Res, 26A, 1395-1404, 1979.

Munsel, D., Kramar, U., Dissard, D., Nehrke, G., Berner, Z., Bijma, J., Reichart, G. -. and Neumann, T.: Heavy metal uptake in foraminiferal calcite: Results of multi-element culture experiments, Biogeosciences, 7, 2339-2350, 2010.

Nehrke, G., Keul, N., Langer, G., De Nooijer, L. J., Bijma, J., & Meibom, A.: A new model for biomineralization and trace-element signatures of Foraminifera tests. Biogeosciences, 10(10), 6759, 2013.

Ní Fhlaithearta, S., Reichart, G.-J., Jorissen, F. J., Fontanier, C., Rohling, E. J., Thomson, J. & de Lange, G. J.: Reconstructing the seafloor environment during sapropel formation using benthic foraminiferal trace metals, stable isotopes, and sediment composition. Paleoceanography, 25, 2010.

Ní Fhlaithearta, S., Fontanier, C., Jorissen, F., Mouret, A., Dueñas-Bohórquez, A., Anschutz, P., Fricker, M. B., Günther, D., de Lange, G. J., and Reichart, G.-J.: Manganese incorporation in living (stained) benthic foraminiferal shells: A bathymetric and in-sediment study in the Gulf of Lions (NW Mediterranean), Biogeosciences Discuss., doi:10.5194/bg-2018-42, in review, 2018.

Nürnberg, D., Bijma, J. and Hemleben, C.: Assessing the reliability of magnesium in foraminiferal calcite as a proxy for water mass temperatures, Geochim. Cosmochim. Ac, 60, 803-814, 1996.

Reichart, G. –., Jorissen, F., Mason, P. R. D. and Anschutz, P.: Single foraminiferal test chemistry records the marine environment, Geology, 31, 355-358, 2003.

Rosenthal, Y., Lear, C. H., Oppo, D. W. and Linsley, B. K.: Temperature and carbonate ion effects on Mg/Ca and Sr/Ca ratios in benthic foraminifera: Aragonitic species *Hoeglundina elegans*, Paleoceanography, 21, doi:10.1029/2005PA001158, 2006.

Rosenthal, Y., Morley, A., Barras, C., Katz, M. E., Jorissen, F., Reichart, G. -., Oppo, D. W. and Linsley, B. K.: Temperature calibration of Mg/Ca ratios in the intermediate water benthic foraminifer Hyalinea balthica, Geochem. Geophys. Geosyst., 12, 2011.

Rosenthal, Y., Boyle, E. A. and Slowey, N.: Temperature control on the incorporation of magnesium, strontium, fluorine, and cadmium into benthic foraminiferal shells from Little Bahama Bank: Prospects for thermocline paleoceanography, Geochim. Cosmochim. Acta, 61, 3633-3643, doi:10.1016/S0016-7037(97)00181-6, 1997.

Russell, A. D. A., Hônisch, B. B. D., Spero, H. J. A. , Lea, D. W. C.: Effects of seawater carbonate ion concentration and temperature on shell U, Mg, and Sr in cultured planktonic foraminifera, Geochim. Cosmochim. Acta, 68, 4347-4361, 2004.

Schenau, S. J., Prins, M. A., De Lange, G. J., Monnin, C.:Barium accumulation in the Arabian Sea: Controls on barite preservation in marine sediments, Geochim. Cosmochim. Acta, 65, 1545–1556, doi:10.1016/S0016-7037(01)00547-6, 2001.

Schmiedl G., Pfeilsticker M., Hemleben C., Mackensen A.: Environmental and biological effects on the stable isotope composition of Recent deep-sea benthic foraminifera from the Mediterranean Sea. Marine Micropaleontology, 51, 129-152, 2004.

Schweizer, M.: Evolution and molecular phylogeny of *Cibicides* and *Uvigerina* (Rotaliida, Foraminifera), PhD thesis, Geologica Ultraiectina, 261, 2006

Spero, H. J., Bijma, J., Lea, D. W., & Bernis, B. E.: Effect of seawater carbonate concentration on foraminiferal carbon and oxygen isotopes. Nature, 390 (6659), 497–500. doi: 10.1038/37333, 1997.

Toyofuku, T. and Kitazato, H.: Micromapping of Mg/Ca values in cultured specimens of the high-magnesium benthic foraminifera, Geochem. Geophys. Geosyst., 6, Q11P05, 2005.

Tyrrell, T and Zeebe, R. E.: History of carbonate ion concentration over the last 100 million years, Geochim. Cosmochim. Acta, 68, 3521-3530, doi:10.1016/j.gca.2004.02.018, 2004.

Van Dijk, I., De Nooijer, L. J., Hart, M. B., & Reichart, G.: The long-term impact of magnesium in seawater on foraminiferal mineralogy: Mechanism and consequences. Global Biogeochemical Cycles, 30(3), 438-446. doi:10.1002/2015GB005241, 2016.

Wit, J. C., de Nooijer, L. J., Barras, C., Jorissen, F. J., and Reichart, G. J.: A reappraisal of the vital effect in cultured benthic foraminifer Bulimina marginata on Mg/Ca values: assessing temperature uncertainty relationships, Biogeosciences, 9, 3693– 3704, doi:10.5194/bg-9-3693-2012, 2012.

Yu, J. and Elderfield, H.: Benthic foraminiferal B/Ca ratios reflect deep water carbonate saturation state, Earth Planet. Sci. Lett., 258, 73-86, doi:10.1016/j.epsl.2007.03.025, 2007.

5

Oxygen and carbon isotope trends in living (stained) benthic foraminifera from the Gulf of Lions (NW Mediterranean)

Shauna Ní Fhlaithearta[1], Christophe Fontanier[2,3,4], Frans Jorissen[5], Gert J. de Lange[1], Gert-Jan Reichart[1,6]

[1]Faculty of Geosciences, Utrecht University, Utrecht, The Netherlands.
[2]Université de Bordeaux, CNRS, Environnements et Paléo-environnements Océaniques et Continentaux, UMR 61125805, F-33600 Pessac, France
[3]FORAM, Foraminiferal Study Group, F-29200, Brest, France
[4]University of Angers, France
[5]CNRS UMR 6112 LPG-BIAF, Angers University, 49045 Angers Cedex, France
[6]Royal NIOZ, Netherlands Institute for Sea Research, department of Ocean Systems.

ABSTRACT

The stable oxygen and carbon isotope composition of the carbonate tests of benthic foraminifera is one of the most commonly used proxies in paleoceanography. Whereas the oxygen isotope signal is interpreted in terms of seawater temperature and global ice volume, the carbon isotope ratio is generally interpreted to reflect carbon flux to the seafloor and water mass . Most studies to date have, however, refrained from looking at both isotope systems in a coupled way. Here we show that the two isotope systems are closely coupled when comparing benthic foraminiferal species with contrasting sediment microhabitats. The strong overall correlation of the carbon and oxygen isotopes suggests that they are primarily controlled by the same process. In the Gulf of Lions, due to the oligotrophic setting and nearly absent temperature gradient over the investigated depth interval, conditions across our bathymetric transect are nearly constant. This exceptional setting allowed us to unravel inherent coupling between carbon and oxygen isotopes. The slope of the correlation between carbon and oxygen isotopes is consistent with a so-called carbonate-ion effect. We argue that this effect acts at the level of the microenvironment around the test. Hence, these coupled oxygen and carbon isotopes cannot be interpreted only in terms of sediment depth, because of this additional impact of the foraminiferal life processes, i.e. vital effects. The data presented here show a major impact of carbonate ions. Whereas in most settings this signal is not directly clear because of other factors, we demonstrate that it is inherently present and should be taken in consideration. Consequently, integrated process-based interpretations require better constraining of all foraminiferal vital effects.

1 | INTRODUCTION

Stable isotope geochemistry of foraminifera is well-established for the reconstruction of paleoenvironmental conditions (e.g., Shackleton, 1974; Bemis et al., 1998; Lea, 2013). Stable oxygen isotopes in foraminiferal carbonate record changes in global ice volume and temperature (Shackleton and Opdyke, 1973) and are the basis of a global oxygen isotope stratigraphy used for correlation and dating (Imbrie et al., 1984). Carbon isotopes are used to trace changes in oceanic water masses and carbon cycling between terrestrial sources and the ocean (Shackleton, 1977; Duplessy et al., 1984). Additionally, paleoproductivity can be constrained using carbon isotopes (Shackleton, 1977). Summarising, stable isotope geochemistry of both benthic and planktonic foraminifera plays an important role in paleo-environmental reconstructions. Still, several issues potentially affecting the fractionation of stable oxygen and carbon isotopes remain unresolved.

Although oxygen and carbon isotopes are the most used proxy in paleoclimate studies, stable isotope fractionation in foraminifera is not yet fully understood. The mechanisms involved in foraminiferal carbon and oxygen isotope fractionation have been extensively studied over the last decades (Mackensen et al., 2000; McCorkle et al., 1997; Spero et al., 1997; Zeebe, 1999). These studies focussed on the ecological processes involved, such as seasonality and habitat, and on the organismal controls on the fractionation of oxygen and carbon isotopes, both for benthic and planktonic species (e.g. Elderfield et al., 2002; Spero et al., 1997; Schmiedl et al., 2004). In fact, in many cases, offsets from equilibrium fractionation have been observed, which are called vital effects. Such vital effects encompass a wide array of kinetic and metabolic fractionation effects (McConnaughey 1989; Wefer and Burger, 1991), biomineralization impact (Zeebe, 1999), symbionts (Wolf-Gladrow et al., 1999) and microhabitat effects (Fontanier, 2006).

Concerning benthic foraminifera, steep geochemical gradients in the first few centimetres of the sediment expose the various species to very different conditions, in function of their species-specific microhabitat preferences. Due to early diagenesis, the first few centimetres of the sediment are characterized by rapid changes in oxygen, nutrients, carbonate chemistry and trace metal availability. Diagenesis is fuelled by ongoing organic matter degradation, which releases CO_2. Therefore, the ambient pore water $\delta^{13}C$ profile, typically shows isotopically depleted values near the sediment water interface, resulting from the degradation of isotopically light organic matter (Grossman, 1984a, 1984b; McCorkle et al., 1985; Grossman, 1987). Foraminiferal taxa calcifying in this environment will mirror this depletion. It has been suggested that this depletion could be maximal for foraminifera living within phytodetritus layers deposited on top of the sediment, a phenomenon known as a the "Mackensen effect" (Mackensen et al., 1993). Deeper in the sediment porewater $\delta^{13}C_{DIC}$ either continues to decrease, due to the ongoing addition of isotopically light CO_2 from organic matter degradation. Conversely, it could also increase again when alkalinity is added due to

carbonate dissolution (Gehlen et al., 1999), although this has not been directly observed yet. Also carbonate speciation will change with depth in sediment, which in turn may affect stable isotopic fractionation during calcification (Zeebe, 1999). Finally, differences in $\delta^{13}C$ observed between individuals have also been related to ontogenetic stage and reproduction mode (asexual/sexual) (e.g., Schmiedl et al., 2004; Staines-Urías and Douglas, 2009; Schumacher et al., 2010; Diz et al., 2012).

Complex interactions between the different factors involved in isotopic fractionation imply that interpretation of carbon and oxygen isotopes in benthic foraminiferal tests requires exhaustive knowledge of ecology, biology and geochemical processes involved. Many studies tried to deconvolve the signal in order to better understand the individual factors as well as the interplay between factors, such as depth of calcification, food preference, reproduction mode, ontogeny, internal pH regulation, test texture (e.g. McCorkle et al., 1990; Mackensen et al., 1993; McCorkle and Keigwin, 1994; Rathburn et al., 1996, 2000; McCorkle et al., 1997; Mackensen et al., 2000; Corliss et al., 2002; Mackensen and Licari, 2004; Schmiedl et al., 2004; Holsten et al., 2004; Fontanier et al., 2006; Eberwein and Mackensen, 2006; Mackensen et al., 2006; Basak et al., 2009; Fontanier et al., 2008a; Staines-Urías and Douglas, 2009). Most of these studies focused, however, either primarily on carbon isotopic or oxygen isotopic fractionation, and only very few also investigated differences in oxygen isotope fractionation as a function of sediment depth (Schmiedl et al., 2004; Fontanier et al., 2006, 2017). Few studies exist that systematically compare oxygen and carbon isotopic signatures of different species and different sediment depth habitats.

Here we investigate the combined oxygen and carbon isotopic fractionation in carbonate tests of living (Rose-Bengal stained) benthic foraminifera collected in the Gulf of Lions (NW Mediterranean). Six stations were sampled along a bathymetric transect between ~ 350 and ~ 2000 m depth in September 2006 (Figure 1). We targeted four taxa *(Hoeglundina elegans, Uvigerina mediterranea, Uvigerina peregrina* and *Melonis barleeanus*) with contrasting microhabitats (Fontanier et al., 2008b). Results are discussed in relation to (1) the quality and the quantity of organic detritus remineralized at the seafloor and (2) the vertical distribution of foraminiferal species in the sediment (i.e. microhabitat). Differences in isotopic signatures are explained in terms of potential controls on species-specific offsets in $\delta^{13}C$ and $\delta^{18}O$ from equilibrium calcite.

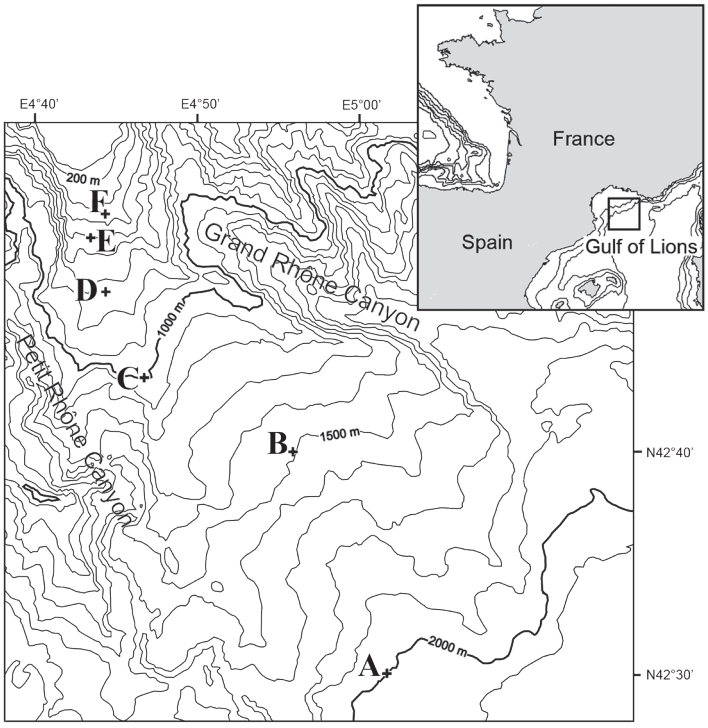

Figure 1 | Study area, bathymetry and geographical position of the different stations (Gulf of Lions, NW Mediterranean).

2 | STUDY AREA

The margin of the Gulf of Lions consists of a large crescent-shaped continental shelf incised by submarine canyons separated by sharp interfluves (Berné and Gorini, 2005). At the scale of the Gulf of Lions, the surface layer (0–200 m) exhibits important seasonal changes in temperature and salinity (Béthoux and Prieur, 1983; Millot, 1990; Béthoux et al., 2002). Below the mixed surface waters, the intermediate layer (Levantine Intermediate Water – LIW) is characterised by a salinity maximum (~ 38.50) and a relative temperature maximum (> 13 °C) (Béthoux and Prieur, 1983; Millot, 1990, Bethoux et al., 2002). The organic matter in the Gulf of Lions may originate from a variety of sources, including riverine input, shelf sediments resuspended at the shelf break, or marine biological production at the sea surface (Buscail and Germain, 1997, Durrieu de Madron et al., 2000). When considering organic carbon content as a function of water depth, a distinct organic carbon maximum is observed at about 1000 meter, with values up to 0.8 weight % (Figure 2, Fontanier et al., 2006). The labile organic matter flux reaching the

sediment-water interface, however, shows a maximum in somewhat shallower water, at about 500 m water depth (Figure 2, Fontanier et al., 2006).

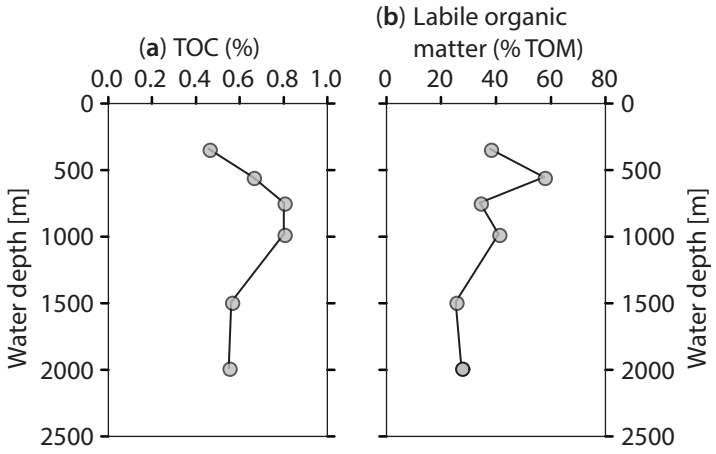

Figure 2 | (**a)** Total organic carbon [%] versus water depth [m]. (**b)** Labile organic matter [%] versus water depth [m]. Data from Fontanier et al., (2008b).

In the present study, we investigate a bathymetric transect comprising 6 sampling stations. All stations were sampled during the BEHEMOTH cruise that took place beginning September 2006 (Table 1). The sites investigated here are located on the interfluve separating the Grand Rhône Canyon from the Petit Rhône Canyon (Figure1). The 6 stations cover a bathymetric transect from ~ 350 to 2000 m water depth. The shallowest site (Station F – 350 m) is bathed by LIW. Station E (552 m) and station D (745 m) are situated in the diffusive boundary separating LIW and Western Mediterranean Deep Water (WMDW). Station C (980 m), station B (1488 m) and station A (1987 m) are bathed by WMDW. Temperature (Fontanier et al., 2008) and salinity (Pierre, 1999) conditions were very similar between all stations (Table 1), which makes these sites ideally suited to investigate the impact of other factors controlling oxygen and carbon stable isotopic fractionation.

Table 1 | Water depth, geographical position, bottom water temperature, bottom water salinity and oxygen penetration depth for water depths 350-1987 m (stations F–A) (adapted from Fontanier et al., 2008b).

Station	Depth (m)	Latitude (N)	Longitude (E)	Bottom water temperature (°C)	Bottom water salinity	Oxygen penetration depth (mm)
F	350	42°52′32	4°42′43	13.2	~ 38.5	20.5 ± 3.3
E	552	42°48′78	4°43′21	13.2	~ 38.5	57.2 ± 4.5
D	745	42°46′66	4°43′91	13.1	~ 38.5	36.5 ± 1.6
C	980	42°43′18	4°46′58	13.1	~ 38.48	50.7 ± 6.3
B	1488	42°38′83	4°56′03	13.1	~ 38.46	141.5 ± 0.0
A	1987	42°28′25	5°00′61	13.1	~ 38.46	197.0 ± 11.0

3 | MATERIALS AND METHODS

3.1 | Foraminiferal sampling

All stations were sampled with a classic Barnett multicorer (Barnett et al., 1984). Each tube has a surface area of about 72 cm^2. The multicorer allowed sampling of the first few decimetres of the surface sediment, collecting the overlying bottom waters and capturing a relatively undisturbed sediment-water interface. The foraminiferal sampling during the BEHEMOTH expedition is described in detail in Fontanier et al., (2008b).

3.2 | Isotopic analyses

The DIC was extracted from seawater with phosphoric acid in an automated preparation device (Thermo Finnigan Gasbench II) coupled online to an isotope ratio mass spectrometer (Thermo Finnigan, Delta V Advantage) to determine its $^{13}C/^{12}C$ ratio. All samples were run at least in duplicate at Utrecht University. Results are reported in δ-notation relative to the V-PDB-scale with an external reproducibility of ± 0.1 ‰ at 2σ.

Isotopic analyses of the foraminiferal calcite were performed on individuals belonging to four benthic foraminiferal taxa *(Melonis barleeanus, Hoeglundina elegans, Uvigerina mediterranea* and *Uvigerina peregrina)*. All individuals analysed come from the > 150 µm size fraction. Analyses of oxygen and carbon isotope ratios were performed at Utrecht University using an automated individual acid bath carbonate preparation device (KIEL III), coupled to a dual-inlet isotope ratio mass spectrometer (Finnigan MAT253). The results were calibrated using an international (NBS-19) and an in-house standard (NAXOS). Precision (1 sigma), based on external standards, is within 0.05 ‰ and 0.08 ‰ for $\delta^{13}C$ and $\delta^{18}O$, respectively. Results are reported in permille (‰) relative to the Vienna Pee Dee Belemnite (V-PDB) standard.

3.3 | Biogeochemical analyses

Total alkalinity of pore water was measured at Utrecht University using an automated titrator (702 SM Titrino, Metrohm) and making Gran plots. The Dickson standard (Dickson, 2010) was analysed every 5 samples to check consistency of the analyses. Dissolved Inorganic Carbon (DIC) was measured using a Total Organic Carbon Analyser (Shimadzu, Model TOC-5050A). Carbonate ion concentrations were calculated using the CO2SYS software (version 01.05; Lewis and Wallace, 1998).

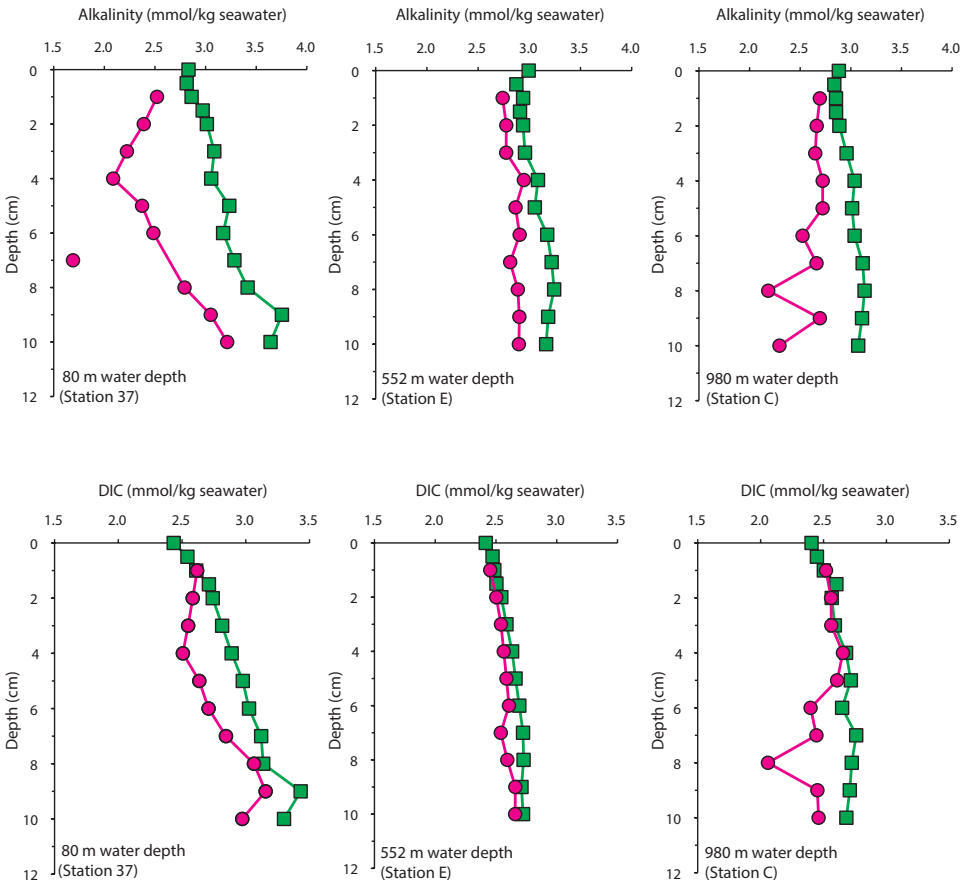

Figure 3 | Pore water alkalinity and DIC for stations 37 (not on map Figure 1), station E and station C. From station 37 (water depth 80 m) no foraminifera were collected and is hence not further used in this study. Green squares indicate samples collected with centrifuging, pink circles were collected using Rhizons. Note the consistently lower DIC and alkalinities of the Rhizon collected pore waters.

Pore water samples used in this study were extracted shortly after core recovery using centrifugation. For comparison, pore water was extracted from a sister core using Rhizon samplers. Rhizon samplers permit less destructive and labour intensive sampling. However, results from total alkalinity and DIC analyses may deviate strongly from the results obtained with centrifuged pore water. For example, data were compared at stations at 980 m and 552 m (this study) and at a station at 80 m (not shown here, station 37, see Goineau et al., 2011). At all three stations, total alkalinity and DIC are lower in pore water extracted using Rhizon samplers compared to the pore water from centrifugation (Figure 3). The fact that a lowered atmospheric pressure is used during pore-water extraction with Rhizon samplers most likely resulted in outgassing of CO_2, lowering DIC concentrations and subsequent precipitation of $CaCO_3$ in the sediment or Rhizons, lowering alkalinity. As such, it is advisable to avoid using Rhizon samplers when studying pore water carbonate chemistry.

4 | RESULTS

4.1 | Pore water carbon isotopes

Carbon isotopes were analysed on all pore water samples at station B (1488 m). The uppermost sample shows a distinct depletion of $\delta^{13}C_{DIC}$ compared to known values for western Mediterranean bottom waters (~ +1 ‰; Pierre, 1999, Schmiedl et al., 2004). All samples below are even more $\delta^{13}C_{DIC}$ depleted. Values for oxygen isotopes in the pore water did not change with depth and are similar to those in the overlying seawater. For the other stations no pore water carbon isotopes were analysed.

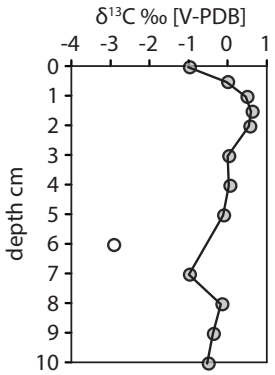

Figure 4 | Plot of pore water $\delta^{13}C_{DIC}$ [‰ V-PDB] at station B (1488 m). An outlier is shown at 6 cm depth.

4.2 | Benthic foraminiferal stable isotopes

4.2.1 | *Depth transect*

The stable carbon isotopic signature of benthic foraminiferal carbonate is relatively more enriched at the shallowest 350 m station, more depleted at 552 m, and returns to more enriched values at the deeper stations (Figure 5). This trend is observed in all species analyzed (*U. mediterranea*, *U. peregrina* and *M. barleeanus*), except in *H. elegans*. The latter species is, however, missing at 552 m water depth, and a subsequent enrichment is still discernible with increasing water depth (Figure 5).

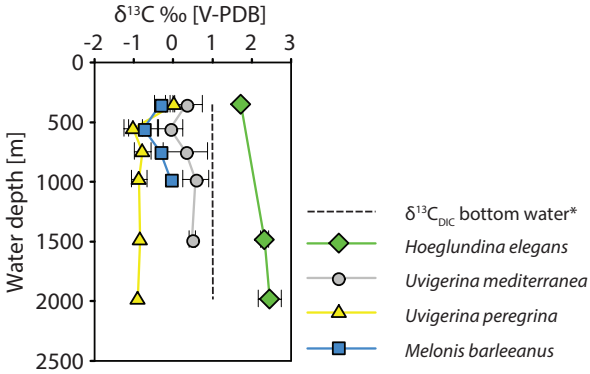

Figure 5 | Plot of average $\delta^{13}C$ [‰ V-PDB] in *Hoeglundina elegans*, *Uvigerina mediterranea*, *Uvigerina peregrina* and *Melonis barleeanus* with increasing water depth [m]. The $\delta^{13}C$ DIC value (dashed line) is based on data from Schmiedl et al., 2004. The spread bars indicate the standard deviation of around the average.

In general, oxygen isotopes in foraminiferal calcite remain relatively stable over the depth interval studied here (Figure 6). For *U. mediterranea* and *U. peregrina*, oxygen isotopes are close to equilibrium at 350 m, drop at 552 m and return to more enriched values at the deeper stations. *Uvigerina mediterranea* exhibits slightly more depleted values at the deepest station. In *M. barleeanus*, oxygen isotopes are stable, apart from a depletion at 980 m depth. Oxygen isotopic values of *H. elegans* become more enriched with increasing water depth (Figure 6).

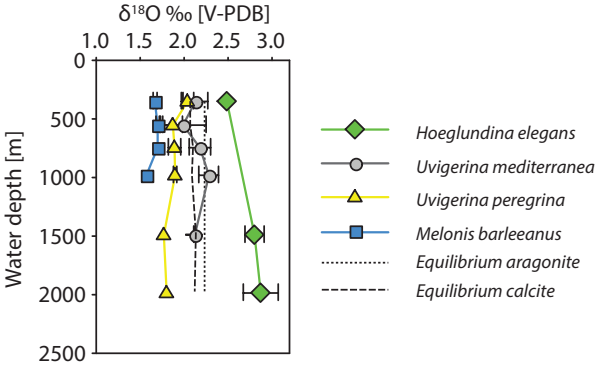

Figure 6 | Plot of average $\delta^{18}O$ [‰ V-PDB] in *Hoeglundina elegans*, *Uvigerina mediterranea*, *Uvigerina peregrina* and *Melonis barleeanus* with increasing water depth [m]. The equilibrium calcite profile $\delta^{18}O$ (dashed line) is calculated using the McCorkle et al., (1997) method based on the Friedman and O' Neill (1977) calcite-water fractionation factor. The spread bars indicate the standard deviation around the average.

4.2.2 | *Changes in foraminiferal stable oxygen and carbon isotopes with sediment depth*

The plots of the foraminiferal stable isotope values as a function of sediment depth (Figure 7 a-b), mostly show data points representing analyses of individual foraminiferal tests. However, for species characterised by smaller test sizes, like *Melonis barleeanus* and *Uvigerina peregrina*, individuals had to be grouped in order to reach the minimum weight required for their analysis (see Table 2 for numbers used per analysis). Although grouping individuals results in a loss of information on inter-individual variability, it has the positive side effect that it increases the robustness of the isotopic value, by averaging inter-specimen variability (Schiffelbein and Hills, 1984; De Nooijer et al., 2014).

In general, the vertical distribution of benthic foraminiferal $\delta^{18}O$-values does not show a trend with sediment depth (1488 m – station B, Figure 7a). The oxygen isotopes in *H. elegans* at 1987 m hint at a slight depletion with sediment depth, but this trend is based on the analyses at 3 depths only. *Uvigerina mediterranea* and *U. peregrina* $\delta^{18}O$ values vary more within the sediment, but without a clear trend, while *M. barleeanus* seems to remain more or less stable with depth in the sediment.

Comparing the different stations, the carbon isotopes (Figure 7b) of *H. elegans* show some variability at the sediment-water interface (1987 m – station A) and a slight enrichment with sediment depth at 1488 m (station B). *U. mediterranea* and *U. peregrina* $\delta^{13}C$ values exhibit more variability within the sediment than *H. elegans* or *M. barleeanus* (Figure 7b). At 552 m, *U. peregrina* $\delta^{13}C$ values appear to become somewhat more depleted with sediment depth. The same is observed at 552 m for *M. barleeanus*, while at the other stations values do not change much with sediment depth.

4.2.3 | *Inter-specific offset in oxygen and carbon isotopes*

Combining all $\delta^{18}O$ and $\delta^{13}C$ data clearly shows the offsets in isotopic signatures between the four species of benthic foraminifera (Figure 8). Moreover, when all stable isotope analyses are combined a strong positive linear correlation ($R^2 = 0.80$) between $\delta^{18}O$ and $\delta^{13}C$ is observed (Figure 8). Looking at the individual species, *U. peregrina* and *M. barleeanus* exhibit the lowest average oxygen and carbon isotopes values, with $\delta^{13}C$ values between -0.88 and -0.53 ‰ and $\delta^{18}O$ values between 1.88 and 1.63 ‰, respectively. Higher average values are observed for *U. mediterranea* (average $\delta^{13}C$ of 0.19 and $\delta^{18}O$ of 2.10 ‰, respectively) and *H. elegans* (average $\delta^{13}C$ of 2.30 and $\delta^{18}O$ of 2.79 ‰, respectively) (Table 2).

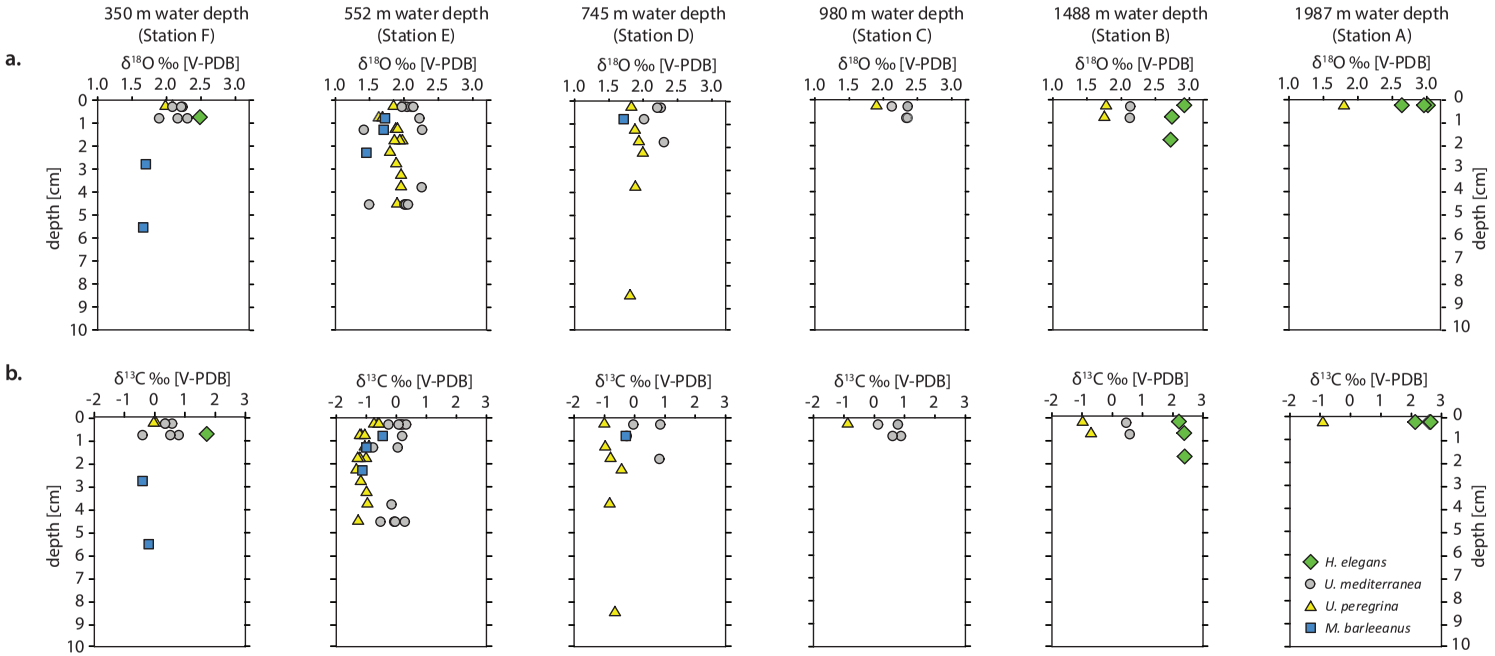

Figure 7 | (**a**) $\delta^{18}O$ measurements of *Hoeglundina elegans*, *Uvigerina mediterranea*, *Uvigerina peregrina* and *Melonis barleeanus* versus depth in sediment [cm]. (**b**) $\delta^{13}C$ measurements of *Hoeglundina elegans*, *Uvigerina mediterranea*, *Uvigerina peregrina* and *Melonis barleeanus* versus depth in sediment [cm].

Table 2 | Oxygen and carbon isotope measurements for *Hoeglundina elegans*, *Uvigerina mediterranea*, *Uvigerina peregrina* and *Melonis barleeanus* from water depths 350–1987 m (stations F–A).

				$\delta^{13}C$ [V-PDB]			$\delta^{18}O$ [V-PDB]		
Station	**Interval (cm)**	**Taxon**	**no. tests**	**value**	**ave.**	**st. dev.**	**value**	**ave.**	**st. dev.**
STATION F									
BTF2	0.5–1	*Hoeglundina elegans*	1	1.72			2.49		
BTF2	0–0.5	*Uvigerina peregrina*	3	0.05			2.09		
BTF2	0–0.5	*Uvigerina peregrina*	1	-0.02	0.02	0.05	1.99	2.04	0.07
BTF2	0–0.5	*Uvigerina mediterranea*	1	0.32			2.22		
BTF2	0–0.5	*Uvigerina mediterranea*	1	0.55			2.07		
BTF2	0–0.5	*Uvigerina mediterranea*	1	0.31			2.20		
BTF2	0.5–1	*Uvigerina mediterranea*	2	-0.43			1.88		
BTF2	0.5–1	*Uvigerina mediterranea*	1	0.76			2.29		
BTF2	0.5–1	*Uvigerina mediterranea*	1	0.48	0.33	0.41	2.15	2.13	0.14
BTF2	2–2.5 & 3–3.5	*Melonis barleeaanus*	2	-0.43			1.69		
BTF2	5–6	*Melonis barleeaanus*	1	-0.23	-0.33	0.14	1.65	1.67	0.02
STATION E									
BTE2	0–0.5	*Uvigerina peregrina*	1	-0.60			1.96		
BTE2	0–0.5	*Uvigerina peregrina*	1	-0.73			2.01		
BTE2	0–0.5	*Uvigerina peregrina*	1	-0.58			1.85		
BTE2	0.5–1	*Uvigerina peregrina*	3	-1.16			1.63		
BTE2	0.5–1	*Uvigerina peregrina*	1	-1.21			1.64		
BTE2	0.5–1	*Uvigerina peregrina*	1	-1.04			1.69		
BTE2	1–1.5	*Uvigerina peregrina*	4	-1.05			1.88		
BTE2	1–1.5	*Uvigerina peregrina*	4	-0.91			1.88		
BTE2	1–1.5	*Uvigerina peregrina*	1	-0.89			1.91		
BTE2	1.5–2	*Uvigerina peregrina*	4	-1.00			1.98		
BTE2	1.5–2	*Uvigerina peregrina*	5	-1.20			1.94		
BTE2	1.5–2	*Uvigerina peregrina*	4	-1.28			1.86		
BTE2	2–2.5	*Uvigerina peregrina*	1	-1.32			1.80		
BTE2	2.5–3	*Uvigerina peregrina*	1	-1.17			1.89		
BTE2	3–3.5	*Uvigerina peregrina*	1	-0.99			1.96		
BTE2	3.5–4	*Uvigerina peregrina*	1	-0.95			1.96		
BTE2	4–5	*Uvigerina peregrina*	5	-1.27	-1.02	0.23	1.90	1.87	0.11

Table 2 | *Continued*

Station	Interval (cm)	Taxon	no. tests	$\delta^{13}C$ [V-PDB] value	ave.	st. dev.	$\delta^{18}O$ [V-PDB] value	ave.	st. dev.
BTE2	0–0.5	*Uvigerina mediterranea*	1	-0.29			2.03		
BTE2	0–0.5	*Uvigerina mediterranea*	1	0.11			2.10		
BTE2	0–0.5	*Uvigerina mediterranea*	1	0.17			2.09		
BTE2	0–0.5	*Uvigerina mediterranea*	1	0.30			2.12		
BTE2	0–0.5	*Uvigerina mediterranea*	1	0.05			1.95		
BTE2	0.5–1	*Uvigerina mediterranea*	1	0.16			2.21		
BTE2	1–1.5	*Uvigerina mediterranea*	1	-0.81			1.40		
BTE2	1–1.5	*Uvigerina mediterranea*	1	0.01			2.25		
BTE2	3.5–4	*Uvigerina mediterranea*	1	-0.19			2.24		
BTE2	4–5	*Uvigerina mediterranea*	1	-0.11			1.99		
BTE2	4–5	*Uvigerina mediterranea*	2	-0.56			1.48		
BTE2	4–5	*Uvigerina mediterranea*	1	0.25			2.01		
BTE2	4–5	*Uvigerina mediterranea*	1	-0.07	-0.08	0.32	2.04	1.99	0.26
BTE2	0.5–1	*Melonis barleeaanus*	2	-0.49			1.71		
BTE2	1–1.5	*Melonis barleeaanus*	2	-1.03	-0.76	0.38	1.69	1.70	0.02
STATION D									
BTD2	0–0.5	*Uvigerina mediterranea*	1	0.82			2.24		
BTD2	0–0.5	*Uvigerina mediterranea*	2	-0.07			2.19		
BTD2	0.5–1.0	*Uvigerina mediterranea*	2	-0.30			2.00		
BTD2	1.5–2	*Uvigerina mediterranea*	1	0.78	0.31	0.57	2.29	2.18	0.12
BTD2	0–0.5	*Uvigerina peregrina*	2	-1.00			1.83		
BTD2	1–1.5	*Uvigerina peregrina*	2	-0.97			1.88		
BTD2	1.5–2	*Uvigerina peregrina*	2	-0.80			1.94		
BTD2	2–2.5	*Uvigerina peregrina*	2	-0.43			2.00		
BTD2	3.5–4	*Uvigerina peregrina*	2	-0.82			1.89		
BTD2	8–9	*Uvigerina peregrina*	1	-0.64	-0.78	0.21	1.81	1.89	0.07
BTD2	0.5–1.0	*Melonis barleeanus*	4	-0.33			1.70		

Table 2 | *Continued*

Station	Interval (cm)	Taxon	no. tests	$\delta^{13}C$ [V-PDB] value	ave.	st. dev.	$\delta^{18}O$ [V-PDB] value	ave.	st. dev.
STATION C									
BC3	0–0.5	*Uvigerina mediterranea*	1	0.74			2.34		
BC3	0–0.5	*Uvigerina mediterranea*	1	0.10			2.11		
BC3	0.5–1.0	*Uvigerina mediterranea*	1	0.85			2.32		
BC3	0.5–1.0	*Uvigerina mediterranea*	1	0.57	0.57	0.33	2.34	2.28	0.11
BC3	0–0.5	*Uvigerina peregrina*	4	-0.87			1.90		
BC3	0.5–1	*Melonis barleeanus*	4	-0.06			1.57		
STATION B									
BTB1	0–0.5	*Uvigerina mediterranea*	1	0.42			2.12		
BTB1	0.5–1.0	*Uvigerina mediterranea*	1	0.54	0.48	0.08	2.11	2.12	0.01
BTB1	0–0.5	*Uvigerina peregrina*	4	-0.98			1.78		
BTB1	0.5–1.0	*Uvigerina peregrina*	4	-0.70	-0.84	0.20	1.76	1.77	0.02
BTB1	0–0.5	*Hoeglundina elegans*	1	2.21			2.93		
BTB1	0.5–1.0	*Hoeglundina elegans*	1	2.38			2.75		
BTB1	1.5–2	*Hoeglundina elegans*	1	2.40	2.33	0.10	2.73	2.80	0.11
STATION A									
BTA1	0–0.5	*Hoeglundina elegans*	1	2.61			3.02		
BTA1	0–0.5	*Hoeglundina elegans*	1	2.64			2.96		
BTA1	0–0.5	*Hoeglundina elegans*	1	2.13	2.46	0.29	2.64	2.87	0.20
BTA1	0–0.5	*Uvigerina peregrina*	5	-0.90			1.80		

4.2.4 | *Inter-individual variation*

The range in $\delta^{13}C$ values observed in all species combined is more than 4 permille, with *U. peregrina* and *M. barleeanus* being most depleted in the heavier carbon isotope. The range in oxygen isotopes values observed is also nearly 4 ‰. Inter-individual variability was calculated using all stable isotope analyses carried out on individual specimens. Comparing the different species studied here, *U. mediterranea* showed highest inter-individual variability, with a standard deviation of 0.40 ‰ for $\delta^{13}C$ and 0.19 ‰ for $\delta^{18}O$, compared to 0.36 ‰ for $\delta^{13}C$ and 0.12 ‰ for $\delta^{18}O$ for *U. peregrina* Table 3.

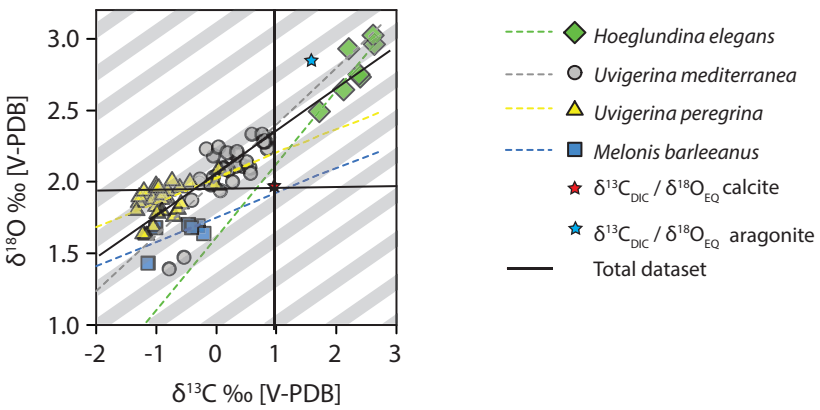

Figure 8 | $\delta^{13}C$ versus $\delta^{18}O$ [‰ V-PDB] in *Hoeglundina elegans*, *Uvigerina mediterranea*, *Uvigerina peregrina*, *Melonis barleeanus* and $\delta^{13}C_{DIC}$ versus $\delta^{18}O_{eq.\ calcite}$.

Table 3 | Inter-individual variation in *Uvigerina mediterranea* and *Uvigerina peregrina.*

	Standard Deviation ‰	
Species	$\delta^{13}C$	$\delta^{18}O$
Uvigerina mediterranea	0.40	0.19
Uvigerina peregrina	0.36	0.12

5 | DISCUSSION

5.1 | Offsets between observed and equilibrium $\delta^{13}C$ values

Remineralisation of (labile) organic matter drives early diagenesis, which results in changes in pore water (carbon) chemistry as a function of sediment depth. Across the bathymetric transect investigated, the average $\delta^{13}C$ value of each species of foraminifera (Figure 5) studied follows the trend in labile organic matter % measured at the seafloor (Figure 2). This most likely reflects organic matter degradation, which releases $\delta^{13}C$ -depleted CO_2 into the surrounding water, which becomes subsequently incorporated into foraminiferal calcite (Mackensen et al., 1993; McCorkle et al., 1997). Comparing the $\delta^{13}C$ values measured in the foraminifera with the in-situ $\delta^{13}C$ of the bottom water DIC shows that all species are depleted in $\delta^{13}C$ relative to bottom water DIC, apart from *H. elegans* (Figure 5). Still, we also notice an offset between the about 1 ‰ reported for the bottom water by Schmiedl et al., (2004) and the about -1 ‰ measured here for the topmost pore water sample. This offset is most likely caused by ongoing degradation of isotopically depleted organic matter and associated release of isotopically light CO_2. For *H. elegans* it furthermore has to be taken into account that this species builds its test from aragonite rather than calcite and that aragonite is relatively enriched in ^{13}C relative to bottom water DIC (1.2–2.1 ‰) (Grossman, 1984). Taking this additional fractionation into

account, the range of $\delta^{13}C$ values measured for *H. elegans* falls within the expected range of aragonite with respect to bottom water. This is in line with the generally assumed niche of this species very close to the sediment water interface.

The absence of a clear gradient in benthic foraminiferal $\delta^{13}C$ as a function of water depth (Figure 5) is in line with the overall meso-oligotrophic conditions across the bathymetric transect. This agrees well with a previous study by Fontanier et al., (2008b), showing that the interfluve on which stations F–A are situated receives substantially less organic matter compared to the nearby canyons. At the shallowest station (350 m) Fontanier et al., (2008b) observed food-depleted conditions, which were attributed to winnowing of organic matter from the seafloor. Indeed, relatively heavy $\delta^{13}C$ values were observed here for *U. mediterranea*, *U. peregrina* and *M. barleeanus* (Figure 3), in line with less isotopically light metabolic CO_2 being admixed. Furthermore the peak in labile organic matter observed at 552 m (Figure 2) is reflected as a dip in $\delta^{13}C$ values observed for all benthic foraminiferal species (Figure 5).

5.2 | Offsets between observed and equilibrium $\delta^{18}O$ values

Stable oxygen isotopes of the different foraminiferal species show little change across the bathymetric transect (Figure 6), in accordance with the virtual absence of a temperature gradient. Also seasonal temperature variability is only on the order of about 0.5 °C (equivalent to a potential $\delta^{18}O$ difference ~ 0.1 ‰; Xavier Durrieu de Madron, pers. com.), which is within the standard deviation observed for most samples. Also variation in $\delta^{18}O_{SW}$ of the Mediterranean Intermediate Water (MIW) and West Mediterranean Deep Water (WMDW) bathing the stations is minimal (1.42–1.45 ‰, (Pierre, 1999)). Accordingly, there is also no variability expected due to potential differences in water masses over the depth interval studied here.

The $\delta^{18}O$ of equilibrium calcite was calculated using the McCorkle et al., (1997) method, which is based on the Friedman and O'Neill (1977) calcite-water fractionation factor. *Melonis barleeanus* exhibits the strongest depletion relative to the calcite-equilibrium calcite, followed by *U. mediterranea*. *Hoeglundina elegans* cannot be compared to equilibrium calcite since it builds its test from aragonite. The equilibrium aragonite line (Figure 6) was calculated based on Kim et al., (2007) aragonite-water fractionation factor. The $\delta^{18}O$ enrichment found here is in agreement with the Marchitto et al., (2014) equation for *H. elegans* $\delta_{carbonate}$ and exhibits only a small offset between the $\delta^{18}O$ of inorganic aragonite, as also reported by Marchitto et al., (2014). The oxygen isotopic values of *U. mediterranea* in this study correspond to equilibrium calcite (offset 0.05 ‰, which is smaller than the analytical uncertainty), in line with the small offset of 0.18 ‰ observed by Fontanier et al., Schmiedl et al., (2004), observed slightly more depleted values (offset of -0.18 ‰) for the same species. *Uvigerina peregrina* is depleted relative to equilibrium calcite in this study by about 0.25 ‰, similar to reported by Fontanier et al., (2006) and Rathburn et al., (1996). Rather surprisingly, Schmiedl et al., (2004) observed *U. peregrina* to be isotopically more enriched (by about 0.40 ‰). *Melonis barleeanus* exhibits a depletion with

respect to equilibrium calcite of about 0.5 ‰, towards lighter values. Importantly the offsets with respect to equilibrium calcite are consistent for the different species at all stations.

5.3 | Microhabitat effects

Although isotope signatures for the different species do not show a clear depth trend (Figure 7a), the differences in average stable isotopic value between the different species, for each core, are in line with known preferential microhabitats for these species. Each benthic foraminiferal species has a preferred microhabitat within the sediment (Jorissen et al., 1995). With respect to the species studied here, *H. elegans U. mediterranea* and *U. peregrina* prefer a shallow infaunal habitat, whereas *Melonis barleeanus* prefers an intermediate infaunal habitat (Schmiedl et al., 2000; Corliss, 1985; Jorissen et al., 1995). Species with a known deep infaunal microhabitat are absent, which corresponds with the oligotrophic setting and hence low fluxes of organic matter at the seafloor. In general, benthic foraminifera record the $\delta^{13}C$ of the pore water in which they calcify, hence isotopically depleted species are thought to calcify deeper within the sediment (Woodruff et al., 1980; McCorkle et al., 1990; Rathburn et al., 1996; Mackensen et al., 2000). The pore water carbon isotopic gradient between ocean bottom water and sediment pore water mostly reflects the addition of isotopically depleted CO_2 from remineralization and may include inputs of isotopically heavier CO_2 from calcite dissolution (Gehlen et al., 1999). As such, it has been suggested that the $\Delta\delta^{13}C$ between shallow living species and deeper living species (e.g. $\Delta\delta^{13}C = \delta^{13}C$ *U. mediterranea* – $\delta^{13}C$ *M. barleeanus*) could be used as an indicator of the organic carbon flux to the sediments (Zahn et al., 1986). In that case, a large $\Delta\delta^{13}C$ between a shallow infaunal species and a deep infaunal species would be indicative of a relatively high organic matter flux. In this study, we do not observe a distinct trend in pore water $\delta^{13}C_{DIC}$ with sediment depth, even though we have only one profile, which is in line with the organic matter starved conditions and high oxygen penetration depth. The fact that we do not observe a clear trend with depth in the sediment is also in line with the absence of a major depth trend in pore water $\delta^{13}C_{DIC}$ (Figure 2). Although the shallowest and deepest living species (*H. elegans and M. barleeanus*, respectively) only occur together at one station, which somewhat limits a comparison, it is clear that between species, differences are still consistent with microhabitat preference. Considering the species combination *Uvigerina mediterranea – M. barleeanus*, the observed offset between these species across three stations remains relatively stable.

The fact that we observed no trends in $\delta^{13}C$ values with depth for even the deepest dweller, *Melonis barleeanus*, indicates that either this species did not calcify at the sediment depth from which it was recovered, or pore water $\delta^{13}C$ gradients were limited. The single available $\delta^{13}C$ pore water profile from1488 m (station B) showed little depletion of pore water $\delta^{13}C$ over a depth of 10 cm. This implies that even when calcifying over different depths in the sediment this species would show little change between depths it was recovered from.

More depleted $d^{13}C$ values generally imply a deeper sediment habitat. Although the isotopic offset, between *U. peregrina* and *U. mediterranea*, shows the latter being consientenly 1.0 ‰ heavier, the average living depth (ALD_{10}) (calculated in Fontanier et al., 2008 for the stations in this study) of *U. mediterranea* is slightly deeper. This difference in ALD is supported by similar results reported in Schmiedl et al., (2004). Still, in the Bay of Biscay exactly the opposite was reported (Fontanier et al., 2006). Fontanier et al., (2006) accordingly suggested that the observed offset in $d^{13}C$ between these species is primarily due to *U. peregrina* preferentially calcifying during eutrophic periods. At these times pore water DIC would have been relatively depleted in $\delta^{13}C$ due to the introduction of labile organic matter into the sediment by macrofaunal bioturbation and its degradation there. We hypothesize therefore that the large isotopic offset between the two species is due to the fact that they don't have the same calcification period, and represent opposite conditions in the yearly productivity cycle, *U. peregrina* being representative for short eutrophic periods and *U. Mediterranean* for the more oligotrophic background conditions.

Although a cross-slope trend in flux of (labile) organic matter is present (Figure 2), differences are apparently too small to result in clear isotopic trends between stations. Although dissolution of carbonates in the pore water could have counteracted potential effects of CO_2 addition through remineralization, we do not have direct evidence of this taking place. This implies that in settings similar to those studied here, i.e. with low sea surface productivity and high sedimentary calcium carbonate contents, differences in isotopic signatures between species do not necessarily reflect organic matter loading and/or sea surface productivity.

5.4 | Oxygen versus carbon isotopes in benthic foraminifera

Plotting the oxygen and carbon isotopes of the individual analyses against each other shows that all data, for all species, plot more or less on a single line (Figure 8). The carbon and oxygen isotopes for individual species are also correlated, showing regression lines more or less parallel to the overall correlation. Remarkably, even the isotopic analyses of *H. elegans* plot on the same line as the overall data, although the regression line for *H. elegans* alone seems somewhat steeper. Schmiedl et al., (2004), who measured stable isotopes in *U. mediterranea* in the Gulf of Lions, noted only a weak covariance in their dataset (Figure 9). However, when only *U. mediterranea* from this data set is considered, the data show a regression curve close to the 0.3 line which represents the data reported here, with slopes of 0.24 and 0.34, depending on the time of the year (Schmiedl et al., 2004). The other species from the Schmiedl et al (2004) data set show little variability and so no correlation between oxygen and carbon stable isotopes is observed.

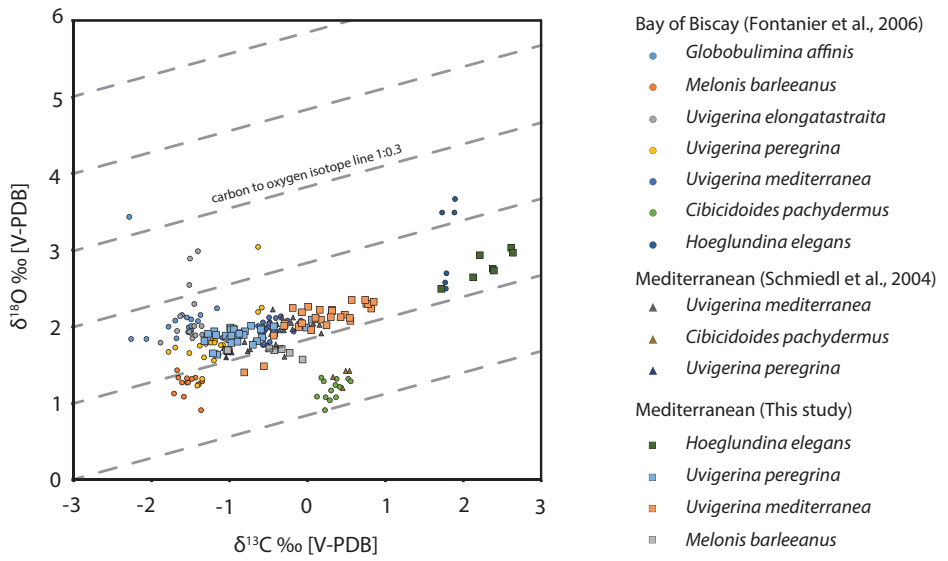

Figure 9 | $\delta^{13}C$ versus $\delta^{18}O$ [‰ V-PDB] for the studies of Fontanier et al., (2006) and Schmiedl et al., (2004) and this study. Data from Fontanier et al., (2006) are based on specimens collected from the Bay of Biscay, other data are based on specimens from the Western Mediterranean. Slope plotted is based on general 1 to 0.3 ‰ $\delta^{13}C_{DIC}$ versus $\delta^{18}O_{eq.\ calcite}$.

The oxygen isotope fractionation between CO_2 (39.5) and CO_3^{2-} (18.4) is 21.1‰ and for carbon isotope fractionation between the same ion pair it is 6.7. The ratio of these two fractionations is 6.7/21.1 = 0.32. This is in close agreement with the observed slopes of the oxygen and carbon isotopes found here. A preliminary review of $\delta^{18}O$ versus $\delta^{13}C$ datasets from two studies from present day and past environments (Schmiedl 2004 and Stap et al., 2010, respectively) show that also for these studies the overall slopes could potentially be explained by shifts in CO_2/CO_3^{2-} and the associated fractions in both carbon and oxygen isotopes.

The observed consistent correlation between oxygen and carbon isotopes in benthic foraminifera suggests that although carbon and oxygen isotopes will primarily reflect the isotopes of the seawater, DIC and temperature, both are also impacted by a common process affecting both isotopes. This is probably especially clear for the samples in this study as all other factors (temperature, isotopic composition of seawater and isotopic composition of the DIC) remain very constant over the interval studied, unlike in most other marine environments. However, also when we plot the data sets of Fontanier et al., (2006, Bay of Biscay) and Schmiedl et al., (2004, Western Mediterranean) together with our data, the total data set still follows the 1:0.3 line between carbon and oxygen isotopes. The fact that this correlation is less clear in the Bay of Biscay and the data set from Schmiedl et al., (2004) is most likely explained by the fact that other factors than the so-called carbonate-ion effect are more important. It appears

that the remarkably constant conditions along the bathymetrical transect in the Gulf of Lions (in terms of temperature, isotopic composition of the bottom water and organic matter remineralisation at the sediment water interface and in the topmost sediment) allow us to single out the effect of carbonate ion concentration.

Also in controlled growth experiments using planktonic foraminifera, specifically set up to target an isolated parameter, a distinct covariance between oxygen and carbon isotopes was observed (Spero et al., 1997). The slope of the covariance for the entire multi-species dataset shown here (0.29) is equivalent to the slope range (0.29–0.33) observed by Spero et al., (1997). Also for cultured benthic specimens (Diz et al., 2012) and benthic foraminifera from the field (Schumacher et al., 2010) similar slopes have been observed previously, albeit for individual species. Diz et al., (2012) show a strong link with ontogeny, which was explained via metabolic processes impacting the direct micro environment around foraminifera. Metabolic processes potentially influence both carbon and oxygen isotopes as the respired CO_2 changes the carbonate chemistry in the micro environment directly surrounding the foraminiferal test. Different metabolic rates result in a different carbonate-ion effect and hence results in an apparent correlation between oxygen and carbon isotopes with a slope of about 0.3.

Spero et al., (1997) explained the covariance observed in planktonic foraminifers as resulting from a carbonate-ion effect, whereby increasing $[CO_3^{2-}]$ (and thus pH) leads to lower $\delta^{18}O$ and $\delta^{13}C$. Whereas this effect is well known and generally accepted for planktonic foraminifera, in benthic foraminifera it is not often invoked to explain observed trends. For instance, Ishimura et al., (2012) noticed a similar covariance in benthic foraminifera but did not ascribe it to a carbonate-ion effect, as species living deeper in the sediment are exposed to lower pH and $[CO_3^{2-}]$, showed lower instead of higher $\delta^{18}O$ and $\delta^{13}C$ values. This is also true for the data set presented here, where the deepest living species, *M. barleeanus,* has relatively low $\delta^{18}O$ and $\delta^{13}C$ values. This implies that the observed correlation between carbon and oxygen isotopes cannot be related to pore water carbonate chemistry alone, but probably also to conditions within the foraminiferal micro-environment. This is in line with the Diz et al., (2012) experiment, where such a correlation was observed although culture water was used with the same isotopic values and carbonate chemistry throughout. Clearly the correlation must be related to changes in the carbonate chemistry on a smaller, i.e. foraminiferal micro-environmental scale. Also calcification itself could result in a carbonate-ion effect as during biomineralization foraminifera actively pump protons from their cytoplasm (De Nooijer et al., 2014, Toyofuku et al., 2017). Different species most likely calcify at a different rate, resulting in species specific offsets.

Variations in carbonate ion concentration affect $\delta^{18}O$ incorporation via kinetic fractionation during the hydration and hydroxylation of CO_2 (McConnaughey et al., 1989; McConnaughey et al., 1997). However, carbonate ion concentrations, calculated from alkalinity and DIC (Figure 3), vary by no more than ~ 100 µmol/kg in core top samples between water depths of 552 m, 980 m and 1488 m (stations E, C and B, respectively), which is equivalent to a $\delta^{18}O$ shift of

0.2 ‰, based on the Spero et al., (1997) $CO_3^{2-}/\delta^{18}O$ relationship. Changes in carbonate chemistry in the metabolic sphere of the foraminifera or at the site of calcification, however, easily exceed this by several orders of magnitude (De Nooijer et al., 2014; Toyofuku et al., 2017).

The average taxon-specific offset between foraminiferal $\delta^{18}O$ and equilibrium calcite $\delta^{18}O$ (Table 4) is in agreement with previous reported offsets (Rathburn et al., 1996; McCorkle 1990 & 1997; Schmiedl et al., 2004; Fontanier et al., 2006; Grossman, 1984a), confirming that $\Delta\delta^{18}O$ offsets are species-specific. If such offsets would reflect differences in carbonate chemistry in the metabolic sphere or at the site of calcification, these differences should reflect species-specific differences in metabolic activity and/or carbonate precipitation rate.

Table 4 | Offsets from equilibrium calcite, this study compared to previously published studies for *H. elegans, U. mediterranea, U. peregrina and M. barleeanus*

	$\Delta\delta^{18}O$ ‰			
	H. elegans	***U. mediterranea***	***U. peregrina***	***M. barleeanus***
This study	0.62	0.05	-0.22	-0.42
Fontanier et al., 2006	0.32	0.18	-0.08	-0.49
Rathburn et al., 1996	0.30	–	-0.25	–
Schmiedl et al., 2004	–	-0.18	0.40	–
McCorkle 1990 1997	–	–	-0.02 – -0.12	-0.53

Our data strongly suggest that CO_2 and proton fluxes into the microenvironment of the foraminifer lead to considerable perturbations in pH and shifts in concentrations of CO_2, HCO_3^-, and CO_3^{2-}. This results in a microenvironment with very different carbonate chemistry than in the surrounding pore water (Wolf-Gladrow et al., 1999; De Nooijer et al., 2008; Toyofuku et al., 2017). We propose here, that it is this change in carbonate chemistry within or close to the foraminifera that is reflected in the $\delta^{18}O/d^{13}C$ relationship observed here. The offset from the idealized overall slope is controlled by either leakage (lower shift) or pumping (upper shift) and a shift in the slope itself is most likely controlled by differences in the initial pool of CO_2/CO_3^{2-} available in the test during the onset of calcification. This implies that some of the interspecific differences observed are due to species-specific differences in metabolic rate and/or rate of calcification. Also intra-specific differences could be related to these parameters.

The intra-generic offset in oxygen isotopes in *U. peregrina* and *U. mediterranea* of 0.27 ‰ is in close agreement with that seen by Schmiedl et al., (≥ 0.2 ‰) (2004) and Fontanier et al., (0.26 ‰) (2006). A mean offset in $d^{13}C$ of approximately 1 ‰ is observed between *U. peregrina* and *U. mediterranea*, with *U. peregrina* being more depleted than *U. mediterranea*. An offset between these two species has been reported in similar studies (Schmiedl et al., 2004; Fontanier et al., 2002; 2006). In line with the interpretation of these isotopic offsets presented here these

differences probably imply differences in metabolic rates and/or rate of calcification. Either the deeper dwelling species have a slower metabolism, or the shallower habitat species calcify at a higher rate. As both processes probably affect the isotopic fractionation to a different extent, it is not possible to fully disentangle these processes here. Still, since calcification requires energy and would be expected to be positively related to calcification rate it is likely that the shallow dwellers both have a higher metabolic rate and calcify at a higher rate, which is in line with the date shown here.

6 | SUMMARY AND CONCLUSIONS

Generally, in field studies, a combination of environmental parameters determine the elemental and isotopic composition of benthic foraminifera. The impact of an individual parameter can only be constrained in the exceptional situation where other parameters are relatively constant. The setting studied here shows only very small differences in temperature, isotopic composition of seawater and organic matter remineralisation, A comparison of benthic foraminiferal species with contrasting sediment microhabitats, shows that the $\delta^{13}C$ and $\delta^{18}O$ isotopic systems are closely coupled. This correlation between carbon and oxygen isotopes, across stations and species, suggests that another process controls the correlation. The slope of the correlation closely corresponds to a carbonate-ion effect. We argue that this carbonate-ion effect is not due to changes in environmental conditions in the sediment, but rather to the changes in the microenvironment immediately around the test, or related to the formation of the test itself. The inherent correlation between carbon and oxygen isotopes also implies that this effect is always present, even when overprinted by other environmental factors.

ACKNOWLEDGEMENTS

We are grateful to the officers, crew, and scientist group aboard the R/V Côte de la Manche during the BEHEMOTH cruise for their valuable collaboration. This project was partially funded by the Darwin Center of Biogeosciences. This paper contributes to the Netherlands Earth Systems Science Center (NESSC – www.nessc.nl).

REFERENCES

Barnett P. R. O., Watson J., Connely D. (1984) A multiple corer for taking virtually undisturbed sample from shelf, bathyal and abyssal sediments. Oceanologica Acta, 7, 399-408.

Basak C., Rathburn A. E., Pérez M. E., Martin J. B., Kluesner J. W., Levin L. A., De Deckker P., Gieskes J. M., Abriani M. (2009) Carbon and oxygen isotope geochemistry of live (stained) benthic foraminifera from the Aleutian Margin and the Southern Australian Margin. Marine Micropaleontology, 70, 89-101.

Berné, S., & Gorini, C. (2005) The Gulf of Lions: An overview of recent studies within the French "Margins" programme. Marine and Petroleum Geology, 22(6–7), 691–693. doi:10.1016/j.marpetgeo.2005.04.004

Bemis, B. E., Spero, H. J., Bijma, J., & Lea, D. W. (1998) Reevaluation of the oxygen isotopic composition of planktonic foraminifera: Experimental results and revised paleotemperature equations. Paleoceanography, 13(2), 150–160. doi:10.1029/98PA00070

Béthoux, J. P., & Prieur, L. (1983) Hydrologie et circulation en Méditerranée nord-occidentale. Pétroles et techniques, 299, 25-34.

Bethoux, J. P., Durieu de Madron, X., Nyffeler, F., & Tailliez, D. (2002). Deep water in the western Mediterranean: Peculiar 1999 and 2000 characteristics, shelf formation hypothesis, variability since 1970 and geochemical inferences. Journal of Marine Systems, 33–34, 117–131. doi:10.1016/S0924-7963(02)00055-6

Buscail, R., Germain, C. (1997) Present-day organic matter sedimentation on the NW Mediterranean margin: Importance of off-shelf export, Limnology and Oceanography, 42, doi:10.4319/lo.1997.42.2.0217

Buscail, R., Pocklington, R., Daumas, R., & Guidi, L. (1990). Fluxes and budget of organic matter in the benthic boundary layer over the northwestern Mediterranean margin. Continental Shelf Research, 10(9–11), 1089–1122. doi:10.1016/0278-4343(90)90076-X

Corliss B. H. (1985) Microhabitat of benthic foraminifera within deep-sea sediments. Nature, 435-438, 1985.

Corliss B. H., McCorkle D. C., Higdon D. M. (2002) Seasonal changes of the carbon isotopic composition of deep-sea benthic foraminifera: Paleoceanography, 17, doi:10.1029/2001PA000664.

De Nooijer L. J., Toyofuku T., Oguri K., Nomaki H., Kitazato H. (2008) Intracellular pH distribution in foraminifera determined by the fluorescent probe HPTS. Limnology and Oceanography: Methods, 6, 610-618.

De Nooijer, L. J., Hathorne, E. C., Reichart, G. J., Langer, G., & Bijma, J. (2014). Variability in calcitic Mg/Ca and Sr/Ca ratios in clones of the benthic foraminifer Ammonia tepida. Marine Micropaleontology, 107, 32–43. doi:10.1016/j.marmicro.2014.02.002

Dickson, A. G. (2010) The carbon dioxide system in seawater: Equilibrium chemistry and measurements. Pp. 17–40 in Guide to Best Practices for Ocean Acidification Research and Data Reporting. U. Riebesell, V. J. Fabry, L. Hansson, and J. P. Gattuso, eds, Chapter 1, EUR 24328 EN, European Commission, Brussels, Belgium.

Diz, P., Barras, C., Geslin, E., Reichart, G. J., Metzger, E., Jorissen, F., & Bijma, J. (2012) Incorporation of Mg and Sr and oxygen and carbon stable isotope fractionation in cultured Ammonia tepida. Marine Micropaleontology, 92, 16-28.

Duplessy, J. C., Shackleton, N. J., Matthews, R. K., Prell, W., Ruddiman, W. F., Caralp, M, Hendy, C. H. (1984) C^{13} record of benthic foraminifera in the last interglacial ocean: implications for the carbon cycle and the global deep water circulation. Quaternary Research 21, 225-243. doi:10.1016/0033-5894(84)90099-1

Durrieu De Madron, X., Abassi, A., Heussner, S., Monaco, A., Aloisi, J. C., Radakovitch, O., Kerherve, P. (2000). Particulate matter and organic carbon budgets for the Gulf of Lions (NW Mediterranean). Oceanologica Acta, 23(6), 717–730. doi:10.1016/S0399-1784(00)00119-5

Eberwein A., Mackensen A. (2006) Regional primary productivity differences off Morocco (NW-Africa) recorded by modern benthic foraminifera and their stable carbon isotopic composition. Deep-Sea Research Part I, 53, 1379-1405.

Elderfield, H., Vautravers, M., Cooper, M. (2002) The relationship between shell size and Mg/Ca, Sr/Ca, $\delta^{18}O$, and $\delta^{13}C$ of species of planktonic foraminifera. Geochemistry, Geophysics, Geosystems 3. doi:10.1029/2001GC000194.

Fontanier C., Jorissen F. J., Licari L., Alexandre A., Anschutz P., Carbonel P. (2002) Live benthic foraminiferal faunas from the Bay of Biscay: faunal density, composition, and microhabitats. Deep-Sea Research I, 49, 751-785.

Fontanier C., Mackensen A., Jorissen F. J., Anschutz P., Licari L., Griveaud C. (2006) Stable oxygen and carbon isotopes of live benthic foraminifera from the Bay of Biscay: microhabitats impact and seasonal variability. Marine Micropaleontology, 58, 159-183.

Fontanier C., Jorissen F. J., Michel E., Cortijo E., Vidal L., Anschutz P. (2008a) Stable oxygen and carbon isotopes of live (stained) benthic foraminifera from Cap-Ferret Canyon (Bay of Biscay). Journal of Foraminiferal Research, 38, 39-51.

Fontanier, C., Jorissen, F. J., Lansard, B., Mouret, A., Buscail, R., Schmidt, S., Kerhervé, P., and Rabouille, C., (2008b). Live foraminifera from the open slope between Grand Rhône and Petit Rhône Canyons (Gulf of Lions, NW Mediterranean). Deep-Sea Research Part I, 55, 1532-1553.

Fontanier, C., Sakai, S., Toyofuku, T., Garnier, E., Brandily, C., Eugene, T., and Deflandre, B. (2017) Stable isotopes in deep-sea living (stained) foraminifera from the Mozambique Channel (eastern Africa): multispecies signatures and paleoenvironmental application. Journal of Oceanography, 73(2), 259–275. doi:10.1007/s10872-016-0401-1

Friedman I., O'Neil J. R. (1977) Compilation of stable isotope fractionations factors of geochemical interest (Geological Survey Professional Paper 440-KK). In: Fleischer, M., (Ed.), Data of Geochemistry, Sixth Edition. U.S. Government Printing Office, Washington, DC, 1-12.

Gehlen, M., Mucci, A., & Boudreau, B. (1999) Modelling the distribution of stable carbon isotopes in porewaters of deep-sea sediments. Geochimica et Cosmochimica Acta, 63(18), 2763–2773. doi:10.1016/S0016-7037(99)00214-8

Grossman, E. L., & Ku, T. -L. (1986). Oxygen and carbon isotope fractionation in biogenic aragonite: Temperature effects. Chemical Geology: Isotope Geoscience Section, 59, 59–74. doi:10.1016/0168-9622(86)90057-6

Grossman E. L. (1984a) Carbon isotopic fractionation in live benthic foraminifera –comparison with inorganic precipitate studies. Geochemica et Cosmochimica Acta, 48, 1505-1512.

Grossman E. L. (1984b) Stable isotope fractionation in live benthic foraminifera from the southern California borderland. Palaeoceanography, Palaeoclimatology, Palaeoecology, 47, 301-327.

Grossman E. L. (1987) Stable isotopes in modern benthic foraminifera: a study of vital effect. Journal of Foraminiferal Research, 17, 48-61.

Holsten J., Stott L., Berelson W. (2004) Reconstructing benthic carbon oxidation rates using $\delta^{13}C$ of benthic foraminifers. Marine Micropaleontology, 53, 117-132.

Ishimura, T., Tsunogai, U., Hasegawa, S., Nakagawa, F., Oi, T., Kitazato, H., Suga, H. and Toyofuku, T. (2012) Variation in stable carbon and oxygen isotopes of individual benthic foraminifera: tracers for quantifying the magnitude of isotopic disequilibrium. Biogeosciences, 9(11), 4353.

Jorissen, F. J., de Stigter, H. C., & Widmark, J. G. (1995) A conceptual model explaining benthic foraminiferal microhabitats. Marine Micropaleontology, 26(1-4), 3-15.

Imbrie, J. & Hays, J. Martinson, Douglas McIntyre, A. Mix, Alan J. Morley, J. Pisias, Nicklas L. Prell, W. J. Shackleton, N. (1984) The Orbital Theory of Pleistocene Climate: Support from a Revised Chronology of the Marine δ18O Record. Milankovich and climate, Part I. 126. 269-305.

Kim S.- T., O'Neil J. R., Hillaire-Marcel C. and Mucci A. (2007) Oxygen isotope fractionation between synthetic aragonite and water: influence of temperature and Mg^{2+} concentration. Geochim. Cosmochim. Acta 71, 4704–4715.

Lea, D.W. (2013) Elemental and Isotopic Proxies of Past Ocean Temperatures. In Treatise on Geochemistry: Second Edition (Vol. 8, pp. 373–397). Elsevier Inc. doi:10.1016/B978-0-08-095975-7.00614-8

Lewis, E., and Wallace, D. W. R. (1998) Program Developed for CO2 Systems Calculations. ORNL/CDIAC-105, Carbon Dioxide Information Analysis Centre, Oak Ridge National Laboratory U.S. Department of Energy, Oak Ridge, Tennessee.

Mackensen A., Licari L. (2004) Carbon isotopes of live benthic foraminifera from the South Atlantic Ocean: Sensitivity to bottom water carbonate saturation state and organic matter rain rates, In: Wefer, G., Mulitza, S., Rathmeyer, V. (Eds.), The South Atlantic in the Late Quaternary – Reconstruction of Material Budget and Current Systems, Springer-Verlag, Berlin, pp. 623-644.

Mackensen A., Hubberten H.- W., Bickert T., Fischer G., Futterer D. K. (1993) $\delta^{13}C$ in benthic foraminiferal tests of *Fontbotia wuellerstorfi* (Schwager) relative to $\delta^{13}C$ of dissolved inorganic carbon in Southern Ocean deep water: implications for Glacial ocean circulation models. Paleoceanography, 6, 587-610.

Mackensen A., Wollenburg J., Licari L. (2006) Low $\delta^{13}C$ in tests of live epibenthic and endobenthic foraminifera at a site of active methane seepage, Paleoceanography, 21, doi:10.1029/2005PA001196.

Mackensen A., Schumacher S., Radke J., Schmidt D. N. (2000) Microhabitat preferences and stable carbon isotopes of endobenthic foraminifera: clue to quantitative reconstruction of oceanic new production. Marine Micropaleontology, 40, 233-258.

Marchitto, T. M., Curry, W. B., Lynch-Stieglitz, J., Bryan, S. P., Cobb, K. M., & Lund, D. C. (2014). Improved oxygen isotope temperature calibrations for cosmopolitan benthic foraminifera. Geochimica et Cosmochimica Acta, 130, 1-11.

McConnaughey, T. (1989) 13C and 18O isotopic disequilibrium in biological carbonates: II. In vitro simulation of kinetic isotope effects. Geochimica et Cosmochimica Acta 53, 163–171.

McConnaughey, T., Burdett, J., Whelan, J. F., Paull, C. K. (1997). Carbon isotopes in biological carbonates: respiration and photosynthesis. Geochim. Cosmochim. Acta 61, 611 –622.

McCorkle D. C., Emerson S. R., Quay P. (1985) Stable carbon isotope in marine pore waters. Earth and Planetary Science Letters, 74, 13-26.

McCorkle D. C., Keigwin L. D. (1994) Depth profile of $\delta^{13}C$ in bottom water and core-top *C. wuellerstorfi* on the Ontong-Java Plateau and Emperor Seamounts. Paleoceanography, 9, 197-208.

McCorkle D. C., Keigwin L. D., Corliss B. H., Emerson S. R. (1990) The influence of microhabitats on the carbon isotopic composition of deep-sea benthic foraminifera. Paleoceanography, 5, 161-185.

McCorkle, D. C., Corliss, B. H., & Farnham, C. A. (1997) Vertical distributions and stable isotopic compositions of live (stained) benthic foraminifera from the North Carolina and California continental margins. Deep-Sea Research Part I: Oceanographic Research Papers, 44(6), 983–1024. doi:10.1016/S0967-0637(97)00004-6

Millot, C. (1990) The Gulf of Lions' hydrodynamics. Continental Shelf Research, 10, 9–11, 885–894. doi:10.1016/0278-4343(90)90065-T

Pierre, C. (1999) The oxygen and carbon isotope distribution in the Mediterranean water masses. Marine Geology, 153, 41-55.

Rathburn A. E., Corliss B. H., Tappa K. D., Lohmann K. C. (1996) Comparison of the ecology and stable isotopic compositions of living (stained) benthic foraminifera from the Sulu and South China Seas. Deep-Sea Research, 43, 1617-1646.

Rathburn A. E., Levin L. A., Held Z., Lohmann K. C. (2000) Benthic foraminifera associated with cold methane seeps on the northern California margin: Ecology and stable isotopic composition. Marine Micropaleontology, 38, 247-266.

Schiffelbein, P., & Hills, S. (1984). Direct assessment of stable isotope variability in planktonic foraminifera populations. Palaeogeography, Palaeoclimatology, Palaeoecology, 48(2–4), 197–213. doi:10.1016/0031-0182(84)90044-0

Schmiedl, G., de Bovée, F., Buscail, R., Charriere, B., Hemleben, Ch., Medernach, L., and Picon, P. (2000) Trophic control of benthic foraminiferal abundance and microhabitat in the bathyal Gulf of Lions, western Mediterranean Sea. Marine Micropaleontology, 40, 167– 188.

Schmiedl G., Pfeilsticker M., Hemleben C., Mackensen A. (2004) Environmental and biological effects on the stable isotope composition of Recent deep-sea benthic foraminifera from the Mediterranean Sea. Marine Micropaleontology, 51, 129-152.

Schumacher, Stefanie, Jorissen, Frans J., Mackensen, Andreas, Gooday, Andrew J. and Pays, Olivier (2010) Ontogenetic effects on stable carbon and oxygen isotopes in tests of live (Rose Bengal stained) benthic foraminifera from the Pakistan continental margin. Marine Micropaleontology, 76, 3–4, 92-103. doi:10.1016/j.marmicro.2010.06.002.

Shackleton, N. J., (1974) Attainment of isotopic equilibrium between ocean water and the benthonic foraminifera genus Uvigerina: isotopic changes in the ocean during the last glacial. Colloques Internationaux du C.N.R.S., 219, 203–208.

Shackleton, N. J. (1977) Carbon 13 in Uvigerina: Tropical rainforest history and the equatorial Pacific carbonate dissolution cycles. Marine science.

Shackleton, N., & Opdyke, N. (1973) Oxygen isotope and paleomagnetic stratigraphy of equatorial Pacific core V28-238: oxygen isotope temperatures and ice volumes on a 105 and 106 year scale. Quaternary Research, 3, 39–55.

Spero, H. J., Bijma, J., Lea, D. W., & Bernis, B. E. (1997) Effect of seawater carbonate concentration on foraminiferal carbon and oxygen isotopes. Nature, 390 (6659), 497–500. doi:10.1038/37333

Staines-Urías F., Douglas R. G. (2009) Environmental and intraspecific dimorphism effects on the stable isotope composition of deep-sea benthic foraminifera from the Southern Gulf of California, Mexico. Marine Micropaleontology, 71, 80–95.

Stap, L., Lourens, L. J., Thomas, E., Sluijs, A., Bohaty, S., & Zachos, J. C. (2010) High-resolution deep-sea carbon and oxygen isotope records of Eocene Thermal Maximum 2 and H2. Geology, 38(7), 607-610. doi:10.1130/G30777.1

Toyofuku, T., Matsuo, M. Y., De Nooijer, L. J., Nagai, Y., Kawada, S., Fujita, K., Reichart, G. J., Nomaki, H., Tsuchiya, M., Sakaguchi, H.and Kitazato, H. (2017) Proton pumping accompanies calcification in foraminifera. Nature communications, 8, 14145. doi:10.1038/ncomms14145

Wefer, G., Berger, W. H. (1991) Isotope paleontology: growth and composition of extant calcareous species. Marine Geology 100, 207-248.

Wolf-Gladrow, D. A., Bijma, J., & Zeebe, R. E. (1999) Model simulation of the carbonate chemistry in the microenvironment of symbiont bearing foraminifera. Marine Chemistry, 64(3), 181–198. doi:10.1016/S0304-4203(98)00074-7

Woodruff F., Savin S. M., Douglas R. G. (1980) Biological fractionation of oxygen and carbon isotopes by recent benthic foraminifera. Marine Micropaleontology, 5, 3–11.

Zahn, R., Winn, K., & Sarnthein, M. (1986) Benthic foraminiferal $\delta^{13}C$ and accumulation rates of organic carbon: Uvigerina peregrina group and Cibicidoides wuellerstorfi. Paleoceanography, 1(1), 27–42.

Zeebe, R. E. (1999) An explanation of the effect of seawater carbonate concentration on foraminiferal oxygen isotopes. Geochimica et Cosmochimica Acta 63, 2001–2007.

Zeebe R. E. and Wolf-Gladrow D. (2001) CO2 in Seawater: Equilibrium, Kinetics, Isotopes. Elsevier Oceanography Series 65.

6

Reconstructing the seafloor environment during sapropel formation using benthic foraminiferal trace metals, stable isotopes, and sediment composition

S. Ní Fhlaithearta[1], G.-J. Reichart[1,2], F. J. Jorissen[3,4], C. Fontanier[3,4], E. J. Rohling[5], J. Thomson[5] and G. J. De Lange[1]

[1]Department of Earth Sciences–Geochemistry, Faculty of Geosciences, Utrecht University, Utrecht, The Netherlands
[2]Alfred-Wegener Institute, Bremerhaven, Germany
[3]Laboratory of Recent and Fossil Bio-Indicators, UPRES EA 2644, Angers University, Angers, France
[4]Laboratoire d'Etude des Bio-Indicateurs Marins, Ile d'Yeu, France
[5]National Oceanography Centre, Southampton, UK

Paleoceanography, vol. 25, PA4225, doi:10.1029/2009PA001869, 2010

ABSTRACT

The evolution of productivity, redox conditions, temperature, and ventilation during the deposition of an Aegean sapropel (S1) is independently constrained using bulk sediment composition and high-resolution single specimen benthic foraminiferal trace metal and stable isotope data. The occurrence of benthic foraminifer, *Hoeglundina elegans (H. elegans)*, through a shallow water (260 m) sapropel, permits for the first time a comparison between dissolved and particulate concentrations of Ba and Mn and the construction of a Mg/Ca–based temperature record through sapropel S1. The simultaneous increase in sedimentary Ba and incorporated Ba in foraminiferal test carbonate, $(Ba/Ca)_{H.\ elegans}$, points to a close coupling between Ba cycling and export productivity. During sapropel deposition, sedimentary Mn content ($(Mn/Al)_{sed}$) is reduced, corresponding to enhanced Mn^{2+} mobilization from sedimentary Mn oxides under suboxic conditions. The consequently elevated dissolved Mn^{2+} concentrations are reflected in enhanced $(Mn/Ca)_{H.\ elegans}$ levels. The magnitude and duration of the sapropel interruption and other short-term cooling events are constrained using Mg/Ca thermometry. Based on integrating productivity and ventilation records with the temperature record, we propose a two-mode hysteresis model for sapropel formation.

1 | INTRODUCTION

The eastern Mediterranean sedimentary record is characterized by the frequent occurrence of organic rich layers, called sapropels (Olausson,1961; Kidd et al.,1978). Sapropels are a sedimentological expression of orbitally induced variations in solar insolation; their occurrence is governed by a 21 kyr periodicity that correlates with precession minima (Rossignol-Strick et al.,1982; Hilgen, 1991; Rohling,1994). According to the most recent synthesis, the youngest sapropel (S1) appears to have formed throughout the eastern Mediterranean between 9.8 and 5.7 ^{14}C kyr B.P. (10.8–6.1 calendar kyr B.P.) (De Lange et al., 2008). Present consensus is that prior to the onset of sapropel formation in SLA9 (~ 9.2 kyr B.P.), continental runoff from the Nile and Northern Borderland rivers intensified (~ 10.5 kyr B.P.), resulting in an increased supply of freshwater (Casford et al., 2002). Consequently, vertical density gradients in the upper water column steepened, leading to restricted deep water formation. Enhanced export productivity during sapropel formation may initially have been fuelled by the input of river derived nutrients, and further sustained by enhanced phosphorus recycling and nitrogen fixation (Olausson, 1961; Vergnaud-Grazzini et al.,1977; Cita et al., 1977; Rossignol-Strick et al., 1982; Rohling and Hilgen, 1991; Sachs and Repeta, 1999; Casford et al., 2002; Rohling et al., 2004; Slomp et al., 2004). Evidence for extensive nitrogen fixation during sapropel conditions invokes oligotrophic surface waters, suggesting that the contribution of river-derived nutrients to surface waters was minor (Sachs and Repeta, 1999).

Furthermore Casford et al., (2002) presented a case for an initial period of 1000–1500 years of nutrient accumulation prior to the onset of sapropel deposition. This would suggest that the nutrient budget for the actual period of sapropel deposition should not be considered in terms of a steady state process, but that it included nutrients imported into the basin during the extensive early phase of flooding. The process involved would be initial deposition on the shelves/slopes, and subsequent remobilization/recycling during the sapropel event. Increased productivity during sapropel deposition is based on a higher export flux of organic matter, reflected in sediment cores by enhanced organic carbon (C_{org}) and biogenic barium content (Thomson et al., 1995; van Santvoort et al.,1996).

The combination of higher organic matter remineralization (Passier et al., 1996) and decreased ventilation resulted in widespread bottom water anoxia (Rohling and Gieskes, 1989; Rohling, 1994). Past anoxia is recognized in sediment cores by an absence of benthic foraminifera, depleted sedimentary Mn concentrations and the presence of reduced mineral species such as pyrite (Passier et al.,1996; Jorissen, 1999; Thomson et al.,1999).

The combination of higher organic matter remineralization (Passier et al., 1996) and decreased ventilation resulted in widespread bottom water anoxia (Rohling and Gieskes, 1989; Rohling, 1994). Past anoxia is recognized in sediment cores by an absence of benthic foraminifera, depleted sedimentary Mn concentrations and the presence of reduced mineral species such as pyrite (Passier et al.,1996; Jorissen, 1999; Thomson et al.,1999).

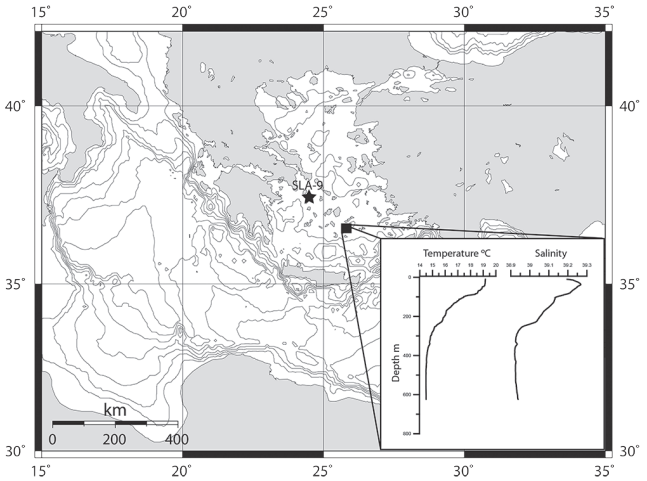

Figure 1 | Map of the Aegean showing the location of core SLA–9. Inset temperature and salinity profile from CTD 588, taken during cruise Meteor 51–3 (courtesy of C. Hemleben).

Discussions of sapropel formation center on the relative roles of enhanced export production and redox controlled enhanced organic matter preservation, in controlling the organic carbon content of sapropels. Both processes not only interact during sapropel formation, but are also intimately linked in proxy data. More recently, sapropel studies have also focused on a centennial scale interruption in sapropel deposition, recognized in cores through out the eastern Mediterranean (Rohling et al., 1997; De Rijk et al., 1999). The sapropel interruption is considered to have resulted from an increase in frequency and intensity of winter cooling, which led to an abrupt collapse of stratification and consequent reoxygenation of bottom waters down to more than 1500 m (Casford et al., 2003) but no deeper than 1800 m (De Lange et al., 2008). Sapropel formation is thus characterized by the complex interplay of productivity and ventilation, with superimposed impacts from abrupt cooling events. Only by using independent multiproxy records can we hope to deconvolve the resulting complex sedimentary phenomena.

Foraminifera have long been used by paleoclimatologists to unravel past changes in the physical and chemical properties of seawater (Parker, 1958; Ruddiman, 1971; Lea and Boyle, 1989; Rosenthal et al., 1997; Lear et al., 2000; Rosenthal et al., 2006; Jorissen et al., 2007). Records of variations in trace metals and stable isotopes can be extracted from the carbonate tests of benthic foraminifera. The benthic foraminifer *Hoeglundina elegans* is of particular interest in trace metal investigation. First, it possesses an aragonitic test that is less susceptible to diagenetic overgrowths than the calcitic shells of most other perforate benthic foraminifera (Boyle et al., 1995). Often, foraminiferal Mn oxide coatings have to be removed from calcitic taxa by elaborate cleaning procedures, which complicates trace metal measurements and may also bias the trace metal record through the preferential removal of the more labile calcium

carbonate phases (Yu et al., 2007). Second, globally, *H. elegans* has a cosmopolitan distribution and lives over a wide range of water depths (Parker, 1958; Lutze and Coulbourn, 1984; Boyle et al., 1995; Hughes et al., 2000; Koho et al., 2008). In a study of the Aegean Sea, Parker (1958) reports the presence of *H. elegans* within a water depth range of 80–1300 m. *Hoeglundina elegans* preferentially lives at or close to the sediment-water interface (Jorissen et al., 1998; Schönfeld, 2001; Fontanier et al., 2002), which is commonly explained in terms of the maximum concentration of labile food particles there (Jorissen et al., 2007), and as such provides a record of the chemistry of oceanic bottom waters and surficial pore waters (Boyle et al., 1995; Reichart et al., 2003; Rosenthal et al., 2006). The combination of these characteristics makes it an ideal candidate for tracking variations in bottom water trace metal concentrations through time.

Core SLA–9 was retrieved with R/V *Aegeo* by gravity corer from the Cyclades Plateau (37°31'N, 24°33'E) in the southwestern Aegean Basin, from a depth of 260 m (Figure 1). The water column is characterized by temperatures ranging from 19 °C at the surface to 14.5 °C at depth (~ 300 m) and salinity ranging from 39.3 to 38.9 (Figure 1, inset). The Aegean currently plays a key role in eastern Mediterranean circulation as a site of deep and intermediate water formation for the entire eastern Mediterranean basin (Theocharis, 1989; Roether et al., 1996; Lascaratos et al., 1999). The sensitivity of this hydrographic link to cold climatic events (Roether et al., 1996) makes the Aegean a key region for study of the causes of eastern Mediterranean reoxygenation at sapropel interruption and termination (Casford et al., 2003; Marino et al., 2007). Studying sapropel formation furthers our understanding of the impact of abrupt climate change on circulation and deep water formation in the Mediterranean. Of broader significance, Mediterranean sapropels offer an ideal test bed for detailed studies of the processes governing organic matter burial, and of the sensitivity of thermohaline ventilation processes to climate change.

In this study, the application of laser ablation-ICP-MS (LA-ICP-MS) to benthic foraminifer *H. elegans* provides a new tool in the reconstruction of bottom water conditions during sapropel deposition. Laser ablation-ICP-MS is virtually non destructive and permits both the repeated analysis of scarce foraminifera and the subsequent measurement of their oxygen and carbon isotope ratios, thus avoiding any potential offsets between individuals. By coupling the dissolved Ba and Mn records, as deduced from *H. elegans*, with their solid phase counterparts, we potentially gain new insights into surface water productivity, biogenic barium preservation, and the evolution of redox conditions throughout the sapropel. We use Mg/Ca thermometry to constrain the duration and magnitude of the cooling during the sapropel interruption. Other centennial scale cooling events, previously suggested by changes in planktonic and benthic foraminiferal assemblage changes (De Rijk et al., 1999; Rohling et al., 2002; Abu-Zied et al., 2008), close to the onset and termination of sapropel S1, are similarly constrained. The uninterrupted presence of *H. elegans* in SLA–9 (Abu-Zied et al., 2008) combined with LA-ICP-MS, thus presents a unique opportunity to better characterize the key forcing mechanisms for environmental change in the Aegean (Casford et al., 2003) and the deep eastern Mediterranean.

2 | MATERIALS AND METHODS

Core SLA–9 was sampled using U channels that were subsampled in a continuous series of 0.5 cm intervals for faunal analysis, and 1 cm intervals for bulk sediment analysis.

For bulk sediment analysis a subsample was freeze-dried and thoroughly ground in an agate mortar. The powder was digested in a mixture of HF, $HNO_3$and $HClO_4$, evaporated to near dryness, before being taken up again in a solution of 1M HCl. Solutions were measured by inductively coupled plasma-optical emission spectroscopy (ICP-OES) (Perkin Elmer Optima 4300DV), with an instrumental precision of better than 3%, for the elements reported. Dilution effects due to varying input rates of carbonate and detrital material are eliminated by normalizing sediment elemental concentrations against Al.

Another part of each subsample was used for foraminiferal preparation, for abundance counts, stable isotopes, shell chemistry, and AMS radio carbon dating. These aliquots were first dried at 50° for 24–48 h, after which they were wet sieved with distilled water and separated into 600, 150, 125 and 63 mm fractions.

For shell chemistry, we picked the aragonitic benthic foraminiferal species *H. elegans* from the > 150 mm fraction. The trace metal composition of *H. elegans* was measured by laser ablation using a deep UV (193 nm) excimer laser (Lambda Physik) with GeoLas 200Q optics. Ablation was performed at a pulse repetition rate of 5 Hz, an energy density of 10 J/cm^2, and a crater size of 20 mm. Ablated particles were measured by a quadrupole ICP-MS (Micromass Platform). Calibration was performed against international glass standard (NIST612), using the Pearce et al., (1997) concentration data and ^{44}Ca as an internal standard, while monitoring the ^{42}Ca and ^{43}Ca minor isotopes. Using a 193 nm wavelength for ablating glass standard and calcite tests minimizes matrix effects (Hathorne et al., 2008). Isotopes used for element quantification were ^{24}Mg, ^{27}Al, ^{55}Mn, ^{138}Ba and ^{208}Pb. All *H. elegans* specimens were ablated twice on their umbilical side. Analytical error (equivalent to 1 sigma), based on the repeated measurement of an external standard, was ± 8% for Ba, ± 8% for Mn, ± 10% for Mg and ± 6% for Sr. Each laser ablation measurement was screened for contamination and diagenetic coatings by monitoring Al, Mn and Pb. On encountering surficial clay contamination (indicated by Al peak) the data integration interval was adjusted to exclude the Al enrichment (see Figure 2). Based on laser ablation profiles, there was no indication of diagenetic Mn coatings on this sample set. As each laser ablation pulse removes approximately 50 nm per pulse, even microscopic coatings of Mn oxides would be detected by this method. Data from single specimen trace metal analyses are prone to scatter due to inter and intraspecimen variations (Sadekov et al., 2005), possibly related to microhabitat and/or vital effects (see Tables A1– A3). We applied a 500 year moving Gaussian window to the benthic foraminiferal trace metal and stable isotope data in order to highlight robust trends.

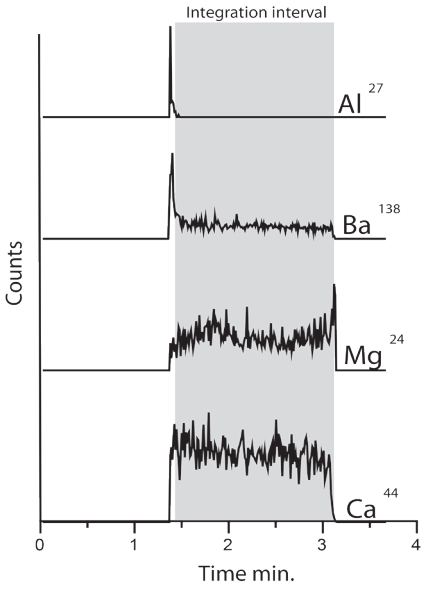

Figure 2 | Example of a laser ablation profile measured in counts per time showing how data integration window (gray shading) is adjusted to include only data unaffected by Al contamination.

Analyses of stable oxygen and carbon isotope ratios based on single specimens of *H. elegans* ($\delta^{18}O_{H.\ elegans}$ and $\delta^{13}C_{H.\ elegans}$) were performed at Utrecht University using an automated individual acid bath carbonate preparation device (KIEL III), coupled to a dual-inlet isotope ratio mass spectrometer (Finnigan MAT253). The results were calibrated using an international (NBS-19) and an in-house standard. Precision (1 sigma), based on external standards, is within 0.05 ‰ and 0.08 ‰ for $\delta^{13}C$ and $\delta^{18}O$, respectively. Results are reported in ‰ relative to the Vienna Pee Dee Belemnite (V-PDB) standard.

Atomic mass spectrometry radiocarbon datings and the age model for SLA–9 have been previously described by Casford et al., (2002, 2007) and Abu-Zied et al., (2008). All dates presented here are given in conventional ^{14}C years. Stable O and C isotope results for the surface-dwelling planktonic foraminiferal species Globigerinoides ruber (white) have been previously described by Casford et al., (2002).

3 | RESULTS

The sapropel interval is characterized by dark olive gray sediments extending from 103 to 84 cm depth, (9000 years B.P. and 7900 years B.P.) followed by light gray muds up to 64 cm (6100 years B.P.) (Figures 3 and 4a). Downward from the sapropel, a continuous transition is observed to light gray sediments, which continue down to about 113 cm depth (10,600 years B.P.).

In core SLA-9, $(Ba/Al)_{sed}$ ratios show a first peak at 9650 years B.P., followed by a sharp drop at 9350 years B.P. (Figure 4d). Immediately thereafter, at 9200 years B.P., $(Ba/Al)_{sed}$ ratios abruptly increase to maximum values, which are attained at 8900 years B.P. Subsequently $(Ba/Al)_{sed}$ ratios remain high until a strong drop starting at about 6350 years B.P. Holocene background levels are reached at 6100 years B.P. Thus the extent of the sapropel from initial onset to termination is between 9200 to 6100 years B.P.

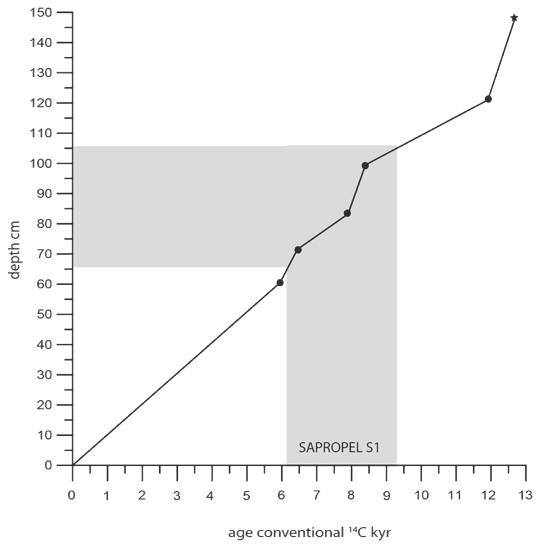

Figure 3 | Age-depth plot for core SLA–9. Black circles indicate ^{14}C measurements; black star indicates planktonic foraminiferal assemblage shift (for details, see Casford et al., (2002)).

The record of low-oxygen tolerant benthic foraminifera for SLA–9 shows an initial increase at around 10250 years B.P. (Figure 4b) (Casford et al., 2003). They attain a first peak at 9650 years B.P., exactly coincident with the first $(Ba/Al)_{sed}$ peak. After a drop to lower values, the percentage of low-oxygen tolerant benthic foraminifera abruptly increases to maximum values at 9000 years B.P. Values remain high until 6400 years B.P., when their percentage sharply decreases until background levels are reached at about 6100 years B.P. The relative abundance of *H. elegans* is generally < 2% throughout the core. Although such low abundances are difficult to quantify because of counting statistics (the entire 150–600 mm fraction has been used without any partitioning or splitting, in order to pick up to 250 specimens from each sample, or as many as present (Abu-Zied et al., 2008); however, within the sapropel sometimes only 80 to 150 specimen were present), concentrations do decrease somewhat during the sapropel (Figure 4b).

The $(Ba/Ca)_{H.\ elegans}$ ratios are stable from the bottom of the core to about 9800 years B.P. From there on they increase until a maximum of about 13 mmol/mol at 8300 years B.P. (Figure 4e). After this, values decrease to a minimum at 7400 years B.P., followed by a second interval with high values from 7300 to 6600 years B.P. After this, values fall back to presapropel ratios.

The $(Mn/Al)_{sed}$ values before and after the sapropel are between 12 and 14 mg/g (Figure 4f). A gradual decrease in $(Mn/Al)_{sed}$ starts at the base of the sapropel, culminating in a minimum of ~ 9 mg/g at about 8200 years B.P. From this point on we observe a gradual increase until about 6300 years B.P., where values abruptly increase to Holocene "baseline values."

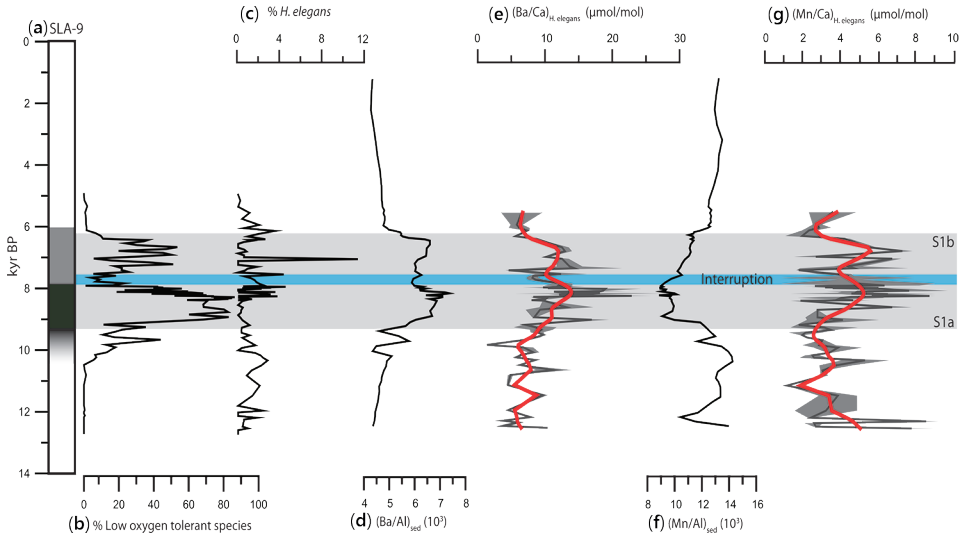

Figure 4 | (**a**) Color description based on core log. (**b**) Percentage low oxygen tolerant benthic foraminifera assemblages (from Casford et al., 2003). (**c**) *Hoeglundina elegans* as percent of total benthic foraminifera assemblage. (**d**) Elemental ratios versus conventional ^{14}C kyr of sedimentary $(Ba/Al)_{sed}$ (Casford et al., 2007). (**e**) Benthic foraminiferal $(Ba/Ca)_{H.\ elegans}$ from core SLA–9. Dark gray line represents $(Ba/Ca)_{H.\ elegans}$ data with standard deviations in gray envelope. Red line represents 500 year Gaussian smoothing of $(Ba/Ca)_{H.\ elegans}$ data. (**f**) Elemental ratios versus conventional ^{14}C kyr of sedimentary $(Mn/Al)_{sed}$. (**g**) Benthic foraminiferal $(Mn/Ca)_{H.\ elegans}$ from core SLA–9. Dark gray line represents $(Mn/Ca)_{H.\ elegans}$ data with standard deviations in gray envelope. Red line represents 500 year Gaussian smoothing of $(Mn/Ca)_{H.\ elegans}$ data. Extents of sapropel and sapropel interruption are indicated by gray and blue shading, respectively.

Oxygen isotopic values of *H. elegans* display considerable scatter until 10,000 years B.P., followed by less variable, rather heavy, values in the younger part of the record. The offset between $\delta^{18}O_{H.\ elegans}$ and $\delta^{18}O_{G.\ ruber}$ is reduced before 12,000 years B.P., but shows no clear systematic variations later in the record (Figure 5).

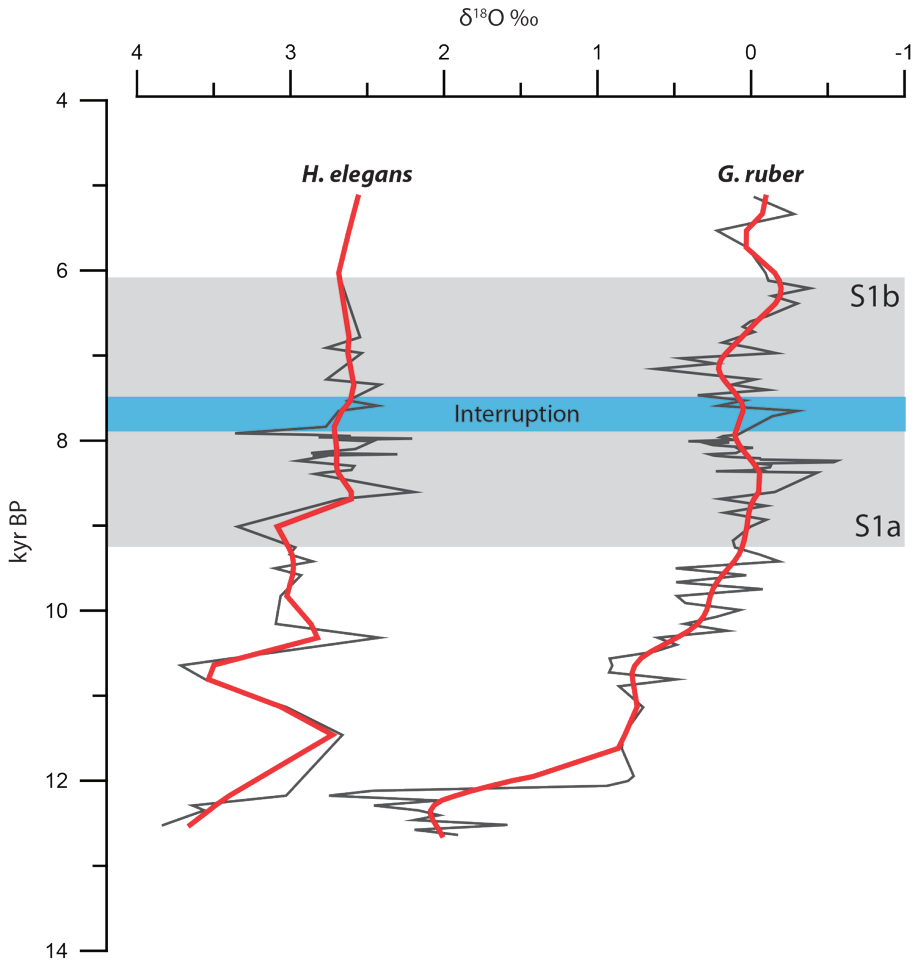

Figure 5 | Oxygen isotope records ‰ of *H. elegans* and *G. ruber* (Casford et al., 2002) versus conventional ^{14}C kyr in core SLA–9. Dark gray lines represent data, overlain with red line representing a 500 year Gaussian smoothing. Sapropel and sapropel interruption are indicated by gray and blue shading, respectively.

The $(Mn/Ca)_{H.\ elegans}$ ratios are low throughout our record (Figure 4g). They exhibit a large scatter and the pattern differs distinctly from the sedimentary $(Mn/Al)_{sed}$ ratio. A clear increase can be observed at about 8500 years B.P. Values remain high until 6700 years B.P. with the exception of a drop culminating at 7400 years B.P. After 6700 years B.P. values drop to a new minimum of 2.5 mmol/mol, at 6300 years B.P. Toward the top of the record, values show as light increase.

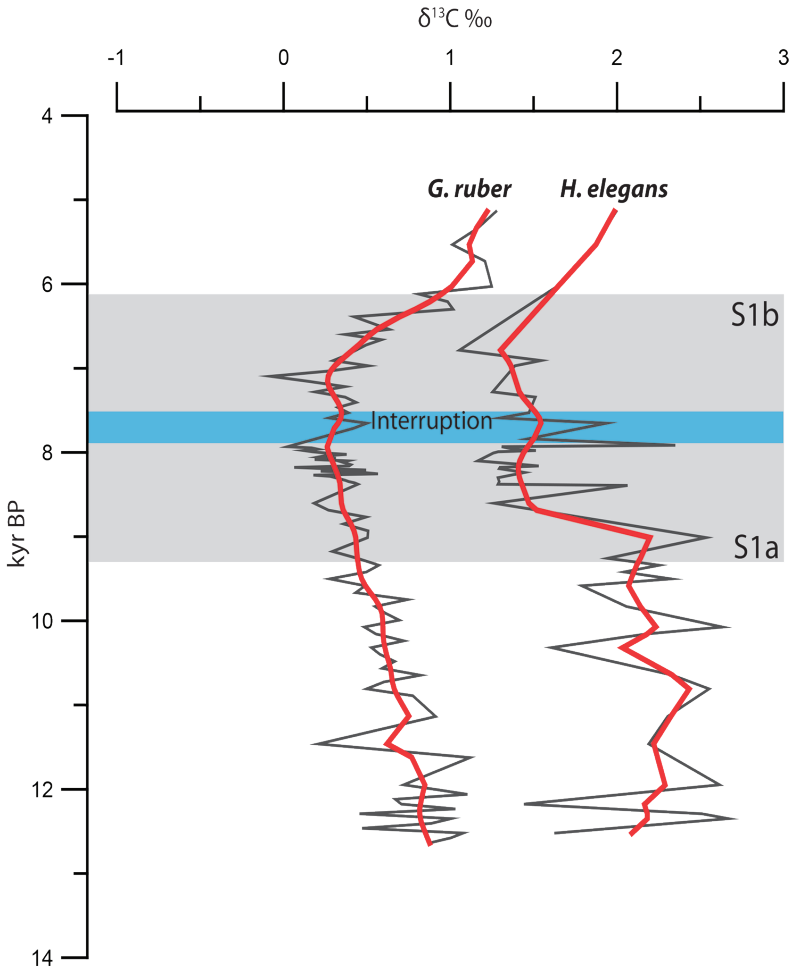

Figure 6 | Carbon isotope records ‰ of *H. elegans* and *G. ruber* (Casford et al., 2002) versus conventional ^{14}C kyr in core SLA–9. Dark gray lines represent data, overlain with red line representing a 500 year Gaussian smoothing. Sapropel and sapropel interruption are indicated by gray and blue shading, respectively.

Throughout the record $\delta^{13}C_{H.\ elegans}$ is heavier than $\delta^{13}C_{G.\ ruber}$ (Figure 6). Also, there is more scatter in the *H. elegans* record (single-specimen analyses) than in the *ruber* record (multiple-specimen analyses), likely related to smoothing effect inherent to multiple-specimen analyses.
Overall, $\delta^{13}C_{H.\ elegans}$ shows the same trend to the $\delta^{13}C_{G.\ ruber}$ trend: a gradual decrease toward the sapropel, culminating in a minimum at around 7100 years B.P. A more pronounced step toward lighter values is observed in $\delta^{13}C_{H.\ elegans}$ at about 9000 years B.P. This more abrupt step in $\delta^{13}C_{H.\ elegans}$causes the isotopic offset between the two species to decrease from this point onward.

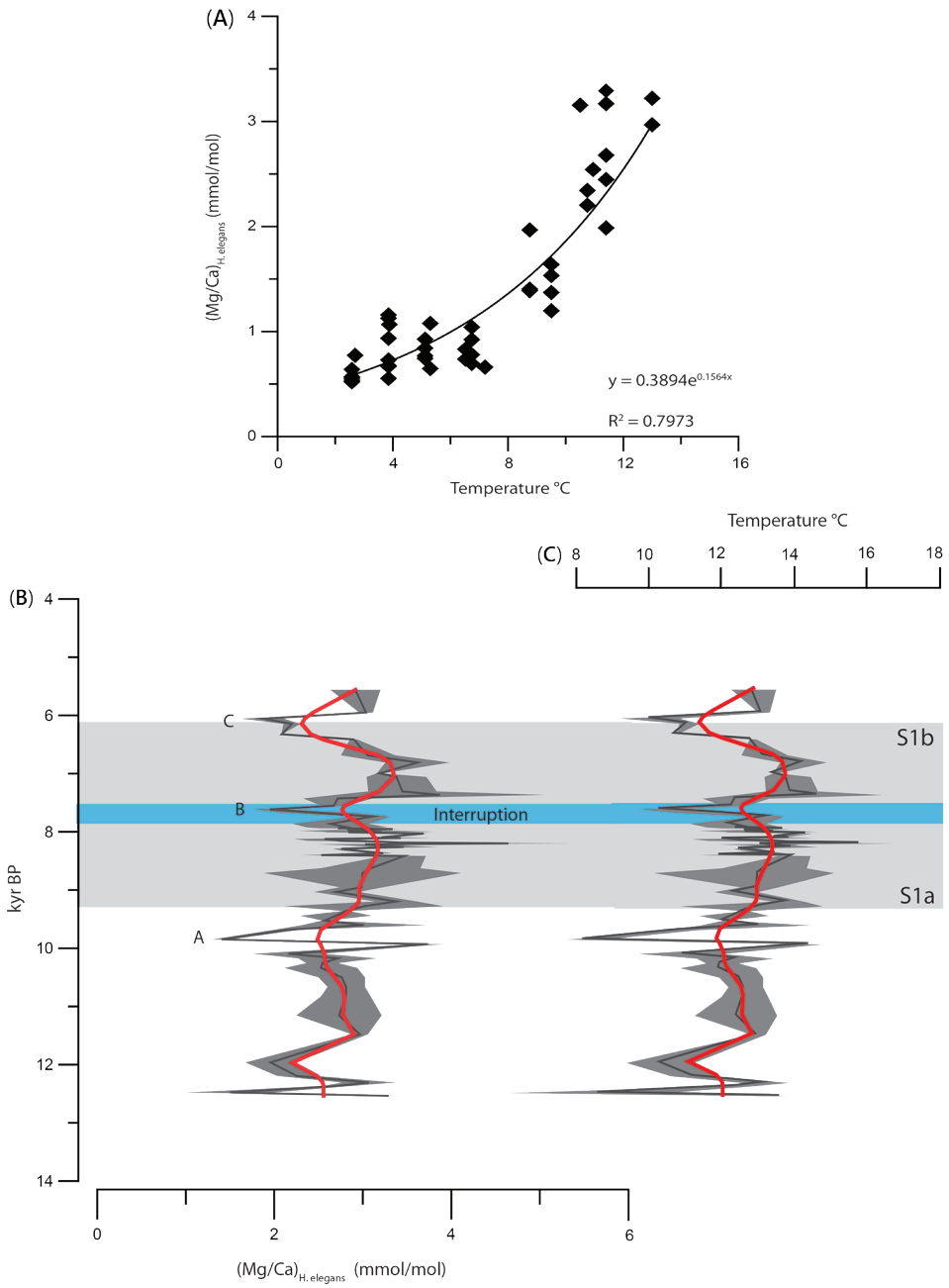

Figure 7 | (**A**) $(Mg/Ca)_{H.\ elegans}$ versus temperature calibration for *H. elegans*, adapted from Reichart et al., (2003). (**B**) $(Mg/Ca)_{H.elegans}$ versus conventional ^{14}C kyr in core SLA–9. Dark gray lines represent $(Mg/Ca)_{H.\ elegans}$ with standard deviations in gray envelope. Red line represents 500 year Gaussian smoothing of underlying data. Cooling events are indicated with letters A–C. Sapropel and sapropel interruption are indicated by gray and blue shading, respectively. (**C**) Temperature in °C as derived from the $(Mg/Ca)_{H.\ elegans}$ calibration versus kyr B.P. for core SLA–9.

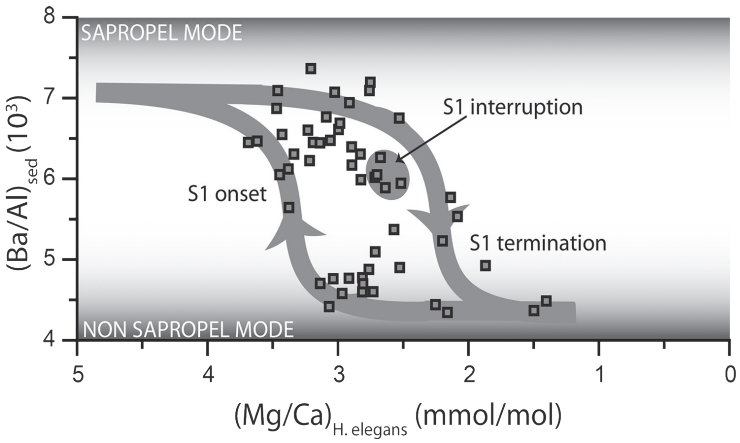

Figure 8 | Hysteresis in shifts from nonsapropel to sapropel mode. $(Mg/Ca)_{H.\ elegans}$ (proxy for temperature) is plotted versus $(Ba/Al)_{sed}$ (proxy for organic carbon) to illustrate the two alternate paths between sapropel and nonsapropel conditions.

The $(Mg/Ca)_{H.\ elegans}$–temperature calibration, adapted from Reichart et al., *(*2003), is best described by an exponential curve ($y = 0.3894e^{0.1564x}$) whereby temperature explains 80% of the variation in $(Mg/Ca)_{H.\ elegans}$ (Figure 7a). The $(Mg/Ca)_{H.\ elegans}$ ratios in SLA–9 fluctuate between 2 and 3.5 mmol/mol (Figure 7b). From 12,500 to 7000 years B.P., values increase from 2.6 to 3.5 mmol/mol. The upper part of the record is interrupted by 3 distinct centennial-scale minima, at 9700 years B.P., 7600 years B.P., and 6000 years B.P. (Figure 7b (A–C)). After 6000 years B.P., values are about 2.9 mmol/mol. From 12,500 years B.P. to 7000 years B.P. the resulting $(Mg/Ca)_{H.\ elegans}$ derived temperature record (Figure 7c) shows a gradual, temperature rise from ~ 12 to 14 °C. Disrupting this general increase in temperature are 3 prominent (~ 3–4 °C) cooling events at 9700 years B.P., 7600 years B.P., and 6000 years B.P. (Figures 7b and 7c (A–C)). However, cooling event A, at 9700 years B.P., is defined by a single data point. After about 6000 years B.P., $(Mg/Ca)_{H.\ elegans}$ ratios sharply increase again, returning to about 13 °C at 5500 years B.P. The Rosenthal et al., (2006) $(Mg/Ca)_{H.\ elegans}$–temperature calibration would suggest unrealistically high temperatures (in the order of 50 °C). The reason for this discrepancy is unclear. Possibly, given that different analytical methods were employed, the leaching phase in classical foraminiferal trace metal analyses preferentially removed a high Mg phase (Lohmann, 1995; Barker et al., 2003) from the more soluble aragonitic shells.

4 | DISCUSSION

4.1 | *Hoeglundina elegans* as a recorder of bottom water conditions during sapropel formation

In the Atlantic Ocean, *H. elegans* is a low to mid bathyal taxon that seems to prefer oligotrophic, oxic conditions (Fontanier et al., 2002). However, the species is also known to be able to tolerate low-oxygen environments, such as the California borderland basins (Douglas and Heitman, 1979; Mackensen and Douglas, 1989). Because of the extreme oligotrophy that characterizes the eastern Mediterranean (Antoine et al., 1995), *H. elegans* can be found at much shallower water depths, similar to other oligotrophic species (De Rijk et al., 2000). However, its low percentages in our core suggest that conditions were close to the tolerance limits of the taxon (Figure 4c), and that the depth of the core location is close to the upper bathymetric limit of this species in the southern Aegean Sea.

Due to the low abundances, only few specimens are available for geochemical analysis per sample. Particular care must therefore be taken to ensure that these scarce specimens are autochthonous. Several arguments converge to show that our *H. elegans* specimens are indeed autochthonous: First, $(Ba/Ca)_{H.\ elegans}$ and $(Mn/Ca)_{H.\ elegans}$ both increase during the sapropel (Figures 4e and 4g), in line with autochthonous *H. elegans* recorded bottom water chemistry during a period of enhanced export flux and/or reduced ventilation. Second, the stepped depletion in $d^{13}C_{H.\ elegans}$ at the sapropel onset, and its return to higher values at the sapropel termination, agree with records of other, more abundant benthic foraminifera from core SLA–9 (Casford et al., 2003). Next, the water depth of 260 m appears to be close to the upper depth limit of *H. elegans* in the Aegean Sea (Parker, 1958) so that reworking from shallower sites would be an unlikely source of *H. elegans* specimens. In general, the percentage of displaced epiphytic and other shallow water taxa is very low in our core, and becomes minimal during the deposition of sapropel S1(Abu-Zied et al., 2008, Figure 9). Finally, although reworking of older, glacial outcrops could also explain the presence of *H. elegans* in our samples, this is ruled out by the following observations: taxa typical of pre-Holocene conditions, such as *Cibicidoides pachydermus*, *Siphotextularia* spp. and *Trifarina angulosa*, are abundant in the pre-Holocene faunas at the bottom of the core (Abu-Zied et al., 2008). In sapropel S1, however, these taxa are present only in trace amounts. Thus, it can be excluded that they have been transported from better oxygenated niches in shallower water, or from reworking of older deposits. All these arguments converge to the conclusion that the occurrence of *H. elegans* is the result of a continuous presence of this taxon at the core locality.

Based on benthic foraminiferal studies of nearby cores, we suspect that the locality of SLA–9 (present water depth 260 m) was positioned several hundreds of meters above the limit of persistently anoxic waters during sapropel times. In fact, also core SL–31 from 430 m depth (Abu-Zied et al., 2008) contains benthic foraminifera throughout, whereas southern Aegean cores GeoTü SL123 from 728 m (Kuhnt et al., 2007) and C40 from 852 m depth (Geraga et

al., 2000) were almost devoid of benthic foraminifera during S1 times. These observations suggest that the limit between oxic and persistently anoxic bottom waters was positioned roughly between 500 and 700 m depth. Core SLA–9 not only shows a continuous presence of benthic foraminifera, but it also shows a continuous presence of low quantities of sediment-surface dwelling taxa, which are usually considered sensitive to low oxygen concentrations (e.g., *H. elegans, Gyroidina* spp.), suggesting that the seafloor at our core locality never became continually anoxic.

4.2 | Productivity in the Aegean during sapropel deposition

Enhanced $(Ba/Al)_{sed}$ ratios indicate that more barium was reaching the seafloor during sapropel formation. Marine sediments contain Ba mainly in the form of biogenic barite ($BaSO_4$) (Dehairs et al.,1980). Biogenic barite forms as microcrystals in decaying organic debris, a process that underpins its use as a proxy for past productivity in Mediterranean waters (Bishop, 1988; Dymond et al., 1996). Enhanced barite burial fluxes are a function of both productivity and preservation (Dymond et al., 1996). On reaching the seafloor, $BaSO_4$ partially dissolves in undersaturated bottom waters (Schenau et al., 2001). The associated release of dissolved Ba to the bottom waters is reflected in enhanced $(Ba/Ca)_{H.\ elegans}$. The degree of dissolution (and thus preservation of $BaSO_4$) depends on the concentration of sulfate and free Ba^{2+} (Church and Wolgemuth, 1972) both of which may be slightly modulated with changes in salinity (Millero and Schreiber, 1982). However, a salinity drop of 1–1.5, equivalent to the drop in salinity associated with increased fresh water runoff during sapropel formation (Rohling, 1994; Rohling, 1999; Kuhnt et al., 2007), results in only an ~ 1% increase in free Ba^{2+}concentration due to reduced complexation, and a decrease in $BaSO_4$ precipitation by 4% at most. Clearly this is irrelevant in comparison to the observed changes. Alternatively, enhanced $(Ba/Ca)_{H.\ elegans}$ could be related to reduced bottom water ventilation, leading to a build up of deeper water Ba^{2+}. Riverine input during sapropel formation may also serve as an additional local source of Ba^{2+} to the Aegean, as river water is enriched in Ba^{2+} relative to surface waters (Martin and Meybeck, 1979; Halland Chan, 2004; Weldeab et al., 2007). However, this influence is deemed negligible in view of the core location in the southern Aegean being remote from any potential river system. Transport of riverine Ba^{2+} is limited because seawater is at or close to saturation with respect to barite. Finally, barium can be scavenged from seawater by adsorption onto Mn oxides (De Lange et al., 1990), thus remobilization of Mn oxides could result in release of Ba^{2+}. The potential amount of adsorbed Ba that could be released from Mn oxides mobilized during S1 formation is negligible (Reitz et al., 2006), whereas that associated with post S1 Mn oxide formation remain fixed during oxygenated conditions. While $(Ba/Ca)_{H.\ elegans}$ ratios and thus bottom water Ba^{2+} undergo a doubling during sapropel formation, their absolute values still remain relatively low and are comparable to intermediate water values in the north Atlantic (Reichart et al., 2003), which suggests that barite remains undersaturated. Such low values exclude a substantial impact of increased bottom water Ba^{2+} concentrations on sedimentary

BaSO4 preservation. In summary, $(Ba/Al)_{sed}$ indicates higher export fluxes, whereas enhanced $(Ba/Ca)_{H.\ elegans}$ during sapropel formation can be attributed to a combination of higher export fluxes and low rates of bottom water ventilation.

4.3 | Bottom water redox conditions

Manganese is a redox sensitive element, which is remobilized from solid phase Mn oxide to dissolved Mn^{2+} during oxygen depleted (suboxic) (Libes, 2009; Burdige, 2006) bottom/pore water conditions (Froelich et al., 1979). Under such conditions, sedimentary Mn ($(Mn/Al)_{sed}$) becomes depleted as Mn^{2+} is released to the bottom waters. *Hoeglundina elegans*, living at the sediment water interface, will record this increased bottom water Mn^{2+} within its test ($(Mn/Ca)_{H.\ elegans}$) (Reichart et al., 2003; Boyle, 1983). The observed anticorrelation in our record between $(Mn/Ca)_{H.\ elegans}$ and $(Mn/Al)_{sed}$ therefore suggests such enhanced Mn mobilization due to suboxic conditions at or close to the sediment water interface. The high variability seen in $(Mn/Ca)_{H.\ elegans}$ during the sapropel probably primarily reflects the highly dynamic nature of Mn cycling at the sediment water interface.

Using variations in $(Mn/Al)_{sed}$ and $(Mn/Ca)_{H.\ elegans}$ profiles as a framework, we propose a five-step evolution of redox conditions in the southern Aegean during sapropel formation, resulting from the interplay of stratification and water mass isolation with ventilation and reoxygenation. Redox changes may also be driven by higher fluxes of organic matter reaching the seafloor. Increased river runoff during sapropel deposition indeed brought with it a higher flux of riverine organic matter to the Aegean (Aksu et al., 1999). However, its contribution to redox variations at the sediment water interface would be minor due to its refractive nature (Burdige, 2005).

Table A1 | Results of Ba single laser ablation analyses, with averages per test where applicable, standard deviation, and standard error per depth, where applicable[a]

Ablation Code	Depth (cm)	Ba/Ca (mmol/mol)	AVE Test	SD Test	AVE Depth	SD Depth	SE Depth
F2-1	56.25	4.86	4.38	0.67	6.55	3.07	0.72
F2-2	56.25	3.91					
F3-1	56.25	7.39	8.72	1.38			
F3-2	56.25	10.14					
F3-3	56.25	8.62					
F4-1	60.25	5.14	5.80	0.92			
F4-2	60.25	6.45					
F5-2	62.25	5.36	7.28	2.72	6.18	1.56	1.07
F5-3	62.25	9.20					
F6-1	62.25	4.86	5.07	0.31			
F6-2	62.25	5.29					
F8-1	64.25	7.61	7.36	0.36			
F8-3	64.25	7.10					
F9-1	68.25	5.80	5.62	0.26			
F9-2	68.25	8.70					
F9-3	68.25	5.43					
F11-3	70.25	8.84	8.77	0.10			
F11-4	70.25	8.70					
F13-2	73.75	12.54					
F15-1	74.25	12.97					
F17-1	75.75	10.43	10.18	0.36			
F17-2	75.75	9.93					
F18-1	76.25	12.54					
F19-1	78.25	12.32	13.66	1.90			
F19-2	78.25	15.00					
F21-1	78.75	9.78	9.46	0.46	14.40	6.99	1.11
F21-2	78.75	9.13					
F22-1	78.75	17.46	19.35	2.66			
F22-2	78.75	21.23					
F23-1	79.25	4.28	4.60	0.46			
F23-2	79.25	4.93					
F24-1	80.25	10.22	9.67	0.77	12.39	3.84	0.51
F24-2	80.25	9.13					
F25-1	80.25	14.64	15.11	0.67			
F25-2	80.25	15.58					
F27-1	80.75	8.26					

Table A1 | *Continued*

Ablation Code	Depth (cm)	Ba/Ca (mmol/mol)	AVE Test	SD Test	AVE Depth	SD Depth	SE Depth
F28-1	81.25	9.20	8.77	0.61	8.13	0.90	0.34
F28-2	81.25	8.33					
F29-1	81.25	7.75	7.50	0.36			
F29-2	81.25	7.25					
F30-1	81.75	9.42	8.62	1.13			
F30-2	81.75	7.83					
F31-1	82.75	17.39	13.66	5.28	12.57	1.54	4.75
F31-2	82.75	9.93					
F33-1	82.75	17.25	11.49	8.15			
F33-2	82.75	5.72					
F35-1	83.25	10.00	0.05	0.37	11.97	2.74	2.08
F35-2	83.25	10.07					
F36-1	83.25	9.78	13.91	5.84			
F36-2	83.25	18.04					
F38-2	83.75	13.19	12.25	1.33	11.90	0.49	0.78
F38-3	83.75	11.30					
F39-1	83.75	12.17	11.56	0.87			
F39-2	83.75	10.94					
F40-2	84.25	10.07			12.95	2.90	1.78
F41-1	84.25	15.00					
F43-1	84.25	10.22	10.91	0.97			
F43-2	84.25	11.59					
F44-1	84.75	11.38	12.79	2.00	12.56	3.36	1.46
F44-2	84.75	14.20					
F45-1	84.75	12.97	15.80	4.00			
F45-2	84.75	18.62					
F46-1	84.75	7.97	9.09	1.59			
F46-2	84.75	10.22					
F48-1	85.25	7.25	7.61	0.51	9.71	2.97	0.65
F48-2	85.25	7.97					
F49-1	85.25	10.87	11.81	1.33			
F49-2	85.25	12.75					
F51-1	85.75	13.77	12.93	1.18			
F51-2	85.75	12.10					
F52-1	86.25	13.33	9.53	5.38	10.43	1.28	1.92
F52-2	86.25	5.72					
F53-1	86.25	11.38	11.34	0.05			

Table A1 | *Continued*

Ablation Code	Depth (cm)	Ba/Ca (mmol/mol)	AVE Test	SD Test	AVE Depth	SD Depth	SE Depth
F53-2	86.25	11.30					
F54-2	86.75	12.75	15.29	3.59	18.99	5.23	
F54-3	86.75	17.83					
F55-1	86.75	22.68					
F56-1	88.75	18.55	18.66	0.15			
F56-2	88.75	18.77					
F57-1	89.25	15.65	18.26	3.69			
F57-2	89.25	20.87					
F58-1	89.75	11.38			11.34	0.05	
F59-1	89.75	12.54	11.30	1.74			
F59-2	89.75	10.07					
F60-1	90.75	11.81	13.26	2.05	12.81	0.64	1.43
F60-2	90.75	14.71					
F61-1	90.75	13.77	12.36	2.00			
F61-2	90.75	10.94					
F62-2	91.25	18.19					
F63-1	91.25	13.91	18.15	6.00			
F63-2	91.25	22.39					
F64-1	91.75	23.84	24.02	0.26	16.45	10.71	0.11
F64-2	91.75	24.20					
F65-1	91.75	8.84	8.88	0.05			
F65-2	91.75	8.91					
F67-2	92.25	18.26	17.83	0.61	16.27	2.20	
F67-3	92.25	17.39					
F68-2	92.25	14.71					
F69-1	92.75	8.62	10.33	2.41			
F69-2	92.75	12.03					
F70-1	92.75	14.64	13.30	1.90	12.10	1.57	1.09
F70-2	92.75	11.96					
F71-1	92.75	12.46	12.68	0.31			
F71-2	92.75	12.90					
G2-2	93.25	12.68					
G5-1	94.25	24.86	22.90	2.77			
G5-2	94.25	20.94					
G7-1	95.25	8.04	8.26	0.31			
G7-2	95.25	8.48					
G8-1	96.25	8.84	10.33	2.10			

Table A1 | *Continued*

Ablation Code	Depth (cm)	Ba/Ca (mmol/mol)	AVE Test	SD Test	AVE Depth	SD Depth	SE Depth
G8-2	96.25	11.81					
G9-1	97.75	9.64	10.04	0.56			
G9-2	97.75	10.43					
G10-1	98.75	7.90	8.01	0.15			
G10-2	98.75	8.12					
G11-1	99.25	9.93	9.82	0.15			
G11-2	99.25	9.71					
G12-1	100.75	16.01	13.19	4.00			
G12-2	100.75	10.36					
G13-1	101.25	10.80	9.28	2.15			
G13-2	101.25	7.75					
G14-1	102.75	8.41					
G14-2	102.75	7.97					
G15-1	103.25	18.77	16.96	2.56			
G15-2	103.25	15.14					
G17-1	104.25	6.88	7.10	0.31			
G17-2	104.25	7.32					
G18-1	104.75	6.30	8.55	3.18			
G18-2	104.75	10.80					
G19-1	105.25	6.09	6.27	0.26			
G19-2	105.25	6.45					
G19R-1	105.25	8.26	9.46	1.69			
G19R-2	105.25	10.65					
G20-1	105.75	8.12	8.80	0.97			
G20-2	105.75	9.49					
G22-1	106.25	9.93	9.78	0.20			
G22-2	106.25	9.64					
G25-1	106.75	8.04	8.59	0.77			
G25-2	106.75	9.13					
G26-1	107.25	6.38	6.99	0.87			
G26-2	107.25	7.61					
G27-1	108.25	1.23	1.38	0.20			
G27-2	108.25	1.52					
G30-1	108.75	5.80	6.81	1.43			
G30-2	108.75	7.83					
G31-1	109.75	7.68	8.30	0.87			
G31-2	109.75	8.91					

Table A1 | *Continued*

Ablation Code	Depth (cm)	Ba/Ca (mmol/mol)	AVE Test	SD Test	AVE Depth	SD Depth	SE Depth
G32-1	110.25	6.59	6.38	0.31			
G32-2	110.25	6.16					
G34-1	110.75	6.16	5.76	0.56			
G34-2	110.75	5.36					
G36-1	111.25	8.41	8.62	0.31			
G36-2	111.25	8.84					
G41-1	113.25	13.19	11.30	2.66			
G41-2	113.25	9.42					
G42-2	114.25	4.86					
G43-1	116.25	4.64	4.49	0.20			
G43-2	116.25	4.35					
G46-1	118.25	9.28	9.75	0.67			
G46-2	118.25	10.22					
G47-1	122.25	4.71	4.53	0.26			
G47-2	122.25	4.35					
G51-3	134.25	3.77					
G52-1	136.25	6.59	5.98	0.87			
G52-2	136.25	5.36					
G53-1	140.25	3.19	3.80	0.87			
G53-2	140.25	4.42					
G54-1	142.25	10.00	10.25	0.36			
G54-2	142.25	10.51					

[a]AVE, average; SD, standard deviation; SE, standard error.

Table A2 | Results of Mn single laser ablation analyses, with averages per test where applicable, standard deviation, and standard error per depth, where applicable[a]

Ablation Code	Depth (cm)	M/Ca (mmol/mol)	AVE Test	SD Test	AVE Depth	SD Depth	SE Depth
F2-1	56.25	2.36	2.09	0.39	2.98	1.26	0.30
F2-2	56.25	1.82					
F3-1	56.25	3.82	3.88	0.46			
F3-2	56.25	3.45					
F3-3	56.25	4.36					
F4-1	60.25	2.00	2.18	0.26			
F4-2	60.25	2.36					
F5-2	62.25	2.00	2.73	1.03	2.27	0.64	0.82
F5-3	62.25	3.45					
F6-1	62.25	2.73	1.82	1.29			
F6-2	62.25	0.91					
F8-1	64.25	2.00	1.73	0.39			
F8-3	64.25	1.45					
F9-1	68.25	0.73	1.36	0.90			
F9-2	68.25	2.91					
F9-3	68.25	2.00					
F11-3	70.25	3.64	3.64				
F11-4	70.25	3.64					
F13-2	73.75	4.91					
F15-1	74.25	6.73					
F17-1	75.75	1.27	2.09	1.16			
F17-2	75.75	2.91					
F18-1	76.25	6.18					
F19-1	78.25	3.27	3.82	0.77			
F19-2	78.25	4.36					
F21-1	78.75	2.36	2.09	0.39	4.14	2.89	0.23
F21-2	78.75	1.82					
F22-1	78.75	6.36	6.18	0.26			
F22-2	78.75	6.00					
F23-1	79.25	1.27	1.18	0.13			
F23-2	79.25	1.09					
F24-1	80.25	2.18	2.45	0.39	3.09	0.90	0.18
F24-2	80.25	2.73					
F25-1	80.25	3.64	3.73	0.13			
F25-2	80.25	3.82					
F27-1	80.75	3.82					

Table A2 | *Continued*

Ablation Code	Depth (cm)	M/Ca (mmol/mol)	AVE Test	SD Test	AVE Depth	SD Depth	SE Depth
F28-1	81.25	6.00	6.27	0.39	3.77	3.54	0.23
F28-2	81.25	6.55					
F29-1	81.25	1.45	1.27	0.26			
F29-2	81.25	1.09					
F30-1	81.75	3.45	3.91	0.64			
F30-2	81.75	4.36					
F31-1	82.75	11.09	7.27	5.40	4.36	4.11	2.00
F31-2	82.75	3.45					
F33-1	82.75	1.27	1.45	0.26			
F33-2	82.75	1.64					
F35-1	83.25	4.36	2.19	67.25	5.77	0.19	1.86
F35-2	83.25	7.45					
F36-1	83.25	3.45	5.64	3.09			
F36-2	83.25	7.82					
F38-2	83.75	1.09	1.91	1.16	2.05	0.19	0.59
F38-3	83.75	2.73					
F39-1	83.75	1.82	2.18	0.51			
F39-2	83.75	2.55					
F40-2	84.25	4.36			4.50	0.19	1.00
F41-1	84.25	4.36					
F43-1	84.25	3.64	4.64	1.41			
F43-2	84.25	5.64					
F44-1	84.75	3.64	4.82	1.67	3.76	0.92	0.69
F44-2	84.75	6.00					
F45-1	84.75	2.18	3.27	1.54			
F45-2	84.75	4.36					
F46-1	84.75	3.45	3.18	0.39			
F46-2	84.75	2.91					
F48-1	85.25	3.27	3.09	0.26	2.59	0.71	0.41
F48-2	85.25	2.91					
F49-1	85.25	2.73	2.09	0.90			
F49-2	85.25	1.45					
F51-1	85.75	6.91	5.45	2.06			
F51-2	85.75	4.00	0.00	0.00			
F52-1	86.25	4.55	3.73	1.16	3.00	1.03	0.45
F52-2	86.25	2.91					
F53-1	86.25	2.18	2.27	0.13			

Table A2 | *Continued*

Ablation Code	Depth (cm)	M/Ca (mmol/mol)	AVE Test	SD Test	AVE Depth	SD Depth	SE Depth
F53-2	86.25	2.36					
F54-2	86.75	5.82	6.64	1.16	5.59	1.48	
F54-3	86.75	7.45					
F55-1	86.75	4.55					
F56-1	88.75	5.64	7.09	2.06			
F56-2	88.75	8.55					
F57-1	89.25	3.45	5.27	2.57			
F57-2	89.25	7.09					
F58-1	89.75	4.91			4.32	0.84	
F59-1	89.75	6.00	3.73	3.21			
F59-2	89.75	1.45					
F60-1	90.75	6.00	4.91	1.54	4.23	0.96	0.95
F60-2	90.75	3.82					
F61-1	90.75	4.36	3.55	1.16			
F61-2	90.75	2.73					
F62-2	91.25	3.82					
F63-1	91.25	2.36	4.73	3.34			
F63-2	91.25	7.09					
F64-1	91.75	6.36	6.27	0.13	4.00	3.21	0.18
F64-2	91.75	6.18					
F65-1	91.75	2.00	1.73	0.39			
F65-2	91.75	1.45					
F67-2	92.25	8.55	7.73	1.16	5.95	2.51	
F67-3	92.25	6.91					
F68-2	92.25	4.18					
F69-1	92.75	3.09	3.55	0.64			
F69-2	92.75	4.00					
F70-1	92.75	5.45	6.09	0.90	5.27	1.50	0.67
F70-2	92.75	6.73					
F71-1	92.75	7.09	6.18	1.29			
F71-2	92.75	5.27					
G2-2	93.25	5.09					
G5-1	94.25	8.00	8.18	0.26			
G5-2	94.25	8.36					
G7-1	95.25	2.91	4.00	1.54			
G7-2	95.25	5.09					
G8-1	96.25	1.82	3.45	2.31			

Table A2 | *Continued*

Ablation Code	Depth (cm)	M/Ca (mmol/mol)	AVE Test	SD Test	AVE Depth	SD Depth	SE Depth
G8-2	96.25	5.09					
G9-1	97.75	3.09	3.27	0.26			
G9-2	97.75	3.45					
G10-1	98.75	4.73	4.09	0.90			
G10-2	98.75	3.45					
G11-1	99.25	1.64	1.27	0.51			
G11-2	99.25	0.91					
G12-1	100.75	6.91	6.18	1.03			
G12-2	100.75	5.45					
G13-1	101.25	2.18	2.18	0.00			
G13-2	101.25	2.18					
G14-1	102.75	2.18					
G14-2	102.75	1.27					
G15-1	103.25	4.91	3.55	1.93			
G15-2	103.25	2.18					
G17-1	104.25	1.27	1.18	0.13			
G17-2	104.25	1.09					
G18-1	104.75	1.27	2.55	1.80			
G18-2	104.75	3.82					
G19-1	105.25	3.82	3.18	0.90			
G19-2	105.25	2.55					
G19R-1	105.25	2.91	2.91	0.00			
G19R-2	105.25	2.91					
G20-1	105.75	0.91	1.55	0.90			
G20-2	105.75	2.18					
G22-1	106.25	1.27	1.36	0.13			
G22-2	106.25	1.45					
G25-1	106.75	1.64	1.64	0.00			
G25-2	106.75	1.64					
G26-1	107.25	2.36	2.45	0.13			
G26-2	107.25	2.55					
G27-1	108.25	2.91	2.27	0.90			
G27-2	108.25	1.64					
G30-1	108.75	2.36	3.27	1.29			
G30-2	108.75	4.18					
G31-1	109.75	2.91	2.82	0.13			
G31-2	109.75	2.73					

Table A2 | *Continued*

Ablation Code	Depth (cm)	M/Ca (mmol/mol)	AVE Test	SD Test	AVE Depth	SD Depth	SE Depth
G32-1	110.25	2.18	1.91	0.39			
G32-2	110.25	1.64					
G34-1	110.75	1.45	2.00	0.77			
G34-2	110.75	2.55					
G36-1	111.25	3.82	4.73	1.29			
G36-2	111.25	5.64					
G41-1	113.25	2.55	2.45	0.13			
G41-2	113.25	2.36					
G42-2	114.25	2.55					
G43-1	116.25	0.55	0.55	0.00			
G43-2	116.25	0.55					
G46-1	118.25	2.55	3.27	1.03			
G46-2	118.25	4.00					
G47-1	122.25	3.82	2.64	1.67			
G47-2	122.25	1.45					
G51-3	134.25	8.00					
G52-1	136.25	1.64	2.00	0.51			
G52-2	136.25	2.36					
G53-1	140.25	2.00	2.09	0.13			
G53-2	140.25	2.18					
G54-1	142.25	8.00	7.18	1.16			
G54-2	142.25	6.36					

[a]AVE, average; SD, standard deviation; SE, standard error.

Table A3 | Results of Mg single laser ablation analyses, with averages per test where applicable, standard deviation and standard error per depth, where applicable[a]

Ablation Code	Depth (cm)	Mn/Ca (mmol/mol)	AVE Test	SD Test	AVE Depth	SD Depth	SE Depth
F2-1	56.25	3.51	3.12	0.55	2.92	0.28	0.21
F2-2	56.25	2.73					
F3-1	56.25	2.75	2.72	0.04	0.00	0.00	0.00
F3-2	56.25	2.68					
F3-3	56.25	2.72					
F4-1	60.25	3.09	3.04	0.08			
F4-2	60.25	2.98					
F5-2	62.25	1.59	1.70	0.15	1.87	0.24	0.14
F5-3	62.25	1.81					
F6-1	62.25	1.87	2.04	0.24			
F6-2	62.25	2.21					
F8-1	64.25	2.27	2.20	0.09			
F8-3	64.25	2.13					
F9-1	68.25	2.09	2.08				
F9-2	68.25	2.91					
F9-3	68.25	2.08					
F11-3	70.25	2.92	2.90	0.04			
F11-4	70.25	2.87					
F13-2	73.75	3.06					
F15-1	74.25	3.62					
F17-1	75.75	3.21	3.19	0.03			
F17-2	75.75	3.17					
F18-1	76.25	3.38					
F19-1	78.25	3.17	3.45	0.39			
F19-2	78.25	3.72					
F21-1	78.75	3.17	3.04	0.18	3.87	1.18	0.21
F21-2	78.75	2.91					
F22-1	78.75	4.41	4.71	0.42			
F22-2	78.75	5.00					
F23-1	79.25	2.44	2.72	0.39			
F23-2	79.25	2.99					
F24-1	80.25	2.38	2.58	0.28	2.67	0.14	0.11
F24-2	80.25	2.77					
F25-1	80.25	2.74	2.77	0.04			
F25-2	80.25	2.80					
F27-1	80.75	1.95					

Table A3 | *Continued*

Ablation Code	Depth (cm)	Mn/Ca (mmol/mol)	AVE Test	SD Test	AVE Depth	SD Depth	SE Depth
F28-1	81.25	2.93	2.81	0.16	2.52	0.41	0.15
F28-2	81.25	2.69					
F29-1	81.25	2.42	2.22	0.27			
F29-2	81.25	2.03					
F30-1	81.75	3.24	3.11	0.20			
F30-2	81.75	2.97					
F31-1	82.75	3.29	2.94	0.50	2.64	0.43	0.39
F31-2	82.75	2.59					
F33-1	82.75	2.76	2.33	0.60			
F33-2	82.75	1.91					
F35-1	83.25	2.54	2.73	0.27	2.82	0.13	0.46
F35-2	83.25	2.92					
F36-1	83.25	2.20	2.92	1.02			
F36-2	83.25	3.64					
F38-2	83.75	2.28	2.64	0.52	2.72	0.10	0.20
F38-3	83.75	3.01					
F39-1	83.75	2.83	2.79	0.06			
F39-2	83.75	2.75					
F40-2	84.25	2.50			3.34	0.07	0.53
F41-1	84.25	3.29					
F43-1	84.25	3.18	3.38	0.29			
F43-2	84.25	3.59					
F44-1	84.75	2.83	2.83		2.83		0.17
F44-2	84.75	2.83					
F45-1	84.75	2.71	2.82	0.17			
F45-2	84.75	2.94					
F46-1	84.75	2.31	2.83	0.74			
F46-2	84.75	3.35					
F48-1	85.25	2.75	2.47	0.40	2.89	0.60	0.27
F48-2	85.25	2.18					
F49-1	85.25	3.58	3.32	0.37			
F49-2	85.25	3.06					
F51-1	85.75	3.64	3.21	0.61			
F51-2	85.75	2.78					
F52-1	86.25	3.44	2.91	0.75	2.84	0.11	0.28
F52-2	86.25	2.38					
F53-1	86.25	2.79	2.76	0.04			

Table A3 | *Continued*

Ablation Code	Depth (cm)	Mn/Ca (mmol/mol)	AVE Test	SD Test	AVE Depth	SD Depth	SE Depth
F53-2	86.25	2.74					
F54-2	86.75	3.24	3.72	0.68			
F54-3	86.75	4.20					
F55-1	86.75	3.65		3.69	0.05		
F56-1	88.75	3.13	3.22	0.12			
F56-2	88.75	3.30					
F57-1	89.25	3.20	3.43	0.32			
F57-2	89.25	3.66					
F58-1	89.75	2.81	2.32	0.41	2.57	0.34	0.36
F59-1	89.75	2.61					
F59-2	89.75	2.04					
F60-1	90.75	3.24	3.01	0.32	2.75	0.37	0.35
F60-2	90.75	2.79					
F61-1	90.75	2.96	2.49	0.67			
F61-2	90.75	2.01					
F62-2	91.25	3.11	3.30	0.32	3.21	0.17	
F63-1	91.25	3.07					
F63-2	91.25	3.53					
F64-1	91.75	3.63	3.55	0.11	3.41	0.20	0.07
F64-2	91.75	3.47					
F65-1	91.75	3.33	3.27	0.09			
F65-2	91.75	3.21					
F67-2	92.25	4.97	5.14	0.24	4.64	0.70	0.35
F67-3	92.25	5.31					
F68-2	92.25	4.15					
F69-1	92.75	2.19	2.86	0.95	3.03	0.53	0.27
F69-2	92.75	3.53					
F70-1	92.75	3.70	3.62	0.11			
F70-2	92.75	3.54					
F71-1	92.75	2.82	2.60	0.31			
F71-2	92.75	2.37					
G2-2	93.25	3.14					
G5-1	94.25	3.73	3.46	0.38			
G5-2	94.25	3.19					
G7-1	95.25	2.83	2.76	0.10			
G7-2	95.25	2.69					
G8-1	96.25	2.81	2.91	0.15			

Table A3 | *Continued*

Ablation Code	Depth (cm)	Mn/Ca (mmol/mol)	AVE Test	SD Test	AVE Depth	SD Depth	SE Depth
G8-2	96.25	3.02					
G9-1	97.75	3.15	3.23	0.11			
G9-2	97.75	3.31					
G10-1	98.75	2.37	2.53	0.23			
G10-2	98.75	2.69					
G11-1	99.25	3.64	3.47	0.24			
G11-2	99.25	3.30					
G12-1	100.75	3.49	3.09	0.56			
G12-2	100.75	2.69					
G13-1	101.25	3.78	3.00	1.11			
G13-2	101.25	2.21					
G14-1	102.75	2.98	2.98	0.24			
G14-2	102.75	2.64					
G15-1	103.25	2.88	2.70	0.25			
G15-2	103.25	2.52					
G17-1	104.25	3.54	3.38	0.23			
G17-2	104.25	3.21					
G18-1	104.75	2.38	3.01	0.90			
G18-2	104.75	3.65					
G19-1	105.25	2.95	2.76	0.26			
G19-2	105.25	2.58					
G19R-1	105.25	2.78	2.81	0.04			
G19R-2	105.25	2.84					
G20-1	105.75	2.41	2.70	0.40			
G20-2	105.75	2.98					
G22-1	106.25	2.55	2.57	0.03			
G22-2	106.25	2.59					
G25-1	106.75	2.52	3.01	0.70			
G25-2	106.75	3.50					
G26-1	107.25	2.03	2.14	0.15			
G26-2	107.25	2.24					
G27-1	108.25	1.33	1.40	0.11			
G27-2	108.25	1.48					
G30-1	108.75	3.85	3.73	0.17			
G30-2	108.75	3.62					
G31-1	109.75	1.88	2.16	0.39			
G31-2	109.75	2.44					

Table A3 | *Continued*

Ablation Code	Depth (cm)	Mn/Ca (mmol/mol)	AVE Test	SD Test	AVE Depth	SD Depth	SE Depth
G32-1	110.25	3.03	2.71	0.45			
G32-2	110.25	2.40					
G34-1	110.75	2.42	2.54	0.18			
G34-2	110.75	2.67					
G36-1	111.25	2.82	2.53	0.41			
G36-2	111.25	2.23					
G41-1	113.25	2.66	2.81	0.21			
G41-2	113.25	2.96					
G42-2	114.25	2.81					
G43-1	116.25	3.07	2.73	0.48			
G43-2	116.25	2.39					
G46-1	118.25	2.90	2.97	0.09			
G46-2	118.25	3.03					
G47-1	122.25	2.16	1.96	0.28			
G47-2	122.25	1.76					
G51-3	134.25	3.07					
G52-1	136.25	2.60	2.72	0.17			
G52-2	136.25	2.84					
G53-1	140.25	1.15	1.50	0.49			
G53-2	140.25	1.84					
G54-1	142.25	3.24	3.28	0.07			
G54-2	142.25	3.33					

[a]AVE, average; SD, standard deviation; SE, standard error.

First (10,300 years B.P. to 9000 years B.P.), a gradual decrease in $(Mn/Al)_{sed}$ prior to sapropel formation resulted from partial mobilization of Mn oxides within the sediments (Figure 4f). Continuously low $(Mn/Ca)_{H.\ elegans}$ suggests that the liberated Mn^{2+} reprecipitated immediately above or near the sediment-water interface, which indicates that bottom waters remained oxygenated. The shift to lighter $\delta^{18}O$ values in both *H. elegans* and *G. ruber* at ~ 10,300 years B.P. is here interpreted to signify a gradual freshening of the entire water column (Figure 5). Based on *G. ruber* alone, Casford et al. (2002) previously interpreted this shift as a strengthening of the summer thermocline. However, as a similar shift to lighter $\delta^{18}O$ values also occurs in the benthic foraminiferal species *H. elegans*, this suggests that it is not a seasonal surface water signal, but rather points to a year-round change, affected the whole watercolumn.

Second (9000 years B.P. to 7900 years B.P. (sapropel S1a), a quick onset of oxygen depleted conditions in the bottom waters resulted in rapid mobilization of Mn oxides from the sediment and a build up of Mn^{2+} at the sediment-water interface, where *H. elegans* calcifies. The increase in $(Mn/Ca)_{H.\ elegans}$ at 9000 years B.P. coincides with an abrupt shift to lighter values in both $\delta^{18}O_{H.\ elegans}$ and $\delta^{13}C_{H.\ elegans}$ (see Figures 5 and 6). The observed depletion in $\delta^{13}C_{H.\ elegans}$ can be explained by an enhanced organic matter flux and subsequent remineralization, releasing ^{13}C depleted DIC at the sediment water interface.

Third (7900 years B.P. to 7500 years B.P.), reventilation of the water column drove the Mn^{2+}/MnO_2 redox front back into the sediment during the sapropel interruption. Consequently $(Mn/Al)_{sed}$ increases, while $(Mn/Ca)_{H.\ elegans}$ decreases (Figures 4f and 4g).

Fourth (7500 years B.P. to 6100 years B.P. (S1b)), reestablishment of suboxic bottom water conditions during the second phase of sapropel deposition led to a renewed migration of the Mn^{2+}/MnO_2 redox front to the sediment water interface, resulting in maximal $(Mn/Ca)_{H.\ elegans}$ values (Figure 4g). Here, $(Mn/Al)_{sed}$ and $(Mn/Ca)_{H.\ elegans}$ no longer exhibit the negative correlation, seen in the previous intervals. Instead $(Mn/Al)_{sed}$ continues to rise gradually until sapropel termination. The absence of expected "low" $(Mn/Al)_{sed}$ values during S1b can be explained as a diagenetic feature due to post depositional reoxygenation of sediments, or "burn down" whereby a downward diffusing redox front converts Mn^{2+} to Mn oxides, thus obscuring the primary $(Mn/Al)_{sed}$ signal (van Santvoort et al., 1996). The drop toward Holocene values starts abruptly at 6800 years B.P., where $(Mn/Ca)_{H.\ elegans}$ rapidly decreases as $d^{13}C_{H.\ elegans}$ and $d^{13}C_{G.\ ruber}$ shift back to heavier values (Figure 6).

Fifth (6100 years B.P. and afterward), complete reventilation of bottom waters at the sapropel termination caused the Mn^{2+}/MnO_2 redox front to migrate back into the sediment. This led to the accumulation of Mn oxides that cause higher $(Mn/Al)_{sed}$ and low $(Mn/Ca)_{H.\ elegans}$.

4.4 | Abrupt centennial-scale cooling events

Abrupt centennial-scale cooling events exert important control on sapropel deposition, as they appear to be responsible for both sapropel interruption and termination (see Figure 7c). Each cooling event (labeled A–C in Figure 7c) results in an approximate drop in temperature of 3–4 °C, independently confirming what previous studies, using different methods, have shown (Rohling et al., 1997; De Rijk et al., 1999; Cacho et al., 2001; Rohling et al., 2002). Cooling event A, though constrained here by a single data point only, may correlate with a short cooling event suggested by planktonic foraminiferal assemblage changes in the Adriatic, at 9500 years B.P. (Rohling et al., 1997; De Rijk et al., 1999). Cooling events B (sapropel interruption) and C (sapropel termination) have been similarly inferred from regional marine records (Rohling et al., 1997; De Rijk et al., 1999; Geraga et al., 2000; Mercone et al., 2001; Rohling et al., 2002). These short-term cooling events are attributed to the strengthening and increase infrequency of winter cooling, driven by changes in intensity of high latitude continental air masses (Theocharis, 1989; Roether et al., 1996; Rohling et al., 2002).

The 3 cooling events are not evident in either the $\delta^{18}O_{G.\ ruber}$ or the $\delta^{18}O_{H.\ elegans}$ records. The absence of these cooling events in $\delta^{18}O_{G.\ ruber}$ has been suggested by Rohling et al., (2002) and Casford et al., (2003) to reflect a seasonal offset between climate forcing and the proxy carrier, as cooling is a winter phenomenon and is thus not recorded by *ruber*, which thrives in the summer mixed layer (Rohling et al., 1997, 2004). However, this cannot explain their absence in the $\delta^{18}O_{H.\ elegans}$ record, because subsurface waters derive from winter time transformation (density increase) of surface waters. We tentatively propose therefore that the cooling events are not observed in the $\delta^{18}O$ records because of a "canceling out" effect. Based on standard oxygen isotope behavior, carbonate formed in fresher waters is more $\delta^{18}O$ depleted and in cool water is more $\delta^{18}O$ enriched. Thus, the simultaneous freshening and cooling of bottom waters during a cooling event would result in a counter balancing effect on $\delta^{18}O_{H.\ elegans}$. For example, a cooling of maximum 4 °C is equivalent to a $\delta^{18}O$ shift of approximately 1 ‰ (Epstein et al.,1951). During S1 times, combined stable isotope and salinity modeling suggests that a +1 ‰ $\delta^{18}O$ effect from temperature reduction might be offset by a ~ 0.6 salinity reduction (Rohling, 1999).

The 9700 years B.P. cooling event occurred 800 years before the sapropel onset. The next cooling event, at about 7700 years B.P. resulted in an interruption of the sapropel, while the final cooling event at 6100 years B.P. shut sapropel formation down completely with renewed ventilation of the Aegean bottom waters. We propose that the nonlinear response to successive cooling events reflects the existence of two alternate states or stable modes, which alternate according to a hysteresis loop (Figure 8) (May, 1977; Scheffer et al., 2001). We constrain the shape of this hysteresis loop for sapropel initiation and termination by plotting $(Ba/Al)_{sed}$ to characterize the "mode" (sapropel or nonsapropel) and $(Mg/Ca)_{H.\ elegans}$ to characterize a key system variable (temperature). The hysteresis is defined by the forward and backward switch from sapropel to nonsapropel mode occurring at different critical conditions (Figure 8). The sapropel mode is marked by increased water column stratification and enhanced export fluxes. Around 7700 years B.P., the sapropel "interruption" coincides with a cooling event similar to that seen at around 6100 years B.P. Yet, after the temperature perturbation is removed, sapropel formation continues after the 7700 years B.P. event, and not after the 6100 years B.P. event (NB, for clarity, we emphasize again that all ages are reported in radio carbon convention years, without corrections). Marine and terrestrial $\delta^{18}O$ records exhibit a mean $\delta^{18}O$ depletion after ~ 7 kyr B.P., suggesting a weakening monsoon (Rohling, 1999; Bar-Matthews et al., 2000; Rohling et al., 2002; Arz et al., 2003; De Lange et al., 2008) which, in interplay with the 6100 years B.P. event, could have facilitated a permanent stop to sapropel formation.

Based on the $(Ba/Al)_{sed}$ versus $(Mg/Ca)_{H.\ elegans}$ plot (Figure 8), the critical thresholds defining the sapropel and nonsapropel mode, can be estimated. The $(Mg/Ca)_{H.\ elegans}$ values reflect bottom water conditions, hence winter temperatures. Although temperature was clearly not the only factor involved, the critical value required to go into sapropel mode was about 14 °C, whereas the temperature tipping the system back to its nonsapropel mode was on the order of

10° C. While this temperature range is relatively limited, it was enough to maintain the stratified conditions first initiated by fresh water input, and thus keep the Aegean in its sapropel state for several thousand years.

5 | CONCLUSIONS AND IMPLICATIONS

This study introduces a promising new application of LA-ICP-MS to benthic foraminifera. The integrated study of dissolved and particulate trace elements allows the better constraint of physiochemical processes at play at the sediment water interface. Trace metal records from *H. elegans* tests show past variations in bottom water chemistry and temperature before, during and after sapropel S1 deposition. Enhanced export fluxes as indicated by our sedimentary $(Ba/Al)_{sed}$ and foraminiferal $(Ba/Ca)_{H.\ elegans}$ occurred particularly during the first phase of sapropel formation. The reduced $(Mn/Al)_{sed}$ and concomitantly enhanced foraminiferal $(Mn/Ca)_{H.\ elegans}$ clearly point to reduced bottom water oxygenation during sapropel deposition. Three distinct cooling events are recorded by the (Mg/Ca) record of *H. elegans*. The last two of these events lead to sapropel interruption and termination, respectively. We propose a hysteresis loop with two stable modes, the sapropel mode and the nonsapropel mode. The stability of the sapropel mode is controlled by "slow variables" such as export productivity and stratification, but is also sensitive to episodic perturbations, such as abrupt cooling events.

APPENDIX A

We present the results of single laser ablation analyses, including averages per test, standard deviation, and standard error per depth, for Ba (Table A1), Mn (Table A2), and Mg (Table A3).

ACKNOWLEDGMENTS

We thank two anonymous reviewers for their suggestions, which greatly improved this manuscript. Also, the support of the crew and captain of R/V *Aegeo* during the sampling campaign for core SLA–9 is gratefully acknowledged. Paul Mason and Gijs Nobbe are thanked for their assistance with LA-ICP-MS. This is publication DW-2009-5004 of the Darwin Center for Biogeosciences, which partially funded this project.

REFERENCES

Abu-Zied, R. H., E. L. Rohling, F. J. Jorissen, Fontanier, J. S. L. Casford, and S. Cooke (2008), Benthic foraminiferal response to changes in bottom-water oxygenation and organic carbon flux in the eastern Mediterranean during LGM to recent times, Mar. Micropaleontol., 67, 46–68, doi:10.1016/j.marmicro.2007.08.006.

Aksu, A. E., T. Abrajano, P. J. Mudie, and Yasar (1999), Organic geochemical and palynological evidence for terrigenous origin of the organic matter in Aegean Sea sapropel S1, Mar. Geol., 153, 303–318, doi:10.1016/ S0025-3227(98)00077-2.

Antoine, D., A. Morel, and J. -M. André (1995), Algal pigment distribution and primary production in the eastern Mediterranean as derived from coastal zone color scanner observations, J. Geophys. Res., 100,16,193–16,209, doi:10.1029/95JC00466.

Arz, H. W., F. Lamy, J. Pätzold, P. J. Müller, and M. Prins (2003), Mediterranean moisture source for an early Holocene humid period in the northern Red Sea, Science, 300, 118–121, doi:10.1126/science.1080325.

Barker, S., M. Greaves, and H. Elderfield (2003), A study of cleaning procedures used for foraminiferal Mg/Ca paleothermometry, Geochem. Geophys. Geosyst., 4(9), 8407, doi:10.1029/ 2003GC000559.

Bar-Matthews, M., A. Ayalon, and A. Kaufman (2000), Timing and hydrological conditions of Sapropel events in the eastern Mediterranean, as evident from speleothems, Soreq cave, Israel, Chem. Geol., 169, 145–156, doi:10.1016/S0009-2541(99)00232-6.

Bishop, J. K. B. (1988), The barite-opal-organic carbon association in oceanic particulate matter, Nature, 332, 341–343, doi:10.1038/ 332341a0.

Boyle, E. A. (1983), Manganese carbonate overgrowths on foraminifera tests, Geochim. Cosmochim. Acta, 47, 1815–1819, doi:10.1016/ 0016-7037(83)90029-7.

Boyle, E. A., L. Labeyrie, and J. -C. Duplessly (1995), Calcitic foraminiferal data confirmed by cadmium in aragonitic Hoeglundina: Application to the Last Glacial Maximum in the northern Indian Ocean, Paleoceanography, 10, 881–900, doi:10.1029/95PA01625.

Burdige, D. J. (2005), Burial of terrestrial organic matter in marine sediments: A re-assessment, Global Biogeochem. Cycles, 19, GB4011, doi:10.1029/2004GB002368.

Burdige, D. J. (2006), Geochemistry of Marine Sediments, Princeton Univ. Press, Princeton, N. J.

Cacho, I., J. O. Grimalt, M. Canals, L. Sbaffi, N. J. Shackleton, J. Schönfeld, and R. Zahn (2001), Variability of the western Mediterranean Sea surface temperatures during the last 25,000 years and its connection with the Northern Hemisphere climatic changes, Paleoceanography, 16(1), 40–52, doi:10.1029/ 2000PA000502.

Casford, J. S. L., E. J. Rohling, R. H. Abu-Zied, S. Cooke, C. Fontanier, M. J. Leng, and V. Lykousis (2002), Circulation changes and nutrient concentrations in the late Quaternary Aegean Sea: A nonsteady state concept for sapropel formation, Paleoceanography, 17(2), 1024, doi:10.1029/2000PA000601.

Casford, J. S. L., E. J. Rohling, R. H. Abu-Zied, C. Fontanier, F. J. Jorissen, M. J. Leng, G. Schmiedl, and J. Thomson (2003), A dynamic concept for eastern Mediterranean circulation and oxygenation during sapropel formation, Palaeogeogr. Palaeoclimatol. Palaeoecol., 190, 103–119, doi:10.1016/ S0031-0182(02)00601-6.

Casford, J. S. L., R. H. Abu-Zied, E. J. Rohling, S. Cooke, C. Fontanier, M. J. Leng, A. Millard, and J. Thomson (2007), A stratigraphically controlled multi-proxy chronostratigraphy for the eastern Mediterranean, Paleoceanography, 22, PA4215, doi:10.1029/2007PA001422.

Church, T. M., and K. Wolgemuth (1972), Marine barite saturation, Earth Planet. Sci. Lett., 15, 35–44, doi:10.1016/0012-821X(72) 90026-X.

Cita, M. B., C. Vergnaud-Grazzini, C. Robert, H. Chamley, N. Ciaranfi, and S. d'Onofrio (1977), Paleoclimatic record of a long deep sea core from the eastern Mediterranean, Quat. Res., 8, 205–235, doi:10.1016/0033-5894(77) 90046-1.

Dehairs, F., R. Chesselet, and J. Jedwab (1980), Discrete suspended particles of barite and the barium cycle in the open ocean, Earth Planet. Sci. Lett., 49(2), 528–550, doi:10.1016/0012- 821X(80)90094-1.

De Lange, G. J., G. Catalano, G. P. Klinkhammer, and G. W. Luther III (1990), The interface between oxic seawater and the anoxic Bannock brine; its sharpness and the consequences for the redox-related cycling of Mn and Ba, Mar. Chem., 31(1–3), 205–217, doi:10.1016/0304- 4203(90)90039-F.

De Lange, G. J., J. Thomson, A. Reitz, C. P. Slomp, M. Speranza Principato, E. Erba, and C. Corselli (2008), Synchronous basin-wide formation and redox-controlled preservation of a Mediterranean sapropel, Nat. Geosci., 1, 606–610, doi:10.1038/ngeo283.

De Rijk, S., A. Hayes, and E. J. Rohling (1999), Eastern Mediterranean sapropel S1 interruption: An expression of the onset of climatic deterioration around 7 ka BP, Mar. Geol., 153, 337–343, doi:10.1016/S0025-3227(98) 00075-9.

De Rijk, S., F. J. Jorissen, E. J. Rohling, and S. R. Troelstra (2000), Organic flux control on bathymetric zonation of Mediterranean benthic foraminifera, Mar. Micropaleontol., 40, 151–166, doi:10.1016/S0377-8398(00) 00037-2.

Douglas, R. G., and H. L. Heitman (1979), Slope and basin benthic foraminifera of the California Borderland, Spec. Publ. Soc. Econ. Paleontol. Mineral., 27,231–246.

Dymond, J., and R. Collier (1996), Particulate barium fluxes and their relationships to biological productivity, Deep Sea Res., Pari II, 43, 1283–1308, doi:10.1016/0967-0645(96)00011-2.

Epstein, S., R. Buchsbaum, H. A. Lowenstam, and H. C. Urey (1951), Carbonate-water isotopic temperature scale, Geol. Soc. Am. Bull., 62, 417–426, doi:10.1130/0016-7606(1951)62 [417:CITS]2.0.CO;2.

Fontanier, C., F. J. Jorissen, L. Licari, A. Alexandre, P. Anschutz, and P. Carbonel (2002), Live benthic foraminiferal faunas from the Bay of Biscay: Faunal density, composition, and microhabitats, Deep Sea Res., Part I, 49, 751–785, doi:10.1016/S0967-0637(01)00078-4.

Froelich, P. N., G. P. Klinkhammer, M. L. Bender, N. A. Luedtke, G. R. Heath, D. Cullen, P. Dauphin, D. Hammond, B. Hartman, and V. Maynard (1979), Early oxidation of organic pelagic sediments of the eastern equatorial Atlantic: Suboxic diagenesis, Geochim. Cosmochim. Acta, 43(7), 1075–1090, doi:10.1016/0016-7037(79)90095-4.

Geraga, M., S. Tsaila-Monopolis, C. Ioakim, G. Papatheodorou, and G. Ferentinos (2000), Evaluation of palaeoenvironmental changes during the last 18,000 years in the Myrtoon basin, SW Aegean Sea, Palaeogeogr. Palaeoclimatol. Palaeoecol., 156, 1–17, doi:10.1016/ S0031-0182(99)00123-6.

Hall, J. M., and L. -H. Chan (2004), Ba/Ca in Neogloboquadrina pachyderma as an indicator of deglacial meltwater discharge into the western Arctic Ocean, Paleoceanography, 19, PA1017, doi:10.1029/2003PA000910.

Hathorne, E. C., R. H. James, P. Savage, and O. Alard (2008), Physical and chemical characteristics of particles produced by laser ablation of biogenic calcium carbonate, J. Anal. At. Spectrom., 23, 240–243, doi:10.1039/ b706727e.

Hilgen, F. J. (1991), Astronomical calibration of Gauss to Matuyama sapropels in the Mediterranean and implication for the geomagnetic polarity time scale, Earth Planet. Sci. Lett., 104, 226–244, doi:10.1016/0012-821X(91) 90206-W.

Hughes, J. A., A. J. Gooday, and J. W. Murray (2000), Distribution of live benthic foraminifera at three oceanographically dissimilar sites in the northeast Atlantic: Preliminary results, Hydrobiologica, 440(1–3), 227–238, doi:10.1023/A:1004131413665.

Jorissen, F. J. (1999), Benthic foraminiferal successions across Late Quaternary Mediterranean sapropels, Mar. Geol., 153, 91–101, doi:10.1016/S0025-3227(98)00088-7.

Jorissen, F. J., I. Wittling, J. P. Peypouquet, C. Rabouille, and J. C. Relaxans (1998), Live benthic foraminiferal faunas off Cape Blanc, NW-Africa: Community structure and micro-habitats, Deep Sea Res., Part I, 45(12), 2157– 2188, doi:10.1016/S0967-0637(98)00056-9.

Jorissen, F., C. Fontanier, and E. Thomas (2007), Paleoceanographical proxies based on deep-sea benthic foraminiferal assemblage characteristics, in Proxies in Late Cenozoic Paleoceanography, Dev. Mar. Geol., vol. 1, edited by C. Hillaire-Marcel and A. de Vernal, pp. 263– 325, Elsevier, New York, doi:10.1016/S1572- 5480(07) 01012-3.

Kidd, R. B., M. B. Cita, and W. B. F. Ryan (1978), Stratigraphy of eastern Mediterranean sapropel sequences recovered during DSDP Leg 42A and their palaeo environmental significance, Initial Rep. Deep Sea Drill. Proj., 42A, 421–443.

Koho, K. A., R. Garcia, H. C. de Stigter, E. Epping, E. Koning, T. J. Kouwenhoven, and G. J. van der Zwaan (2008), Sedimentary labile organic carbon and pore water redox control on species distribution of benthic foraminifera: A case study from Lisbon–Setúbal Canyon (southern Portugal), Prog. Oceanogr., 79(1), 55–82, doi:10.1016/j.pocean.2008.07.004.

Kuhnt, T., G. Schmiedl, W. Ehrmann, Y. Hamann, and C. Hemleben (2007), Deep-sea ecosystem variability of the Aegean Sea during the past 22 kyr as revealed by benthic foraminifera, Mar. Micropaleontol., 64, 141–162, doi:10.1016/j. marmicro.2007.04.003.

Lascaratos, A., W. Roether, K. Nittis, and B. Klein (1999), Recent changes in deepwater formation and spreading in the eastern Mediterranean Sea: A review, Prog. Oceanogr., 44(1–3), 5–36, doi:10.1016/S0079-6611(99) 00019-1.

Lea, D., and E. Boyle (1989), Barium content of benthic foraminifera controlled by bottom-water composition, Nature, 338, 751–753, doi:10.1038/338751a0.

Lear, C. H., H. Elderfield, and P. A. Wilson (2000), Cenozoic deep-sea temperatures and global ice volumes from Mg/Ca in benthic foraminiferal calcite, Science, 287, 269–272, doi:10.1126/science.287.5451.269.

Libes, S. M. (2009), Introduction to Marine Biogeochemistry, pp. 316–317, Academic, San Diego, Calif.

Lohmann, G. (1995), A model for variation in the chemistry of planktonic foraminifera due to secondary calcification and selective dissolution, Paleoceanography, 10(3), 445–457, doi:10.1029/95PA00059.

Lutze, G. F., and W. T. Coulbourn (1984), Recent foraminifera from the continental margin of northwest Africa: Community structure and distribution, Mar. Micropaleontol., 8(5), 361–401, doi:10.1016/0377-8398(84)90002-1.

Mackensen, A., and R. G. Douglas (1989), Down-core distribution of live and dead deep-water benthic foraminifera in box cores from the Weddell Sea and the California continental borderland, Deep Sea Res., Part A,36, 879–900,doi:10.1016/0198-0149(89)90034-4.

Marino, G., E. J. Rohling, W. I. C. Rijpstra, F. Sangiorgi, S. Schouten, and J. Sinninghe-Damste (2007), Aegean Sea as driver of hydrographic and ecological changes in the eastern Mediterranean, Geology, 35(8), 675– 678, doi:10.1130/G23831A.1.

Martin, J. M., and M. Meybeck (1979), Elemental mass-balance of material carried by major world rivers, Mar. Chem., 7, 173–206, doi:10.1016/0304-4203(79)90039-2.

May, R. M. (1977), Thresholds and breakpoints in ecosystems with a multiplicity of stable states, Nature, 269, 471–477, doi:10.1038/ 269471a0.

Mercone, D., J. Thomson, R. H. Abu-Zied, I.W. Croudace, and E. J. Rohling (2001), High-resolution geochemical and micropalaeontological profiling of the most recent eastern Mediterranean sapropel, Mar. Geol., 177, 25–44, doi:10.1016/S0025-3227(01)00122-0.

Millero, F. J., and D. R. Schreiber (1982), Use of the ion pairing model to estimate activity coefficients of the ionic components of natural waters, Am. J. Sci., 282, 1508–1540, doi:10.2475/ajs.282.9.1508.

Olausson, E. (1961), Studies of deep-sea cores, in Reports of the Swedish Deep-Sea Expedition 1947–1948, vol. 8, pp. 353–391, Swed. Nat. Sci. Res. Counc., Stockholm.

Parker, F. L. (1958), Eastern Mediterranean foraminifera, in Reports of the Swedish Deep-Sea Expedition 1947–1948, vol. 8, pp. 217–283, Swed. Nat. Sci. Res. Counc., Stockholm.

Passier, H. F., J. J. Middelburg, B. J. H. van Os, and G. J. de Lange (1996), Diagenetic pyritisation under eastern Mediterranean sapropels caused by downward sulphide diffusion, Geochim. Cosmochim. Acta, 60, 751–763, doi:10.1016/0016-7037(95)00419-X.

Pearce, N. J. G., W. T. Perkins, J. A. Westgate, M. P. Gorton, S. E. Jackson, C. R. Neal, and S. P. Chenery (1997), A compilation of new and published major and trace element data for NIST SRM 610 and NIST SRM 612 glass reference materials, Geostand. Newsl., 21, 115–144, doi:10.1111/j.1751-908X.1997.tb00538.x.

Reichart, G. -J., F. Jorissen, P. R. D. Mason, and P. Anschutz (2003), Single foraminiferal test chemistry records the marine environment, Geology, 31, 355–358, doi:10.1130/0091- 7613(2003)031<0355:SFTCRT>2.0.CO;2.

Reitz, A., J. Thomson, G. J. de Lange, and C. Hensen (2006), Source and development of large manganese enrichments above eastern Mediterranean sapropel S1, Paleoceanography, 21, PA3007, doi:10.1029/2005PA001169.

Roether, W., B. B. Manca, B. Klein, D. Bregant, Georgopoulos, V. Beitzel, V. Kovacevic, and A. Luchetta (1996), Recent changes in eastern Mediterranean deep waters, Science, 271, 333–335, doi:10.1126/science.271.5247.333.

Rohling, E. J. (1994), Review and new aspects concerning the formation of eastern Mediterranean sapropels, Mar. Geol., 122, 1–28, doi:10.1016/0025-3227(94)90202-X.

Rohling, E. J. (1999), Environmental control on Mediterranean salinity and $\delta^{18}O$, Paleoceanography , 14 (6), 706 –715, doi:10.1029/ 1999PA900042.

Rohling, E. J., and W. C. Gieskes (1989), Late Quaternary changes in Mediterranean intermediate water density and formation rate, Paleoceanography, 4, 531–545, doi:10.1029/ PA004i005p00531.

Rohling, E. J., and F. J. Hilgen (1991), The eastern Mediterranean climate at times of sapropel formation: A review, Geol. Mijnbouw, 70, 253–264.

Rohling, E. J., F. Jorissen, and H. C. De Stigter(1997), 200 year interruption of Holocene sapropel formation in the Adriatic Sea, J. Micro-palaeontol., 16, 97–108, doi:10.1144/jm.16.2.97.

Rohling, E. J., P. A. Mayewski, R. H. Abu-Zied, J. S. L. Casford, and A. Hayes (2002), Holocene atmosphere-ocean interactions: Records from Greenland and the Aegean Sea, Clim. Dyn., 18, 587–593, doi:10.1007/s00382-001- 0194-8.

Rohling, E. J., et al. (2004), Reconstructing past planktic foraminiferal habitats using stable isotope data: A case history for Mediterranean sapropel S5, Mar. Micropaleontol., 50, 89–123, doi:10.1016/S0377-8398(03)00068-9.

Rosenthal, Y., E. A. Boyle, and N. Slowey (1997), Temperature control on the incorporation of magnesium, strontium, fluorine, and cadmium into benthic foraminiferal shells from Little Bahama Bank: Prospects for thermocline paleoceanography, Geochim. Cosmochim. Acta, 61, 3633–3643, doi:10.1016/ S0016-7037(97)00181-6.

Rosenthal, Y., C. H. Lear, D. W. Oppo, and K. Linsley (2006), Temperature and carbonate ion effects on Mg/Ca and Sr/Ca ratios in benthic foraminifera: Aragonitic species Hoeglundina elegans, Paleoceanography, 21, PA1007, doi:10.1029/2005PA001158.

Rossignol-Strick, M., W. Nesteroff, P. Olive, and C. Vergnaud-Grazzini (1982), After the deluge: Mediterranean stagnation and sapropel formation, Nature, 295, 105–110, doi:10.1038/ 295105a0.

Ruddiman, W. F. (1971), Pleistocene sedimentation in the equatorial Atlantic: Stratigraphy and faunal paleoclimatology, Geol. Soc. Am. Bull., 82, 283–302, doi:10.1130/0016-7606 (1971)82[283:PSITEA] 2.0.CO;2.

Sachs, J. P., and D. J. Repeta (1999), Oligotrophy and nitrogen fixation during eastern Mediterranean sapropel events, Science, 286, 2485–2488, doi:10.1126/science.286.5449.2485.

Sadekov, A. Y., S. M. Eggins, and P. De Deckker (2005), Characterization of Mg/Ca distributions in planktonic foraminifera species by electron microprobe mapping, Geochem. Geophys. Geosyst., 6, Q12P06, doi:10.1029/ 2005GC000973.

Scheffer, M., S. Carpenter, J. A. Foley, C. Folke, and B. Walker (2001), Catastrophic shifts in ecosystems, Nature, 413, 591–596, doi:10.1038/35098000.

Schenau, S. J., M. A. Prins, G. J. De Lange, and Monnin (2001), Barium accumulation in the Arabian Sea: Controls on barite preservation in marine sediments, Geochim. Cosmochim. Acta, 65, 1545–1556, doi:10.1016/S0016- 7037(01)00547-6.

Schönfeld, J. (2001), Benthic foraminifera and pore-water oxygen profiles: A re-assessment of species boundary conditions at the western Iberian margin, J. Foraminiferal Res., 31(2), 86–107, doi:10.2113/0310086.

Slomp, C. P., J. Thomson, and G. J. de Lange (2004), Controls on phosphorus regeneration and burial during formation of eastern Mediterranean sapropels, Mar. Geol., 203, 141–159, doi:10.1016/S0025-3227(03)00335-9.

Theocharis, A. (1989), Deep water formation and circulation in the Aegean sea, in Reports in Meteorology and Oceanography, edited by H. Charnock, pp. 335–359, Harvard Univ., Cambridge, Mass.

Thomson, J., N. C. Higgs, T. R. S. Wilson, I. W. Croudace, G. J. de Lange, and P. J. M. van Santvoort (1995), Redistribution and geochemical behaviour of redox-sensitive elements around S1, the most recent eastern Mediterranean sapropel, Geochim. Cosmo-chim. Acta, 59, 3487–3501, doi:10.1016/ 0016-7037(95)00232-O.

Thomson, J., D. Mercone, G. J. De Lange, and P. J. M. Van Santvoort (1999), Review of recent advances in the interpretation of eastern Mediterranean sapropel S1 from geochemical evidence, Mar. Geol., 153, 77–89, doi:10.1016/S0025-3227(98)00089-9.

van Santvoort, P. J . M., G. J. de Lange, J. Thomson, H. Cussen, T. R. S. Wilson, M. Krom, and K. Strohle (1996), Active post-depositional oxidation of the most recent sapropel (S1) in sediments of the eastern Mediterranean, Geochim. Cosmochim. Acta, 60, 4007–4024, doi:10.1016/S0016-7037(96) 00253-0.

Vergnaud-Grazzini, C., W. B. F. Ryan, and Bianca Cita (1977), Stable isotopic fractionation, climate change and episodic stagnation in the eastern Mediterrane an during the late Quaternary, Mar. Micropaleontol., 2,353–370, doi:10.1016/0377-8398(77)90017-2.

Weldeab, S., D. W. Lea, R. R. Schneider, and Andersen (2007), 155,000 years of West African monsoon and ocean thermal evolution, Science, 316, 1303–1307, doi:10.1126/ science.1140461.

Yu, J., H. Elderfield, M. Greaves, and J. Day (2007), Preferential dissolution of benthic foraminiferal calcite during laboratory reductive cleaning, Geochem. Geophys. Geosyst., 8, Q06016, doi:10.1029/2006GC001571.

Nederlandse samenvatting

De toename in de gemiddelde temperatuur op aarde heeft ervoor gezorgd dat het klimaat ingrijpend verandert, dit heeft gevolgen voor mens en natuur. De toename van koolstofdioxide in de atmosfeer, welke wordt veroorzaakt door menselijke activiteiten, heeft geleid tot een stijging van de gemiddelde mondiale temperatuur. De veranderingen in het klimaatsysteem zijn ingrijpend en complex. Deze complexiteit van klimaatverandering maakt het erg moeilijk om de gevolgen te voorspellen, zowel op korte als lange termijn.

Om beleid te ontwikkelen op het gebied van klimaatmitigatie en klimaatadapatie zijn betrouwbare voorspellingen van klimaatsveranderingen essentieel. Om dat mogelijk te maken zijn verschillende klimaatmodellen ontwikkeld. Klimaatmodellen worden meestal gevalideerd met historische gegevens van instrumenteel verkregen (direct gemeten) archieven van temperaturen, neerslag en koolstofdioxide concentraties. Echter, deze archieven bevatten meestal geen data die ver teruggaan in de geschiedenis (<150 jaar) en het bereik van de metingen is daardoor beperkt. Daarentegen biedt het geologische archief de mogelijkheid gegevens te vergelijken met een veel langere historie en daardoor ook een groter bereik in temperatuur, neerslag en koolstofdioxideconcentraties (CO_2). Dus, om de betrouwbaarheid van klimaatmodellen en scenario's voor hoge CO_2 concentraties te testen, is het cruciaal om gebruik te maken van data van klimaatperioden uit het verleden, het liefst ook met hoge CO_2 concentraties. Dit vereist echter wel dat adequate tools beschikbaar zijn om het klimaat in het verleden te reconstrueren.

Klimaatreconstructies zijn gebaseerd op zogenaamde 'proxies'. Proxies zijn kwantitatieve parameters (b.v. jaarringbreedte van bomen) die een relatie hebben met een parameter die nu niet meer te meten is (b.v. de hoeveelheid neerslag in een bepaald jaar, in het verleden). Een proxy kan worden gekalibreerd door middel van veldonderzoek, in het laboratorium of door het onderling vergelijken met andere proxies.

Foraminiferen zijn eencellige mariene organismen met een uitwendig kalkskelet. Tijdens de vorming van hun kalkskelet nemen deze foraminiferen spoormetalen en isotopen op, welke hun milieuomgeving weerspiegelt. Daardoor zijn foraminiferen zeer geschikt als proxy voor het reconstrueren van klimaatsveranderingen in het geologisch verleden. Bijvoorbeeld, de zuurstof- en koolstofisotopenratio's in deze kalkskeletten correleren met de veranderingen in zeewatertemperatuur, watermassa en voedselbeschikbaarheid. De stabiele zuurstof- en koolstofisotopensamenstelling van de schelpen van foraminiferen is één van de meeste gebruikte proxies om klimaatsverandering in het geologische verleden te reconstrueren.

Echter, opgenomen spoormetalen en isotopen in het kalkskelet van foraminiferen kunnen ook worden beïnvloed door de carbonaatchemie van het water, de habitatvoorkeur en de groeisnelheid van de foraminiferen. Een robuuste interpretatie van de informatie uit foraminiferen proxies vereist daarom kennis over de invloed van deze verschillende factoren.

Dit kan worden bereikt door een zogenaamde "multi-proxy" benadering toe te passen. Enkele relevante voorbeelden van een dergelijke benadering worden in deze dissertatie beschreven, met name het gebruik van foraminiferen die leven in en op de zeebodem (benthische) en hun organische, element en isotopensamenstelling.

Deze dissertatie beschrijft de ontwikkeling en toepassing van proxies op basis van benthische foraminiferen. Het doel is een beter begrip te krijgen van deze proxies en daarmee onze kennis van klimaatveranderingen in het verleden te vergroten. De verschillende toegepaste benaderingen zijn opgenomen in de hoofdstukken twee tot en met vijf. Het laatste hoofdstuk (zes) geeft een gedetailleerde beschrijving van het toepassen van proxies gebaseerd op de spoormetalen samenstelling van foraminiferen schelpen van Middellandse Zee sediment archieven.

In hoofdstuk 2 is de organische geochemische samenstelling van de organische lagen onderzocht in foraminiferen, als potentiële proxy voor de $\delta^{18}O$ en $\delta^{13}C$ waarden van het zeewater en/of de $\delta^{13}C$ van de voedselbronnen (i.e. het trofische niveau). De macromoleculaire en stabiele isotoop samenstelling van de organische lagen zijn gekarakteriseerd met behulp van Curie-punt pyrolyse-GC-MS. De metingen laten zien dat de organische lagen proteïne en polysacharide bevatten die gebonden zijn in een complexe macromoleculaire structuur. Zowel chitineafgeleiden als sporen van guaiacols en syringols zijn gevonden. Hoewel alle organische lagen van de vijf onderzochte soorten foraminiferen chitineafgeleiden en proteïnen bevatten, varieerde de relatieve bijdrage van de verschillende bestanddelen tussen deze soorten aanzienlijk. De fractionering tussen zeewater en organisch materiaal is consistent ook terug te zien in de stabiele zuurstofisotopen samenstelling van de organische lagen. Dit betekent dat de organische lagen een potentiële onafhankelijke bron van informatie zijn voor het bepalen van de stabiele zuurstofisotoop samenstelling van het zeewater in het verleden. Daarentegen laat een tracer experiment zien dat de $\delta^{13}C$ van de organische lagen juist de voedselbronnen van foraminiferen reflecteren. Deze verschillende fractioneringsroutes voor zuurstof- en koolstofisotopen hebben belangrijke implicaties voor het potentiële gebruik van foraminiferen gebonden organisch materiaal als proxy-signaaldragers. Echter, voor geavanceerd gebruik van deze aanpak, moeten er nog belangrijke analytisch verbeteringen worden gemaakt, met name het verkleinen van het minimaal monstergewicht voor een meting. Recente ontwikkelingen in de nano-onderzoekanalyses van stabiele koolstofisotopen, waarmee met zeer kleine hoeveelheden organisch materiaal de isotopische samenstelling gemeten kan worden (Van Roij et al., 2017), in combinatie met de benadering beschreven in Hoofdstuk 2, creëert een heel nieuw veld in het foraminiferenonderzoek.

In hoofdstuk 3 zijn mangaan/calcium ratio's in foraminiferen schelpen gemeten als potentiële proxy voor paleo-redox condities in marine sedimenten. Dit is onderzocht in combinatie met de habitatvoorkeuren van foraminiferen. In de eerste paar centimeters van de oceaanbodem heeft mangaan een consequente gradiënt. Dit komt overeen met de leefdieptes van verscheidene soorten van foraminiferen. Dit maakt dat mangaan zeer

geschikt is voor een dergelijke studie. Hoofdstuk 3 laat de incorporatie van mangaan zien in foraminiferen carbonaat over een dieptetransect in de Golf van Lions, in de noordwestelijke Middellandse Zee. Mangaan concentraties in de schelpen van levende foraminiferen soorten – *Hoeglundina elegans*, *Melonis barleeanus, Uvigerina mediterranea*, *Uvigerina peregrina* – zijn gemeten met behulp van laserablatie ICP-MS. In sedimentporiewater monsters was te zien dat de mangaanconcentratie afnam met toenemende waterdiepte, wat consistent is met de afname van de depositie van organisch materiaal met waterdiepte. Verschillen in organisch materiaal depositie op het sediment-water oppervlak beïnvloedde de diepte tot waar het zuurstof in het sediment diffundeert en dus ook de mangaan-poriewaterprofielen. De Mn/Ca waarden van het kalkskelet van de verschillende soorten foraminiferen correleren met de gemeten poriewatergeochemie. De geobserveerde verschillen tussen de soorten is in overeenstemming met de verschillen in leefdieptes en de gemeten opgeloste Mn-gradiënten. Wel vereist de toepassing van deze proxy relatieve stabiele milieuomstandigheden, omdat Mn/Ca ratio's in foraminiferen ook de historische dynamiek van specifieke leefdieptes van foraminiferen en de Mn-cyclus reflecteren.

Hoofdstuk 4 onderzoekt de opname van andere spoormetalen, zoals magnesium, barium en strontium, in het kalkskelet van foraminiferen langs een dieptetransect met verschillende water en sedimentdiepte in de Golf van Lions, in de noordwestelijke Middellandse Zee. Het doel hiervan was om inzicht te krijgen in het verband tussen de spoormetalen in het kalkskelet van foraminiferen en de ecologische voorkeuren van de verschillende foraminiferen soorten. Magnesium-, strontium- en bariumconcentraties in de schelpen van de foraminiferen soorten *Hoeglundina elegans*, *Melonis barleeanus, Uvigerina mediterranea*, *Uvigerina peregrina* zijn gemeten met behulp van laserablatie ICP-MS. Bij een toename van de waterdiepte bleven de Mg/Ca en Sr/Ca ratio's relatief stabiel, waarbij Mg/Ca waardes een veel hogere spreiding tussen de verschillende individuen vertoonde. Mg/Ca en Sr/Ca waarden zijn vergeleken met reeds bestaande temperatuurkalibraties en tonen de toepasbaarheid voor de Middellandse zee aan. *Uvigerina peregrina* toonde daarbij duidelijk andere Mg/Ca karakteristieken dan *Uvigerina mediterranea.* Het advies is daarom om deze twee soorten niet te groeperen in een enkele empirische Mg/Ca temperatuur kalibratie. Sr/Ca in *H. elegans* lijkt de temperatuur te volgen zoals verwacht mag worden op basis van bestaande kalibraties. De veranderingen van Ba^{2+} in het sediment zijn niet zichtbaar in de Ba/Ca ratio's van dezelfde foraminiferen schelpen, hoewel deze afkomstig zijn uit dezelfde kernen, terwijl foraminiferen de Mn poriewaterchemie uit het verleden wel registreren (hoofdstuk 3). *Hoeglundina elegans* toonde gemiddeld een hogere bariumconcentratie ten opzichte van andere soorten, wat waarschijnlijk wordt veroorzaakt doordat de schelp van deze foraminifeer wordt gemaakt van aragoniet (anders dan de calciet schelpen van de andere soorten). Wanneer de verschillen in Ba/Ca waarden tussen de verschillende soorten worden vergeleken, blijkt dat de foraminiferen waarvan de schelp is opgebouwd uit calciet de hoogste Ba concentratie hebben bij degene die het diepst in het sediment leven. Dus, hoewel de Ba/Ca voor individuen niet direct overeenkomen met

de in-situ concentraties, is de ecologische voorkeur van foraminiferen wel duidelijk zichtbaar in soort specifieke Ba opname.

Hoofdstuk 5 behandelt de invloed van de carbonaatchemie in het porie-water op de stabiele koolstof- en zuurstofisotopen fractionering in de schelp van foraminiferen. De stabiele zuurstof- en koolstofisotopensamenstelling van de schelpen van benthische foraminiferen is één van de meeste gebruikte proxies in paleoceanografie. Waar het zuurstofisotopensignaal een proxy is voor zeewatertemperatuur en het mondiale ijsvolume, wordt de koolstofisotopen-ratio over het algemeen gezien als een proxy voor watermassa en het koolstofgehalte op de zeebodem. Echter de meeste bestaande studies bestuderen de verbinding tussen beide isotopensystemen niet. Dit hoofdstuk laat zien dat de koolstof- en zuurstofisotopen in de kalkskeletjes van verschillende foraminiferen, die op verschillende leefdieptes in het sediment voorkomen, verbonden zijn. De sterke correlatie tussen de koolstof- en zuurstofisotopen van de soorten suggereert dat deze primair worden gestuurd door hetzelfde proces. In de Golf van Lions heersen bijna constante milieuomstandigheden, ongeacht waterdiepte, welke de mogelijkheid geven de correlatie tussen koolstof en zuurstofisotopen in het kalkskelet van foraminiferen te achterhalen. De helling van de correlatie is consistent met die van de carbonaationconcentratie, bekend van planktonische foraminiferen. Omdat de gekoppelde zuurstof- en koolstofisotopen niet strikt kunnen worden geïnterpreteerd in termen van de leefdieptes van de verschillende soorten in het sediment, is het aannemelijk dat een extra impact van de biologie van de foraminiferen een rol speelt.

In hoofdstuk 6 wordt het afzettingsmilieu van de Oost Middellandse Zee in combinatie met de sediment geochemie en metingen van sporenelementen in foraminiferen schelpen onderzocht. De ontwikkeling van productiviteit, redox omstandigheden, temperatuur en watermassaverversing gedurende de afzetting van een sapropel (S1) in de Egeïsche zee is hier onderzocht. De continue aanwezigheid van de foraminifeer *Hoeglundina elegans* (*H. elegans*) door de gehele sapropel, maakt het voor het eerst mogelijk de opgelost Ba en Mn in het bodemwater te vergelijken met de reconstructie van temperatuur op basis van Mg/Ca tijdens de afzetting van S1. Een synchrone toename van barium in het sediment en in de schelp van de foraminiferen wijzen op een sterke correlatie tussen Ba cyclus en de export productiviteit. Tijdens de vorming van een sapropel was het mangaan in het sediment gereduceerd, wat overeenkomt met de hier gereconstrueerde versterkte Mn^{2+} mobilisatie van sedimentaire Mn-oxides onder suboxische omstandigheden. De daarmee samenhangende hogere opgeloste Mn^{2+} concentraties worden gereflecteerd in de hoge Mn/Ca waarden in de foraminiferen schelpen. Dit komt overeen met de huidige observaties in de Golf van Lions (Hoofdstuk 3). Door Mg/Ca ratio te gebruiken voor de reconstructie van de bodemwater temperatuur in de sapropel is de omvang en de duur van de interruptie van de sapropel en andere korte koude episodes nu bekend. Het integreren van de reconstructie van de productiviteit en de zuurstofgehaltes van het bodemwater met temperatuurarchieven suggereert een hysterese

tijdens een sapropel afzetting, wat te zien is de abrupte afwisselingen tussen twee semi-stabiele perioden van het Middellandse Zee systeem.

VOORUITBLIK

Voor geavanceerd onderzoek en een fundamenteel begrip van de toestand van het klimaat en de oceanen, zullen proxies altijd belangrijk blijven. Terwijl er overeenstemming is over dat de opwarming van de aarde wordt veroorzaakt door stijging in de CO2 concentraties in de atmosfeer, is de gevoeligheid van het klimaatsysteem op de atmosferische CO2 concentratie nog altijd onderwerp van debat. Meer accurate en robuuste proxies zijn essentieel voor ons begrip van het klimaat in het verleden. Deze proxies kunnen helpen om de condities te bepalen die geleid hebben tot de verschillende klimaatsveranderingen in het verleden, en zijn daarmee essentiële tools voor het verbeteren van voorspellingen van toekomstige klimaatveranderingen. Echter, voor enkele componenten in het oceaan-klimaatsysteem zijn proxies nog niet voldoende ontwikkeld. Er bestaan bijvoorbeeld veel proxies voor zeewatertemperatuur (zoals Mg/Ca, Uk37 en "clumped" isotopen thermometrie), terwijl andere parameters (zoals de toegift van organische materiaal en het zuurstofgehalte van het bodemwater) veel moeilijker te bepalen zijn, of te koppelen zijn aan één enkel proces. Het is duidelijk dat meerdere factoren één enkele proxy beïnvloeden (zoals de Ba/Ca in foraminiferen wordt beïnvloed door watermassa, diagenetische cycli dichtbij het sediment-waterinterface en het zoutgehalte). Daarom is er meer werk nodig op het gebruik van multi-proxy benadering om de deze parameters te ontrafelen, zoals gedaan in deze dissertatie. Een betere definiëring van ecologische factoren (factoren die bepalen *welke* foraminifeer *waar* verkalkt) zowel in water als in het sediment, zijn noodzakelijk om de geochemische foraminiferen proxies meer robuust en accuraat te maken. Het samenbrengen van de (micro)leefdieptevoorkeur van foraminiferen, levenscyclus en ontogenetische veranderingen, de impact van levensprocessen en biomineralisatie in een gemeenschappelijk model zou meer inzicht kunnen geven in potentiële onnauwkeurigheden van de toegepaste proxies. Daarnaast zou dit ook meteen de proxy-gebaseerde reconstructies via een Bayesiaanse benadering kunnen verbeteren, waardoor de koppeling van meervoudige element bepalingen met meervoudige milieuomstandigheden de voorspellende kracht van proxies verbeteren. De schelpen van foraminiferen zijn in dat opzicht ideaal omdat de compositie zowel elementair als isotopisch een drager is van verscheidene signalen. Echter, dit vraagt nog wel om aanvullende gecontroleerde groei-experimenten, veldcalibraties en modelstudies voordat ze kunnen worden toegepast.

Acknowledgements

For a while there finishing this thesis was looking *a bit shaky*. That it is finished is a credit to all the people who have shared their time, expertise, support, friendship and love.

Thank you all.

Gert-Jan, your generosity of spirit is boundless, as is your determination to see this finished. Thank you.

Gert, thank you for sharing your fascination for marine geochemistry and for indulging my favourite part of the job, that of going on marine expeditions.

To the dissertation commission members, thank you for taking the time to evaluate this thesis and participate in its defense.

To my co-authors, thank you for cooperating on various chapters of this thesis. In particular I would like to thank Frans, for your enduring patience and Christophe, for always responding so quickly to any of my questions.

Thank you to the dedicated technicians both at the university and on board ship, who strive to carry out the best possible analyses: Helen, Dineke, Pieter, Gijs, Arnold and Karel.

To my paranymphs, José, thank you for keeping your promise, made many years ago, to be my paranymph. Lavinda, when help is needed, you are there. Thank you.

Thank you to my friends and former colleagues from my time working at Utrecht University. I learned something new from each and every one of you. Lucy, after all those years, you were willing to help me with last minute text editing. Thank you.

Thank you to my friends and family at home. Adèle, Carola, Clíodhna, Karen and Rose, it's good to know that you are there for me.

My friends in the Netherlands, thank you for your support and for opening your homes to me where I could peacefully procrastinate and work on this thesis.

Sonja, Nico†, Sterre and Yuna, dank voor jullie oneindige betrokkenheid en praktisch ondersteuning door de jaren heen. Nico, een lievere schoonvader had ik niet kunnen wensen. Dank je.

My parents, Bríd and Seán, thank you for all of your love and support. Always.

My siblings, Aoife, Dara, Áine and Laoise, thank you for knowing when to ask, 'is *it* almost finished?' and when to pretend like *it* doesn't exist.

Dúana, Aedín and Ruán, you are the most wonderful antithesis of support I can imagine [*cue Ruán waking for his feed*].

Wouter, pre-children: without you this thesis may still have happened, but everything else would have been a mess. Wouter, with children: without you this thesis would not have happened. Your love and support brought me here today. Bedankt.

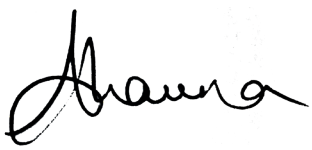

Curriculum vitae

Shauna Ní Fhlaithearta was born on the 14th of March, 1980, on the Aran Islands, Ireland. She attended University College Cork where she graduated in 2002 with a BSc. in Earth Sciences (1st class honours). After spending several months working for the National Seabed Survey at the Geological Survey of Ireland, she moved to the Netherlands to start an MSc. in Earth Systems Science at Wageningen University and Research. During her MSc. she completed an internship at the Royal Netherlands Institute for Sea Research, focussed on the effect of iron limitation on diatom growth. For her MSc. thesis she studied the inorganic geochemistry of a sediment core from a brine lake in the Eastern Mediterranean Sea. During her MSc. she spent 7 weeks at sea on board the RV Pelagia. After graduation she began her PhD at Utrecht University, within the Darwin Center for Biogeosciences. Her PhD project focussed on the development of foraminiferal based proxies in the Mediterranean Sea. After her PhD Shauna spent several years working for a hydrographic consultancy in Utrecht. Since 2017 she works at Wageningen University and Research – Library, as an Information Specialist.